DESIGN AND MANUFACTURING OF FUNCTIONALIZED HEXAGONAL BORON NITRIDE REINFORCED MULTI-SCALE EPOXY COMPOSITES WITH ENHANCED THERMAL CONDUCTIVITY

by

MOSTAFA MEHDIPOUR AGHBOLAGH

Submitted to the Graduate School of Engineering and Natural Sciences

in partial fulfilment of

the requirements for the degree of Doctor of Philosophy

Sabanci University

July 2025

DESIGN AND MANUFACTURING OF FUNCTIONALIZED HEXAGONAL BORON NITRIDE REINFORCED MULTI-SCALE EPOXY COMPOSITES WITH ENHANCED THERMAL CONDUCTIVITY

Approved by:

Prof. MEHMET YILDIZ. . . . . .
(Dissertation Supervisor)

Prof. BURÇ MISIRLIOĞLU. . . . . .

Assoc. Prof. BEKIR DIZMAN. . . . . .

Assoc. Prof. BERTAN BEYLERGIL. . . . . .

Assoc. Prof. HASAN ULUS. . . . . .

Date of Approval: July 23, 2025

ABSTRACT

DESIGN AND MANUFACTURING OF FUNCTIONALIZED HEXAGONAL BORON NITRIDE REINFORCED MULTI-SCALE EPOXY COMPOSITES WITH ENHANCED THERMAL CONDUCTIVITY

MOSTAFA MEHDIPOUR AGHBOLAGH

Materials Science and Engineering, Ph.D. Dissertation, July 2025

Dissertation Supervisor: Prof. Mehmet Yıldız

Dissertation Co-Supervisor: Prof. Burcu Saner Okan

Keywords: boron nitride, carbon fiber, thermal conductivity, epoxy

This thesis tackles the issue of poor heat dissipation in aerospace composites by using a multi-scale interface engineering strategy with hexagonal boron nitride (h-BN) and carbon fibers (CF) in epoxy. By optimizing h-BN content and applying surface modifications (acid/thermal treatments and silanization), thermal conductivity improved by up to 123%, with enhanced mechanical strength. Amino-silane treatment further increased conductivity but introduced brittleness. Incorporating modified h-BN into CF composites via electrospraying formed aligned thermal networks, achieving 2.31 W/mK thermal conductivity and a 127% rise in flexural modulus. The study shows that interface engineering can significantly improve both thermal and mechanical performance for aerospace use.

ÖZET

FONKSİYONELLEŞTİRİLMİŞ ALTIGEN BOR NİTRÜR TAKVİYELİ ÇOK ÖLÇEKLİ EPOKSİ KOMPOZİTLERİN GELİŞTİRİLMİŞ TERMAL İLETKENLİK İLE TASARIMI VE ÜRETİMİ

MOSTAFA MEHDIPOUR AGHBOLAGH

Malzeme Bilimi ve Mühendisliği, Doktora Tezi, July 2025

Tez Danışmanı: Prof. Dr. Mehmet Yıldız

Tez Eş Danışmanı: Prof. Dr. Burcu Saner Okan

Anahtar kelimeler: bor nitrür, karbon fiber, termal iletkenlik, epoksi

Bu tez, havacılık kompozitlerinde ısı yayılımını artırmak amacıyla, hekzagonal bor nitrür (h-BN) ve karbon fiber (CF) içeren epoksi kompozitlerde çok ölçekli arayüz mühendisliği uygulamıştır. h-BN'in boyutu ve miktarı optimize edilerek ısı iletkenliği %123'e, eğilme modülü ise %127'ye kadar artırılmıştır. Yüzey modifikasyonları ve amino-silan işlemleri, ısı iletkenliğini ve arayüz uyumunu geliştirmiştir. Elektropüskürtme ile CF yapısına entegre edilen modifiye h-BN, hem ısı hem de mekanik özelliklerde önemli iyileşmeler sağlamıştır. Çalışma, arayüz mühendisliğinin havacılık ve ısı yönetimi uygulamaları için etkili bir yöntem olduğunu ortaya koymaktadır.

ACKNOWLEDGMENTS

I would like to express my sincere gratitude to all those who supported and contributed to the completion of this thesis.

First and foremost, I would like to extend my deepest thanks to my supervisor, Prof. Dr. Mehmet Yıldız, for his invaluable guidance, insightful advice, and continuous support throughout the course of this research. His encouragement to explore various aspects of the field, his recognition of my achievements, and his constructive feedback during challenges have been instrumental to my academic and personal growth.

I am especially grateful to my co-supervisor, Prof. Dr. Burcu Saner Okan, for her patient guidance, unwavering encouragement, and expert insights throughout the research process. Her support has been crucial in bringing this work to completion, and I am truly thankful for her dedication and mentorship.

I would also like to express my appreciation to my dear research colleague, Dr. Semih Doğan, for his collaboration, helpful discussions, and contributions throughout this journey.

My heartfelt thanks go to my family, whose unconditional love, support, and belief in me have been a constant source of strength. Their encouragement has always motivated me to reach my full potential and pursue my dreams.

Finally, I gratefully acknowledge the financial support provided by the Turkish Energy, Nuclear and Mineral Research Agency – National Boron Research Institute (TENMAK-BOREN) under project number 2020-31-07-15-002.

TABLE OF CONTENT

LIST OF TABLES

LIST OF FIGURES

1. INTRODUCTION

Hexagonal boron nitride (h-BN) offers a range of valuable benefits, making it highly versatile material in various applications. Known for its exceptional thermal stability (up to 1000 °C in air and 1400 °C in vacuum) and high thermal conductivity (600 W/ mK), h-BN is ideal for use in high-temperature environments and as a heat dissipation material in electronics. H-BN exhibits high thermal conductivity primarily due to efficient phonon transport within its crystal lattice. Its strong in-plane covalent bonds and low atomic mass facilitate rapid phonon propagation, enabling effective heat transfer. Additionally, the highly ordered hexagonal structure of h-BN reduces phonon scattering, further enhancing thermal conductivity. Unlike metals, where electrons dominate heat transfer, in h-BN the phonon-based mechanism allows it to maintain high thermal conductivity while remaining electrically insulating, making it ideal for thermal management in electronic devices. It also has excellent electrical insulation properties, which makes it suitable for applications requiring both thermal conductivity and electrical insulation (band gap 5 eV), something rare among materials. Additionally, h-BN has outstanding chemical resistance and lubricating properties, making it useful as a solid lubricant in extreme conditions. Its layered structure, similar to graphite, allows it to be exfoliated into nanosheets for use in nanotechnology, coatings, and composite materials. Table 1 shows the comparing properties of h-BN with other materials used in thermal management applications.

Table 1.1 Comparing thermal conductivity properties of carbon based, ceramics and metals.

Materials	**Fillers**	**Thermal conductivity W/m-K**
Carbon based	Carbon nanotubes (CNT)	2800-6000
	Graphite	100-400
	Pitch based carbon fiber	530-1100
Ceramics	**Hexagonal boron nitride (h-BN)**	**600**
	Beryllium oxide	260
	Aluminum nitride	200
	Aluminum oxide	20-29
Metals	Cu	483
	Au	345
	Al	204
	Ni	158

The design and development of multifunctional h-BN reinforced thermoset epoxy matrix is being used in aerospace engineering and aviation applications, nowadays. Composite materials based on h-BN can improve the performance of materials used in aerospace applications by combining properties such as lightness, high strength, high thermal conductivity, and durability (Dong et al., 2024). However, before incorporating h-BN into the epoxy matrix, its surface needed to be modified due to its inherently high chemical stability and limited reactivity with epoxy resins. This surface inertness hinders effective interfacial bonding, which is crucial for enhancing the composite's overall thermal and mechanical performance. Therefore, appropriate surface functionalization strategies are essential to promote stronger interfacial interactions between h-BN and the epoxy matrix.

Various techniques for surface modification of h-BN have been explored in the works of literature, including chemical and mechanical exfoliation (Gautam & Chelliah, 2021), thermal treatment (He et al., 2019; Yu et al., 2016), and more. Certainly, among these approaches, chemical and thermal treatment processes are highly advantageous and facilitate the large-scale functionalization of h-

BN particles. In this context, incorporating a substantial quantity of hydroxyl (OH) groups onto the h-BN surface enhances both the bonding capability and adhesion force between h-BN and epoxy. Lingyun et al. stirred h-BN in sodium hydroxide solution at 120 ºC for 48 h and then filtered and washed (Huang et al., 2020). After oxidation process, the enhanced FTIR peak at 3416 cm^{-1} is related to the stretching vibration of B–OH was shown. Also, Jae et al. (Lee et al., 2019) transferred h- BN to sulfuric acid solution and mixed at 200 °C for 5 h, followed by washing, filtering and drying. No tools were used to show exactly the OH groups on the surface of h-BN particles. Generally, the amount of O-H group added to h-BN in an acidic environment is low and, and the rate of oxidation is not determined well (S. Zhang et al., 2017). Muratov et al. (Muratov et al., 2015a)compared the heat treatment process with different acid treatment processes for evaluating the amount of joint O-H groups in h-BN particles and the maximum hydroxyl group obtained in h-BN particles which were heat treated. The heat treatment process can increase the plane distances through in-plane direction and activate the surface for connection with oxygen and hydrogen derived from the air. The main disadvantage of heat treatment is the employment of high temperatures. In another study, Mostovoy et al. (Mostovoy et al., 2020) subjected h-BN particles to annealing at 1100 ºC for 1 h to increase hydrophilicity to the surface of h-BN. The incorporation of just 0.05 - 1.0 wt. % h-BN additives into the epoxy composition resulted in a notable improvement, increasing the thermal conductivity coefficient by 52–217%, strength by 53%, and tensile elastic modulus by 37%.

Also, to enhance wettability, achieve uniform distribution, and optimize h-BN particle-epoxy interface interactions, the silanization process (including amine groups) stands out as one of the most effective surface functionalization methods following the completion of the oxidation process (Lunelli et al., 2019). For instance, Hyunwoo et al. (Oh & Kim, 2019) silanized the surface of h-BN with vinyltriethoxysilane, and it was directly linked with the polymethyl methacrylate (PMMA) during the composite fabrication step. As a result, at a BN content of 70 wt.%, the composite exhibited an obvious thermal conductivity enhancement, with a value that was 17.8 times higher than that of PMMA about 3.73 (W/mK) Jaehyun et al. (Wie et al., 2020) silanized boron nitride with polysilazane (PSZ) and three different silanes, glycidoxypropyltrimethoxysilane (GPTMS), aminopropyltriethoxysilane (APTES), and mercaptopropyltrimethoxysilane (MPTMS), via hydrolysis and condensation. An epoxy composite containing the BN surface modified with PSZ and APTES had the highest thermal conductivity of 11.8 (W/mK) at a filler

fraction of 75 wt.%. Its thermal conductivity was 62 times higher than that of the neat epoxy. Moreover, Tuğrul et al. (Seyhan et al., 2017) functionalized the surface of boron nitride nanosheets (BNNSs) with vinyl-trimethoxy silane (VTS) coupling agent. Thermal conductivity of the neat PP sheets, which is about 0.22 (W/mK), was shown to increase to 0.41 (W/mK) when they were mixed with 5 wt.% of functionalized h-BNs. Kiho et al. (Kim et al., 2014) used two surface modified agents, 3-glycidoxypropyltrimethoxysilane (KBM-403) and 3-chloropropyltrimethoxysilane (KBM-703), and introduced them onto the surfaces of hydroxyl-functionalized boron nitride using a simple sol–gel process to act as fillers in the thermally conducting composites. The thermal conductivities of the composites containing 70 wt.% BN particles treated with the KBM-403 and KBM-703 were 4.11 and 3.88 (W/mK), respectively, compared to 2.92 (W/mK) for the composite without surface treatment. By Seokgyu in (Ryu et al., 2019), h-BN particles were silanized with amino propyl triethoxysilane (APTES) and aniline trimer (AT). The thermal conductivity of the composite containing 30 wt.% BN particles treated with the APTES and AT agents was 0.72 (W/mK), compared to 0.48 (W/mK) for the composite without surface treatment.

Building upon this background, the study first focused on enhancing the surface properties of h-BN for improved compatibility with epoxy matrices through chemical and thermal treatments. It includes chemical methods like the Hummer method, base and acid treatments to introduce functional groups, followed by thermal treatment at 1000 °C to enhance stability. Silanization will then bond silane molecules to h-BN, improving dispersion and boosting thermal conductivity and mechanical properties. The study also compares different solvents (water, ethanol and hexane) to optimize the process for creating high performance composites with excellent heat dissipation and mechanical strength.

The intricacy of the preparation of composite based on h-BN not only affects the properties of the materials during the process but also impacts the thermal conductivity of the resulting materials. Electrospinning and electrospraying methods, nowadays, offer a straightforward and auspicious approach for creating high-thermal-conductivity composites. Electrospraying is an electrohydrodynamic phenomenon driven process. The fibers produced using the electrospraying method exhibit exceptional alignment, facilitating the placement of fillers within the fibers in a highly oriented fashion. Kisang et al. (Sabri et al., 2021) employed the electrospray deposition method for the introduction of carbon nanotubes (CNTs) onto the surface of glass fiber (GF). The morphology of the resultant CNTs-GF hybrid revealed uniform and homogeneous deposition of

CNTs across the GF surface. Notably, the electrosprayed CNTs-GF exhibited a 34% increase in fracture toughness compared to the reference sample without electrospraying. Moreover, Dong et al. (D. L. Zhang et al., 2018) successfully used the electrospinning technique to create a composite of modified boron nitride (m-BN) within a polyvinylidene fluoride (PVDF) matrix, resulting in a material with impressive thermal conductivity and flexible mechanical properties. Within the m-BN/PVDF composites, m-BN is uniformly dispersed and exhibits an ordered orientation, forming a thermal conduction pathway along the direction of the fibers. As a result, the thermal conductivity of the m-BN/PVDF film can reach 7.29 (W/mK) with the inclusion of 30 wt.% m-BN. Additionally, these composites demonstrate enhanced mechanical characteristics, boasting a tensile strength of 24.06 MPa.

To address these objectives, the second phase of the study developed advanced coating processes using electrospraying and dip coating to apply h-BN or functionalized h-BN onto carbon fibers. A stable h-BN solution must first be formulated by optimizing concentration, solvent, and dispersant. Electrospraying parameters like voltage, flow rate, and nozzle distance fine-tuned to achieve uniform coating. Dip coating explored as an alternative method. Both techniques compared to identify the most effective process for enhancing thermal conductivity and mechanical strength in the coated carbon fibers.

To enhance the inter fiber bonding, hot pressing has been employed. Hot pressing these days is used much more for composite production, especially for thermal management applications. During hot press, we can reach high levels of densities through composite production, the number of scattering centers for phonon movement is decreasing, and thermal conductivity increasing. In (Gu et al., 2017) initially, a micrometer boron nitride/polyamide acid (mBN/PAA) compound was synthesized using electrospinning technology, followed by the fabrication of dielectric, thermally conductive mBN/polyimide (mBN/PI) composites saw the hot press at 320 ℃ under 5 MPa for 20–30 min. The resulting mBN/PI composite, containing 30 wt.% m-BN, exhibits a notably high thermal conductivity coefficient of 0.696 (W/mK). In (Y. Liu et al., 2022), an ultrasound fiber separation methodology was considered to infuse ceramic materials with continuous carbon fibers (CFs), and then low temperature hot pressing was employed to enhance its durability. Optimal carbon coating thickness was found to be crucial for achieving high fracture resistance. By producing a carbon interface with a thickness of approximately 110 nm, the resulting composite achieved impressive flexural strength, fracture toughness, and work of fracture values, measuring

388.3 MPa, 10.04 MPa·$m^{1/2}$, and 2380 J/m^2, respectively. Consequently, low temperature hot pressing proved to be an effective method for producing high-performance ceramic matrix composites. In (M. Liu et al., 2023), a multilayered composite of glass fiber and reinforced graphene nanoplatelets (GNP) into polypropylene was created. The GNPs were blended with a polypropylene-graft-maleic anhydride (PP-MAH) compatibilizer through a melt mixing process and subsequently coated onto the GF mats. Layer-by-layer assembly was carried out by sandwiching prepared coated fiber and then applying the hot press at 150 ºC with a pressure of up to 0.5 MPa. Remarkably, the stiffness and strength of the GFRP exhibited significant enhancements, increasing by approximately 3 GPa (25%) and about 120 MPa (95%), respectively, with the incorporation of 1.7 vol% of GNP into the composite.

So, in the third phase of the research, the study explored the thermal conductivity and mechanical properties of h-BN/CF composites manufactured by hot press, mold casting and manual extrusion with different structural conFigureurations, including filler-matrix and multilayered systems, to find optimal conditions for performance. Composites with varying h-BN filler content (5 wt.%, 10 wt.%, 20 wt.%, and 60 wt.%) were produced, with lower concentrations using mold casting and higher using manual extrusion. The impact of filler loading on properties analyzed with different characterization tools. For multilayered systems, alternating layers of carbon fibers and h-BN/epoxy resin hot-pressed to investigate heat and stress distribution. The study aims to identify the best structural conFigureurations for superior thermal and mechanical performance.

The incorporation of h-BN particles into epoxy matrices has been a subject of significant interest due to the potential enhancement of thermal and mechanical properties in composite materials. The particle size of h-BN plays a crucial role in influencing these properties, offering tunability and optimization for specific applications. The thermal conductivity of epoxy composites is greatly affected by the size of h-BN particles. Generally, h-BN particles which have higher interactions with the epoxy matrix, enhancing heat transfer through the material, resulting in improved thermal conductivity (Ambreen & Kim, 2020). Consequently, the thermal performance of the composite can be finely tuned by adjusting the particle size of h-BN. The mechanical properties of epoxy composites, including tensile strength, flexural strength, and hardness, are influenced by the dispersion and interaction of h-BN particles within the matrix. Yuezhan et al. mentioned the manufacturing of a hybrid composite that combined chemically linked hexagonal boron nitride (h-BN) with reduced graphene oxide (rGO) and incorporated through thermoplastic polyurethane

(TPU) (Bashir et al., 2023). This hybrid network structure, when employed as a filler in polymer composites, substantially enhances through-plane thermal conductivity, reaching 4.63 (W/mk) with just 3 wt.% BN content. Furthermore, the composite exhibits improved mechanical properties, particularly under tension. In one of the studies, Seyhan et al. (Seyhan et al., 2017) detailed the surface functionalization of boron nitride nanosheets (BNNSs) using the vinyl-trimethoxy silane (VTS) coupling agent to render their surface more hydrophilic. Achieving a weight content of 5 wt.% of functionalized h-BNs, the nanocomposites with silanized BNNS demonstrated the highest thermal conductivity values, reaching 0.41 (W/mK).

Although a significant body of literature exists on epoxy-based thermoset composites, many studies report substantial deviations in out-of-plane (through-thickness) thermal conductivity values and notable losses in mechanical properties, particularly when high thermal conductivity fillers are incorporated. Addressing these limitations requires a comprehensive approach that simultaneously improves heat transport in the thorough-thickness direction while preserving or enhancing structural integrity. This thesis advances the state of the art by delivering outcomes in multiple domains, including the functionalization of hexagonal boron nitride (h-BN) to improve interfacial compatibility, the modification of carbon fiber surfaces to strengthen fiber–matrix adhesion, and the strategic regulation of interphase and interface properties. Through this multi-faceted strategy, the research establishes effective pathways to achieve directional thermal conductivity control without compromising — and in some cases enhances the mechanical performance of epoxy composites. This thesis is structured into five interrelated chapters, each addressing a critical aspect of multi-scale interface engineering for enhanced thermal and mechanical performance in epoxy composites. Chapter 2 presents a comprehensive experimental study on the effects of hexagonal boron nitride (h-BN) particle size and loading ratio on the thermal and mechanical behavior of epoxy systems. Chapter 3 focuses on enhancing directional thermal conductivity in h-BN reinforced epoxy composites through the development of robust interfacial bonding strategies. Chapter 4 combines experimental validation and numerical modeling to investigate the influence of silane concentration on the interfacial effects in silanized h-BN/epoxy composites. Chapter 5 explores how functionalized h-BN particle interphase and interface regulation, combined with structural design, affect the directional thermal conductivity and mechanical performance of carbon fiber/epoxy composites. Finally, Chapter 6 integrates the findings into a multi-scale interface engineering approach, demonstrating how physical and

chemical interactions can be tailored to control directional performance in h-BN and carbon fiber-reinforced composites. Together, these chapters provide a systematic pathway for controlling heat transport and mechanical integrity in advanced composite systems, with direct relevance to aerospace and thermal management applications.

2. A COMPREHENSIVE EXPERIMENTAL STUDY ON THE EFFECTS OF HEXAGONAL BORON NITRIDE PARTICLE SIZE AND LOADING RATIO ON THERMAL AND MECHANICAL PERFORMANCE IN EPOXY COMPOSITES

Harnessing the potential of hexagonal boron nitride (h-BN) in epoxy composites for tailoring thermal conductivity is a promising avenue in materials science. However, achieving balanced enhancements in both in-plane and through-plane directions remains a challenge that requires innovative solutions. The primary objective of this research is to evaluate how thermal and mechanical characteristics of an epoxy matrix are affected by the size and amount of h-BN particles. To achieve this goal, h-BN particles with varying sizes (micro and nano) are incorporated into the epoxy matrix at different weight ratios spanning from 0.5 wt. % to 20 wt. % using a pre-dispersion technique. The epoxy composites reinforced with h-BN through a molding process exhibit enhanced mechanical and thermal performance in contrast to the pristine epoxy material. During the flexural test, acoustic emission data is collected to identify the initiation and progression of damage within the specimens under testing conditions. The most notable enhancement in thermal conductivity is observed when incorporating 20 wt.% of micron-sized h-BN particles. This leads to a remarkable 107% increase in the in-plane direction and an impressive 112% increase in the through-plane direction. These results can be attributed to the formation of a three-dimensional thermally conductive network by the larger h-BN particles, which extends the path of phonon scattering. Furthermore, there are significant improvements in both flexural modulus and tensile modulus. Epoxy composites containing 10 wt.% of micron-sized h-BN experience an approximate 42% increase, while those with 20 wt.% of the same particles display a substantial 47% rise in these properties. This study effectively addresses the challenges associated with tailoring the thermal properties of epoxy composites, opening up new opportunities for applications in various industries, including electronics, aerospace and thermal management systems.

2.1 Review

The electrical systems and components used in modern airplanes are highly developed and powerful resulting in the generation of heat dissipation and large amounts of waste heat. The accumulated heat from the onboard electronics, oil and hydraulic systems, avionics bay cooling, and weapons modules must be effectively dissipated in order to maintain thermal stability and prevent material failure (Muratov et al., 2015b). Herein, there is a growing demand to enhance thermal conductivity of thermoset and thermoplastic polymeric composites by designing polymer chains and blending with metallic, ceramic, carbon and natural micron- and nano-sized fillers. However, polymeric composites especially thermoset composites used in structural parts of airplanes still suffer from a poor thermal conductivity in the range of 0.1–0.3 W/mK due to the random orientation of molecular chains or the defects like a loop, voids, impurities, and chain dangling ends occurred in the structure. These defects give rise to phonon scattering and considerable reduction in phonon's mean free path, thereby decreasing the thermal conductivity, which causes the failure of polymer composites when the temperature increases. Hence, a growing focus on designing complex and high-powered electronics components and systems can mitigate waste heat by utilizing a larger quantity of fillers that can effectively manage thermal conductivity in epoxy resin.

Hexagonal boron nitride (h-BN), also known as white graphene, is a promising thermally conductive dielectric material for thermal management systems since its theoretical in-plane thermal conductivity is reported as 600 W/mK at room temperature (Yuan et al., 2019). Therefore, numerous attempts are conducted to incorporate h-BN particles into epoxy matrix at different loading ratios. For instance, Gu et al.(Gu et al., 2012) investigated the effect of the loading ratio of neat and micron-scale BN particles modified by silane coupling agent, g-aminopropyl triethoxy silane (KH550) on the thermal and mechanical properties, and it is shown that the thermal conductivity and flexural strength improved by 58% and 13% for 10 wt. % neat BN concentration, respectively. The composites filled with modified BN possess have better thermal conductivity. The thermal conductivity coefficient reached 1.1 W/mK with the addition of 60 wt. % modified BN. In another work, Tang et al. demonstrated that the thermal conductivity value of epoxy composites is enhanced by 58% by the addition of 7 wt. % methyl tetrahydrophthalic anhydride

modified h-BN. In addition, Hou et al. (Mostovoy et al., 2020) showed that the thermal conductivity of epoxy composite based on neat micron h-BN increased by composite based on h-BN microparticles, modified by surface coupling agent 3-aminopropyl triethoxy silane (APTES). The thermal conductivity is 1.178 W/mK with loading of 30 wt. % modified BN particles, which is 6.14 times higher than that of pure epoxy resin, whereas a lower value of 1.037 W/mk could be obtained by adding the same content of raw BN particles. It was also shown that the thermal conductivity does not increase linearly with the addition of h-BN into the matrix. Rather, this increase follows an exponential trend, especially noticeable with higher h-BN content (Huang et al., 2020), (Peng et al., 2022). These results indicate that the thermal conductivity of epoxy resin could be increased by using h-BN particles significantly, however there is still lack of information to control the thermal conductivity in-plane and through thickness directions based on selective composite design and manufacturing with the suitable and scalable process (Ahmad et al., 2023). In other words, a systematic approach is required to get optimum in-plane and through-thickness thermal conductivity results in epoxy systems. This involves determining the ideal particle size and aspect ratio of h-BN particles while considering interfacial properties. Moreover, although high filler loading enhances heat conductivity, it also results in a substantial reduction in the mechanical properties of epoxy systems during the manufacturing phase.

To the best of our knowledge, no prior research has been devoted to the determination of optimal h-BN particle size and concentration to tailor both through-thickness and in-plane thermal conductivity. This research also aims to enhance or at least maintain mechanical performance of the epoxy matrix and thereby use acoustic emission analysis to investigate how particle size affects the failure behavior and overall mechanical performance of the manufactured composite. To this end, two distinct h-BN particle sizes are employed, and a solvent-based dispersion method is utilized to achieve a completely intercalated composite structure with an appropriate concentration threshold of h-BN. The utilization of an ethanol-based pre-dispersion method yields a rapid and scalable manufacturing process, effectively dispersing the h-BN particles without compromising the inherent qualities of the epoxy resin. Having ensured uniform dispersion, this approach facilitates efficient heat and load transfer within the composite, ultimately resulting in enhanced thermal and mechanical characteristics of the epoxy composites. Thus, this study offers insights into the combined influence of h-BN particle size and concentration within the epoxy matrix, leading to the augmentation of both thermal and mechanical properties.

2.1 Experimental

2.1.1 Materials

Hexagonal boron nitride (h-BN) nanoparticles measuring 120 nm are acquired from Bortek Company in Turkey. h-BN with varying particle sizes, ranging from 4 to 10 μm, is sourced from Civelek Porselen Company, also in Turkey. The epoxy resin system Sika Biresin® CR131/CH132-5 is procured from Tekno Chemicals Inc. in Turkey. This particular resin system is well suited for infusion applications due to its low viscosity and is commonly employed in the production of high-performance fiber-reinforced composite materials. Absolute ethanol with a purity level of 99% is obtained from Sigma Aldrich. All agents are used in their unaltered, analytical-grade forms.

2.1.2 Manufacturing of h-BN reinforced epoxy composites

The reference plates are produced by combining CR131 epoxy with CH132-5 hardener at a specific ratio (100:28 by weight), using a high-speed mixer for 1 minute at 1000 rpm. After the mixing process, the solution is subjected to a 25 min degassing procedure in a vacuum chamber to eliminate any trapped air and volatile reaction products. Subsequently, the degassed mixture is poured into a preheated aluminum mold and then cured in an oven at 100°C for 5 hours. As for the production of h-BN-reinforced epoxy composite plates, the pre-dispersion method is employed, utilizing a weight percentage ranging from 0.5 wt.% to 20 wt.%. Micron- and nano-sized h-BN particles are first sonicated in ethanol for 1 hour and then introduced into the epoxy, followed by an additional 2-hour sonication period. All sonication steps are performed in an ice bath to maintain appropriate temperature conditions. The resulting homogeneous h-BN/ethanol/epoxy solution is stirred using a magnetic stirrer for 2 days to eliminate ethanol. After incorporating the CH132-5 hardener and repeating the degassing procedure as employed for the reference epoxy, the mixture is cast into a preheated aluminum mold and subjected to the same curing process as the reference epoxy plate. Following this curing step, both the reference and h-BN-reinforced epoxy composites

are cut to precise dimensions, adhering to relevant test standards. Figure S1 presents a process schematic for the preparation of the h-BN epoxy mixture.

2.2.3 Characterization

The chemical and morphological properties of h-BN particles are scrutinized using various analytical tools. A Renishaw inVia Reflex Raman Microscope, equipped with a 532 nm edge laser, is employed at room temperature. Additionally, X-ray photoelectron spectroscopy (XPS) analysis is conducted with a Thermo Scientific instrument. For the study of crystallographic properties, X-Ray Diffraction (XRD) is performed using a Bruker D2 Phaser diffractometer with a CuKα radiation source. Thermal characteristics of the materials are examined using a Mettler Toledo Thermal Analyzer (TGA/DSC 3+), with a heating rate of 3°C/min from room temperature to 1000°C. The thermal conductivity values (k) for both in plane and through-thickness directions of the reference and h-BN reinforced epoxy composite samples are determined employing the hot disc method with a TPS 2500 S device. To elucidate the interfacial interactions between the matrix and filler in the composite structures as a function of h-BN amount and particle size, various destructive and non-destructive techniques are employed. Namely, tensile and 3-point bending tests are performed by Instron 5982 Static Universal Test Machine (UTM) fitted with a 10 kN load cell with the crosshead speed of 2 mm/min in accordance with the standards of ASTM D 638 and ASTM D 790, respectively. The cross-sectional analyses of specimens after tensile tests and the examinations of h-BN particle morphologies are conducted with a Leo Supra 35VP Field Emission Scanning Electron Microscope (SEM) from Carl Zeiss AG in Jena, Germany. Dynamic mechanical analysis (DMA) is carried out on specimens with dimensions of 65 mm in length and 10 mm in width, utilizing a DMA Q800 instrument from TA Instruments. The experiments are performed in a dual cantilever mode with a heating rate of 3°C/min, covering the temperature range from room temperature to 150°C at a frequency of 1 Hz. Acoustic emission (AE) analysis is carried out during 3-point bending tests on specimens. Mistras PCI 2 AE apparatus along with AEwin PCI2-4 software is used to record the acoustic signals during mechanical testing. Two wideband PICO-type AE sensors, operating within a range of 200–750 kHz and with a resonance frequency of 550 kHz, are employed for this analysis to avoid data loss in case one of the sensors gets detached

during the test. Time domain waveforms are utilized to detect acoustic emission hits occurring during damage formation and propagation. These waveforms are amplified using Mistras 0/2/4 preamplifiers with a gain of 20 dB. To ensure clean and noise-free recordings, a data-recording threshold of 45 dB is established. The acoustic emission signals are collected with the following parameters, a 150-µs hit definition time, a 300-µs hit lockout time, and a 50-µs peak definition time. The AE sampling rate is set to 2 MHz, and the strain value associated with each acoustic hit is recorded using an analog voltage from a tensile test machine. Following the mechanical tests, the collected AE data is subjected to filtering in the frequency domain between 20 and 800 kHz, utilizing an 8th-order Bessel band pass filter as a postprocessing step using Noesis 7 software. Both time domain and frequency domain parameters are then extracted as the primary features of the acoustic signals.

2.3 Results & Discussion

2.3.1 Characteristics of micron- and nano-sized h-BN particles

Surface chemistry and morphology play a pivotal role in the dispersion quality of fillers within a polymer matrix. Thus, the mechanical and thermal properties of the resulting composites are significantly affected by the surface characteristics of these reinforcements and their interactions with the epoxy matrix. The atomic composition and surface structure of h-BN particles can directly influence their dispersion behavior within the epoxy matrix. In this study, we employed morphological and spectroscopic techniques to characterize two distinct types of h-BN particles. Figures 2.1a and 2.1b present scanning electron microscope (SEM) images of micron-sized and nano-sized h-BN particles, revealing the presence of flat-like h-BN particles. Particle size analysis results indicate that the micron-sized h-BN particles measures between 4-10 µm, while the nano-sized h-BN particles have a particle size of 120 nm. The SEM images also confirm that the disparities in particle sizes and the sheet dimensions of micron-sized h-BN are noticeably greater in comparison to nano-sized h-BN.

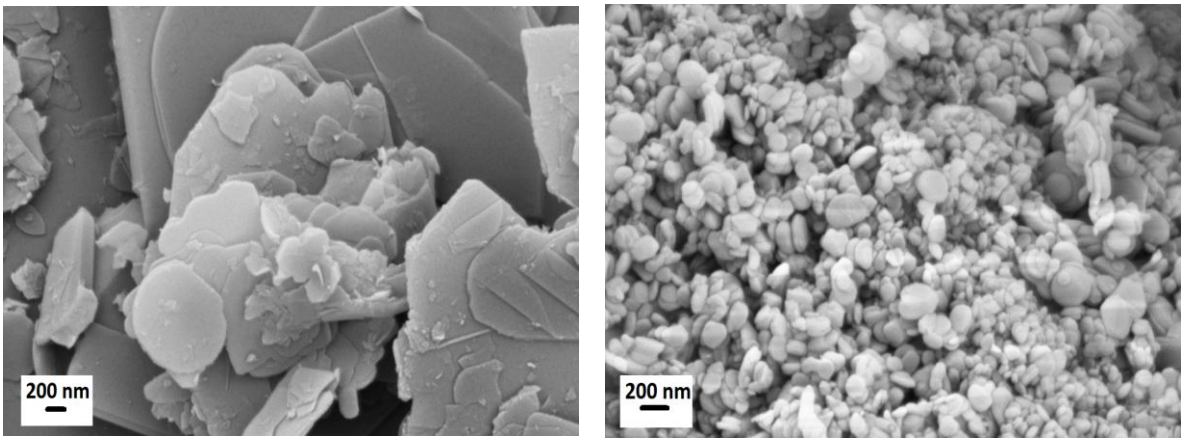

(a) (b)

Figure 2.1 SEM images of (a) micron- and (b) nano-sized-h-BN particles

As stated previously, the elemental compositions of the micron- and nano-sized h-BN particles are analyzed by XPS to understand the relation of h-BN surface chemistry with the epoxy matrix. Table 2.1 summarizes XPS results of neat micron- and nano-sized h-BN particles, and Figure. S4 shows XPS survey scan spectra of h-BN particles. The results indicated that nano-sized h-BN has higher oxygen and carbon content than micron-sized h-BN. The intensity of N1s of micron-sized h-BN is greater than that of nano-sized h-BN; in addition, O1s, N1s, C1s, and B1s signals are observed at approximately 532 eV, 398 eV, 285 eV, and 190 eV, respectively, for both micron- and nano-sized h-BN, as seen in Figure. S4.

Table 2.1 The elemental compositions of neat micron- and nano-sized h-BN particles.

Sample	**N (at %)**	**B (at %)**	**O (at %)**	**C (at %)**
Micron h-BN	70.94	16.44	4.08	8.55
Nano h-BN	50.84	27.93	8.70	12.53

Figure 2.2 shows XRD patterns of micron- and nano-sized h-BN particles, and peaks found at 9°, 18°, 28°, 37°, and 48° refer to the characteristic hexagonal basal planes, (101), (102), (004), and (110), respectively. There is no significant difference in TGA curves and Raman spectra of micron-

and nano-sized h-BN particles, and the results are provided in Figure. S2 and S3, respectively, in the supporting information document.

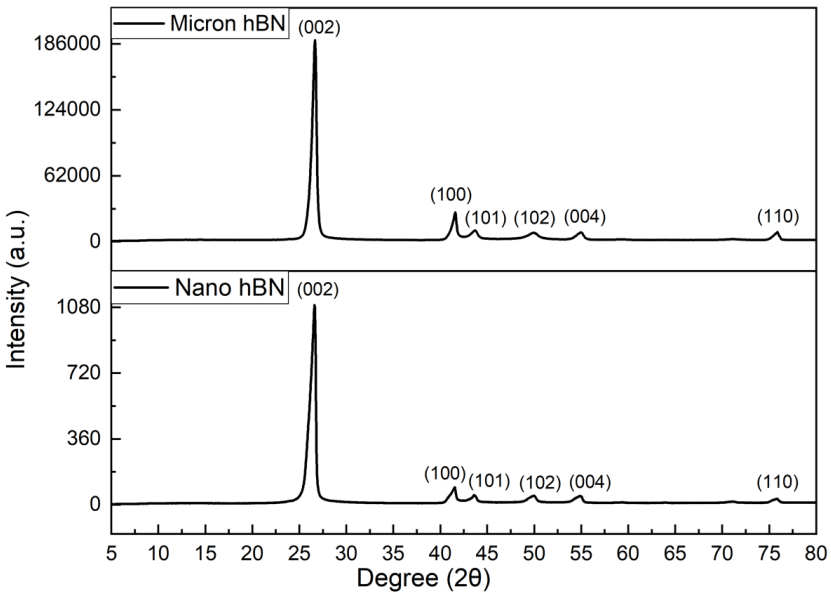

Figure 2.2 XRD patterns of micron- and nano-sized h-BN particles.

2.3.2 Effect of particle size and h-BN loading ratios on mechanical and thermomechanical behavior of epoxy composites

This section delves into the impact of particle size and loading ratios of h-BN particles on mechanical and thermomechanical performance. Figurers 3a and 3b illustrate the stress-strain curves from tensile tests conducted on both the pristine epoxy and h-BN reinforced epoxy composites, encompassing various concentrations of micron- and nano-sized h-BN particles. As the h-BN particle concentration increases, the stress-strain curve exhibits a steeper slope, signifying an augmentation in the elastic modulus for both micron- and nano-sized h-BN reinforced composites. The neat epoxy displays an elastic modulus of 2985±87 MPa and a tensile strength of 81±2.4 MPa. However, in the case of micron-sized h-BN reinforced composites, there is a notable decrease in failure strain values, indicating that the resulting composite becomes more brittle compared to both the neat epoxy and the nano-sized h-BN reinforced composites. Conversely, the failure strain values for nano-sized h-BN reinforced composites remain nearly

equivalent to those of the neat epoxy. The comparison of improvements in tensile strength and elastic modulus with micron- and nano-sized h-BN particles is demonstrated in Figureures 3c and 3d, respectively. The incorporation of 20 wt.% of micron-sized h-BN particles in the epoxy matrix results in 46.9% increase in elastic modulus, which is approximately three times higher than that achieved by adding 20 wt.% of nano-sized h-BN particles. This greater enhancement in elastic modulus with micron-sized h-BN particles can be attributed to their larger size and higher aspect ratio, which effectively constrain crack propagation, immobilize epoxy chains, and transfer stress between micron-sized h-BN and the epoxy through a more extensive surface contact area. It is worth noting, however, that increasing the loading ratio of micron-sized h-BN particles can have a detrimental effect on the tensile strength of epoxy. This is due to the uneven distribution of h-BN particles and poor stress transfer between the h-BN and the epoxy, resulting in a maximum reduction of 20.6% for 10 wt. % of h-BN. The addition of h-BN generates various stress concentration points within the epoxy resin as the content of h-BN increases. On the other hand, nano-sized h-BN has a minimal impact on the mechanical properties of the epoxy due to local stress caused by the stiffening effect of the brittle cross-linked polymers and poor connections between fillers and matrix, leading to a reduction in tensile strength (Park et al., 2018). Table S2 and S3 summarize the tensile strength variation for micron- and nano-sized h-BN particles as a function of particle concentration.

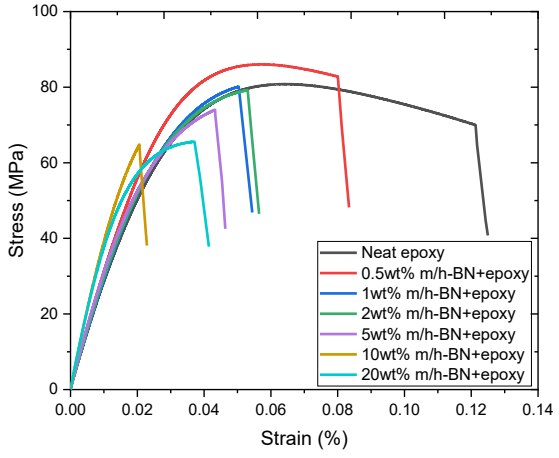

(a)

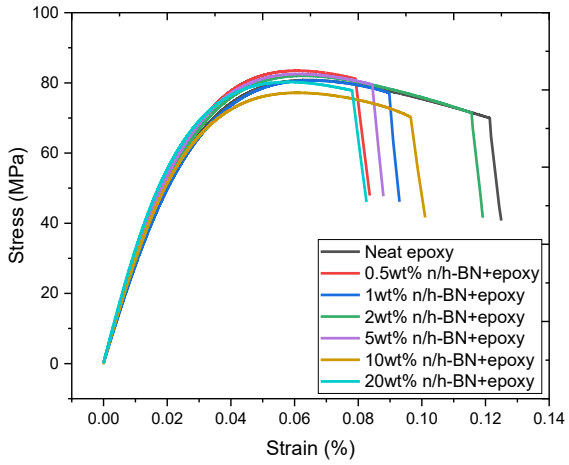

(b)

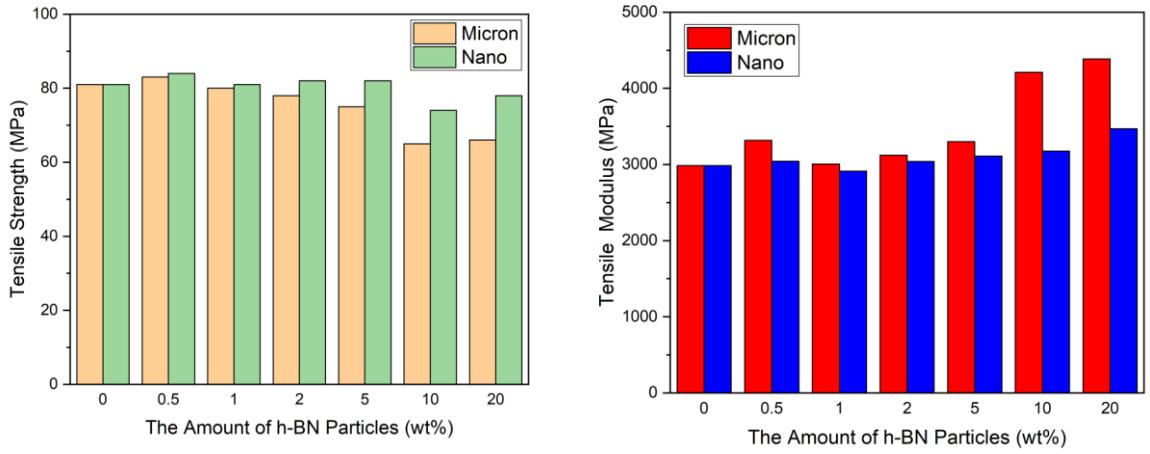

(c) (d)

Figure 2.3 The tensile stress-strain curves for (a) epoxy composites reinforced with micron-sized h-BN and (b) those reinforced with nano-sized h-BN at various loading ratios, and a comparison of the enhancements in (c) tensile strength and (d) tensile modulus concerning h-BN particle size.

The flexural stress-strain curves for the neat epoxy, as well as micron- and nano-sized h-BN particle reinforced epoxy composites with varying loading ratios ranging from 0.5 wt. % to 20 wt. %, are shown in Figure 4a and 4b. Similar to the tensile tests, an increase in h-BN particle concentration lead to a decrease in ductility and an increase in brittleness in the composites. However, the reduction in ductility is less pronounced in the composites reinforced with nano-sized h-BN particles. The flexural strength values are also found to be significantly decreased with the increase of micron-sized h-BN particles. Figure. 4c and 4d illustrate the flexural strength and flexural modulus values of the neat epoxy and h-BN reinforced epoxy composites as a function of h-BN type and concentration. Both micron- and nano-sized h-BN/epoxy composites demonstrate a gradual increase in flexural modulus values. Specifically, the 10 wt. % micron-sized h-BN particle reinforced epoxy composites exhibits a higher flexural modulus (by approximately 40.62%) than the neat epoxy. This is due to the wider surface interaction area between the micron-sized h-BN particles and the epoxy, which enables more efficient load transfer compared to nano-sized h-BN particles. As a result, the flexural modulus values are much higher in the case of micron-sized h-BN reinforced epoxy composites (Hassan et al., 2019). In contrast, nano-sized h-BN particles render an enhancement in flexural modulus without much deterioration, even at high concentrations (such as 20 wt. % h-BN). Additionally, there is no significant change in the flexural

strength, and the nano-sized h-BN particles have a positive effect on the flexural modulus, which is 15.2% higher than that of the neat epoxy. The homogeneous dispersion of nano-sized h-BN particles is maintained even at high concentration levels, whereas the upper limit for homogeneous dispersion of micron-sized h-BN particles in the epoxy matrix is found to be at the 10 wt. % loading level. The decrease in flexural strength values of the micron-sized h-BN reinforced epoxy composites can be attributed to the formation of h-BN particle agglomerates, which reduce the interaction areas between the h-BN particles and the load transfer capability between the particles and the epoxy. As the h-BN particle concentration increases, the epoxy matrix becomes saturated, resulting in the development of voids and mesh-like structures that further reduce the flexural strength of composites containing excessive h-BN. This non-uniform distribution and agglomeration of h-BN particles in the epoxy matrix have been previously demonstrated in a similar study by Han et al.(Sroka et al., 2016) on BN-nanosheets in the epoxy matrix. Poor interfacial adhesion between h-BN particles and the epoxy matrix is a common issue, making it difficult to transfer and distribute the applied load uniformly in the matrix. However, this problem can be addressed through surface treatment of h-BN particles. A previous study by Wattanakul et al. (Shen et al., 2019) demonstrated that surface treatment of h-BN particles can enhance the interfacial adhesion and dispersion of the particles in the epoxy matrix, leading to improved mechanical properties of the resulting composites. Table S3 and S4 summarize the flexural modulus, strength, and the calculated improvement percentages.

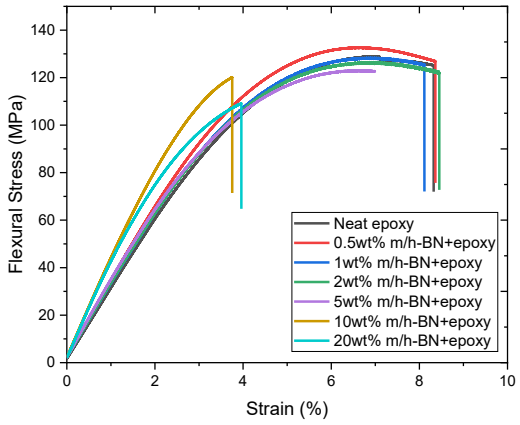

(a)

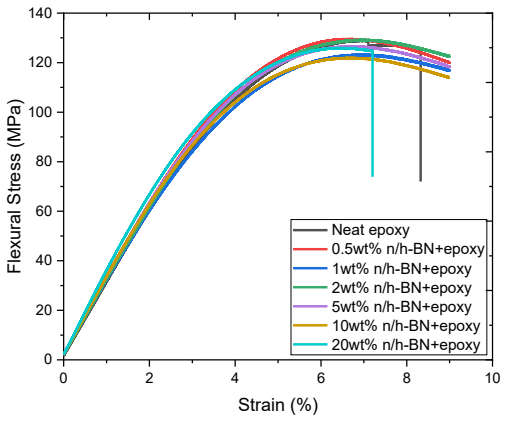

(b)

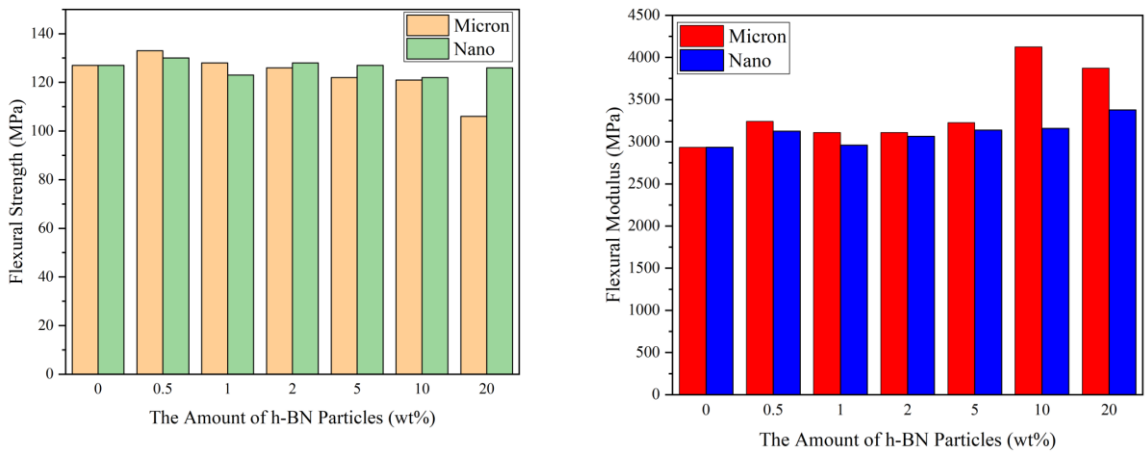

(c) (d)

Figure 2.4 Flexural stress-strain curves of (a) micron- and (b) nano-sized h-BN reinforced epoxy composites at different loading ratios, and the improvement comparison of (c) flexural strength and (d) flexural modulus in terms of h-BN particle size

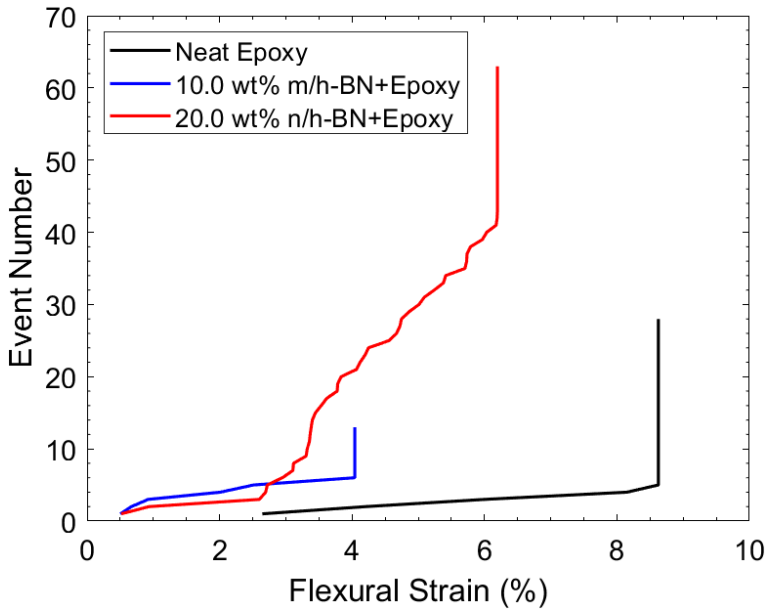

Figure 2.5 Cumulative sum of acoustic events of neat epoxy, 10% micro h-BN/epoxy and 20% nano h-BN/epoxy flexural tests.

To qualitatively elucidate the effect of h-BN particle size on the mechanical behavior of h-BN/epoxy composite, acoustic emissions (AE) analysis is performed on the specimens during mechanical testing. In the case of the flexural specimens, AE events (the elastic waves generated

by the material during deformation or failure) are recorded and compared for neat epoxy, 10% micro-reinforced and 20% nano-reinforced samples. The cumulative sum of acoustic events with respect to flexural strain is plotted in Figure 5. The results show that the addition of h-BN particles increases the brittleness of the epoxy, regardless of the reinforcement size. This is attributed to the hindering effect of the particles on polymeric chain mobility. However, the nano-reinforced specimen exhibits significantly higher acoustic events at intermediate strain values, indicating that the nano h-BN particles can delay failure through micro crack formation. This toughening mechanism counteracts the brittleness caused by chain restriction and leads to a higher strain capacity. As a result, there is no reduction in strength when compared to pure epoxy. In contrast, the micro-reinforced specimen does not show any toughening mechanisms, resulting in a lower strength value caused by a lower strain capacity. These results suggest that nano-sized h-BN particles can improve the toughness of the epoxy matrix, while micron-sized h-BN particles may have a detrimental effect on the material's mechanical properties.

Flat-like particles offer a substantial surface area, and the mechanical performance of epoxy is influenced by their size and aspect ratio. When h-BN particles are large and have a high aspect ratio, they aid in the effective transfer of stress between the epoxy and h-BN particles, as well as prevent polymer chain movement (Bashir et al., 2023). The mechanical properties of epoxy can be improved by adjusting the loading ratio, which inhibits crack propagation and provides effective stress transfer. However, exceeding a certain concentration level may cause a decrease in mechanical properties due to the formation of bubbles and stress concentration regions caused by particle aggregation. On the other hand, high-quality dispersion of h-BN particles and strong adhesion between h-BN and epoxy can enhance the mechanical performance of the composites by preventing stress concentration areas from forming in the material. Improved wettability and reduced coefficient of friction of layered h-BN particles lead to fewer voids and agglomerated particles. However, excessive use of h-BN particles negatively affects the mechanical properties. Despite this drawback, incorporating h-BN particles into the composite can result in higher thermal conductivity, which will be discussed in the following paragraphs.

The analysis of storage modulus and tan δ curves is an effective method to evaluate the reinforcing efficiency of particles under different temperatures and stress conditions. Figurers 6a and 6b illustrate the changes in the storage modulus of epoxy, particle size, and h-BN concentration. The storage modulus shows a direct correlation with the amount of micron- and nano-sized h-BN

particles, similar to the flexural modulus in bending tests. The increase in storage modulus can be attributed to the improvement in load-bearing capacity and stiffness of the epoxy due to the addition of high-stiffness h-BN particles. Furthermore, increasing the concentration of h-BN particles allows for more particles to connect to the epoxy, contributing to the enhancement in storage modulus (S. Zhang et al., 2017). Moreover, the uniform distribution of inflexible h-BN particles creates effective pathways for load transfer, thereby facilitating load transfer via the h-BN/epoxy interfaces. Additionally, the chemical bonding between the h-BN particles and epoxy constrains the mobility of the epoxy's molecular chains in the vicinity of the h-BN particles, resulting in an increase in the storage modulus. The storage modulus exhibits a decline with rising temperature due to relaxation in the mobility of the epoxy chains, followed by a steep drop in the high-temperature range, known as the glass transition region (Xiao et al., 2020a).

The glass transition temperature is the temperature range at which polymer chains transition from a rigid, glassy state to a more flexible, rubbery state. Figures 6c and 6d display the temperature-dependent changes in the loss factor, and the T_g values of the samples can be compared based on the peak points of the graphs, as a function of particle size and concentration. The T_g is a property that relates to the molecular mobility of polymers, which can be affected by factors such as chain rigidity, linearity, and packing. The Figures reveal only minor variations in the T_g of the epoxy composites upon the addition of both micron- and nano-sized h-BN particles, which could be attributed to the restriction of segmental motion of the polymer chains in the vicinity of the filler-matrix interface (Y. Wang et al., 2019). In contrast, the moderate decrease can be reduced by the reduction of the cross-linked density in the composite and low interfacial interaction between h-BN particles and epoxy matrix (Yuan et al., 2019).

The magnitude of tan δ serves as an indicator of a material's energy dissipation characteristics. Figurers 6c and 6d depict an increase in tan δ with the incorporation of micron- and nano-sized h-BN particles, and the highest value is attained in the epoxy with 10 wt. % of micron-sized h-BN. This increase can be attributed to the interaction between the h-BN and epoxy molecules, whereby a low tan δ value indicates a robust interaction. As a result of this strong interaction, chain entanglement occurs in the vicinity of the fillers, hindering the epoxy's chain mobility.

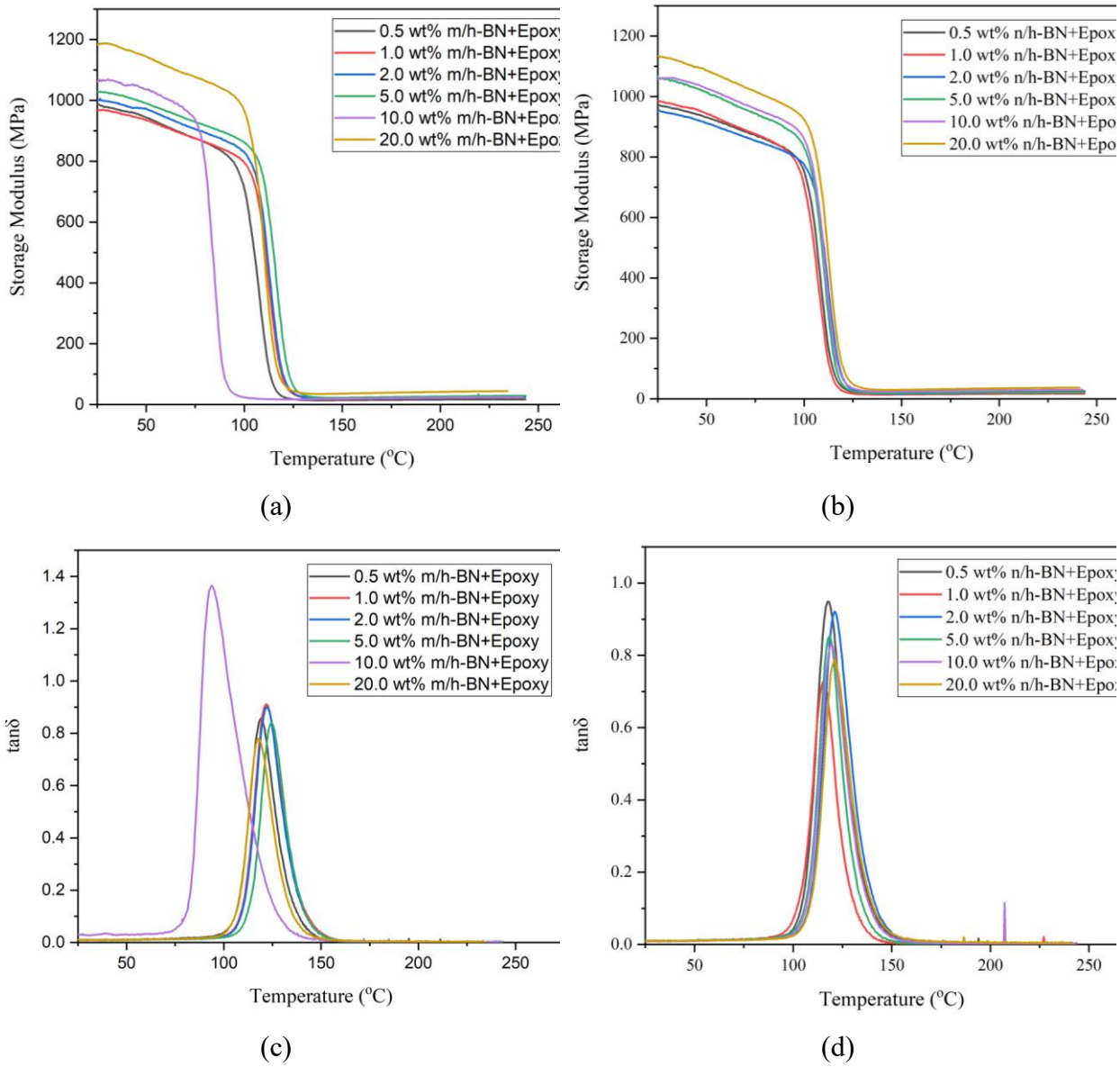

Figure 2.6 Temperature sweep of the storage modulus of (a) micron-sized and (b) nano-sized h-BN reinforced epoxy composites and damping ratio curves of (c) micron-sized and (d) nano-sized h-BN reinforced epoxy composites.

2.3.3 Customizing Thermal Conductivity in Epoxy Composites through Varying Particle Size and Loading Ratios of h-BN Particles

The thermal conductivity of composite materials is influenced by various factors such as the constituent materials, their intrinsic thermal conductivity values, filler concentration, size and shape. This is because composites are made up of different types of materials that interact with each other, affecting the overall thermal conductivity of the resulting composite. Therefore, it is crucial to consider these factors when designing composite materials with desired thermal conductivity properties (W. Yang et al., 2025). To improve the thermal conductivity properties of composite materials, several strategies can be employed. One such approach is to create highly thermally conductive pathways within the composite material. Additionally, reducing the interfacial resistance between the filler and matrix can also enhance thermal conductivity. Furthermore, minimizing thermal resistance arising from lattice defects, impurities, boundaries, and phonon-phonon scattering through conductive pathways can further improve the thermal conductivity of composite materials. By employing these methods, composite materials can be designed with improved thermal conductivity properties for various applications (Kuila et al., 2025).

The thermal conductivity values of epoxy in both in-plane and through-through-thickness directions are illustrated in Figure 7a and 7b, respectively, as a function of h-BN particle size and concentration. It is evident that, at all concentration levels, the use of micron-sized h-BN particles in the epoxy results in higher thermal conductivity values compared to those obtained with nano-sized h-BN particles. This phenomenon can be attributed to the heat transport mechanism in non-metals, which involves the flow of phonons. The larger size of the micron-sized h-BN particles reduces the number of interfacial areas between the h-BN and epoxy, which in turn diminishes phonon scattering through the conductive pathways. Consequently, there is a significant enhancement in thermal conductivity for particles with wider interfacial surface areas. Moreover, the large particles create thick and highly stable conductive pathways that cannot be disrupted by other particles at the boundaries of these pathways (Gul et al., 2023). Another factor that affects the thermal conductivity values of composites is the loading level of the filler particles. Increasing the loading levels of both micron- and nano-sized h-BN particles can improve the thermal conductivity values, but this improvement occurs in a non-linear manner. Specifically, the

percentage improvement in thermal conductivity is higher at higher loading levels compared to lower loading levels, as depicted in Figure 7a and 7b. This can be explained by the initiation of thermally conductive pathways, which is facilitated by the formation of filler connections at high filler concentration levels. The thermal conductivity values of the neat epoxy are 0.222 W/mK in the in-plane direction and 0.231 W/mK in the through-thickness direction. The differences in these values between the two directions can be attributed to the molecular chain alignments of the epoxy. However, the thermal conductivity values can be improved by incorporating micron- and nano-sized h-BN particles, with the maximum values in the in-plane and through-thickness directions reaching 0.46 W/mK and 0.49 W/mK, respectively. The addition of 20 wt. % micron-sized h-BN results in a 107.2% and 112.1% increase in thermal conductivity values for the in-plane and through-thickness directions, respectively. These values are approximately two times higher than those obtained with the use of nano-sized h-BN particles. A reduction in thermal conductivity is noted at a 2 wt. % concentration of nano h-BN, as illustrated in Figure 7(a). This decline is likely due to the impeded movement of phonons within the matrix. In solid materials, lattice vibrations (phonons) predominantly govern thermal conductivity. When these phonons transition from the matrix to the filler, an increase typically occurs, given h-BN's higher thermal conductivity. However, at lower concentrations of h-BN, particularly in the nanoscale, phonons may struggle to effectively navigate pathways to fully access the nano h-BN phases, thus leading to the observed reduction.

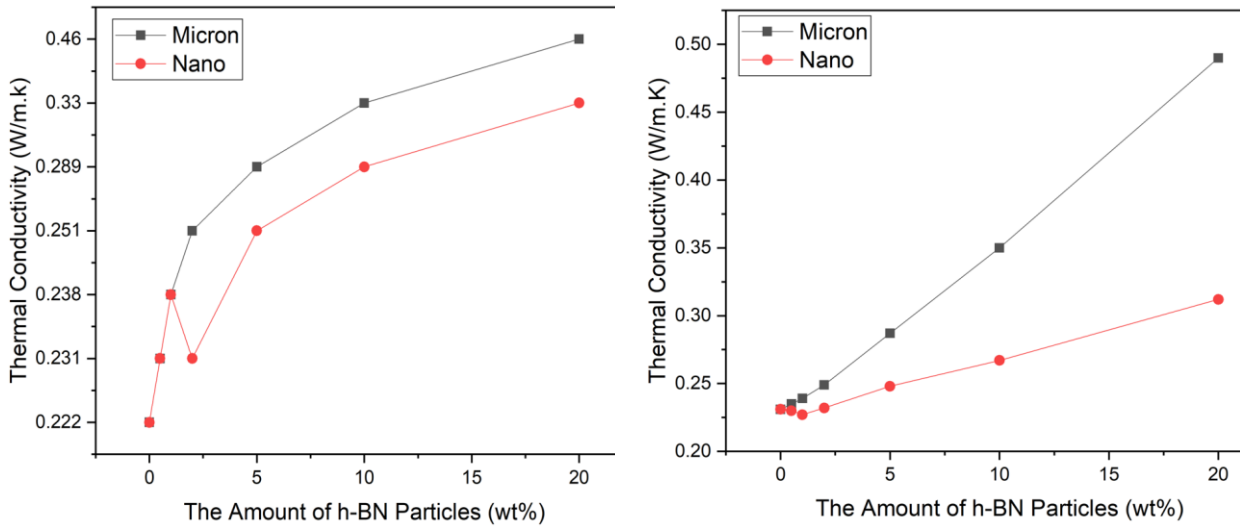

(a) (b)

Figure 2.7 The comparison of thermal conductivity values of the epoxy composites in (a) in-plane and (b) through-thickness directions as a function of particle size and concentration of h-BN.

2.3.4 Fracture surface analysis

SEM images in Figure 8 illustrate the fractured surfaces of the neat epoxy, 10 wt.% micron-sized h-BN reinforced epoxy composites, and 10 wt.% nano-sized h-BN reinforced composites after tensile loading. At different magnifications, Figure 8a and 8b display the fracture surface morphology of the neat epoxy specimen, which has a smooth surface characteristic of brittle fracture, indicating low fracture toughness. Figure 8c and 8d show the fracture surfaces of the 10 wt.% micron-sized h-BN reinforced epoxy composite, which also exhibits a brittle fracture nature and smoother surface compared to neat epoxy due to the inclusion of 10 wt. micron-sized h-BN . As previously mentioned, the composite material containing 10 wt.% micron-sized h-BN is more brittle than the neat epoxy, as confirmed by the SEM analysis. On the other hand, the fracture surface of the 10 wt.% nano-sized h-BN reinforced epoxy composite in Figure. 8e and 8f are significantly rougher than the other specimens. The roughness is correlated with toughening and additional surface formation during the crack mechanisms. The crack deflection, twisting, and tilting lead to the formation of the rough surface area, and this surface morphology points out the

efficient energy dissipation characteristics. Moreover, the uniform roughness of the fracture surface of the 10 wt.% nano-sized h-BN reinforced epoxy composite implies the homogeneous dispersion of h-BN in epoxy without any observable agglomerations and improved interfacial bonding between nano-sized h-BN and epoxy (Zanjani et al., 2016). In Figure 8d, a particular segment of the composite featuring micron h-BN is highlighted, revealing a distribution of the reinforcement phase. The reinforcement phase manifests in hexagonal shapes with a uniform distribution.

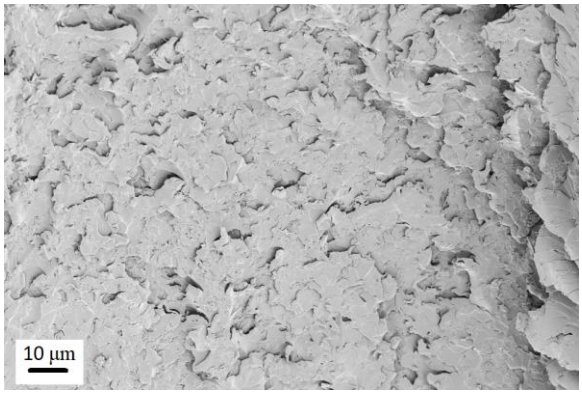

(a)

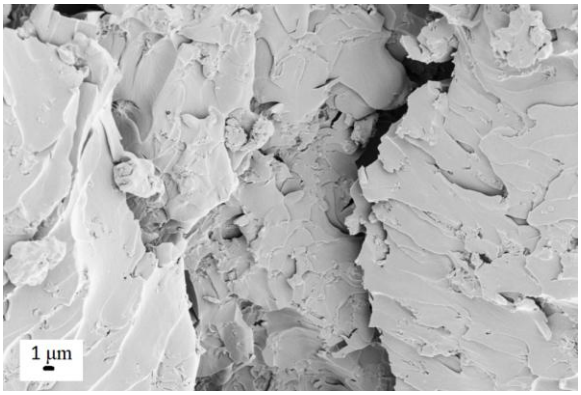

(b)

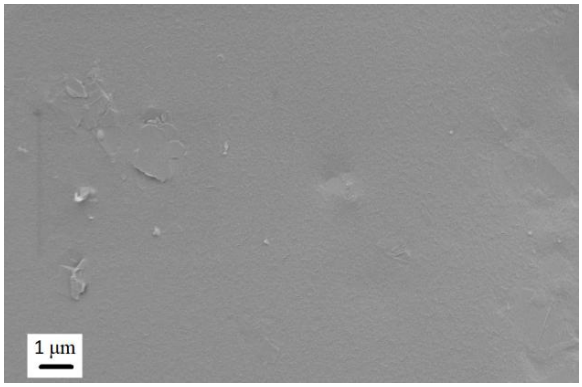

(c)

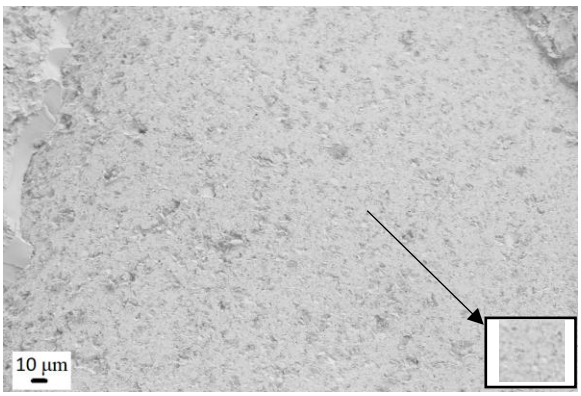

(d)

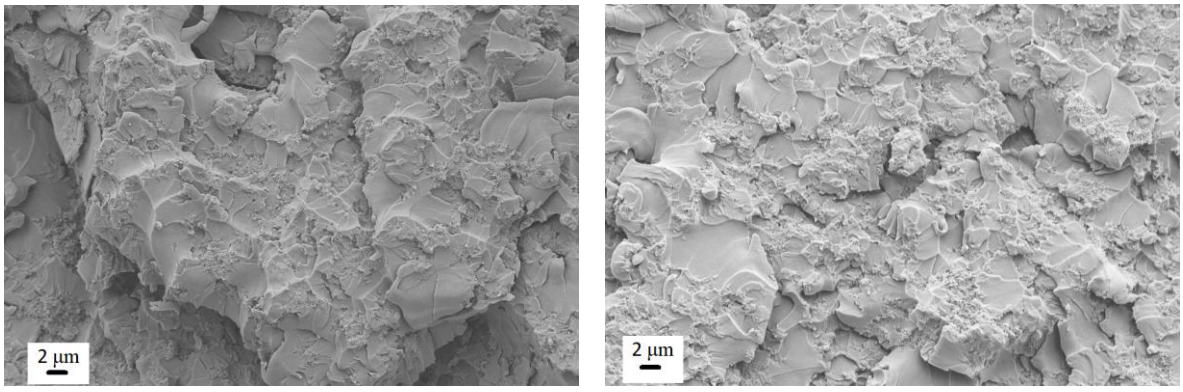

(e) (f)

Figure 2.8 SEM images of the fracture surfaces after tensile test (a,b) neat epoxy (c,d) 10 wt. % micron-sized h-BN reinforced epoxy composite, and (e,f) 10 wt. % nano-sized h-BN reinforced epoxy composites.

2.4 Conclusion

In the present study, thermal conductivity values of h-BN reinforced epoxy composites in in-plane and through-thickness directions are significantly enhanced by providing the incremental loading and tailoring the particle size of h-BN to maintain thermal stability and prevent damage to the composites structure at high filler loadings. A fast, up-scalable, and cost-effective pre-dispersion method is employed to incorporate micron- and nano-sized h-BN in epoxy to obtain a highly dispersed and stable h-BN/epoxy mixture. It is observed that the micron-sized h-BN particles (20 wt. %) were much more effective than nano-sized h-BN particles so that the thermal conductivity of epoxy was enhanced by 107% and 112% in in-plane and through-thickness directions. The tensile and 3-point bending tests are also carried out to determine optimum h-BN size distribution and concentration for better mechanical performance with high thermal conductivity. The epoxy modified with 20 wt. % micron-sized h-BN showed a 47% improvement in tensile modulus, whereas the epoxy contained 10 wt. % micron-sized h-BN provided a 41% improvement in the flexural modulus. In contrast, 20 wt. % nano-sized h-BN concentration improved the tensile and flexural modulus values of epoxy by 16% and 15%, respectively. Furthermore, DMA test results

confirmed that the dispersion of micron- and nano-sized h-BN in a wide weight range did not affect the thermomechanical characteristics of epoxy; thereby, the thermal consistency of epoxy was preserved even at high temperatures. This study of the correlation between particle size and concentration provides fresh perspectives on thermal management in polymer matrix composites employed in structural applications. Serving as a roadmap, this study facilitates the development of innovative designs and adaptable, multi-scale composites with customized functionalities.

Supplementary

The details of the stepwise production route of the micron and nano-sized h-BN reinforced epoxy composites are given in Figure. S1.

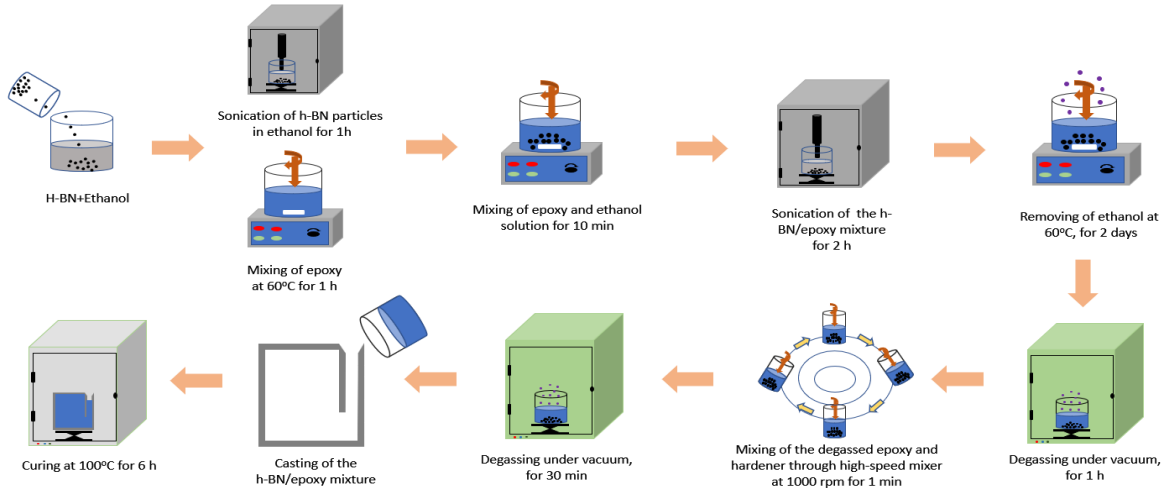

Figure 2.S1 The schematic representation of the fabrication of the micron and nano-sized h-BN reinforced epoxy composites.

Figure 2. S2 exhibits the TGA curves of the neat micron and nano-sized h-BN particles.

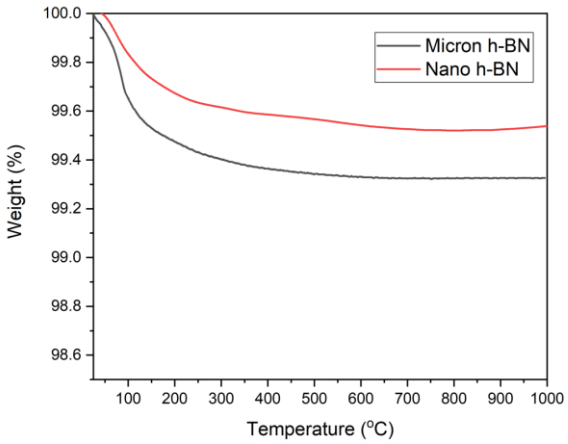

Figure 2.S2 TGA curves of micron and nano-sized h-BN particles

Figure 2.S3 exhibits the Raman spectra of micron and nano-sized h-BN particles.

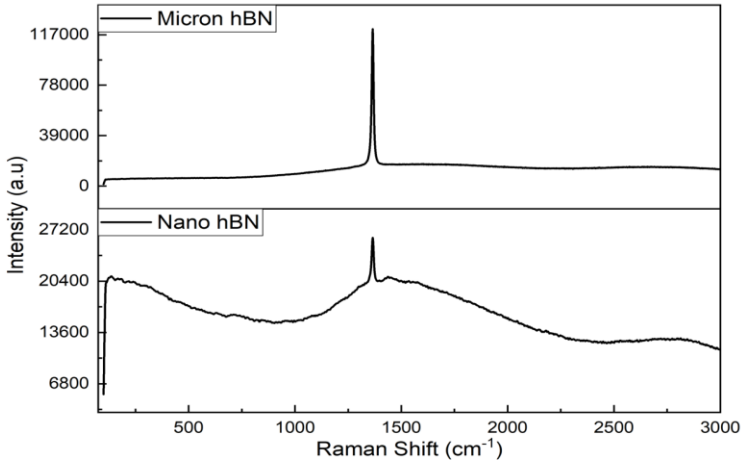

Figure 2.S3 Raman spectra of micron and nano-sized h-BN particles

Figure 2.S4 shows the XPS survey scan spectra of micron and nano-sized h-BN particles.

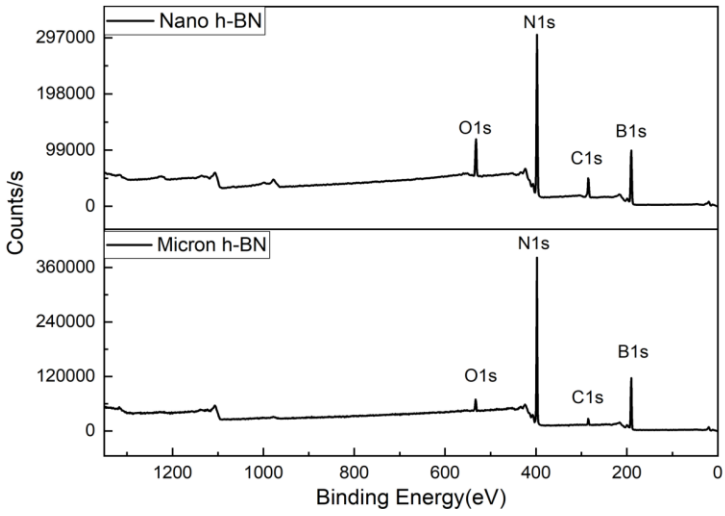

Figure 2.S4 XPS survey scan spectra of micron and nano-sized h-BN particles

Tables S1 and S2 show the tensile strength and modulus values and their improvement percentages of the micron and nano-sized h-BN reinforced epoxy composites as a function of loading ratio, respectively.

Table S.1 Tensile strength and modulus values and their improvement percentages of micron-sized h-BN reinforced epoxy composites as a function of loading ratio.

Sample	**Elastic Modulus (MPa)**	**Improvement (%)**	**Tensile Strength (MPa)**	**Improvement (%)**
Neat epoxy	2985±87	-	81±2.4	-
0.5 wt% m/h-BN+Epoxy	3317±77	11.0	83±6.1	1.6
1.0 wt% m/h-BN+Epoxy	3006±49	0.6	80±0.8	-1.4

2.0 wt% m/h-BN+Epoxy	3122±29	4.6	78±2.5	-4.3
5.0 wt% m/h-BN+Epoxy	3330±33	11.5	75±2.5	-7.5
10.0 wt% m/h-BN+Epoxy	4211±90	41.1	65±5.0	-20.6
20.0 wt% m/h-BN+Epoxy	4387±83	46.9	66±0.9	-18.9

Table 2.S2 Tensile strength and modulus values and their improvement percentages of nano-sized h-BN reinforced epoxy composites as a function of loading ratio

Sample	**Elastic Modulus (MPa)**	**Improvement (%)**	**Tensile Strength (MPa)**	**Improvement (%)**
Neat epoxy	2985±87	-	81±2.4	-
0.5 wt% n/h-BN+Epoxy	3043±61	1.9	84±0.5	2.7
1.0 wt% n/h-BN+Epoxy	2913±23	-2.4	81±0.4	-0.9
2.0 wt% n/h-BN+Epoxy	3039±41	1.8	82±0.2	0.9
5.0 wt% n/h-BN+Epoxy	3111±82	4.2	82±0.2	1.1
10.0 wt% n/h-BN+Epoxy	3175±53	6.3	74±7.3	-9.0

20.0 wt% n/h-BN+Epoxy	3468±30	16.1	78±6.5	-4.5

Tables S3 and S4 demonstrate the flexural modulus and strength values and their improvements of the epoxy composites as a function of loading ratio.

Table 2.S3 Flexural modulus and strength values and their improvements of micron-sized h-BN particles reinforced epoxy composites as a function of loading ratio

Sample	**Flexural modulus (MPa)**	**Improvement (%)**	**Flexural strength (MPa)**	**Improvement (%)**
Neat epoxy	2934±93.8	-	127±2.1	-
0.5 wt% m/h-BN+Epoxy	3241±9.5	10.46	133±0.7	4.72
1.0 wt% m/h-BN+Epoxy	3109±42.4	5.96	128±1.77	0.78
2.0 wt% m/h-BN+Epoxy	3119±19.7	6.31	126±1.03	-0.78
5.0 wt% m/h-BN+Epoxy	3227±11.1	9.98	122±2.49	-3.14
10.0 wt% m/h-BN+Epoxy	4126±47.7	40.62	121±3.01	-4.74
20.0 wt% m/h-BN+Epoxy	3872±83.7	31.95	106±2.30	-16.37

Table 2.S4 Flexural modulus and strength values and their improvements of nano-sized h-BN particles reinforced epoxy composites as a function of loading ratio

Sample	Flexural modulus (MPa)	Improvement (%)	Flexural strength (MPa)	Improvement (%)
Neat epoxy	2934±93.8	-	127±2.1	-
0.5 wt% n/h-BN+Epoxy	3124±39.0	6.47	130±1.15	2.36
1.0 wt% n/h-BN+Epoxy	2959±22.2	0.85	123±0.83	-3.14
2.0 wt% n/h-BN+Epoxy	3065±41.8	4.46	128±1.47	0.78
5.0 wt% n/h-BN+Epoxy	3138±12.8	6.95	127±0.78	0.0
10.0 wt% n/h-BN+Epoxy	3159±39.9	7.67	122±1.25	-3.94
20.0 wt% n/h-BN+Epoxy	3378±52.0	15.13	126±1.08	-0.79

The thermal conductivity values of micron-sized h-BN reinforced epoxy composites in in-plane and through-thickness directions as a function of loading ratio are shown in Table S5 and Table S6.

Table 2.S5 The thermal conductivity of micron-sized h-BN reinforced epoxy composites in in-plane and through-thickness directions as a function of loading ratio

Samples	In-Plane Thermal Conductivity (W/m.K)	Improvement (%)	Through-thickness Thermal Conductivity (W/m.K)	Improvement (%)
Neat Epoxy	0.222	---	0.231	---
0.5 wt% m/h-BN+Epoxy	0.231	4.1	0.235	1.7
1.0 wt% m/h-BN+Epoxy	0.238	7.2	0.239	3.5
2.0 wt% m/h-BN+Epoxy	0.251	13.5	0.249	7.8
5.0 wt% m/h-BN+Epoxy	0.289	30.2	0.287	24.2
10.0 wt% m/h-BN+Epoxy	0.330	48.6	0.350	51.5
20.0 wt% m/h-BN+Epoxy	0.460	107.2	0.490	112.1

Table 2.S6 The thermal conductivity of nano-sized h-BN reinforced epoxy composites in in-plane and through-thickness directions as a function of loading ratio

Samples	In-Plane Thermal Conductivity (W/m.K)	Improvement (%)	Through-thickness Thermal Conductivity (W/m.K)	Improvement (%)
0.5 wt% n/h-BN+Epoxy	0.224	0.9	0.230	-0.4
1.0 wt% n/h-BN+Epoxy	0.223	0.5	0.227	-1.7
2.0 wt% n/h-BN+Epoxy	0.224	0.9	0.232	0.4
5.0 wt% n/h-BN+Epoxy	0.252	13.5	0.248	7.4
10.0 wt% n/h-BN+Epoxy	0.257	15.8	0.267	15.6
20.0 wt% n/h-BN+Epoxy	0.312	40.5	0.312	35.1

Damping ratio, glass transition temperature and storage modulus values of micron- and nano-sized h-BN reinforced composites are presented in Table S7 and Table S8.

Table 2.S7 Damping ratio, glass transition temperature and storage modulus values of micron-sized h-BN reinforced composites

Sample	$tan\delta_{max}$	Glass transition temperature (^oC)	Storage Modulus at 25^oC (MPa)
Neat Epoxy	0.74	120.39	900.1
0.5 wt% m/h-BN+Epoxy	0.85	119.07	989.76
1.0 wt% m/h-BN+Epoxy	0.91	120.39	966.46
2.0 wt% m/h-BN+Epoxy	0.92	121.36	999.85
5.0 wt% m/h-BN+Epoxy	0.84	123.20	1026.16
10.0 wt% m/h-BN+Epoxy	1.36	119.50	1060.33
20.0 wt% m/h-BN+Epoxy	0.77	121.40	1182.31

Table 2.S8 Damping ratio, glass transition temperature (T_g) and storage modulus values of nano-sized h-BN reinforced composites

Sample	**$tan\delta_{max}$**	**T_g (^oC)**	**Storage Modulus at 25^oC (MPa)**
Neat Epoxy	0.74	120.39	900.1
0.5 wt% n/h-BN+Epoxy	0.95	117.84	972.10
1.0 wt% n/h-BN+Epoxy	0.72	115.33	986.76
2.0 wt% n/h-BN+Epoxy	0.92	121.10	953.24
5.0 wt% n/h-BN+Epoxy	0.85	118.29	1067.38
10.0 wt% n/h-BN+Epoxy	0.82	119.20	1057.59
20.0 wt% n/h-BN+Epoxy	0.78	120.70	1133.63

3. ENHANCING DIRECTIONAL THERMAL CONDUCTIVITY IN HEXAGONAL BORON NITRIDE REINFORCED EPOXY COMPOSITES THROUGH ROBUST INTERFACIAL BONDING

Establishing a robust interfacial bond between hexagonal plate shape Boron Nitride (h-BN) and the Epoxy matrix is essential for enhancing heat transfer, which is difficult because of h-BN's low surface energy, tendency to clump together, and the chemical inertness of the epoxy matrix. This research shows different techniques for treating the surface of h-BN fillers by applying acids and thermal processes to activate the surface. The silanization process was used to increase the Silane content on the face of activated h-BN in order to make it more compatible with the epoxy matrix. XPS analysis revealed silicon peaks (Si2s peak at 150.1 eV and Si2p peak at 100.3 eV) in the spectrum of silane-treated samples. Heat treatment resulted in the production of more oxygen molecules on the shell of h-BN compared to the acid treatment. Here, the primary focus was on examining how surface treatment affects thermal conductivity performance in both in-plane and through-through-thickness paths. There was an increase in the epoxy's thermal conductivity perpendicular to the plane, going from 0.21 (W/mK) to 0.47 (W/mK), showing a remarkable 123.8% enhancement by adding 10 wt.% of silane-modified-thermal treated h-BN particles. The improvement resulted from effectively silanizing the exterior boundary of h-BN particles, enhancing connection and distribution in the epoxy medium. Surface modification of h-BN-epoxy composites improves thermal conductivity, leading to better heat conduction in thermal management systems, benefiting industries like aerospace, automotive, and energy systems.

3.1 Review

The growing importance of efficient heat dissipation is largely driven by the ever-increasing energy demands of modern electronic devices, aerospace components, and industrial machinery. As these technologies advance, the need to manage and dissipate heat effectively has become a

critical issue, especially as devices become smaller and more powerful, leading to greater heat generation in confined spaces. In industries such as electronics, where components are packed densely, the inability to efficiently dissipate heat can lead to performance degradation, reduced lifespan, and even device failure. Similarly, in aerospace and industrial machinery, excessive heat buildup can impair functionality, compromise safety, and reduce energy efficiency. Consequently, addressing the challenge of heat dissipation has become a major area of focus for researchers and engineers who are striving to develop energy efficient systems that can handle higher thermal loads. This challenge has spurred significant innovation in the design of materials and composites that can effectively manage heat, leading to advancements in thermal management solutions that are critical for sustaining the performance and reliability of next generation technologies (Moore & Shi, 2014), (X. Zhang et al., 2021).

Epoxy composites are widely preferred in the structural parts, but they suffer limited thermal conductivity around 0.15–0.35 (W/mK). Among several attempts published in the literature published, the thermal conductivity of epoxy composite based is enhanced by underfilling materials like hexagonal boron nitride (h-BN) as a thermally conductive inorganic filler and offers a potential pathway to improve the thermal conductivity of epoxy resins (Gong et al., 2021). Several studies utilize h-BN at different loadings by using it as received or functionalized with different groups in epoxy composite based.

Recently in (Shi et al., 2020), the in-plane thermal conductivity of h-BN/epoxy composites reached a thermal conductivity of 1.2 (W/mK) at filler loading (12 wt.%). One should be aware that the epoxy used in this study inherently possesses an in-plane thermal conductivity of approximately 1 (W/mK). In another study (S. Wang et al., 2022), the application raw and functionalized micron sized h-BN examined. They prepared highly thermally conductive epoxy/h-BN composites with 1.05 (W/mK) increasing five times higher than 0.202 (W/mK) of unfilled epoxy resin. In addition, In (S. Wang et al., 2022), an epoxy/h-BN composite with a significantly enhanced through-plane thermal conductivity of 1.52 (W/mK) at 30 wt.% filler loading of h-BN with an average particle size of 10 μm has prepared, studies indicate that both particle size and filler loading ratio are critical factors in controlling thermal conductivity (in work the average particle size used is 2 μm). Additionally, Li et al. (S. Li et al., 2021) achieved an increase in thermal conductivity, raising it from 0.29 (W/mK) to 0.62 (W/mK), through a series of composites based on polytetradecyl acrylate (PTA) by using a solution-based blending technique involving Boron Nitride (BN) content

changing from 5% to 20%. While raw h-BN boasts high thermal conductivity when used as a filler with moderate loading, various challenges arise, including issues like low flow capability, poor wettability, surface delamination, and escalating costs. Simultaneously, the low wettability of h-BN leads to weak interface bonding with other polymeric materials, resulting in the aggregation of h-BN particles within polymeric matrices (X. Li et al., 2017). Therefore, addressing these challenges involves improving the surface wettability of h-BN through techniques such as chemical functionalization or coating with hydrophilic materials. This approach can enhance compatibility and attachment between h-BN particles and the polymer base.

The surface modification of h-BN holds significant importance in evaluating the maximum loading ratios in epoxy composites. This is a critical consideration as the loading ratio of h-BNs is significantly influenced by structural factors like surface affinity and surface area, directly impacting thermal conductivity. Saher et al. (Gul et al., 2023) with high degree of the alignment of h-BN platelets at 60 wt.% h-BN filler loading reached maximum value of in-plane thermal conductivity 12.45 (W/mK). Various techniques for surface modification of h-BN have been explored in the literature, including chemical and mechanical exfoliation (H. Yi et al., 2022) plasma-arc method, chemical and thermal treatment (Mostovoy et al., 2020), ball-milling treatment, and more. Among these techniques, chemical and thermal treatment processes provide to control the surface characteristics of h-BN structures. For instance, in (Namba et al., 2019), a thermal conductivity of 0.748 (W/mK) in polyimide/boron nitride composites, exhibiting a 4.6-fold increase compared to pure polyimide had been achieved, thanks to the incorporation of 40 wt.% acid-treated micron scale h-BN particles with the typical diameter of particles of 5 μm. In this context, incorporating a substantial quantity of hydroxyl (OH) groups onto the h-BN surface enhances both the bonding capability and adhesion force between h-BN and epoxy. Addressing this issue, Muratov et al. conducted a comparative study of thermal treatment processes and various acid treatment methods to achieve the maximum hydroxyl group coverage on the surface of h-BN particles. Encouragingly, it has been demonstrated that thermal heat treatment is a more environmentally friendly option as it does not involve the use of chemicals during the process. In another investigation, Mostovoy also annealed h-BN particles at 1100 ºC for 1 h, with the incorporation of just 0.05 - 1.0 wt.% h-BN additives into the epoxy with a notable improvement in the thermal conductivity coefficient by 52.0–217%, strength tensile and tensile elastic modulus by 53.0% and 37.0%, respectively. On the other hand, to enhance wettability, achieve uniform

distribution, optimize particle-epoxy interface interactions, and enhance matrix-particle affinity, the silanization process (including amine groups) stands out as one of the most effective surface functionalization methods following the completion of the oxidation process (Ma et al., 2011). After introducing hydroxyl groups onto the face of hexagonal boron nitride (h-BN), it becomes crucial to graft silane molecules onto these groups to establish a strong interfacial connection with an epoxy matrix. The addition of hydroxyl groups creates active sites on the h-BN surface, which can enhance its reactivity. However, to ensure effective bonding with the epoxy resin, these hydroxyl groups need to be further modified by silane molecules. A study by Lee et al (Lee et al., 2019) demonstrated a significant improvement in thermal conductivity, reaching about 0.35 (W/mK) at 10 wt.% h-BN (with the typical diameter of particles 1 μm) for silanized samples incorporated into epoxy. Furthermore, Zhang et al. (S. Zhang et al., 2017) synthesized Boron Nitride (BN) (the average particle size 2 μm) silanized with various silane agents and the surface-modified BN exhibited an exceptional thermal conductivity of 0.686 (W/mK) with a filler fraction of 40 wt.%. Moreover, Seyhan et al. detailed the surface functionalization of boron nitride nanosheets (BNNSs) using the Vinyl-Trimethoxy Silane (VTS) coupling agent incorporated into polypropylene (PP) and demonstrated the highest thermal conductivity values, reaching 0.41 (W/mK) at 5 wt.%. These findings indicate the effectiveness of different surface treatments for enhancing the thermal conductivity of epoxy composites reinforced with BN derivatives. Notably, the maximum heat transfer was achieved in (Xiao et al., 2020b), where the epoxy composites were prepared using 70 wt.% h-BN powders (the average particle size 12 μm) and surface modified with 3-GlycidoxypropyltrimethoxySilane (KBM/403) and 3-ChloropropyltrimethoxySilane (KBM/703), resulting in thermal conductivities of 4.11 and 3.88 (W/mK), respectively, in the comparison to 2.92 (W/mK) for the composite not included silanes at 50 wt.%. The incorporation of silane-modified h-BN particles into epoxy resin stands as a highly effective strategy for significantly enhancing thermal conductivity, offering improved dispersion, enhanced adhesion, and tailored surface properties. Incorporating KBM-403 into the composites effectively hindered stress propagation, leading to improved storage modulus. Specifically, the elastic modulus of the (KBM/403-treated BN) composite surpassed that of the (KBM/03-treated BN) case. Gül et al. [64] further emphasized the importance of careful filler selection in optimizing the overall performance of composite materials. Their research provides crucial insights into the current focus on enhancing adhesive joint performance, underscoring the broader implications of composite engineering.

Additionally, Salunke and Gopalan (Salunke & Gopalan, 2021) provided a comprehensive review of the advancements in boron nitride/epoxy composites, with a particular emphasis on their thermal and electrical behaviors. These properties are especially important for applications within electronic and electrical components, where heat management and conductivity are paramount. Moreover, Jia et al. explored a variety of strategies aimed at optimizing interfacial thermal resistance within thermally conductive polymer composites, offering valuable perspectives on improving the efficiency and functionality of these materials. Their work contributes to a growing body of knowledge on how to enhance the thermal performance of polymer-based composites, which is crucial for their application in high-performance industries.

To conclude, silanization and the attachment of functional group on the surface of h-BN enhance boundary interactions with the chosen polymer but the process and suitable viscosity together with curing time depending on the functionalized h-BN are needed to define to reach repeatable thermal conductivity. Physico-chemical properties of h-BN should link with the epoxy matrix regarding the surface oxygen groups and aspect ratio of the selected particle to attain high thermal conductivity at the optimum loading ratio. To the best of our knowledge, this study showed a pathway starting from chemical treatment to thermal modification by tailoring surface chemistry and providing a high degree of wettability even at 60 wt.% loading of micron sized h-BN in adhesive form. A stepwise functionalization process has been applied to h-BN particles by starting from oxidation to thermal activation to silanization with the integration of extensive silane-based chain groups. Then, epoxy composite manufacturing was carried out by mold casting method to follow a systematic h-BN loading procedure to get homogeneity in the targeted structure. The relation between functional groups and thermal conductivity by highlighting the direction of conductive pathways was explained with comprehensive characterization for the first time.

3.2 Experimental Part

3.2.1 Materials

Hexagonal boron nitride (h-BN) with a particle size of 1-2 μm and 99.5% purity was obtained from Civelek Porselen Company in Turkiye. The silane coupling agent, 3-aminopropyltriethoxysilane (APTES, >98%), was supplied by Sigma-Aldrich. Nitric acid (HNO3, 70%), sulfuric acid (H2SO4, 99%), acetic acid (glacial, 100%), and ethanol (absolute) were purchased from Isolab and used without further purification. A high Tg thermosetting resin system, Sika Biresin® CR131, along with the CH132-5 hardener, was provided by Tekno Chemicals Inc., Turkiye, and was selected for its suitability in infusion applications due to its low viscosity.

3.2.2 Surface functionalization of h-BN particles

Two distinct hydroxylation procedures, one involving chemical modification in an acidic medium and the other thermal modification, were applied to h-BN particles to evaluate differences between the two approaches. These methods were selected for their suitability for mass production, ease of setup, and effectiveness in increasing oxygen content on the surface of h-BN particles. The goal was to create a modified h-BN surface that enhances interaction with silane molecules through covalent bonds. This surface modification improves the chemical bonding and compatibility between h-BN particles and the polymer base, resulting in better dispersion and interfacial adhesion in h-BN composite materials. Initially, the chemical modification of h-BN particles was performed in an acidic medium. Following this, the hydroxylation process was achieved through thermal modification to introduce hydroxyl (-OH) molecules onto the h-BN (N. Yang et al., 2016).

3.2.2.1 Chemical modification of h-BN particles with acid treatment

The surface activation of h-BN was accomplished through a hydroxylation process, which increased the oxygen content on the h-BN surface oxidized. This improvement enhanced the interaction between h-BN particles and silane molecules during silanization. Additionally, exfoliation was performed to enlarge the surface area, promoting stronger interactions between oxygen (O) and silicon (Si) atoms. As a result, this process created a larger and more reactive surface, enabling the formation of stronger and more stable chemical links between the h-BN particles and the silane molecules (Berktas et al., 2021).

In this process, 2 μm-sized h-BN the powder was uniformly distributed in a solution of Sulfuric and Nitric acids in a 3:1 volume ratio. A total of 5.0 g of h-BN was placed in a 500 mL reaction vessel, and 225 mL of H_2SO_4 and 75 mL of HNO_3 were gradually added to the vessel while stirring in an ice bath. The magnetic stirrer was employed for continuous stirring of the mixture and reflux condenser at 50 °C for 24 hours. After this period, the mixture gradually cooled to an ambience temperature, and the acid solution was filtered out. The resulting h-BN was then washed multiple times with distilled water to adjust the pH from strongly acidic to neutral. Finally, the acid-treated hydroxylated h-BN product was subjected to drying in a vacuum oven at 50.0 °C for 24 hours.

3.2.2.2 Thermal modification of h-BN particles with heat treatment

Direct thermal treatment at ambient conditions was used to process h-BN microparticles, offering a scalable alternative for conducting the hydroxylation process. According to the results of this study, this method proved to be the most proficient at introducing hydroxyl (O-H) molecules onto the surface of h-BN particles, outperforming acid treatment. By using high temperatures to facilitate exfoliation, this approach not only reduces production time but also supports the potential for mass production. The combination of high-temperature exfoliation and the addition of OH groups significantly enhance the reactivity and functionality of h-BN particles, making them more suitable for thermal management applications (Ozyigit et al., 2024).

In this procedure, 5.0 g of h-BN powder (Particle Size: 2 μm) was placed in a ceramic crucible and endured to thermal-treatment at 1000 °C for 5 minutes with air exposure. The furnace was brought

to the desired temperature with a heating rate of 5.0 °C/min, then thermal treatment, the furnace was allowed to cool down to room temperature. Once cooled, the thermally treated hydroxylated h-BN was collected from the ceramic crucible.

3.2.3 Silanization process of hydroxylated h-BN particles

Two different hydroxylated h-BN samples were used in the silane modification process: one was prepared through chemical treatment, and the other through thermal treatment. To modify the surface of these hydroxylated h-BN samples, APTES, a silane coupling applied agent, was applied. This agent served as a chemical bridge between the h-BN samples and the silanization reaction, improving the compatibility between the materials (Berktas et al., 2020).

3.2.3.1 Synthesis of silane modified-acid treated h-BN

Surface modification with a silane coupling agent, specifically APTES (3-aminopropyl)-triethoxysilane, was conducted according to a procedure described in the literature (Hou et al., 2014) to augment the interfacial interaction between Epoxy and hydroxylated h-BN particles, thereby enhancing the compatibility and adhesive properties of the h-BN/epoxy composite materials. Through the functionalization of h-BN surfaces, the silane coupling agent facilitates stronger chemical bonding between the filler loaded and the polymer base, ultimately improving the overall performance and thermal conductivity properties of the h-BN/epoxy composites. Silane modification was conducted on 3 g of acid-treated hydroxylated h-BN using a 5 wt.% solution of APTES in h-BN. The mixture was sonicated for 30 min in 120 mL of toluene solution. Following that, the mixture was thereafter brought to reflux at 110 ℃ under a nitrogen atmosphere with magnetic persistently stirring for 8 h. Following cooling to room temperature, the reaction mixture was filtered through a Buchner funnel and thoroughly washed three times with distilled water and ethanol. The silane-modified, acid-treated h-BN was subsequently dried in a vacuum oven at 50°C for 24 h.

3.2.3.2 Synthesis of silane modified-thermal treated h-BN

The silane modification of h-BN microparticles, which already possessed hydroxyl (-OH) groups, was achieved using APTES (3-aminopropyl)-triethoxysilane. In this process, 5.0 g of hydroxylated h-BN were dispersed in 1000 mL of distilled water containing the 5% APTES (v, v) with the aid of an ultrasonic probe sonicator for 15 min. The h-BN suspension was then refluxed at 80 °C in an oil vessel for 4 h. Adding acetic acid was done to bring the pH index of the reaction mixture to 5. After cooling to room temperature, the reaction mixture was filtered and washed twice with distilled water. The silane-modified, thermally treated h-BN was subsequently dehydrated in a vacuum oven at 50 ˚C for 24 hours to eliminate any remaining solvent.

3.2.3.3 The selection of an ideal surface modification process

Table 1 provides a comparative summary of the reaction conditions and yields for both hydroxylation and silanization processes. Initially, successful surface hydroxylation of h-BN was achieved through chemical modification under strongly acidic conditions, yielding favorable results. Additionally, to enhance the efficiency of the hydroxylation process and establish a scalable alternative, direct thermal treatment of raw h-BN was conducted at 1000 °C for 5 min under an air atmosphere. This thermal modification was found to be more environmentally friendly because it did not involve chemical use during the process. Moreover, thermal modification significantly reduced the surface activation time by only 5 min. Notably, the yield of thermally treated h-BN exceeded that of acid-treated h-BN.

Table 3.1 Summary of the synthesis conditions for functionalized h-BN particles.

Sample Name	Silane coupling agent	The ratio of APTES/h-BN (wt.%)	Reaction Medium	Reaction Temperature (°C)	Time (h or min)	Reaction Yield (wt.%)
Acid-treated h-BN	-	-	Strong acid mixture (H_2SO_4+HNO_3)	50	24 h	72
Thermal-treated h-BN	-	-	Air	1000	5 min	95
Silane modified-acid treated h-BN	APTES	1	Toluene	110	8 h	27
Silane modified-thermal treated h-BN	APTES	0.25 to 1	Water	80	4 h	40

3.2.4 Incorporation of functionalized h-BN into epoxy matrix

The fabrication of h-BN reinforced Epoxy base composites involved the use of surface-modified h-BN particles. Specifically, individual mixes were prepared by combining 17.5 g of CR131 epoxy with 1.75 g of each of the following: untreated h-BN, acid-treated hydroxylated h-BN, thermally treated hydroxylated h-BN, silane-modified acid-treated h-BN, and silane-modified thermally treated h-BN to prepare the 10 wt. % loading filler composite samples. After a 30-minute mixing

period, 4.9 g of CH132-5 hardener was introduced into each mixture. The resulting blend was transferred into a pre-heated aluminum mold and then cured in an oven at 100°C for 5 h. Furthermore, composite materials containing a 60 wt.% filler loading of both pristine h-BN and silanized h-BN were fabricated to explore the influence of loading ratio on the interaction forces between the fillers and epoxy, as well as the resulting changes in thermal conductivity. The manufacturing process mirrored that of the 10 wt.% cases, albeit with a higher ratio between filler and epoxy, elevated from 10 wt.% to 60 wt.%. Moreover, varying quantities of silanized h-BN were synthesized for the 60 wt.% loading to probe the optimal silane concentration and enhance the effective adhesion to hydroxylated h-BN. In the 10 wt.% loading case, the ratio of APTES to h-BN was maintained at 1. However, for the 60 wt.% cases, a range of APTES/hydroxylated h-BN ratios were explored, with varying amounts of APTES/hydroxylated h-BN ranging from 0.25 to 1. The outcomes underscored the critical role of adjusting the silane concentration in achieving peak thermal conductivity. Notably, the maximum thermal conductivity was attained at a ratio of 0.5, beyond which thermal conductivity experienced a decline. These findings emphasize the importance of precise control over the silane content to optimize the thermal properties of the h-BN composite materials. Figure 1 provides a visual representation of the hydroxylation and silanization stages in the synthesis pathway of h-BN.

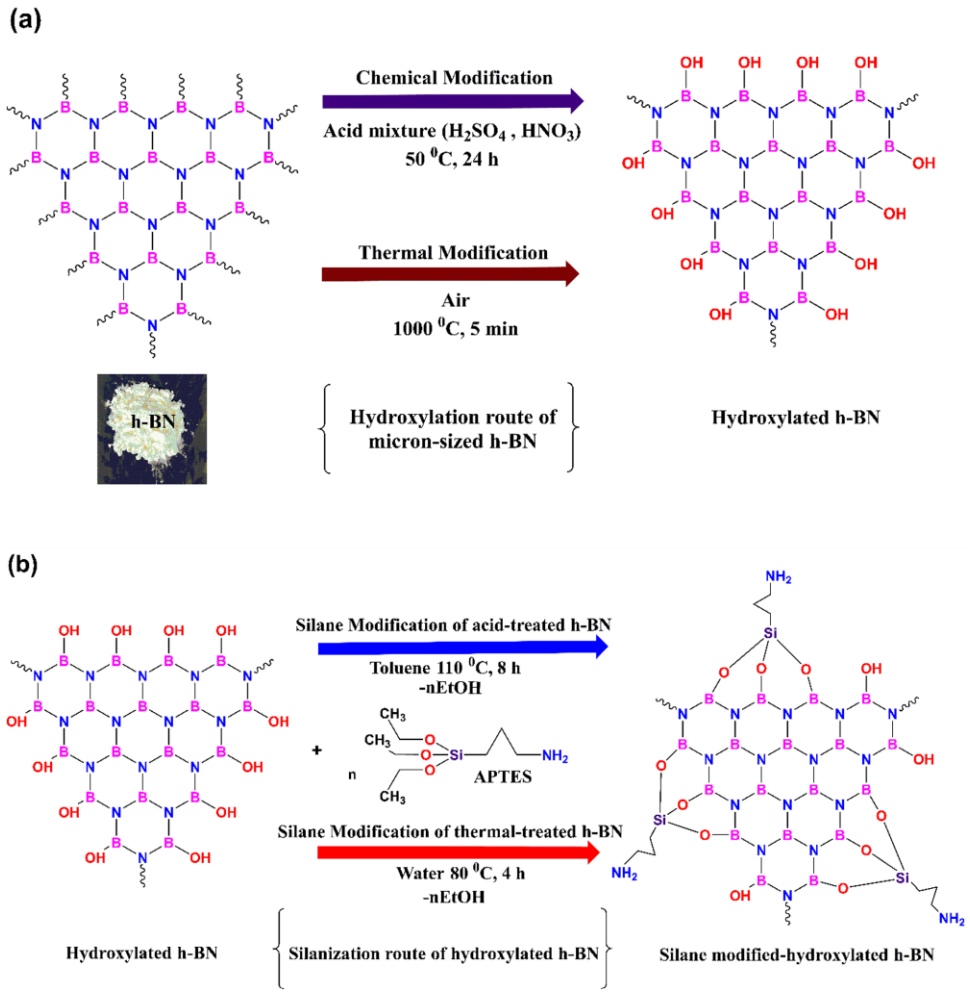

Figure 3.1 Schematic illustration of (a) hydroxylation and (b) silanization processes of h-BN.

3.2.5 Characterization

Functionalized h-BN particles were thoroughly analyzed using a combination of spectroscopic and gravimetric characterization methods. Fourier transform infrared spectroscopy (FT-IR) was conducted to identify functional groups and provided crucial insights into the surface modifications of h-BN. The appearance or disappearance of peaks, corresponding to spectral data of stretching and bending vibrations in the FT-IR, supported the proposed structural changes. FT-IR spectra were collected using an ATR-equipped spectrometer, covering the range of 4000–650 cm^{-1} to detect active groups on the h-BN surface. Additionally, Raman spectroscopy was conducted to investigate the molecular structure and vibrational characteristics of micron-sized h-

BN particles. A Renishaw in Via Reflex-Raman/Microscope, equipped with a 532 nm edge laser, was utilized at room temperature to scan the data range of 100–3500 cm^{-1}.

Thermogravimetric analysis (TGA) was performed with the aid of a Mettler-Toledo TGA/DSC 3+ thermal analyzer, where the samples were heated with a progression of 10 K/min from 25°C to 1000°C under a 50 mL/min O_2 flow to assess thermal stability. Surface morphologies were evaluated using a Leo-Supra/35VP Field Emission Scanning Electron Microscope (FE-SEM). For crystallinity and structural analysis, X-ray diffraction (XRD) was performed using a Bruker-D2/Phaser instrument with a CuKα radiation source, scanning the range of $2\theta = 5°$ to 55°, to identify characteristic h-BN peaks post-functionalization. The Thermo Scientific K-Alpha was employed to determine the chemical and elemental compositions of the modified h-BN microparticles by using X-ray photoelectron spectroscopy (XPS). Furthermore, the thermal conductivity (TC) of the h-BN filler reinforced into epoxy composites were measured using the hot-disc method with a TPS-2500/S device, assessing both in-plane and through-thickness thermal conductivity. Detailed methods for calculating TC values can be accessed in the supplementary document.

3.3 Results and Discussion

3.3.1 Structural Characterization of surface-functionalized h-BN particles

Analyzing the structure of surface-functionalized h-BN particles involves a comprehensive understanding of variations in the h-BN/epoxy material's composition, morphology, and properties of the material following surface modification, which can be used for different kinds of composite systems, such as filler-matrix and multilayered structures. Surface functionalization often involves the introduction of new chemical groups onto the surface of h-BN particles. In this context, Figure 2a shows comparative FTIR spectra data of micron-sized h-BN and surface-functionalized h-BN particles. First, the stretching and bending vibration peaks of h-BN were determined to define its structure of h-BN before the modification process. It exhibited two characteristic peaks: a broad absorption peak around 1307 cm^{-1} belonging to B (Boron)-N (Nitrogen) stretching, and at 763

cm^{-1} belonging to B-N-B bending. In the following XPS section, the results will show that h-BN particles parallel have B and N atoms, and the surface of the particles is occupied with Oxygen and Carbon (C). The amount of them, especially for O is low showing neat micron h-BN particles reacted with the atmosphere and carry O and C. After chemical and thermal modification of h-BN, a new stretching vibration peak at 3197 cm^{-1} belonging to B-OH stretching and 841 cm^{-1} belonging N-O stretching were determined in FT-IR spectra as well characteristic absorption peaks of h-BN. Moreover, the B-OH stretching peak had a high intensity over the period of the thermal-treatment of micron h-BN. This peak confirms the presence evidence of hydroxyl groups on the surface of h-BN during the hydroxylation. These B-OH bonds are formed as crystalline structures on the surface of h-BN confirmed by XRD results shown in Figure 2b. In the succeeding stage, the silanization process on the surface of hydroxylated BN particles showed absorption peaks at 2961 cm^{-1} and 2804 cm^{-1} which correspond to the asymmetric/symmetric stretching of molecules of CH_2 groups, and at 1101 cm^{-1} and 1023 cm^{-1} which are related to Si-O-Si in the silane molecule, respectively. The intensity peak of the Si-O-Si stretching of silane modified-thermal treated was much stronger than that of silane modified-acid treated h-BN. Also, these results indicated that the silanization of thermal-treated h-BN proved efficient treatment than the silanization of acid-treated h-BN particles since the chemical formation of B-OH and Si-O bonds at the molecule structure of h-BN was verified successfully in the thermal treated sample.

To verify this verification, XRD analysis was completed to identify the crystalline phase and determine the crystallite size of the synthesized particles. The XRD peak patterns of h-BN and surface-functionalized h-BN particles are shown in Figure 2b. All h-BN derivatives have similar XRD patterns except for thermal-treated h-BN and each XRD pattern showed that the sharp and intense peak at 2θ (degree)=26.60º (002) corresponds to the crystallographic/plane of the h-BN graphitic structure. The weaker intensity peaks in XRD patterns correspond to 2θ=41.55º (100), 43.63º (101), 49.87º (102) and 54.89º (004), respectively. On the other hand, the XRD pattern of thermal-treated h-BN revealed a new peak at 2θ=27.55º (010) for (Boric acid) H_3BO_3. The new peak corresponding to H3BO3 diffraction is the formation of B-OH covalently grafted on the surface of h-BN. This phenomenon emerges after the acid treatment of h-BN due to process conditions at low temperatures and inhibited decomposition of h-BN. Subsequently, boric acid is likely to form during the decomposition and exfoliation of h-BN at temperatures as high as 1000 ºC. In response to the attachment of the APTES molecule to the surface of hydroxylated h-BN, Si-

O bonds were formed, and the boric acid peak disappeared. The same peak groups that are like neat micron h-BN were detected because of the amorphous structure of the silane molecule in the XRD pattern. In addition, the degree of crystallinity and amorphous phase calculated by X-ray peak diffractions are shown in Table S1. Remarkably, the highest crystallinity was achieved by thermal treated h-BN particles, and the changes in XRD peaks were complementary to the peaks defined in FTIR.

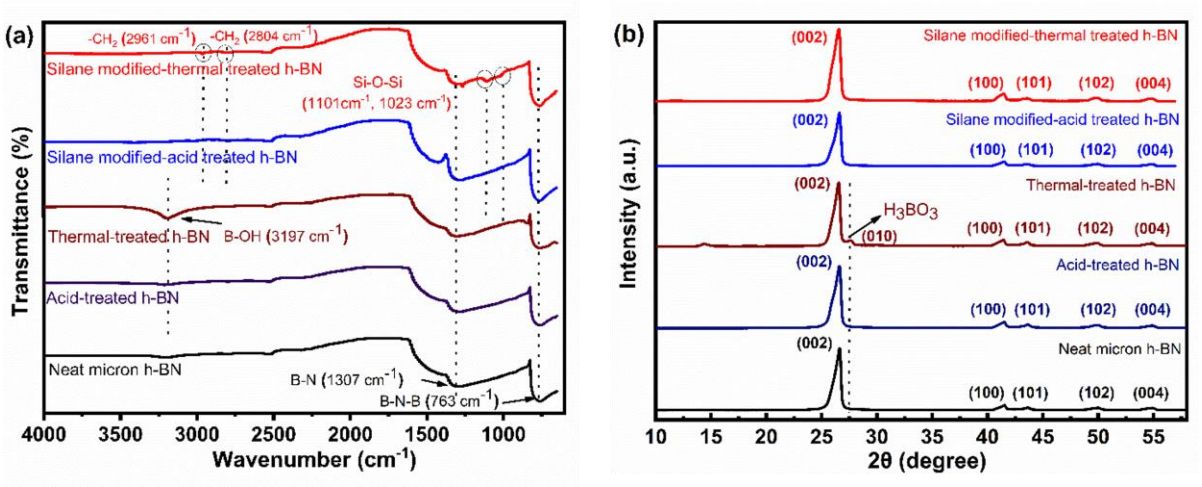

Figure 3.2 (a) FT-IR spectra and (b) XRD patterns of neat h-BN, acid-treated h-BN, thermal-treated h-BN, silane modified-acid treated h-BN, and silane modified-thermal treated h-BN samples.

During this research, XPS was applied to explore the bonding and chemical composition of h-BN, with hydroxylation and silanization processes and XPS spectra data of pure micron h-BN, h-BN treated with acid, h-BN treated thermally, h-BN modified with silane after acid treatment, and h-BN modified with silane after thermal treatment conducted in Figure 3. The elemental compositions of h-BN and modified h-BN particles can be found in Table S2. The wide-scan XPS spectrum of h-BN validated its chemical compositions as 70.94 %(N), 16.44 %(B), 4.08 %(O), and 8.55 %(C), respectively. The oxygen level rose from 4.08% to 15.83% due to the attachment of hydroxyl molecules groups to the B atoms at the edges of h-BN through thermal processing. O1s analyses of hydroxylated h-BN revealed the manifestation of Boron-OH bonds peaks closing to 531.9 eV and 531.6 eV during each hydroxylation stage. Following silanization, the presence of APTES molecule on the acid-treated h-BN led to a decrease in oxygen percentage from 15.83%

to 3.63%. Moreover, the nitrogen percentage in h-BN modified with acid and APTES rose from 46.24% to 53.43%. Additionally, the XPS spectrum showed successful attachment of the modification to the surface through the bonding of the APTES silane coupling agent onto the acid-treated h-BN particles, with Si2s peak at 150.1 eV and Si2p peak at 100.3 eV, as depicted in Figure. 3. During heating of h-BN particles, the O1s and C1s peaks grew stronger while the B1s and N1s peaks weakened, showing that oxygen and carbon were successfully incorporated onto the surface of the particles. Table 2 summarizes the specific bonds corresponding to the binding energies of h-BN and functionalized h-BN particles.

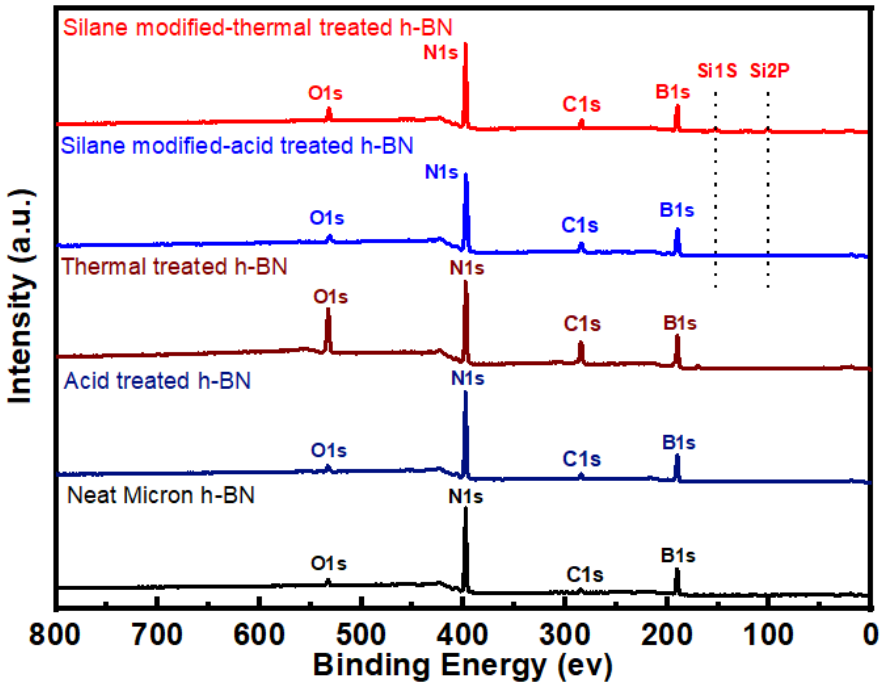

Figure 3.3 XPS survey scan spectra of neat h-BN, acid-treated h-BN, thermal-treated h-BN, silane modified-acid treated h-BN and silane modified-thermal treated h-BN.

Table 3.2 The specific bonds correspond to the binding energies of micron-sized h-BN and functionalized h-BN particles.

Sample Name	N1s(eV)/ Bond type		B1s(eV)/ Bond type		O1s(eV)/ Bond type		C1s(eV)/ Bond type		Si2p(eV)/ Bond type	
h-BN	397.7	N-B N-C	189.6	B-N	531.6	B-O C-O O-H	284.5	C-C C=C	-	Si-C Si-O
Acid-treated h-BN	397.7		189.6		531.9		284.5		-	
Thermal-treated h-BN	397.3		189.1		531.6		284.5		-	
Silane modified-acid treated h-BN	397.2		189.8		531.0		284.5		100.3	
Silane modified-thermal treated h-BN	397.4		189.8		531.0		284.5		100.2	

The thermogravimetric analysis (TGA) curves of neat h-BN, acid-treated h-BN, thermal-treated h-BN, silane-modified acid-treated h-BN, and silane-modified thermal-treated h-BN are presented in Figure 4 to examine the effects of surface modification on h-BN and assess its thermal stability. The TGA results, summarized in Table 3, provide key thermal data including the starting decomposition temperatures (T_{on}) and the highest observed decomposition temperatures (T_{dm}) and the percentage of remaining substance at 1000˚C. The observed weight decreasing done in the temperature ranges of 308.9˚C–506.8˚C for neat h-BN, 209.8˚C–425.5˚C for acid-treated h-BN, 101.7˚C–163.0˚C for thermal-treated h-BN, 333.5˚C–473.4˚C for silane-modified acid-treated h-BN, and 289.3˚C–461.1˚C for silane-modified thermal-treated h-BN. Upon comparing the thermal stabilities of the surface-modified h-BN derivatives, it was found that acid-treated h-BN and

silane-modified acid-treated h-BN exhibited higher thermal stability than the thermal-treated and silane-modified thermal-treated counterparts.

It is also important to clarify that in this study, thermal stability refers to the extent to which a material's weight changes with increasing temperature. The thermal stability of a material is an indicator of its ability to withstand high temperatures without undergoing significant decomposition or chemical change. As depicted in Figure 4, both the acid-treated h-BN and the silane-modified acid-treated h-BN exhibit remarkable thermal stability. These materials do not experience any significant weight loss or gain as the temperature increases, indicating their resistance to thermal degradation. The absence of weight change suggests that these surface-modified h-BN derivatives maintain their structural integrity and composition even at elevated temperatures, making them suitable for applications where high thermal stability is crucial. On the other hand, thermal-treated h-BN lost only 6.7 % of its weight during O2 flow due to its hydroxyl groups which are 13.67 wt. % of oxygen abundance on surface hydroxylated h-BN. The observed thermal behavior indicates that micron-sized h-BN retains its thermal stability even after surface modification, demonstrating high thermal resistance up to 1000 ˚C. Besides, the grafting of silane molecules onto the hydroxylated h-BN structure did not adversely affect its thermal stability.

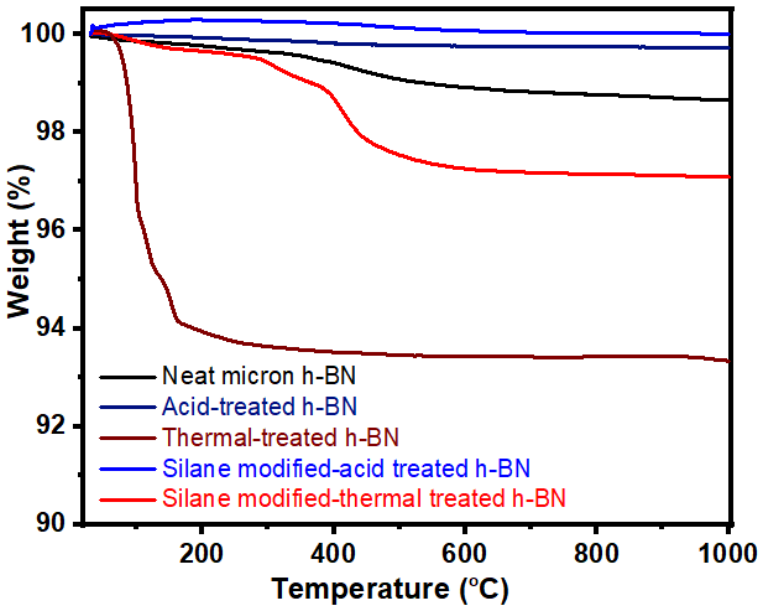

Figure 3.4 TGA curves of neat h-BN, acid-treated h-BN, thermal-treated h-BN, silane modified-acid treated h-BN, and silane modified-thermal treated h-BN

Table 3.3 TGA results of h-BN and functionalized h-BN particles.

Sample Name	TGA (˚C)		Remaining substance amounts at 1000 ˚C (%)
	T_{on}	T_{dm}	
h-BN	308.9	506.8	98.64
Acid-treated h-BN	209.8	425.5	99.73
Thermal-treated h-BN	101.7	163.0	93.30
Silane modified-acid treated h-BN	333.5	473.4	99.98
Silane modified-thermal treated h-BN	289.3	461.1	97.10

T_{on}: On-set temperature, starting to decomposition changes.

T_{dm}: Highest observed decomposition temperatures.

In addition to the mentioned characterization techniques, Raman spectra of the neat h-BN, acid-treated h-BN, thermal-treated h-BN, silane modified-acid treated h-BN and silane modified-thermal treated h-BN as shown in Figure S1 (refer to supporting Info) depicted the Raman-active high energy phonon peak at 1365 cm-1 correlated with B-N vibration mode. Notably, there was no significant shift observed in the B-N vibration mode following the surface modification process of h-BN.

3.3.2 Surface Morphology Analysis of functionalized h-BN fillers

The dispersion behavior and effectiveness of reinforcing materials within a polymer matrix are primarily governed by their surface morphology and chemical properties. Achieving optimal dispersion and strong interfacial interactions is essential, as these factors significantly influence the overall effectiveness characteristics of the composite h-BN/Epoxy materials. In this study, the impact of the silanization process on the morphology of micron hexagonal boron nitride (h-BN) particles was assessed using scanning electron microscopy (SEM). Various treatment and

modification methods were employed to enhance the surface chemistry and morphology of the h-BN particles, with the goal of improving their performance in composite applications.

As depicted in Figure 5(a), the untreated (neat) h-BN particles exhibit a flake-like morphology, with varying diameter-to-length ratios. Additionally, these particles tend to agglomerate and display smooth surfaces, primarily due to the absence of surface functional groups. However, Figure 5 further illustrates that the morphology of the h-BN particles can be tuned through specific surface treatment techniques. For instance, as shown in Figure 5(b), the acidic treatment did not significantly alter the size or overall morphology of the h-BN particles, though a slight exfoliation effect was observed. Moreover, the surface of the acid-treated particles appeared smoother compared to the untreated ones.

On the other hand, after heat treatment, the h-BN particles experienced agglomeration, as evidenced in Figure 5(c). This observation aligns with the X-ray diffraction (XRD) results, which suggest that the increased surface energy stemming from the reduced particle size—contributes to this agglomeration. Additionally, the lack of a suitable dispersing medium exacerbates this effect, leading to clustering of the particles. Figure 5(d) demonstrates that following the silanization process applied to the acid-treated particles, the overall morphology remained consistent, retaining a layered structure. This indicates that silanization does not drastically alter the surface morphology post-acid treatment.

In contrast, Figure 5(e) highlights the lamellar structure of APTES (3-aminopropyltriethoxysilane)-heat-treated h-BN particles. After the silanization process, the lamellae reduced in size, but the layered structure remained intact. The APTES molecules facilitated separation between the h-BN sheets, contributing to a more distinct and dispersed morphology.

In summary, the SEM analysis, as demonstrated in Figure 5, confirms that the exfoliation and morphology modification of h-BN flakes can be effectively controlled through chemical and thermal treatments. Importantly, these processes did not lead to destructive changes in the flake structure, which is essential for maintaining h-BN's exfoliation behavior in epoxy matrices. Therefore, the preparation of an intercalated structure in the composite manufacturing process is considered important to facilitate heat conduction between the platelet structures.

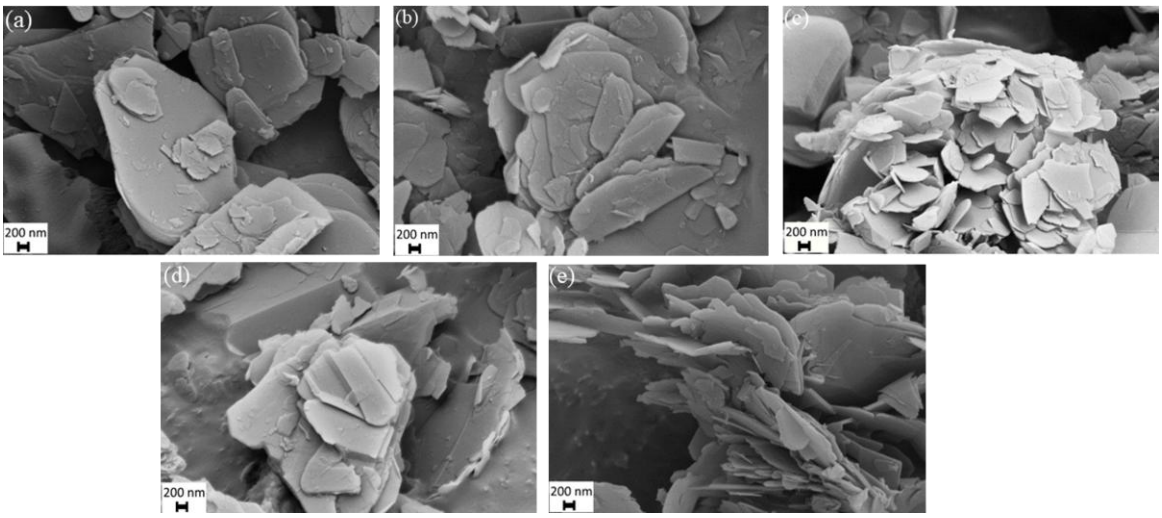

Figure 3.5 FE-SEM images of (a) h-BN, (b) acid-treated h-BN, (c) thermal-treated h-BN, (d) silane modified-acid treated h-BN, (e) silane modified-thermal treated h-BN.

3.3.3 Thermal Conductivity Analysis

Thermal conductivity is an essential characteristic that explains how well a material can conduct heat. Experimental methods and calculations are used to analyze the efficiency of a material in conducting thermal energy. The equation for calculating thermal conductivity in a solid with scattering centers under a thermal gradient can be expressed as the Boltzmann equation given below (Gaonkar & Vaidya, 2020), (Omini & Sparavigna, 1997):

$$\mathrm{TC} = \frac{8l_1 \emptyset_0^{1.5}}{9\pi^2\sqrt{2}h_1^2 \mathrm{TM}^{0.5}} 2\int_0^1 y^2 \frac{\partial \omega_\mathrm{T}}{\partial y} \omega_\mathrm{T} \frac{e^{\eta\omega_\mathrm{T}}}{[e^{\eta\omega_\mathrm{T}}-1]^2} \xi_\mathrm{T}(y)dy \int_0^1 y^2 \frac{\partial \omega_\mathrm{L}}{\partial y} \omega_\mathrm{l} \frac{e^{\eta\omega_\mathrm{l}}}{[e^{\eta\omega_\mathrm{l}}-1]^2} \xi_\mathrm{y}(y)dy$$

With consideration:

$$l_1 = Q_D h_1, \eta = \frac{\hbar}{k_B T h_1} \sqrt{\left(\frac{\emptyset_0}{2M}\right)}$$

Q_D is the value of the radius of the Debye/sphere index, h_1 is the nearest neighbor distance, and M is the nominal mass M of the reticular centers, T is temperature, $\emptyset_0$ is the energy in units of the pair potential U is measured based on y, which is a dimensionless parameter related to the distance between particles centers and k_B is the Boltzmann constant.

By considering $\omega_T = \omega_L = y$ and $\xi_T(y) = \xi_y(y) = 1$, we can reach to following equation:

$$TC = \frac{8l_1 \emptyset_0^{1.5}}{9\pi^2\sqrt{2}h_1^2 TM^{0.5}} \times 3e^{\eta} \int_0^1 y^3 \frac{e^y}{[e^{\eta y} - 1]^2} dy$$

According to equation this last equation, thermal conductivity is related to M which determines the rate of scattering centers, consequently with increasing the vacancies through composite, thermal conductivity is decreasing. Through thickness and in-plane thermal conductivity were measured for the four different functionalized h-BN fillers at 10 wt.% loading ratios in epoxy compared to neat h-BN filled epoxy are presented in comparative manner in Figure 6 (a). The neat epoxy showed 0.21 (W/mK), and for the composite containing neat h-BN, out-plane thermal conductivity was increased to 0.34 (W/mK). TC value did not change for acid-treated h-BN samples and silane-modified acid-treated h-BN. At the same time, the TC value did not alter (0.36 W/mK) for the composite filled loading with thermally treated h-BN, compared to the composite prepared from neat micron h-BN. However, TC was enhanced and reached 0.47 (W/mK) for silane-modified thermal treated h-BN, which is higher than the reported value reported in the literature published (W. Wang et al., 2022). Silanization based on XPS results can increase Si2p peak to 3.5% and silane molecules on the surface of h-BN particles can fill vacancies between particles and epoxy interfaces and silane molecules are like a bridge through particles and matrix. Based on equation (2), decreasing vacancies between particles and the epoxy, and improving the interface connectivity of h-BN particles to the epoxy resin which directly decreases M and affects the thermal conductivity, and in-plane and through-plane TC are increased. All the composites increased in-plane and through-plane TC related to neat epoxy. In this way, in-plane TC improved about 42.8% by adding neat h-BN to the composite. In other cases, for instance, silane modified thermal treated h-BN, in-plane TC increased 34.7% and reached 0.31 (W/mK) at the loading ratio of 10wt %. To provide further clarification, Figure. 6(b) presents a schematic representation of heat transfer within h-BN/epoxy composites, illustrating the impact of various interfaces on thermal conduction. This diagram helps visualize how the inclusion of different types of hexagonal boron nitride (h-BN) fillers affects the thermal conductivity of the composite material. As shown in the Figure, when neat h-BN is incorporated into the epoxy matrix, phonons quasiparticles representing the quantized modes of vibrations that carry thermal energy can effectively reach the h-BN particles. Due to the inherently high thermal conductivity of h-BN, these phonons can travel

more efficiently through the composite, leading to an overall increase in thermal conductivity. The high thermal conductivity of h-BN is attributed to its unique hexagonal lattice structure, which facilitates rapid phonon transport. In the case of silanized h-BN, the addition of silane molecules, specifically those with an APTES (3-aminopropyltriethoxysilane) structure, plays a crucial role in modifying the interface between the h-BN particles and the epoxy matrix and decreasing M. The silane molecules act as molecular bridges, enhancing the interfacial bonding between h-BN and the polymer matrix. These bridges help to improve mechanical wave phonon conduction through the interface by reducing thermal boundary resistance. This more efficient phonon movement further increases the thermal conductivity of the h-BN/epoxy composites, as it allows for a more continuous pathway for heat flow. Overall, the schematic in Figure 6(b) demonstrates how the reinforcement with both neat and silanized h-BN leads to improved thermal properties of the composites, emphasizing the importance of interface engineering in optimizing the thermal efficiency of polymer-based composite materials.

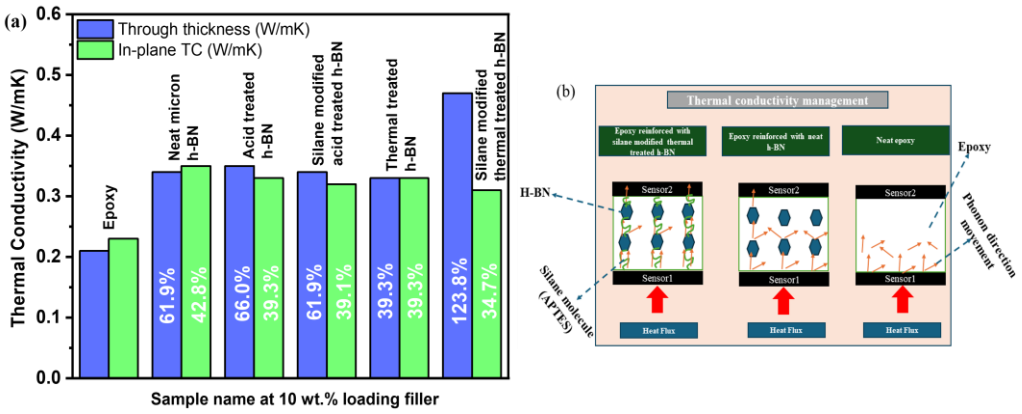

Figure 3.6 (a) Experimental results of through-thickness and in-plane thermal conductivity values of h-BN/epoxy composites with 10 wt.% loading filler, (b) a schematic revealing the effects of various interfaces on heat conduction of the composites.

FE-SEM is used to analyze the surface morphologies of both pure epoxy and h-BN/epoxy composites containing 10 wt.%, with the resulting images shown in Figure 7. As anticipated, the neat epoxy displayed a noticeably smooth surface with some gaps, as depicted in Figure 7a, which can be credited to the lack of any extra substances. Figure 7b shows that adding micron-sized h-BN to the epoxy resin interrupted the flow, causing untreated h-BN particles to clump together

and increasing the rate of hole formation. The inclusion of acid-treated h-BN particles, as shown in Figure 7c, caused some unevenness in the composites, but reduced the rate of hole formation compared to using untreated h-BN. In the composite with heat-treated h-BN (shown in Figure 7d), there was a notable decrease in epoxy vacancies related to flow. Nevertheless, the most significant enhancement was seen in the APTES-treated h-BN/epoxy composite (Figure 7e), resulting in a more condensed structure with reduced inhomogeneity and vacancies. The silane-treated h-BN powders, thanks to an enhanced interface with the epoxy resin, achieved superior dispersion in the epoxy, resulting in decreased voids. This enhanced distribution, along with the lack of non-uniformity and empty spaces, can greatly increase thermal conductivity by decreasing obstacles for phonon movement and promoting easier phonon mobility within the composite. As a result, adding APTES-treated h-BN enhances both the structural integrity and thermal management capabilities of the composite, showing potential for use in applications that need effective heat dissipation.

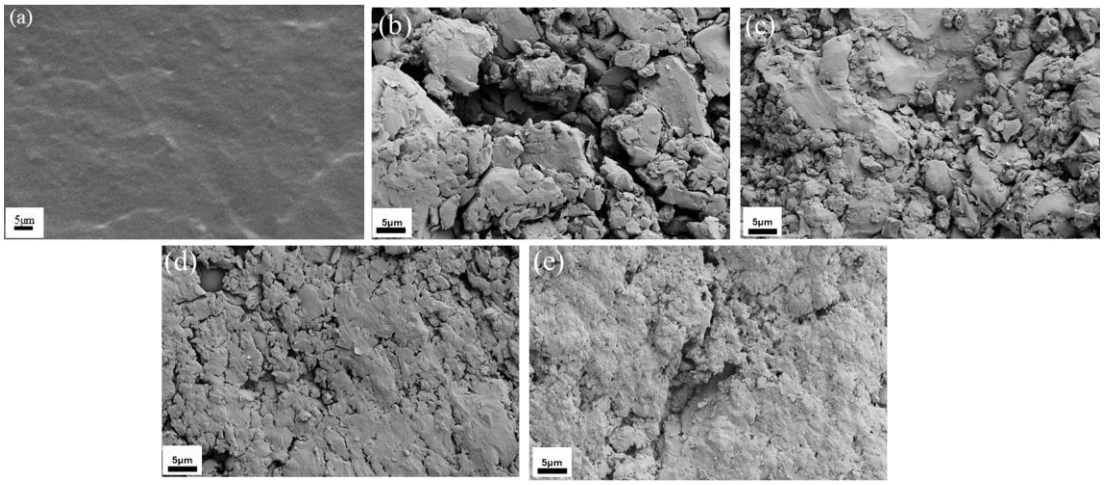

Figure 3.7 FE-SEM images of the (a) neat epoxy and h-BN/epoxy composites contain 10 wt.% (b) micron-sized h-BN, (c) acid treated h-BN d) thermal-treated h-BN, (e) silane modified-thermal treated h-BN.

After that the definition of suitable method, silane modified thermal treated h-BN fillers was selected to reach the highest loading ratio up to 60 wt.% to make an epoxy paste. The in-plane thermal conductivity (TC) was analyzed for composites containing 60% filler with different numbers of silanes and their results are presented in Figure 8. The thermal conductivity of neat

epoxy increased to 1.4 (W/mK) after the addition of 60 wt.% h-BN filler. In the case of samples with Silane/thermal treated h-BN (0.5:1), TC showed an increase, reaching a maximum value of 1.7 (W/mK). This represents a remarkable increase of 709%. However, for composites with 60 wt.% Silane/thermal treated h-BN (0.75:1), TC decreased to 1.5 (W/mK) compared to the optimum value and further decreased to 1.2 (W/mK) for fillers with Silane/thermal treated h-BN (1:1). The remarkable optimum TC value of 1.7 (W/mK) observed in this study surpasses findings from other sources.

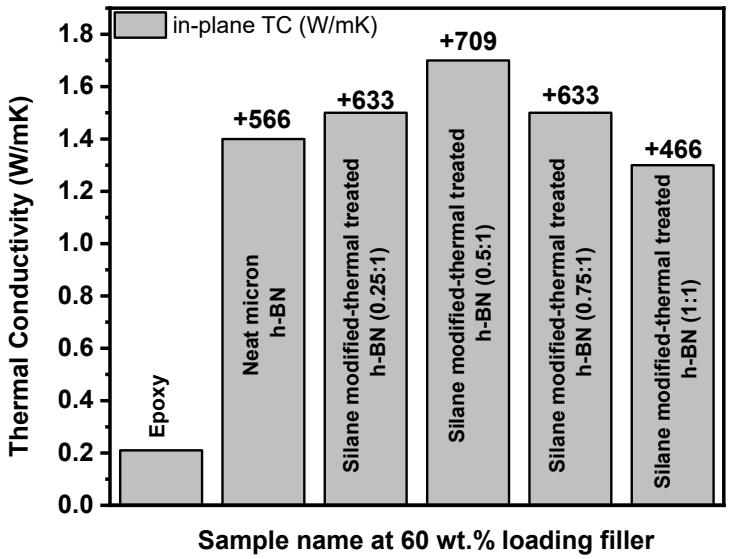

Figure 3.8 Comparing in-plane thermal conductivity results of neat h-BN with silanized samples with 60 wt.% content loading.

The surface morphology of the modified h-BN/epoxy composite with a 60 wt.% filler loading is analyzed using FE-SEM, with images are displayed in Figure 9 at various magnifications. Figure 9a to 9c illustrate the incorporation of silane/thermal treated h-BN at a ratio of 0.5:1, identified as the optimal condition for maximizing thermal conductivity. The images reveal a packed structure formed within the composite, which facilitates phonon movement through the material, thereby enhancing its thermal conductivity. This detailed structural analysis underscores the effectiveness of the silane/thermal treatment in improving the composite's thermal properties.

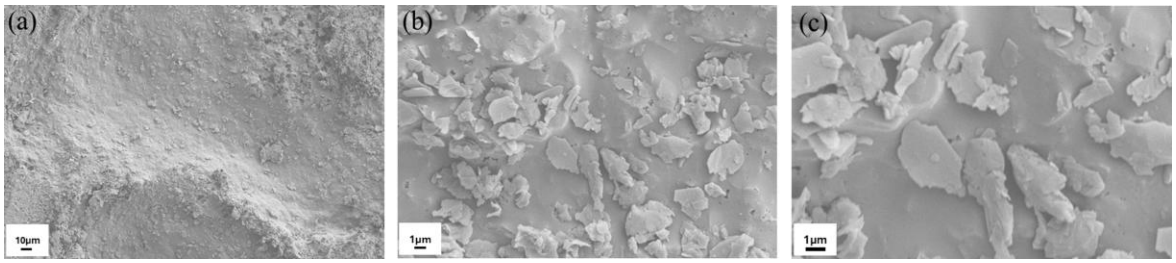

Figure 3.9 FE-SEM images of the composites contain 60 wt.% filler silane/thermal treated h-BN (0.5:1) /epoxy at different magnification of (a) 1000, (b) 10K and (c) 20K.

To sum up, Table 4 provides a thorough summary of the results. This table shows the differences in oxygen content, silicon content, crystallinity, weight loss at 1000 ˚C, and in-plane thermal conductivity depending on the fillers and loading ratios used. The data shows that both the filler type and the loading ratio have a significant impact on the properties of the composite. In thermal management applications, it is essential to adjust these factors in order to enhance the effectiveness of h-BN composites. In particular, the treatment of hexagonal boron nitride (h-BN) with silane had a significant effect on the thermal conductivity characteristics of the composites created in this research. Through the process of silanization, the introduction of silane molecules altered the structure and bonding properties of h-BN combined with epoxy, resulting in an improved interfacial thermal conductivity between the two materials and promoting more efficient heat transfer at the interface. Moreover, phonon scattering within the composite materials was decreased by the silanization process. Phonons, the main conductors of heat in non-metallic materials, usually disperse at boundaries and flaws, reducing thermal conduction. Silanization decreased phonon scattering by enhancing bonding and reducing defects, resulting in improved thermal conductivity of the composite. Table 4 presents useful information on how various combinations impact the performance of the material, helping choose the best filler type and loading ratio for certain uses. By precisely fine-tuning these factors, the thermal conductivity and overall efficiency of h-BN composites can be improved, making them better suited for utilization in different thermal management situations. This optimization is crucial for creating high-performance composites that satisfy the strict criteria of modern thermal management systems.

Table 3.4 A detailed overview of the findings of h-BN reinforce composite properties.

Filler Name	The loading ratio of h-BN /epoxy(wt. %)	Oxygen content (at %)	Silicon content (at %)	Crystallinity (%)	Weight loss at 1000 ˚C (%)	In-plane thermal conductivity (W/mK)
Pristine h-BN	10	4.08	0	70.1	1.3	0.34
Acid treated h-BN	10	5.72	0	61.1	0.2	0.35
Thermal treated h-BN	10	13.67	0	72.2	6.7	0.33
Silane/acid treated h-BN	10	3.63	1.18	69.3	0.01	0.35
Silane/thermal treated h-BN	10	5.40	3.50	71.2	2.9	0.47
Silane/thermal treated h-BN	60	5.40	3.50	71.2	2.9	1.70

3.4 Conclusions

Epoxy composites are commonly employed in different sectors because of their outstanding mechanical characteristics; nonetheless, they frequently display inadequate thermal conductivity. On the other hand, micron hexagonal boron nitride (h-BN) exhibits high thermal conductivity, which suggests it could be a valuable ingredient for improving the thermal efficiency of epoxy composites. Surface modification techniques have been used to enhance the compatibility and adhesion of h-BN with the Epoxy matrix.

Heating h-BN results in the addition of hydroxyl groups, increasing the oxygen level from 4.08% to 13.67%, whereas exposure to acid further boosts it to 15.83%. These changes on the surface improve the bonding between h-BN and epoxy. Moreover, silane coupling agents, like APTES, are employed to establish chemical connections between the two substances. Following silanization, the acid-treated h-BN surface exhibited a reduction in oxygen content from 15.83% to 3.63%, confirming the efficacy of the silanization procedure. Likewise, heating h-BN resulted in lowered oxygen levels and a rise in silane content (3.50%), indicating that treating with silane not only decreases oxygen content but also adds functional groups that enhance bonding with the epoxy matrix. The research points out substantial advancements in directional thermal conductivity. Thermally treated h-BN reinforced epoxy composites modified with silane showed enhanced through-plane thermal conductivity from 0.21 (W/mK) to 0.47 (W/mK), and in-plane conductivity from 0.21 W/mK to 0.31 W/mK, with a 10 wt.% filler loading. Additionally, when incorporating a 60 wt.% h-BN filler, the thermal conductivity of pure epoxy significantly jumped from 0.31 W/mK to 1.4 W/mK. These findings are vital for sectors like electronics, aerospace, and automotive, where enhanced heat dispersion and specific thermal attributes in composite materials are necessary.

Supplementary

Table 3.S1 Crystallinity and amorphous degrees of functionalized h-BN particles derived from the XRD characterization.

Sample Name	Crystallinity (%)	Amorphous (%)
h-BN	70.1	29.9
Acid-treated h-BN	61.1	38.9
Thermal-treated h-BN	72.2	27.8
Silane modified-acid treated h-BN	69.3	30.7

Silane modified-thermal treated h-BN	71.2	28.8

Table 3.S2 The elemental composition of h-BN and functionalized h-BN particles.

Sample Name	**N (at %)**	**B (at %)**	**O (at %)**	**C (at %)**	**Si (at %)**
h-BN	70.94	16.44	4.08	8.55	-
Acid-treated h-BN	45.85	35.55	5.72	12.88	-
Thermal-treated h-BN	31.18	38.50	13.67	16.65	-
Silane modified-acid treated h-BN	53.43	28.55	3.63	13.20	1.18
Silane modified-thermal treated h-BN	38.96	42.84	5.40	9.30	3.50

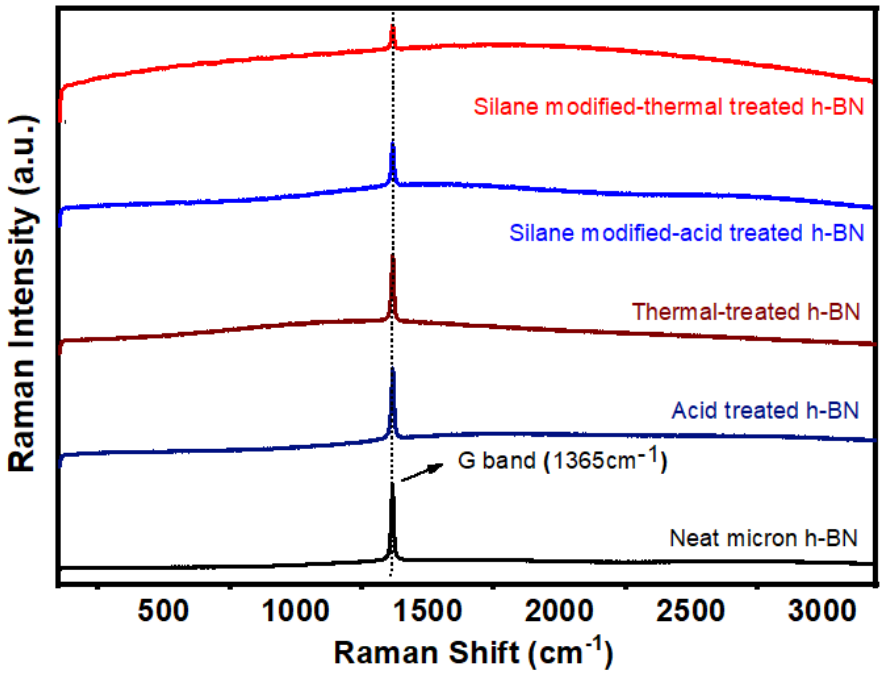

Figure 3.S1 Raman spectra of neat micron h-BN, acid-treated h-BN, thermal-treated h-BN, silane modified-acid treated h-BN and silane modified-thermal treated h-BN.

4. EXPERIMENTAL VALIDATION AND NUMERICAL MODELING OF INTERFACIAL EFFECTS IN SILANIZED HEXAGONAL BORON NITRIDE (H-BN) REINFORCED EPOXY COMPOSITES BY TAILORING SILANE CONCENTRATION

This study investigates the use of h-BN particles as fillers, focusing on tailoring surface chemistry to enhance the thermal conductivity of epoxy composites. By enriching the interface between h-BN particles with amino-silane groups and the epoxy matrix through controlled surface modification, thermal performance, and interfacial bonding were improved. To achieve a high degree of functionalization, h-BN particles were oxygenated to 13.6 atomic percent (at. %) through thermal treatment, followed by reduction using 3-amino-propyl-3-ethoxy-silane (APTES), which increased the amino content by 3.5% at. % under optimized reaction conditions. During composite manufacturing, 10 wt.% functionalized h-BN particles were reinforced into the epoxy matrix, increasing bulk thermal conductivity by 53%, from 0.2 W/mK to 0.34 W/mK. Heat flux simulations with ANSYS confirmed the interface interactions and thermal performance, with silanized h-BN achieving the highest heat flux of 70 W/mm², aligning well with experimental results. While silanization improved thermal conductivity by strengthening interfacial bonding between h-BN and the epoxy matrix, it introduced brittleness, making the composites stiffer and more fragile. However, the silanized h-BN composite showed a 57.14% increase in toughness compared to neat h-BN, while the highest flexural modulus of 4126 MPa was achieved with neat h-BN.

4.1 Review

Electronic devices are integral to modern life, yet overheating can severely damage components like circuits and capacitors. Prolonged heat exposure leads to issues such as short circuits, micro-cracks, and structural deformation, ultimately impairing device performance (Kasirer & Meir, 2022). Efficient heat transfer away from the device is crucial to ensure safe dissipation into the

environment. High-thermal-conductivity materials play a vital role in this process, facilitating direct and effective heat conduction, making them well-suited for electronic applications.

Polymer composites with excellent thermal conductivity are increasingly utilized to enhance heat dissipation in thermal management applications. In polymers, heat is primarily transferred by phonons, which are collective vibrations within the ordered atomic or molecular structures of condensed matter (Purohit & Satapathy, 2016). However, phonons encounter scattering mechanisms such as Umklapp phonon-phonon scattering, phonon-impurity scattering, phonon-electron scattering, and phonon-boundary scattering, which hinder heat transfer. Due to their high porosity, polymers typically exhibit low thermal conductivity (~0.2 W/mK), limiting their effectiveness in thermal management. Adding boron nitride (BN) significantly improves thermal conductivity, as its hexagonal lattice structure and strong B–N bonds enable efficient phonon transport along the basal plane. With an intrinsic thermal conductivity of 250–300 W/mK, BN is an ideal filler for enhancing the thermal performance of polymers in advanced applications (Yuan et al., 2019). Incorporating hexagonal boron nitride (h-BN) into polymers like epoxy has shown promising results in improving thermal conductivity. However, interfacial boundary scattering between h-BN and the epoxy matrix can limit the overall thermal conductivity. To address this, various surface modification methods for h-BN have been explored, including chemical and mechanical exfoliation (Park et al., 2018), plasma-arc techniques, chemical and thermal treatments, and ball-milling. Among these methods, silanization has emerged as a precise and effective surface modification method, enhancing the compatibility and interaction between h-BN and polymer matrices by improving thermal and mechanical properties through three key applications: bonding organic resins with silanized fillers, using silane coupling agents as coatings, and treating surfaces for enhanced adhesion and resistance to environmental factors. Wie et al. demonstrated that h-BN modified with polysilazane (PSZ) and aminopropyltriethoxysilane (APTES) achieved a thermal conductivity of 11.8 W/mK at 75 wt. % filler loading. Similarly, Liu et al. synthesized a dual matrix composite of carbon and h-BN, achieving enhanced flexural strength and improved thermal performance through a silanization process (F. Liu et al., 2021). Seyhan et al. functionalized the surface of boron nitride nanosheets (BNNSs) using vinyl-trimethoxy silane (VTS). The maximum thermal conductivity achieved was 0.35 W/mK for the silanized sample at a 10 wt. % filler loading (Seyhan et al., 2017). Other studies have further highlighted the role of silanization in improving thermal conductivity, such as Seyhan et al.'s work

on vinyl-trimethoxy silane (VTS) functionalized BNNSs in polypropylene (Seyhan et al., 2017). Lee et al.'s integration of silanized h-BN into an epoxy matrix (Lee et al., 2019). Furthermore, Yongbo et al. functionalized h-BN nanosheets (BNNS) using 3-aminopropyltriethoxysilane (APTES) to prepare an A-BNNS/epoxy resin (EPN) coating. With the addition of 15 wt. % A-BNNS, the composite achieved optimal coating performance, reaching a thermal conductivity of 0.64 W/mK. Mehdipour et al. (Mehdipour et al., 2025) highlighted the benefits of silane-modified h-BN, achieving a 123.8% increase in through-plane thermal conductivity with 10 wt. % loading, emphasizing the importance of robust interfacial bonding. These findings underline the need for optimizing h-BN size, surface treatments, and loading ratios to balance thermal and mechanical properties. Seokgyu et al. modified hexagonal boron nitride (h-BN) using aminopropyl triethoxysilane (APTES) through a casting method. With 10 wt. % of APTES-treated h-BN, the composite achieved a thermal conductivity of 0.28 W/mK.

Composite manufacturing processes also significantly influence thermal conductivity. Techniques such as vacuum degassing during mixing and curing eliminate air pockets, enhancing material homogeneity and thermal performance. The vacuum casting method has been shown to be a direct and effective approach for producing high-thermal-conductivity composites, utilizing vacuum pressure to eliminate air from the mold, ensuring precise material shaping and making it particularly well-suited for casting plastics and rubber components with intricate designs and high accuracy. Hongda et al. demonstrated that incorporating h-BN nanoflakes into epoxy resin via vacuum casting achieved a thermal conductivity of 0.29 W/mK at 10 wt. % filler loading (H. Yang et al., 2019). Incorporating additional materials, such as nanocellulose fibers (CNF), has further enhanced composite thermal conductivity. In addition, theoretical models and simulation tools, like ANSYS software, complement experimental studies by providing insights into the factors influencing thermal conductivity, such as h-BN size, orientation, and interfacial thermal resistance. Yingying et al. highlighted the importance of such simulations in predicting and optimizing the performance of h-BN/polymer composites (Sun et al., 2020). Priyabrat et al. investigated the impact of particle size on the mechanical and thermal properties of teak wood dust (TWD)-reinforced polyester composites, presenting both experimental and simulation results. Additionally, in another study, they fabricated composites by incorporating varying amounts of aluminum oxide and pine wood dust into polyester resin, also including simulated analyses (Pradhan et al., 2025). In all these studies, a strong correlation was observed between the

experimental and simulated results, demonstrating the reliability and consistency of the findings. Consequently, these studies highlight the importance of incorporating simulation models alongside experimental tests, as they reveal a gap between theoretical explanations and supporting experimental data for neat or modified h-BN incorporated into polymeric matrices like epoxy, where theoretical models often lack sufficient experimental validation detail.

In the current study, the effects of varying silanization rates using 3-Aminopropyltriethoxysilane (APTES) molecules were explored to determine the optimal surface treatment for h-BN particles and evaluate their impact on the thermal and mechanical performance of epoxy composites, supported by theoretical validation. A key innovation of this work lies in its focus on the silanization process combined with vacuum degassing to enhance composite fabrication. H-BN particles are silanized at different ratios and incorporated into epoxy under vacuum conditions with filler loadings of 5, 10, and 20 wt. %. The vacuum degassing process eliminates air pockets, ensuring precise particle integration and improved material homogeneity. Under optimal silanization conditions, thermal conductivity is expected to achieve its maximum potential. ANSYS software simulations are employed to visualize the effects of surface modification on heat flux transfer between the epoxy matrix and h-BN particles, providing valuable insights into how silanization alters interfacial interactions and enhances heat dissipation. By introducing a novel 15-minute silanization method and optimizing manufacturing through vacuum degassing, this study offers a comprehensive pathway to unlocking the potential of filler-matrix composites for advanced thermal management applications. The findings emphasize the synergy between surface treatment and composite design, bridging theoretical and practical advancements in this field.

4.2 Materials and Methods

4.2.1 Materials

Micron-sized hexagonal boron nitride (h-BN) with a purity of 99.5 %, a particle size distribution ranging from 10 to 20 micrometers, a bulk density between 0.25 and 0.35 g/cm^3, crystal sizes measuring 4 to 7 nm, and a total oxygen content less than 0.5 %, was sourced from BORTEK Co.

(Turkiye). Ethanol (>99.9 %), acetic acid (>99.9 %), 3-Aminopropyl triethoxysilane (APTES), and hexane (>99 %) were obtained from ISOLAB Co. All chemicals were used as received without further purification. Epoxy (Biresin-CR131) and hardener (Biresin CH132-5) were employed for the composite component.

4.2.2 Surface activation of h-BN and functional additive development routes

In our previous studies, hydroxyl groups were introduced onto the surface of h-BN and graphene through different activation methods to prepare the materials for the silanization process. In the current study, after heat activation to oxidize the surface of h-BN, an additional functional group was attached via silanization to improve interfacial interactions by bridging the matrix and reinforcement. For this, 30 g of neat h-BN were placed in an electric furnace and heat-treated at 1000 °C for 5 min with a heating rate of 5 °C/min, followed by cooling in the furnace. Next, 30 g of the heat-activated h-BN were dispersed in 300 mL of a hexane-APTES solution with varying APTES ratios (95–x) using an ultrasonic homogenizer for 10 min, where x represents the volume of APTES (in mL) per gram of heat activated h-BN. The tested APTES ratios were 0.25, 0.50, 0.75, and 1, denoted as silane modified-h-BN (x:1). The suspension was stirred with a magnetic stirrer at room temperature for 10 min, followed by the addition of 15 drops of acetic acid and further stirring for 5 min. The resulting mixture was filtered and washed twice with water, then dried at 80 °C for 1 h. Notably, the h-BN modification in this work took only 1.5 h to yield the final compound, a significant improvement in efficiency compared to other methods in the literature.

4.2.3 Neat h-BN or modified h-BN reinforced epoxy composite production

Initially, 250 g of ethanol was mixed with the filler, either neat h-BN or Silane modified-h-BN (x:1) and sonicated for 2 h to ensure uniform dispersion. In the next step, 350 g of epoxy was heated to 60°C. Once the sonication was complete, the filler-ethanol mixture was added to the epoxy and stirred for 48 h at 50 °C to facilitate the evaporation of ethanol. After the evaporation

process, degassing was conducted for 60 min to remove any trapped air bubbles and ensure a homogenous mixture. After that, 98 g of hardener was incorporated into the epoxy-filler mixture and stirred thoroughly before undergoing another round of degassing for 30 min. This step is crucial for enhancing the mechanical properties of the final composite by eliminating voids. Subsequently, the prepared mixture was poured into molds and cured at 100 °C for 5 h to achieve optimal cross-linking and strengthen the composite structure. Throughout this process, composite fillers were incorporated at varying weight percentages of 5 %, 10 %, and 20 %. A schematic representation of the processes involved in creating the h-BN/epoxy composite is illustrated in Figure 1. Additionally, the compositions of the specimens are summarized in Supplementary File Table S.1, providing a detailed overview of the ratios and types of materials used in each formulation. This comprehensive approach aims to optimize the thermal and mechanical properties of the resulting composites for various applications.

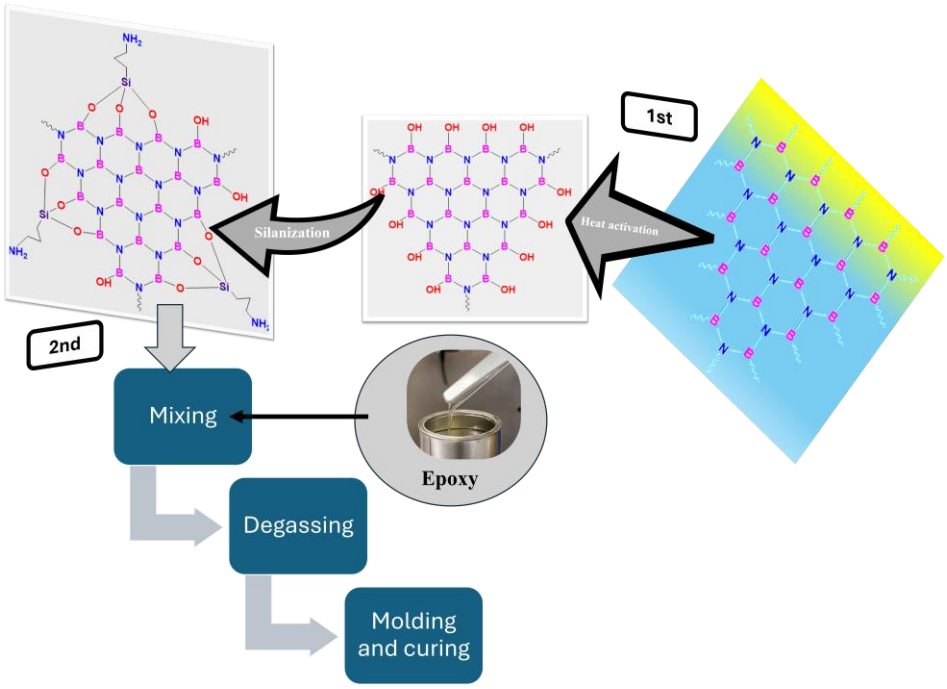

Figure 4.1 A schematic representation of manufacturing neat h-BN and silanized h-BN epoxy composites.

4.2.4 Characterization

Fourier transform infrared (FTIR) spectra were recorded using an IS10 FT-IR spectrometer. Thermogravimetric analysis (TGA) was conducted with a Mettler Toledo thermal analyzer (TGA/DSC 3+) at a heating rate of 10 K/min, covering a temperature range from 25 °C to 1000 °C in a nitrogen atmosphere. To assess the crystallinity of the samples, X-ray diffraction (XRD) analysis was performed with a Bruker D2 PHASER Desktop instrument, utilizing CuKα radiation over a 2θ range of 5 ° to 80 °. The Thermo Scientific K-Alpha was employed to determine the chemical and elemental compositions of the modified h-BN microparticles by using X-ray photoelectron spectroscopy (XPS). Surface morphologies were examined using a Leo Supra 35VP Field Emission Scanning Electron Microscope (FE-SEM). Thermal conductivity (TC) measurements were conducted using a Hot Disk C02-12. The elastic modulus and tensile strength of the composites were determined following ASTM D638 standards, with a knife-edge extensometer used to record extension data during testing at a cross-head speed of 2 mm/min. Flexural properties were evaluated through three-point bending tests in accordance with ASTM D790, maintaining a span-to-thickness ratio of 16:1. Additionally, samples measuring 65 x 10 x 4 mm were subjected to Dynamic Mechanical Analysis (DMA) using a Mettler Toledo DMA device. The testing was performed in single cantilever mode at a heating rate of 3 °C/min, a frequency of 1 Hz, and a temperature range of 25 to 250 °C. A minimum of five specimens from each group were tested to ensure reliable results.

4.3 Results and Discussion

4.3.1 Chemical characteristics of functional h-BN particles

In the intimal part, oxygenation and reduction of h-BN particles were carried out to provide a high degree of exfoliation in the epoxy matrix by making bridges with amine groups of the epoxy. In the stepwise procedure, heat activation was applied under an oxygen environment to provide a high degree of oxygen groups on the h-BN surface and then APTES groups were attached to the

activated groups. Different APTES ratios were applied to reach a high degree of silane content by monitoring spectroscopic and gravimetric methods. To examine the surface characteristics of h-BN particles before and after functionalization, FTIR is applied to identify the chemical bonds and functional groups. The FTIR spectra for various samples, including neat h-BN, heat-activated h-BN, and silane-modified h-BN (x:1) at different ratios, are presented in Figure 2. In the FTIR analysis, a prominent absorption peak at 1321 cm^{-1} corresponds to the in-plane covalent B–N stretching vibration of raw boron nitride (BN). Additionally, the peak observed around 775 cm^{-1} is indicative of the B–N–B out-of-plane bending vibration, while the peak at approximately 1500 cm^{-1} is associated with N–H vibration, which is often observed in nitrogen-containing compounds. The FTIR spectra of heat-activated h-BN confirmed the presence of O–H groups and N–O bonds, as evidenced by the peaks at 3220 cm^{-1} and 841 cm^{-1}, respectively. These peaks suggest that surface modifications have occurred due to heat treatment. In samples silanized at a ratio of x = 0.25, a minimal siloxane peak is observed, indicating the initial incorporation of silane molecules. As the silanization ratio increases, the O–H group peak diminishes, and the intensity of the siloxane peak increases. This trend suggests effective silanization of the h-BN surface, with a clear siloxane peak remaining prominent up to an optimum silanization level of x = 0.25. Notably, the intensity of the Si–O peak observed in this study surpasses that reported in previous literature, indicating a more successful modification process. Overall, these findings illustrate the effectiveness of silanization in enhancing the properties of h-BN, providing insights into the structural changes that occur during surface modification (L. Yang et al., 2020).

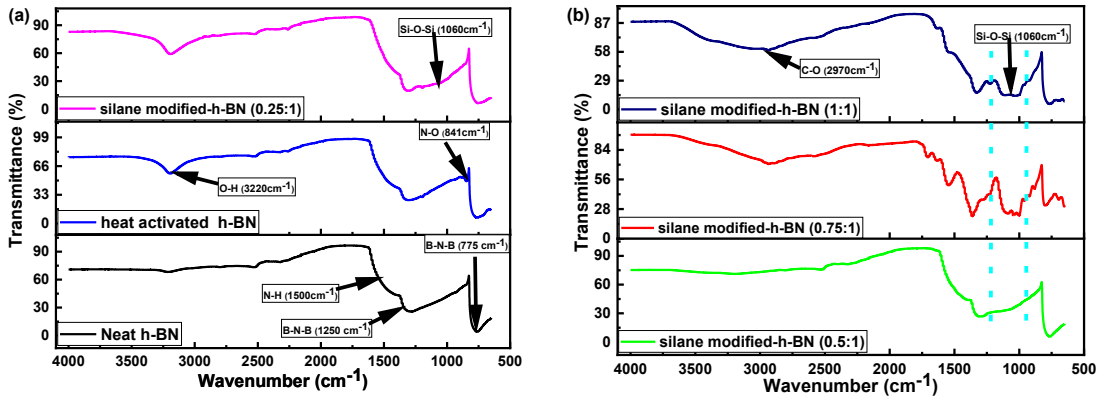

Figure 4.2 FTIR spectra (a) comparison of neat h-BN, heat activated h-BN and silane modified-h-BN (0.25:1=silane amount: h-BN), b) comparison of Silane modified-h-BN (0.5:1), Silane modified-h-BN (0.75:1) and Silane modified-h-BN (1:1) samples by increasing silane.

To further validate the findings, X-ray diffraction (XRD) analysis was conducted to identify the crystalline phases and determine the crystallite size of the synthesized particles. The XRD patterns reveal distinct peaks associated with the (002), (100), (101), (102), (004), and (110) planes, which are characteristic of the hexagonal crystal structure of boron nitride. These peaks are illustrated in Figure S1a of the supplementary document. The heat treatment process notably altered the crystal structure of the neat h-BN. In particular, new peaks corresponding to the (100), (111), and (105) planes emerged, indicating the formation of a new compound, $B(OH)_3$. Overall, the XRD results corroborate the modifications observed in the FTIR analysis, providing a comprehensive understanding of the structural changes that occur during the synthesis and treatment of h-BN. This detailed characterization underscores the significance of thermal processing in tailoring the properties of boron nitride for various applications in composite materials. In the silane modified-h-BN (0.25:1) sample, distinct peaks associated with $B(OH)_3$ were observed following the silanization process. However, these peaks exhibited lower intensity compared to those found in the heat-activated h-BN, which aligns well with the findings from the FTIR analysis. This reduction in peak intensity suggests that while silanization allows for some retention of the $B(OH)_3$ phase, the incorporation of silane molecules may be competing with the boron tri hydroxide for structural space or bonding sites. As illustrated in Figure S1b, when silanization is carried out at a higher ratio, the peaks corresponding to $B(OH)_3$ completely disappear. This phenomenon indicates a significant alteration in the sample's structure due to the dominance of the silane network, which

appears to mask or replace the crystalline features of $B(OH)_3$. The transition from a crystalline to an amorphous structure, attributed to the high ratio of silane, suggests that the silane molecules may effectively envelop the boron trihydroxide, thereby inhibiting its crystallinity. The complete disappearance of the $B(OH)_3$ peaks underscores the profound impact that silanization can have on the structural characteristics of h-BN. This change not only reinforces the effectiveness of the silane treatment in modifying the surface properties of h-BN but also highlights the potential for tuning the interactions between the filler and the matrix in composite materials.

The TGA results were also analyzed to quantify the hydroxy groups (O-H) added to h-BN. As depicted in Figure 3 (a), neat h-BN exhibited minimal weight loss when heated to 1000 °C, approximately 1.4%. However, for heat-activated h-BN, two distinct weight loss regions were observed around 90 °C and 120 °C. Additionally, for silane-modified-h-BN samples, weight loss occurred between 220 °C and 650 °C, indicating the departure of silane molecules. Considering that the melting point of APTES molecules is around 200 °C, the decomposition of APTES occurred beyond this temperature (Sun et al., 2016). The weight loss observed in APTES-treated h-BN particles indicates the extent of silanization. The highest weight loss was observed in Silane modified-h-BN (1:1), reaching 18 %. The weight loss observed in other APTES-treated h-BN particles decreased with decreasing the silane content.

In the current research, XPS was employed to investigate the bonding and chemical compositions of h-BN, focusing on the hydroxylation and silanization processes applied to modify the h-BN material. The XPS spectra for neat h-BN, heat-activated h-BN, and h-BN modified with silane groups following thermal treatment are presented in Figure 3 (b). The wide scan XPS spectrum of h-BN confirmed its chemical composition, revealing the presence of 70.94 at. % nitrogen (N), 16.44 at. % boron (B), 4.08 at. % oxygen (O), and 8.55 at. % carbon (C). This analysis underscores the significant nitrogen content characteristic of h-BN, which is critical for its unique properties. The oxygen content increased from 4.08 at. % to 15.83 at. % as a result of the attachment of hydroxyl groups to the boron atoms at the edges of h-BN during thermal processing. This hydroxylation process is crucial as it enhances the material's hydrophilicity and potentially improves its interaction with polymer matrices in composite applications. Following the silanization process, the presence of 3-aminopropyltriethoxysilane (APTES) molecules on the heat-activated h-BN resulted in a notable increase in silicon peaks within the XPS spectra. This increase signifies the successful attachment of silane groups to the h-BN surface, enhancing its

compatibility with organic matrices. The intensity of the silicon peaks reached its maximum in the silane-modified-h-BN sample at a silane ratio of 1:1. Overall, the XPS results provide comprehensive insights into the chemical modifications occurring in h-BN through hydroxylation and silanization.

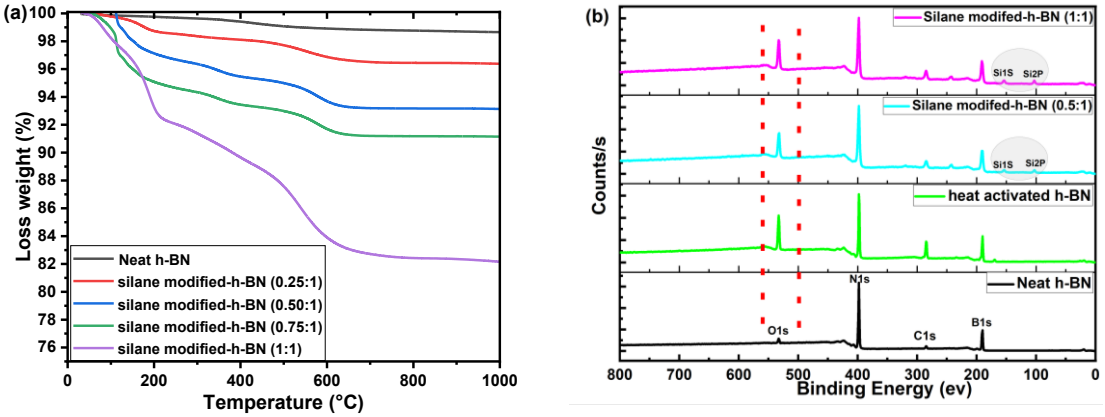

Figure 4.3 (a) TGA curves of neat h-BN, Silane modified-h-BN (0.25:1), Silane modified-h-BN (0.5:1), Silane modified- h-BN (0.75:1) and Silane modified- h-BN (1:1), and XPS survey scans (b) for neat h-BN, heat activated h-BN, silane modified-h-BN (0.5:1), and Silane modified-h-BN (1:1).

4.3.3 Mechanical properties of silanized h-BN reinforced epoxy composites

The relationship between the chemistry of hexagonal boron nitride (h-BN) and its mechanical properties when incorporated into an epoxy matrix is primarily influenced by surface chemistry, particle-matrix interactions, and chemical modifications such as silanization. These factors determine how well h-BN integrates with the matrix and transfers stress, playing a critical role in enhancing or limiting the composite's mechanical behavior. Understanding the effects of these chemical treatments and interactions is essential for optimizing the performance of h-BN/epoxy composites, ensuring improvements in strength, stiffness, and overall durability. Tensile tests were conducted to evaluate the mechanical properties of the samples, with the results illustrated in Figure 4. The data clearly indicates that as the filler percentage of neat h-BN increases, there is a noticeable decrease in tensile strength, which drops from 81.4 MPa to 65.98 MPa. Concurrently,

the tensile modulus shows a significant increase, rising from 2985.3 MPa to 4211.36 MPa for the 10 wt. % hBN + epoxy composite. This trend suggests that while the addition of h-BN enhances the stiffness of the composite, it negatively impacts the tensile strength, leading to a more brittle behavior. Interestingly, the incorporation of silanized h-BN samples results in an even more pronounced reduction in tensile strength, indicating a higher rate of decline compared to the neat h-BN composites. This further decrease implies that the silanization process may not effectively mitigate the brittleness associated with the filler, which can be attributed to the potential incompatibility between the modified filler and the epoxy matrix. In particular, the samples treated with a high concentration of 3-aminopropyltriethoxysilane (APTES) exhibited the most significant decline in tensile properties. This observation highlights the potentially detrimental effects of excessive silane content, which may disrupt the interfacial bonding within the composite, leading to reduced load-bearing capacity. It is important to note that a composite of silane modified-h-BN (1:1) with epoxy with 10 wt.% filler loading was also fabricated; however, the conditions for casting were suboptimal. This is illustrated in Figure S.2, which highlights the challenges encountered during the fabrication process. As a result, no tests were conducted for this composite. Toughness is also the ability of a material to absorb energy and plastically deform without fracturing and it is referred to as the area under tensile stress and tensile strain. Consequently, the toughness details of h-BN/epoxy and silanized h-BN/epoxy were calculated and further details regarding the tensile modulus and strength can be found in Tables 1 and 2. It is evident that the 10 wt. % h-BN+epoxy composite exhibits superior mechanical properties. However, when considering toughness characteristics (Figure S.3), the 10 wt. % silane-modified h-BN (0.25:1) + epoxy composite proves to be a better option.

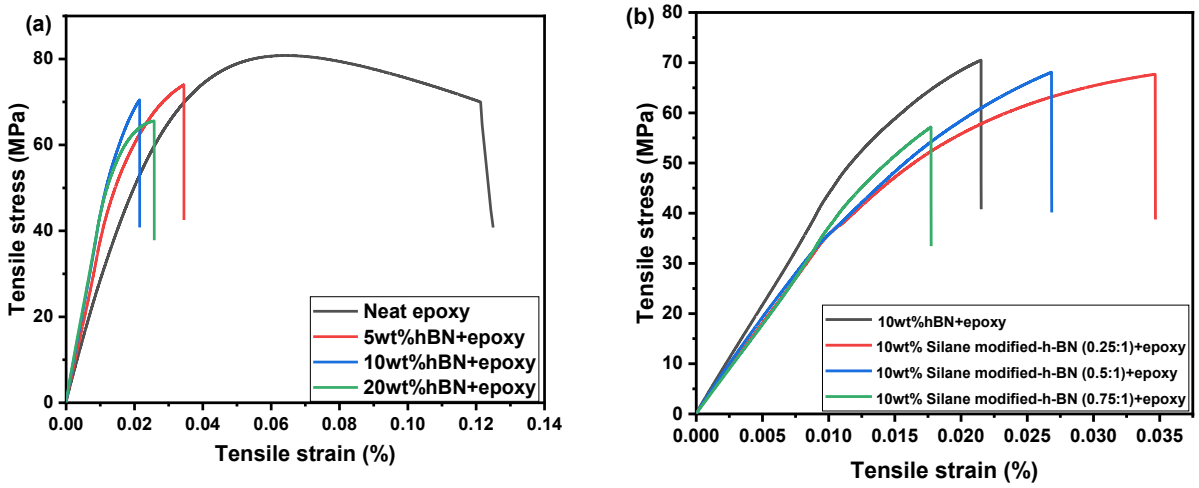

Figure 4.4 (a) Comparison tensile stress-strain curves of neat h-BN reinforced epoxy composites by loading ratio of 5 wt. %, 10 wt. % and 20 wt. % and (b) silanized h-BN reinforced epoxy composites by a loading ratio of 10 wt.% by changing silane content.

Table 4.1 Tensile modulus, strength and toughness results of neat h-BN reinforced epoxy composites by the loading ratios of 5 wt. %, 10 wt. % and 20 wt. %.

Sample	Tensile modulus (MPa)	Improvement (%)	Tensile strength (MPa)	Improvement (%)	Toughness (MPa)	Improvement (%)
REF-EP	2985.3±87	-	81.4±2.40	-	6.90	-
5wt%hBN+epoxy	3329.92±32.90	11.52	75.28±2.51	-7.51	1.10	-84.05
10wt%hBN+epoxy	4211.36±90.30	41.06	70.65±5.01	-13.57	0.70	-89.85
20wt%hBN+epoxy	4386.86±82.52	46.94	65.98±0.98	-18.94	0.60	-91.30

Table 4.2 Tensile modulus, strength and toughness results of silanized h-BN reinforced epoxy composites at loading ratio of 10 wt. % by changing silane content.

Sample	Tensile modulus (MPa)	Improvement (%)	Tensile strength (MPa)	Improvement (%)	Toughness (MPa)	Improvement (%)
10wt%hBN+epoxy	4211.36±90.30	-	70.65±5.01	-	0.70	-
10wt% Silane modified-h-BN (0.25:1)+epoxy	3915.36±92.30	-7.02	63.85±5.60	-10.46	1.10	57.14
10wt% Silane modified-h-BN (0.5:1)+epoxy	3620.16±96.54	-14.03	63.31±4.54	-10.20	0.60	-14.28
10wt% Silane modified-h-BN (0.75:1)+epoxy	3472.03±27.70	-17.54	62.73±3.50	-11.42	0.10	-85.71

Three-point bending tests were conducted to further investigate the mechanical behavior of the samples, and the results are illustrated in Figure 5. The data clearly demonstrate that as the content of neat h-BN increases, there is a corresponding decrease in flexural strength, which declines from 127 MPa to 109 MPa. Despite this reduction in strength, the flexural modulus exhibits a significant increase, rising from 2934 MPa to 4126 MPa. This suggests that while the addition of h-BN enhances the stiffness of the composite, it adversely affects its ability to withstand flexural loads. Furthermore, the incorporation of silanized h-BN samples leads to an additional decrease in flexural strength. This trend indicates that the modification process may influence the structural integrity of the composite, potentially due to the altered interfacial interactions between the silane-treated filler and the epoxy matrix. Such interactions can affect the load transfer efficiency within the composite, contributing to the observed decline in flexural performance. Detailed results

regarding the flexural properties, including flexural strength and modulus, are summarized in Table S2 and Table S3. This comprehensive analysis of the three-point bending tests provides valuable insights into the mechanical behavior of h-BN-filled epoxy composites.

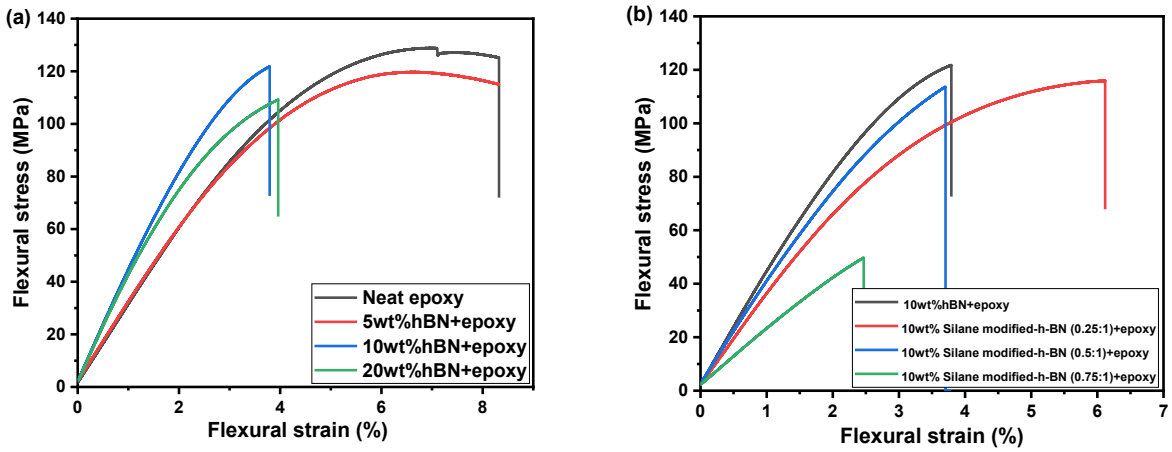

Figure 4.5 (a) Comparison flexural stress-strain curves of neat h-BN reinforced epoxy composites by loading ratio of 5 wt. %, 10 wt. % and 20 wt. % and (b) silanized h-BN reinforced epoxy composites by a loading ratio of 10 wt. % by changing silane content.

Dynamic mechanical analysis (DMA) was performed to evaluate the storage modulus, loss modulus, and tan delta of the samples, as are illustrated in Figure 6 and 7. The results reveal three distinct zones during the temperature sweep. Part I corresponds to the glassy state of the material, which is characterized by elasticity and minimal molecular motion. Zone II marks the rubbery phase transition region, where the material begins to exhibit increased mobility of the polymer chains. Finally, Part III indicates a fully rubbery phase, where the material displays significant flexibility and energy dissipation. Throughout these zones, all tested samples demonstrated similar behaviors, indicating consistency in their mechanical responses. Notably, the DMA results show that incorporating silane-modified-h-BN samples into the epoxy matrix raises the glass transition temperature compared to the neat h-BN/epoxy composite. This enhancement suggests that the silanization process effectively improves the thermal stability of the composite. For instance, at a filler loading of 5 wt. %, the transition temperature for epoxy containing neat h-BN was 101 °C.

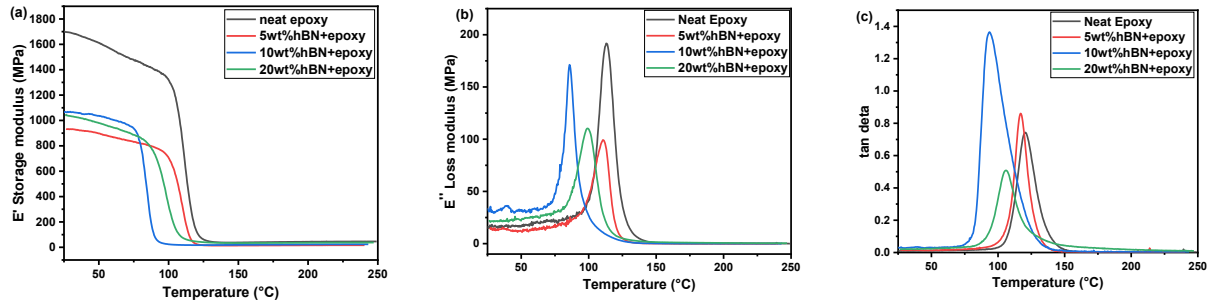

Figure 4.6 Comparison of DMA curves (a) changes of E' storage modulus (b) E" loss modulus and (c) the tan delta of neat h-BN reinforced epoxy composites by loading ratio of 5 wt. %, 10 wt. % and 20 wt. % as a function of temperature.

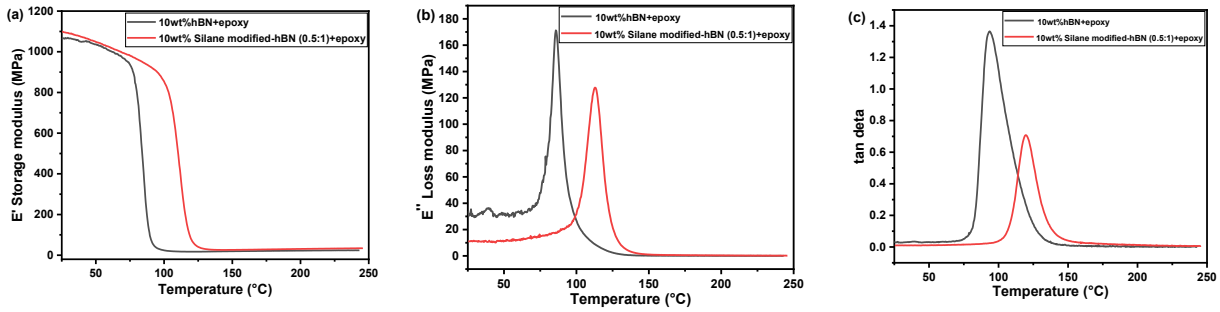

Figure 4.7 Comparison of DMA curves (a) changes of E' storage modulus (b) E" loss modulus and (c) the tan delta of silanized h-BN reinforced epoxy composites at a loading ratio of 10 wt. % as a function of temperature.

4.3.4 The effect of functionalization of h-BN surfaces on the bulk thermal conductivity of epoxy composites

Bulk thermal conductivity is a crucial factor in applications where hexagonal boron nitride (h-BN) is incorporated into epoxy, particularly in fields requiring efficient heat dissipation, such as electronics, aerospace, and energy storage systems. Due to its high thermal conductivity and excellent electrical insulation, h-BN serves as an ideal filler for improving the thermal performance of epoxy composites. This combination enables the composite to transfer heat effectively while maintaining electrical insulation, making it valuable for a range of high-performance applications. Bulk thermal conductivity (TC) was evaluated for composites with filler loadings of 5, 10, and 20

wt. % and the results are presented in Figure 8. When 5 % h-BN was added to the epoxy matrix, the thermal conductivity increased to 0.28 W/mK, indicating an initial improvement in heat transfer properties. As the filler percentage increased to approximately 10 wt. %, the neat h-BN demonstrated a significant increase in thermal conductivity, rising by nearly 50% to reach 0.33 W/mK. Interestingly, samples treated with APTES at a lower concentration also achieved a thermal conductivity of 0.33 W/mK. However, the optimum thermal conductivity was observed at 10% filler loading of silane modified-h-BN (0.5:1), which reached approximately 0.34 W/mK. In contrast, higher amounts of APTES led to a decrease in thermal conductivity, resulting in a TC value of only 0.23 W/mK. This indicates that there is an optimal level of APTES that enhances thermal conductivity, beyond which the benefits diminish. In our previous research (Mehdipour et al., 2025), we investigated two types of silanization processes and similarly identified a trend where the highest thermal conductivity was achieved at a specific concentration of APTES. The underlying reasons for this behavior will be explored in the subsequent section using ANSYS software. Preliminary simulations conducted with ANSYS suggest that silanization modifies the surface morphology of h-BN, which can significantly influence heat flux and, consequently, the overall thermal conductivity of the composite. The insights gained from this study highlight the critical role of filler loading and surface treatment in optimizing the thermal properties of h-BN/epoxy composites.

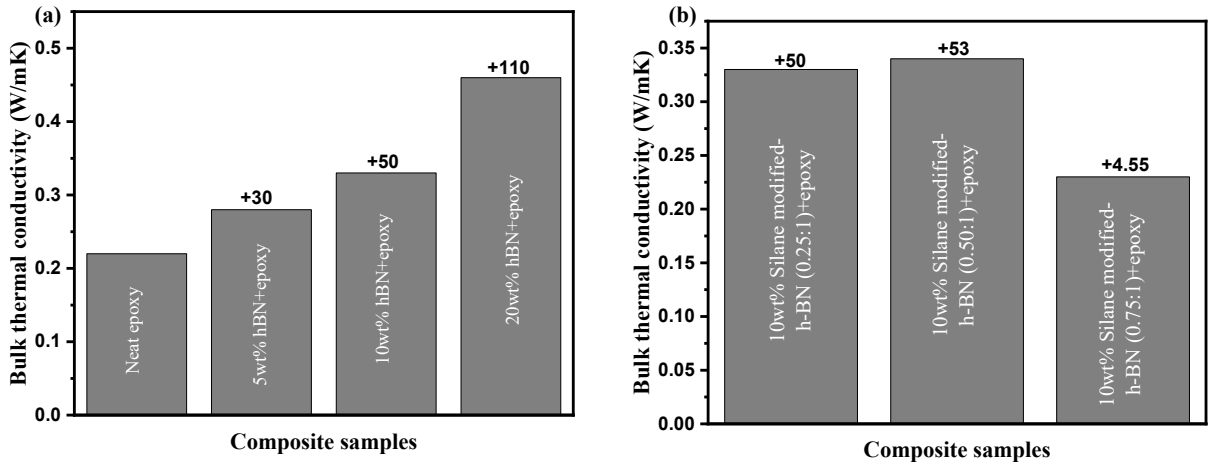

Figure 4.8 Comparison of bulk TC of (a) neat h-BN reinforced epoxy composites by loading ratio range from 5 wt. % to 20 wt. % and (b) silane-modified h-BN epoxy composites at 10 wt. % loading ratios.

4.3.5 Thermal conductivity simulation of neat or modified h-BN/epoxy composites

Numerical modeling in the steady state mode is an essential tool in the field of composite materials, providing insights into prediction capability, optimization of material properties, and failure analysis that drive innovation and performance in various applications by different software (Dericiler et al., 2021). A straightforward finite element model was developed using ANSYS to simulate the thermal transport properties of polymer composites filled with oriented hexagonal boron nitride (h-BN) and silanized h-BN. This numerical model was validated against experimental data obtained in the preceding sections. Initially, the epoxy resin was modeled in ANSYS, where a solid representation of the resin was created. After completing the modeling process, the structure was analyzed using ANSYS software. Detailed representations of the modeling process can be found from various perspectives in Figure 9 (a1, a2, a3). Following this, the composite material consisting of neat h-BN was modeled and simulated within ANSYS. The details of this specific model are also illustrated in Figure 9 (b1, b2, b3). It is important to note that the surface of the neat h-BN exhibits a rough structure, as evidenced by scanning electron microscope (SEM) images presented in the supplementary document (Figure S.4). The irregularities on the h-BN surface are filled with air pockets, making the h-BN/epoxy composite a

combination of three components: neat h-BN, epoxy resin, and air. This comprehensive modeling approach allows for a better understanding of the thermal behavior of the composite materials, providing valuable insights for optimizing their performance in various applications.

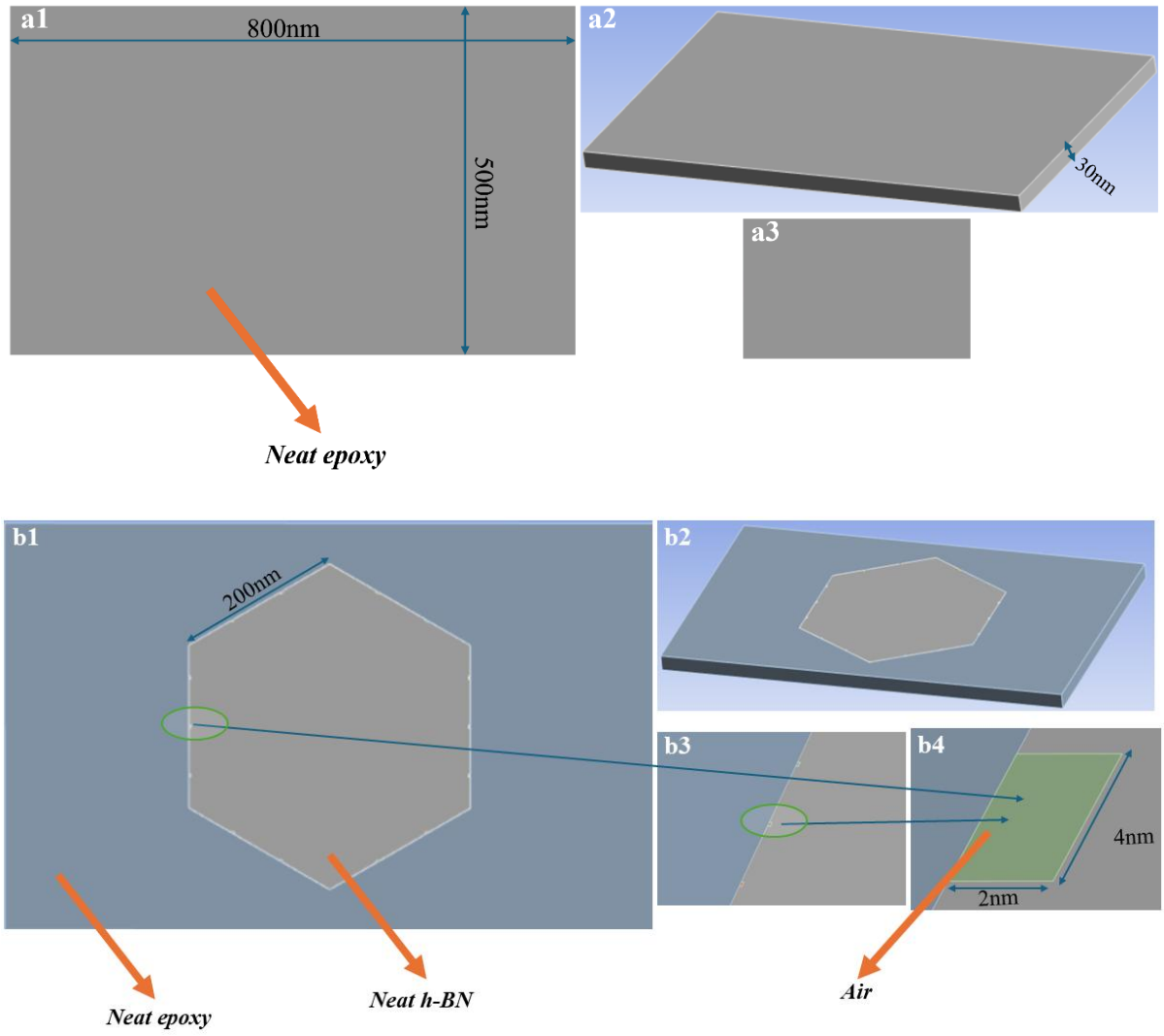

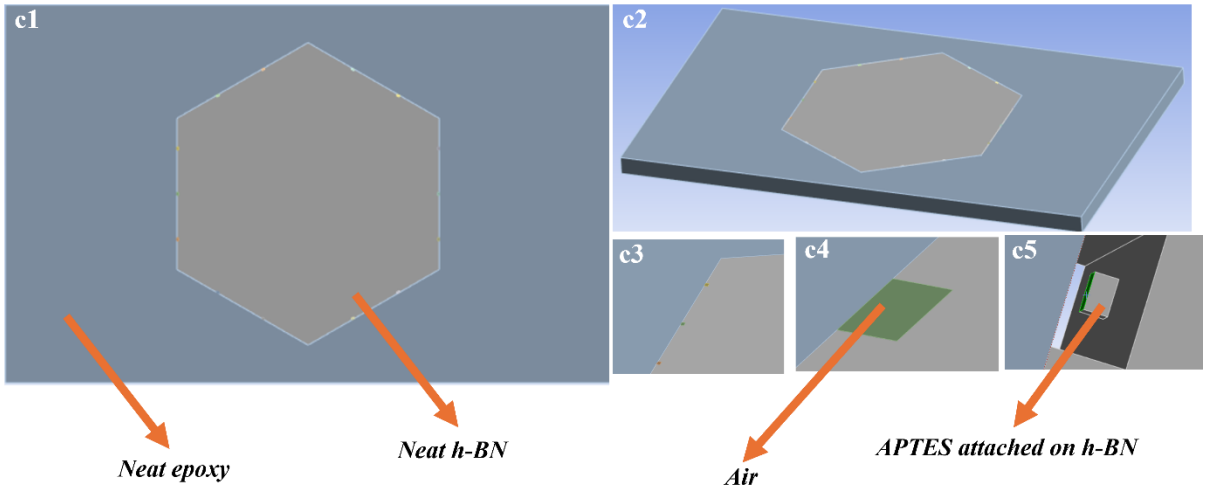

Figure 4.9 Modeling done in ANSYS of (a) epoxy (b) neat h-BN/epoxy and (c) silanized h-BN/epoxy.

For the modeling of the silanized composites, certain assumptions were made for the attachment of silane groups on the surface of h-BN to clarify the interaction in the interphase within this study. The structure of the silane molecule, specifically (3-Aminopropyl) triethoxysilane (APTES), used in this work is illustrated in Figure S.5 (a). In ANSYS, the bulk component can be considered based on the structure of the APTES molecule; thus, the silane component is represented as shown in Figure S.5 (b). Moreover, the thermal conductivity of APTES, when covalently bonded to the surface of h-BN, is assumed to be equivalent to that of h-BN itself. To model the effects of varying amounts of silane on the surface of h-BN, APTES in Figure S.5 (b) is treated as a single bulk unit. As the number of APTES increases, additional bulk units are incorporated into the ANSYS model. In this study, the models with 7, 14, and 21 bulk units of APTES were created and simulated. Further details regarding the characteristics of silanized h-BN are provided in Figure 9 (c1, c2, c3, c4, and c5).

The meshing parameters for each model were configured using criteria based on bounding box diagonal (9.4×10-7), minimum edge length (6.4×10-10), and element size (5959). The mesh setup for the neat epoxy model is depicted in Figure S.6 (a), illustrating the structure's uniformity. For the neat h-BN/epoxy composite, meshing details are shown in Figure S.6 (b,c), where adjustments accommodate the added h-BN particles, maintaining accuracy in element size and connectivity. Similarly, Figure S.6 (d,e,f) presents the meshing layout for the silanized h-BN/epoxy composite,

with refinements to account for interfacial effects induced by the silane treatment, ensuring that the model captures variations in thermal behavior. This approach allows for a robust simulation of each composite's response under thermal loads, providing a high-resolution analysis of mesh conditions across different materials.

The boundary conditions for the models were established in alignment with experimental tests, starting with an initial temperature set at room temperature. A heat flux of 3×10-5 W was applied to one surface of the model. The boundary conditions are specific to the neat epoxy are illustrated in Figure S.7 (a,b), while the conditions for the neat h-BN/epoxy and silanized h-BN/epoxy composites were set to match those of the neat epoxy model, as shown in Figure S.7 (c,d). This setup enables a detailed examination of the influence of silane treatment on the thermal behavior of the composite materials, providing insights into the heat transfer improvements attributed to silanization.

After completing the modeling and applying the boundary conditions, all samples including neat epoxy, h-BN/epoxy composites, and silanized h-BN/epoxy composites were analyzed using ANSYS. The results of the heat flux analysis are presented in Figure. 10. Heat flux distribution for neat epoxy is shown from various perspectives in Figure 10 (a1, a2, and a3), while the neat h-BN/epoxy composite is illustrated in Figure 10 (b1, b2, and b3). The results for silanized samples, featuring increasing amounts of APTES bulk, are depicted in Figure 10 (c1, c2, c3/d1, d2, d3/e1, e2, e3). A critical observation is that the addition of neat h-BN to the epoxy matrix leads to an increase in heat flux. Similarly, the incorporation of APTES bulk units also enhances heat flux; however, beyond an optimal concentration, further increases in APTES result in a decline in heat flux. In most of the existing literature, the addition of silane molecules is reported to enhance the bonding with epoxy, thereby improving heat flux and thermal conductivity. However, there is little discussion regarding the observed decrease in thermal conductivity after a certain level of silane incorporation. The ANSYS models developed in this study indicate that thermal conductivity is influenced by more than just chemical bonding; surface morphology modifications due to APTES significantly affect the heat flux across the h-BN surface. The average heat flux trend as APTES bulk amounts increase is displayed in Figure. 11, highlighting the importance of optimizing the amount of silane added to achieve maximum thermal performance.

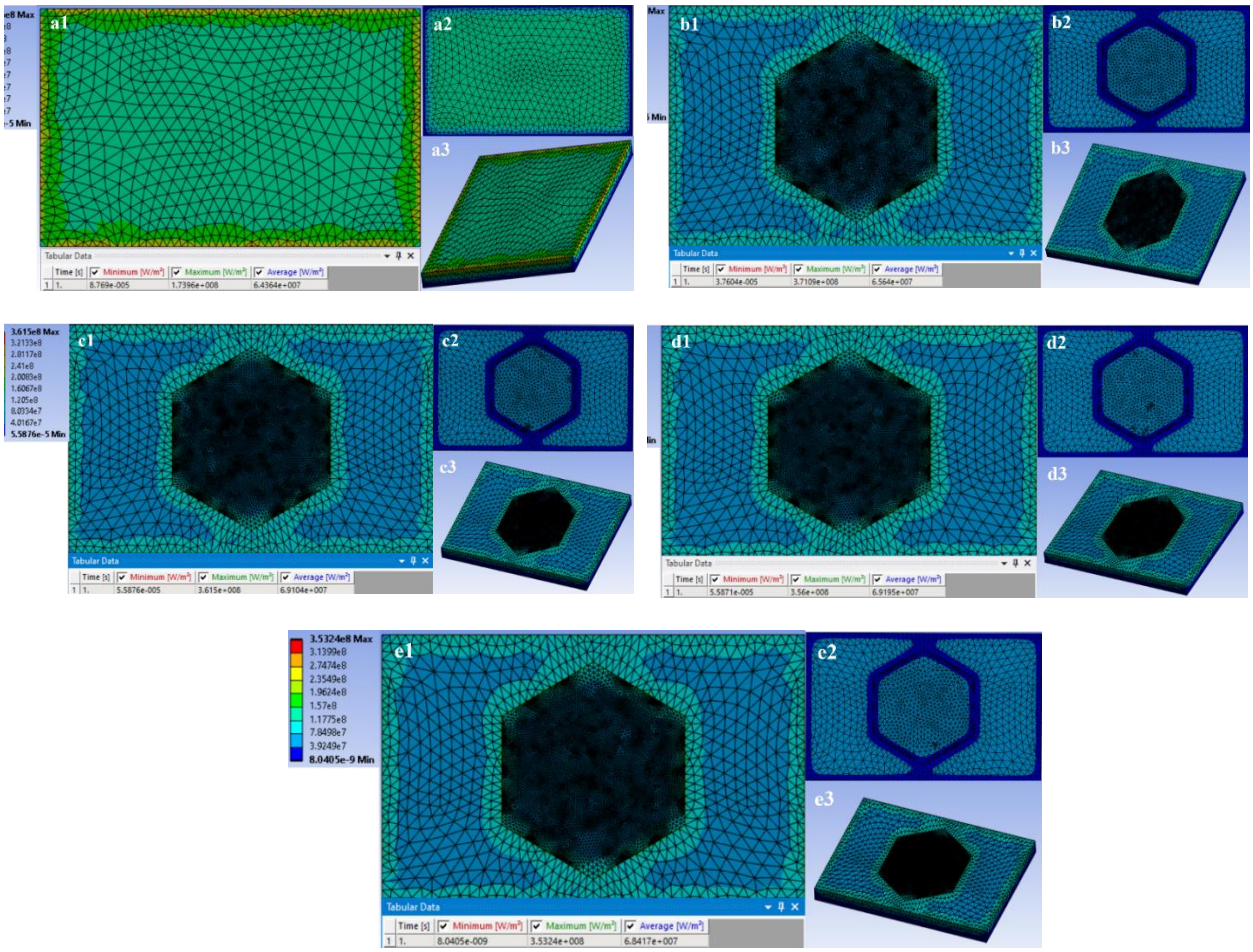

Figure 4.10 Simulation models performed by ANSYS of (a) epoxy (b) 10 wt.% neat h-BN+epoxy and (c, d, e) 10 wt. % silane modified-h-BN+epoxy.

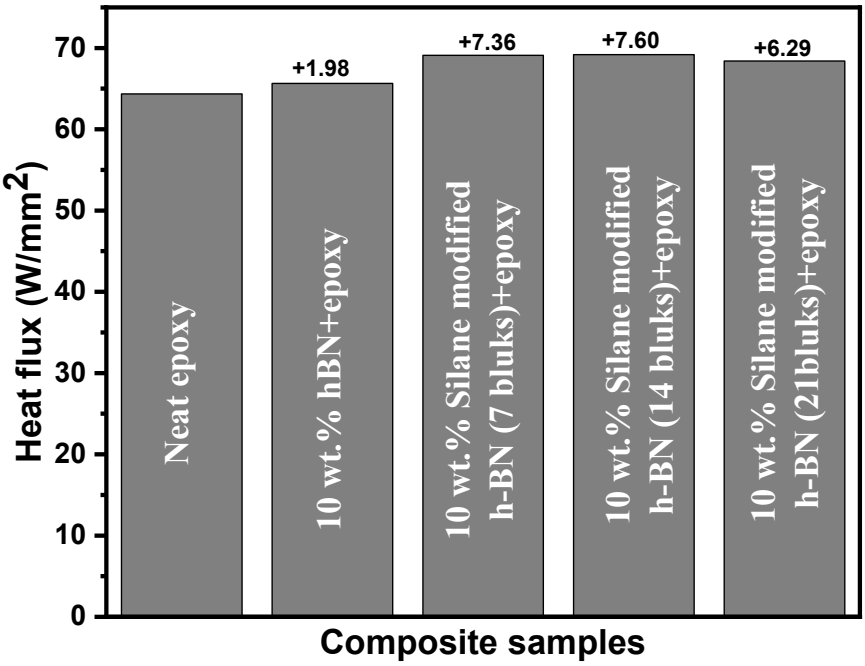

Figure 4.11 The changes in the average heat flux of epoxy, neat h-BN/epoxy, and silanized h-BN/epoxy specimens at the loading ratio of 10 wt. %.

4.3.6 Cross-section analysis of neat or modified h-BN/epoxy composites

To investigate the microstructure of the composites, Scanning Electron Microscopy (SEM) was used, and the results are presented in Figure 12. The SEM images illustrate the microstructures of various epoxy composites: Figure 12 (a) shows 10 wt. % h-BN+epoxy, Figure 12 (b) displays 10 wt.% silane modified-h-BN (0.25:1)+epoxy, Figure. 12 (c) presents 10 wt.% silane modified-h-BN (0.50:1)+epoxy, and Figure. 12 (d) highlights 10 wt .% silane modified-h-BN (0.75:1)+epoxy. Additionally, the microstructure of neat epoxy is provided in Figure. S.4 for reference. In the SEM images of epoxy reinforced with neat h-BN and most of the silanized h-BN composites (Figure 12 (b-c)), a uniform structure can be observed from the cross-sectional view, indicating that the addition of h-BN or lower amounts of silane-modified h-BN does not significantly alter the internal microstructure of the epoxy matrix. This uniformity suggests consistent dispersion of the filler particles within the epoxy, which is crucial for maintaining consistent thermal and mechanical properties. However, the microstructure of the composite containing 10 wt. % silane modified-h-

BN (0.75:1) (Figure 12 (d)) reveals a different scenario. It exhibits higher porosity and the presence of voids, which could be attributed to the release of gases during the reaction between the epoxy and the increased amount of silanized h-BN particles during the composite fabrication process. This reaction likely leads to the formation of bubbles or voids within the matrix as the silane molecules react with epoxy. When comparing Figure 12 (a-c), the similarity in microstructure aligns with the theory presented in the previous section, which suggested that in h-BN reinforced epoxy composites, heat flux is significantly influenced by surface morphology. The silanization process modifies the surface of the h-BN particles, which in turn aids in altering the heat flux properties of the composite. However, when using a higher concentration of silane, as in the 10 wt. % silane modified-h-BN (0.75:1) composite, the excess silane reacts more aggressively with the epoxy, leading to gas release and the formation of voids. These voids negatively impact the thermal conductivity and mechanical properties of the composite, as discussed earlier, by introducing areas of poor thermal conduction and structural weaknesses. This demonstrates the importance of optimizing the silane concentration to balance the benefits of surface modification without compromising the integrity of the composite.

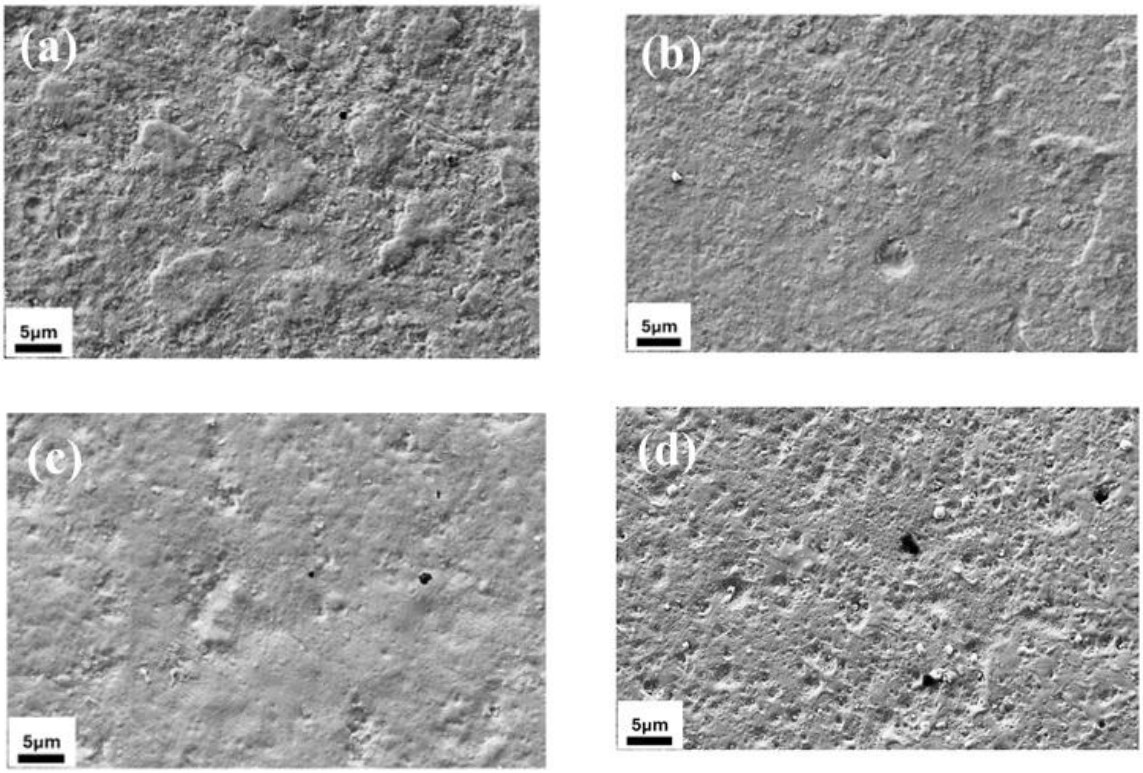

Figure 4.12 SEM images of (a) 10 wt. % h-BN+epoxy, (b) 10 wt. % silane modified-h-BN (0.25:1)+epoxy, (c) 10 wt. % silane modified-h-BN (0.50:1)+epoxy, and (d) 10 wt. % silane modified-h-BN (0.75:1)+epoxy.

4.4 Conclusion

In this study, surface modification of h-BN particles through thermal treatment followed by silanization with APTES was successfully employed to improve the compatibility and adhesion between h-BN and the epoxy matrix by improving interfacial interactions. Silanized h-BN samples exhibited a maximum thermal conductivity of 0.34 W/mK at an optimal APTES-to-heat activated-h-BN ratio of 0.5:1, beyond which thermal conductivity decreased, consequently, this ratio was selected for further composite manufacturing. This trend of thermal conductivity behavior was validated through simulations using ANSYS software, where both neat h-BN/epoxy and silanized h-BN/epoxy were modeled. The simulation results confirmed that thermal conductivity increased

to an optimal level before declining with excess silane content, aligning with the experimental data. The maximum heat flux in silanized h-BN/epoxy was 70 W/mm², a 7.6 % improvement compared to neat epoxy. In terms of mechanical performance, the introduction of silanized samples resulted in a more pronounced decrease in tensile strength compared to neat h-BN samples, a trend also observed in three-point bending tests. However, toughness was significantly better in the silane-modified h-BN (0.25:1) composites, showing a 54 % improvement over neat h-BN. The highest flexural modulus in this work for the composite was reached with 10 wt. % h-BN+epoxy, about 4126 MPa. Overall, the study demonstrates that surface modification through silanization significantly enhances the thermal conductivity and interfacial bonding in epoxy-based composites, making them more suitable for thermal management applications. However, it also highlights the importance of controlling the silane content to balance thermal and mechanical performance. The enhancement of mechanical and thermal conductivity properties in the developed h-BN/epoxy composites paves the way for their application in advanced aerospace technologies. These composites show significant potential for mass production, offering an efficient solution for dissipating heat generated by electronic devices in high-performance environments. The combination of improved properties and scalability makes these materials highly suitable for demanding applications, where thermal management and structural integrity are critical.

Supplementary

Table 4.S1 Summary of the manufacturing conditions of h-BN/epoxy composites.

Sample	Filler	Matrix	Filler loading ratio of filler/matrix (wt.%)	Curing temperature (°C)	Curing time (h)
REF-EP	-	epoxy	0	100	5
5wt%hBN+epoxy	Neat h-BN	epoxy	5	100	5

10wt%hBN+epoxy	Neat h-BN	epoxy	10	100	5
20wt%hBN+epoxy	Neat h-BN	epoxy	20	100	5
10wt% Silane modified-h-BN (0.25:1)+epoxy	Silane modified-h-BN (0.25:1)	epoxy	10	100	5
10wt% Silane modified-h-BN (0.5:1)+epoxy	Silane modified-h-BN (0.5:1)	epoxy	10	100	5
10wt% Silane modified-h-BN (0.75:1)+epoxy	Silane modified-h-BN (0.75:1)	epoxy	10	100	5

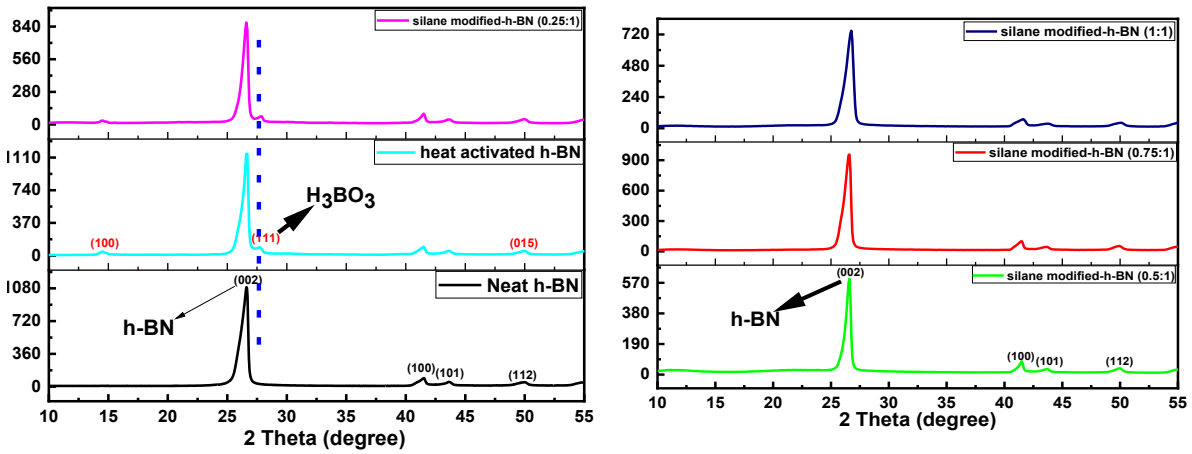

a b

Figure 4.S.1 XRD patterns results (a) for neat micron h-BN, heat activated h-BN, Silane modified-h-BN (0.25:1), b) Silane modified-h-BN (0.5:1), Silane modified-h-BN (0.75:1) and Silane modified h-BN (1:1).

Figure 4.S.2 The 10 wt. % silane modified-h-BN (0.75:1) + epoxy sample during the composite production process.

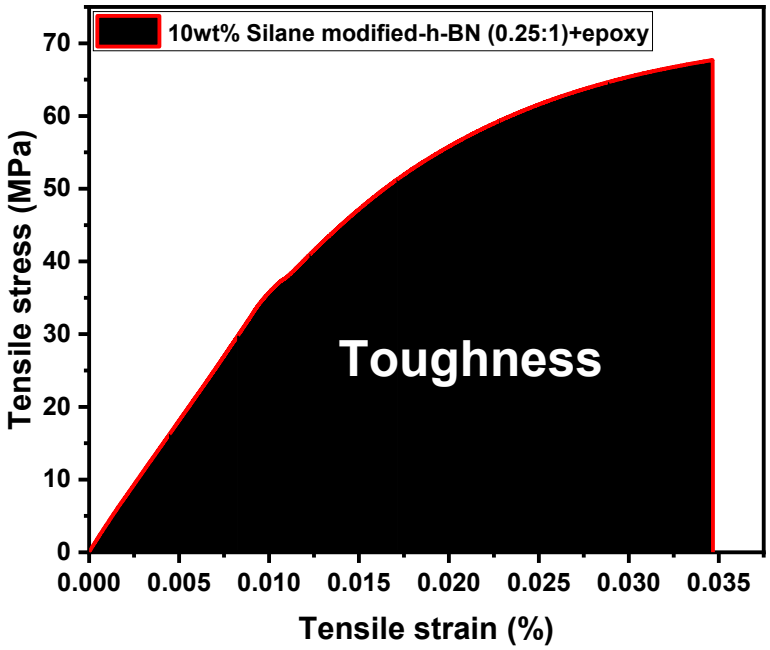

Figure 4.S.3 The toughness curve of silane modified-h-BN (0.25:1).

Table 4.S2 The summary of flexural modulus and strength results of neat h-BN reinforced epoxy composites by loading ratio of 5 wt. %, 10 wt. % and 20 wt. %.

Sample	Flexural modulus (MPa)	Improvement (%)	Flexural strength (MPa)	Improvement (%)
REF-EP	2934±93.80	-	127±2.10	-
5wt%hBN+epoxy	3227±11.15	9.98	122±2.49	-3.14
10wt%hBN+epoxy	4126±47.79	40.62	121±3.01	-4.74
20wt%hBN+epoxy	3872±83.79	31.95	106±2.30	-16.37

Table 4.S3 The summary of flexural modulus and strength results of silanized h-BN reinforced epoxy composites at loading ratio of 10 wt. % by changing silane content.

Sample	Flexural modulus (MPa)	Improvement (%)	Flexural strength (MPa)	Improvement (%)
10wt%hBN+epoxy	4126±47.79	40.62	121±3.01	-4.74
10wt% Silane modified-h-BN (0.25:1)+epoxy	3407±53.57	16.10	109±8.23	-14.20
10wt% Silane modified-h-BN (0.5:1)+epoxy	3599±89.47	22.66	110±5.98	-13.40
10wt% Silane modified-h-BN (0.75:1)+epoxy	2110±72.93	-28.08	48.0±1.70	-62.20

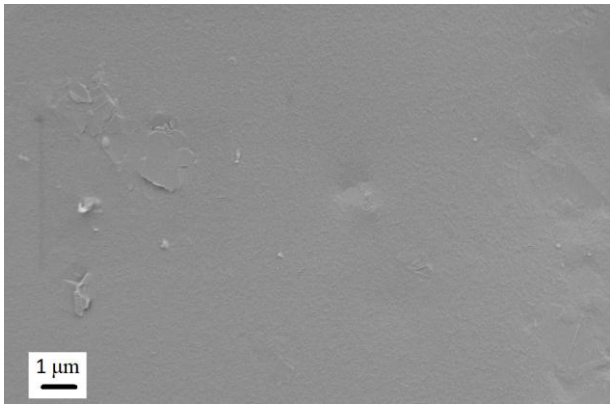

(a)

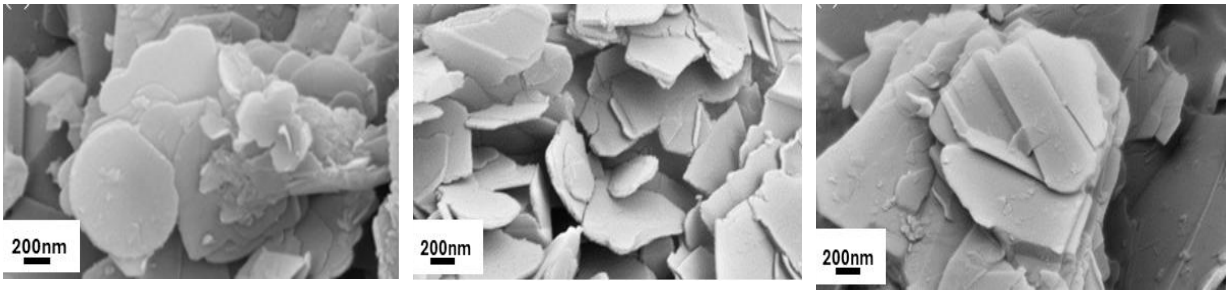

(b) (c) (d)

Figure 4.S4 SEM images of (a) Neat epoxy (b) neat h-BN, (c) heat activated h-BN, and (d) APTES modified h-BN particles (silane modified-h-BN (0.50:1)).

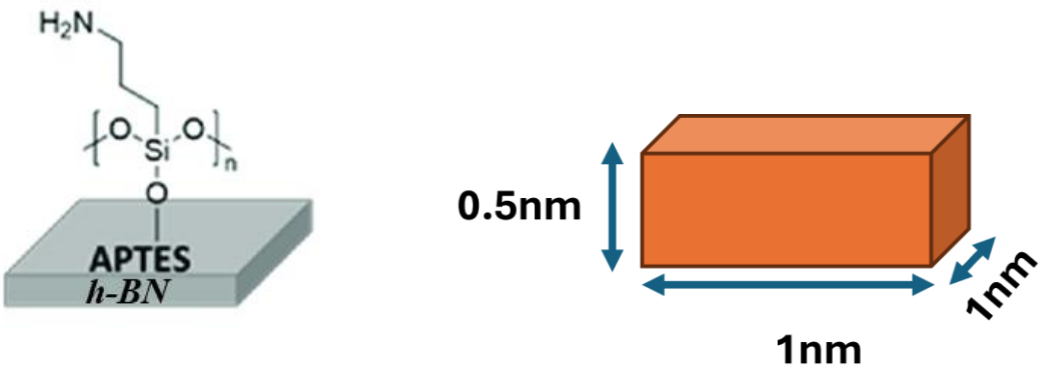

(a) (b)

Figure 4.S5 Modeling of APTES considered in the ANSYS software.

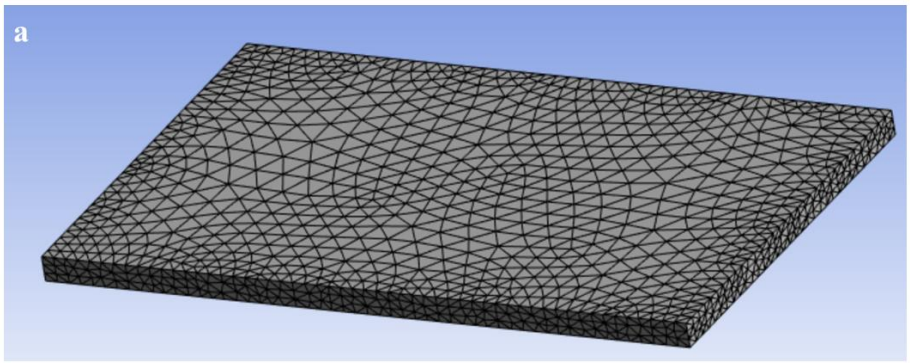

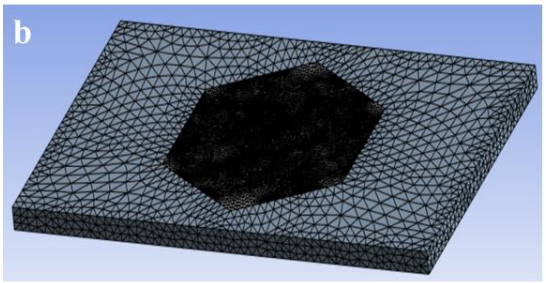

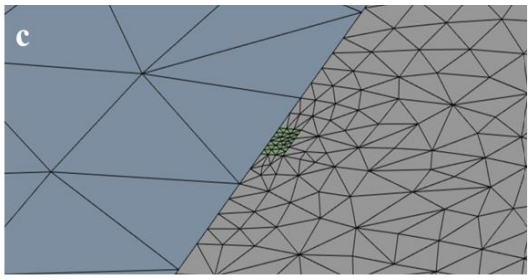

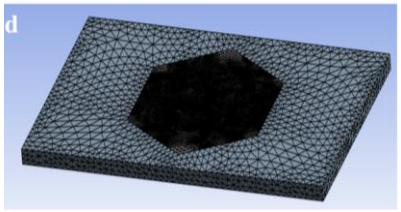

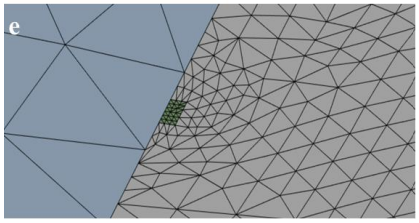

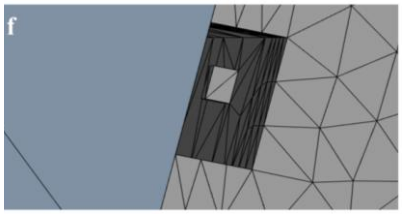

Figure 4.S6 The mesh conditions done in ANSYS of (a) epoxy (b,c) neat h-BN/epoxy and (d,e,f) silanized h-BN/epoxy.

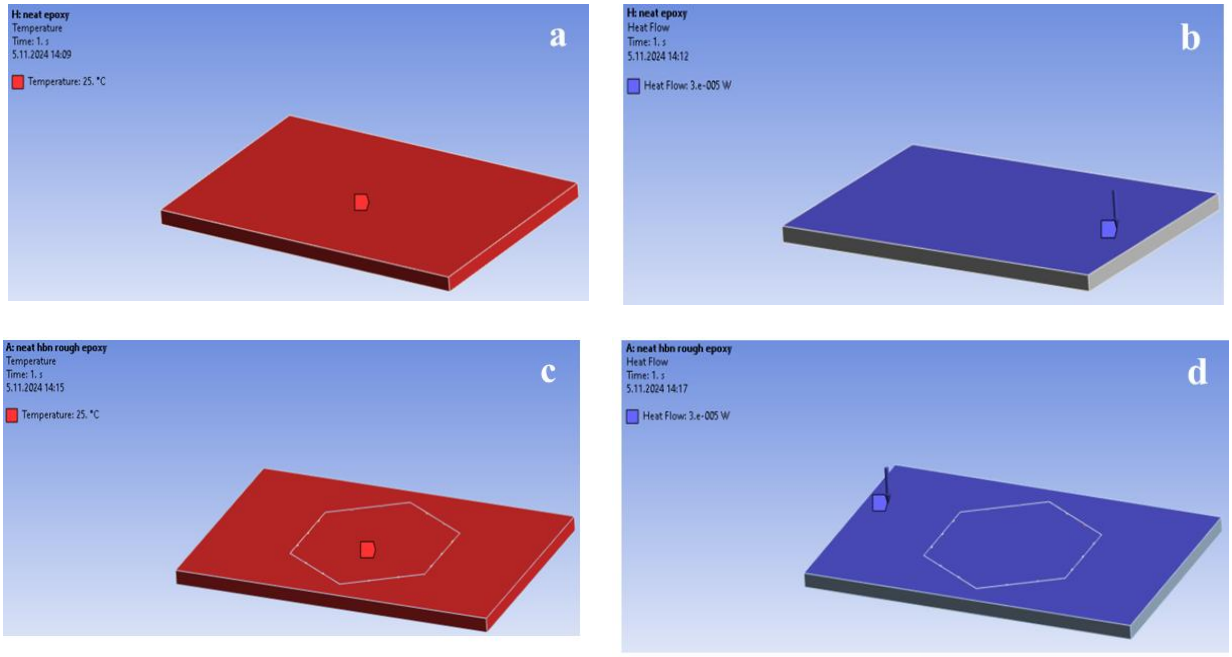

Figure 4.S7 The boundary conditions done in ANSYS of (a,b) epoxy (c,d) neat h-BN/epoxy and silanized h-BN/epoxy.

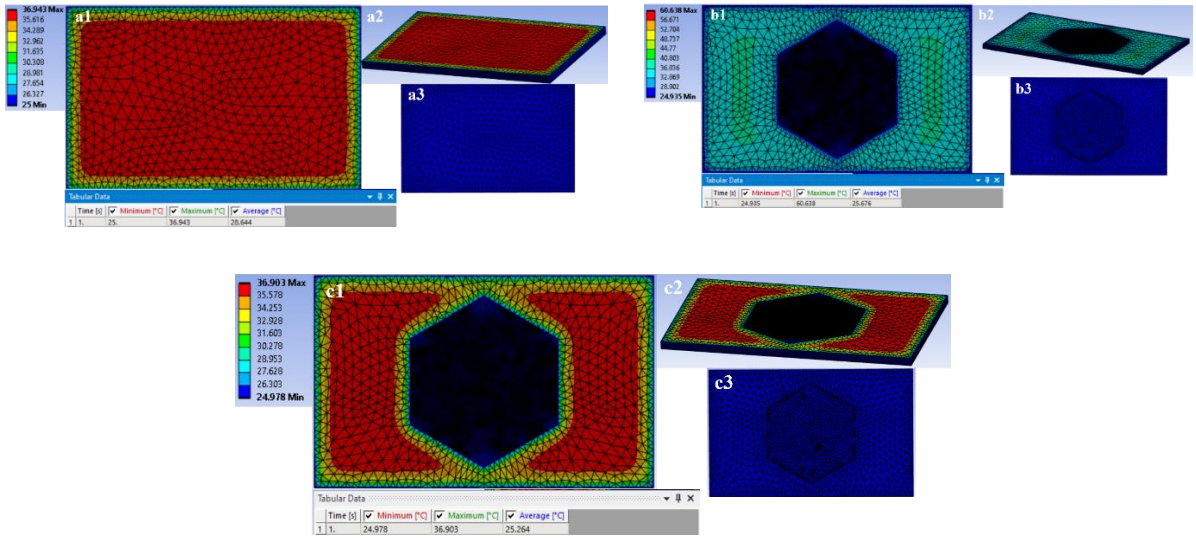

Figure 4.S8 Temperature distribution models by ANSYS of (a) epoxy (b) 10 wt. % neat h-BN/epoxy and (c) silanized BN/epoxy samples.

5. INFLUENCE OF FUNCTIONALIZED H-BN PARTICLE INTERPHASE AND INTERFACE REGULATION WITH STRUCTURAL DESIGN ON THE DIRECTIONAL THERMAL CONDUCTIVITY AND MECHANICAL PERFORMANCE OF CARBON FIBER/EPOXY COMPOSITES

This study highlights the importance of interfacial adhesion between carbon fiber (CF) and the epoxy matrix by adopting a novel approach that combines untreated and silane-treated h-BN in a multilayered structure. The interface was engineered by electrospraying h-BN particles, while the interphase was modified by incorporating up to 20% h-BN into the epoxy matrix. The highest out-of-plane thermal conductivity of 2.31 W/mK, a 116% increase compared to the reference value of 1.07 W/mK, was achieved by sizing CF with silanized h-BN through electrospraying, in conjunction with the 20% h-BN-loaded epoxy matrix. Conversely, the incorporation of h-BN in the epoxy alone resulted in the best mechanical performance, with approximately a 46.4% increase in elastic modulus, a 105% improvement in flexural modulus, and a nearly 5% increase in Charpy impact strength. Based on CT scan results, the resizing of CF fabrics improved directional thermal conductivity in CF/epoxy composites with controlled.

5.1 Review

Electronic devices, such as computers, mobile phones, smart televisions, transistors, diodes, and cameras, rely on electric current for transmitting information. As these devices continue to be smaller in physical size the components are more prone to overheating (Bianco et al., 2022). To prevent thermal loading, it is crucial to efficiently remove the heat generated by the device and dissipate it into the environment. Materials with high thermal conductivity are particularly effective in this regard, as they can better manage and conduct heat. In electronic devices, the thermal conductivity of polymers is governed by phonon heat conduction, but they often have a relatively low thermal conductivity, around 0.2 W/mK (L. Yi et al., 2022). This is due to their low

mean free path for phonons, which can limit their effectiveness in thermal management applications and this fact can cause polymers to overheat. Consequently, there is a strong drive-in high-performance composite to develop polymer-based materials having different fiber forms and micro/nano fillers that excel in both thermal conductivity and mechanical properties.

Carbon fiber (CF) composites, known for their superior strength-to-weight ratios, are widely used in various applications but suffer from insufficient thermal conductivity. Incorporating boron nitride (BN) fillers into the carbon fiber-polymer matrix could potentially address this shortcoming (Kong et al., 2023). Hexagonal boron nitride (h-BN), with its two-dimensional structure, demonstrates impressive thermal conductivity of up to 600 W/mK, comparable to nanostructured carbon materials, while also offering superior chemical stability, increased heat resistance, and exceptional electrical insulating properties, making it an ideal choice for fillers in thermally conductive composites. In the literature, there are several attempts to utilize h-BN particles in the thermoplastic or thermoset polymer matrix to tailor the conductivity. In one of the studies demonstrated by Bahsir et al. a hybrid composite of chemically linked h-BN and reduced graphene oxide (rGO) in thermoplastic polyurethane significantly enhanced through-plane thermal conductivity to 4.63 W/mK with just 3 wt.% BN content. In another study conducted by Liu et al. (M. Liu et al., 2020), thermally conductive polypropylene (PP) composites, created using PP as the matrix with BN and alumina (Al_2O_3) through melt blending and injection, achieved a thermal conductivity of 0.54 W/mK with volume fractions of 9.09% BN and 8.10% Al_2O_3 (a significant 157.14% increase in thermal conductivity compared to unfilled PP).

There is a growing trend to control the interface between reinforcement and matrix by activating fabric surface properties and functionalizing epoxy matrix. Electrospraying is a promising technology by an electrohydrodynamic phenomenon and powered by voltage that provides functionality on the selected fiber matrix without the removal of sizing. In our previous study, graphene sheets were efficiently electrosprayed on carbon fabric by providing suitable load transfer between reinforcing fiber and epoxy and tailoring mechanical performance of the developed composites (Zanjani et al., 2016). In our another work, the impact of graphene modification on both the fabric and matrix was examined by analyzing viscoelastic response, self-heating, and deicing properties. With the suitable suspensions having nanomaterials, it becomes possible to functionalize carbon or glass fabrics and produce functional structural composites. There are several coating studies in the literature to activate the fabric surfaces in the composite

structures. For instance, Sabri et al.utilized the electrospraying deposition technique to apply carbon nanotubes (CNTs) onto glass fiber (GF) surfaces and then incorporating into epoxy resin. Examination of the resulting CNTs-GF hybrid showed a uniform and even distribution of CNTs over the GF surface. Significantly, the electrosprayed CNTs-GF demonstrated a 34% enhancement in fracture toughness of CNT coated GF composite when compared to the reference specimen. In one of the studies, a maximum tensile strength of 364 MPa was demonstrated by a composite consisting of carbon fiber and h-BN, which is notably lower than the 600 MPa maximum strength achieved in the CF+/EP-20%hBN composite studied in this work (H. & Peter, 2018). It is crucial to graft silane molecules onto the surface of h-BN to establish a strong interfacial connection with an epoxy matrix, in this study, the intensity of the Si-O peak was found to be greater than the intensity reported.

In order to get an ideal fiber matrix composite structure with nanomaterials, it is significant to tailor the surface properties of nanomaterials and keep the mechanical integrity by improving interfacial bonding between reinforcement and matrix and reducing the stress concentrations and thus targeting the highest heat transfer. In this study, three different conFigureurations were designed to tailor the thermal conductivity in both in-plane and out-of-plane directions: h-BN applied on the fabric, incorporated into the resin, and both, with h-BN functionalized using APTES to enhance interfacial interactions and reduce stress concentrations through conduction pathways. This approach provides high thermal conductivity, which has not been previously reported, and even at high loadings, mechanical performance is preserved by incorporating h-BN through an electrospraying process. Various strategies have been proposed to explain the interactions in glass fiber-reinforced epoxy composites, particularly those involving h-BN and glass (F. Chen et al., 2021). However, our study extends this understanding by demonstrating the enhanced interactions of h-BN, employed as a ceramic filler, within a carbon matrix. This highlights a notable difference arising from the distinct nature of the composite matrix components, facilitated by bridging through functional groups. The comprehensive package detailing all the key parameters including electrospraying techniques, hot pressing methods, the incorporation of h-BN, the silanization process for h-BN, and the development of a multilayered structure with enhanced thermal conductivity and mechanical properties was investigated by supporting spectroscopic, gravimetric and morphological characterizations and addressing physical/chemical interactions.

5.2 Experimental Part

5.2.1 Materials

Hexagonal boron nitride (h-BN) with a particle size ranging from 1 to 5 μm and a purity of 99.5% was acquired from Civelek Porselen Company in Turkiye. 3-aminopropyltriethoxysilane (APTES, 0.946 g/mL, >98%), silane coupling agent was provided by Sigma-Aldrich. Acetic acid (glacial, %100), and ethanol (absolute) were purchased from Isolab. n-hexane was employed as a solvent in the silanization reaction as received from Tekkim. All agents were utilized directly without undergoing any additional purification processes. Sika Biresin® CR131 (based on 50%–100% bisphenol A diglycidyl ether (DGEBA), 10%– 20% bisphenol F diglycidyl ether (DGEBF), and 5%–10% 1,4-bis (2,3 epoxypropoxy) butane) with CH132-5 hardener (based on triethylenetetramine [TETA]) were supplied by Tekno Chemicals Inc., Turkiye. This resin system was appropriate for infusion applications because of its low viscosity and is generally used to manufacture high-performance fiber-reinforced composite parts. Plain carbon fabrics with a weight of 200 gsm provided by Dost Chemistry company were used for the manufacturing of the h-BN reinforced epoxy-based composites.

5.2.2 Thermally activated h-BN particles

The surface of h-BN underwent activation through a thermal treatment process, leading to an increase in the oxygen content on its surface. This enhancement promoted the interaction between h-BN particles and silane molecules during silanization, thereby improving their compatibility and adhesion. Furthermore, exfoliation was employed to increase the surface area available for interaction, facilitating bonding between oxygen and silicon atoms. In this way, 5.0 g of h-BN powder, with particle sizes ranging from 1 to 5 μm was loaded into a ceramic crucible. The crucible was then subjected to thermal treatment at 1000 °C for 5 min in the presence of air. The furnace temperature was ramped up to 1000 °C at a rate of 5 °C/min. Afterward, the furnace was gradually

cooled to room temperature, and the thermally treated h-BN was retrieved from the ceramic crucible. The reaction yield of the thermal treatment process is 95 wt%.

5.2.3 Synthesis of silanized h-BN

The silanization of h-BN in composite production is crucial for several reasons. It enhances dispersion, and adhesion, and prevents agglomeration of h-BN particles within the polymer matrix. Additionally, it improves thermal conductivity and chemical compatibility. These benefits collectively lead to stronger, more uniform composites with better thermal management and long-term stability. Therefore, 5.0 g of thermally treated micron h-BN were dispersed in 150 mL of n-hexane containing 1.25 mL of APTES (v, v) using an ultrasonic probe sonicator for 15 min. Then, 15 drops of acetic acid were added to the reaction mixture to bring the pH value of the reaction mixture to 4-5. The reaction mixture was stirred with the help of a magnetic stirrer at room temperature for 15 min. After cooling to room temperature, the reaction mixture was filtered and washed twice with distilled water. The silane-modified-thermally treated h-BN was subsequently dried in a vacuum oven at 80 ˚C for 1 h to remove any remaining solvent.

5.2.4 Manufacturing h-BN/carbon fiber reinforced epoxy composites

5.2.4.1 Fabric coating by Electrospraying of h-BN particles

Process parameters can influence the quality of the product achieved by electrospraying. The effect of the variation of the process parameters including applied voltage (7, 10, 12, and 14 kV), flow rate (80, 160, 240, and 320, 400 µl/min), and distance (5, 7, and 10 cm) were evaluated. The experiments were carried out based on a Design software (DOE) as shown in Table S1 provided in the supplementary document. The electrospraying was carried out on the area of 5x5 cm2 carbon fiber fabrics to determine the optimum condition. The obtained results showed that at lower applied voltages (7 kV) and lower distances (5 cm), no electrospraying occurred and only drops of the solutions fell on the surface of the carbon fibers. By increasing the applied voltage to 14 kV and

distance of 7 cm, electrospraying happened with the formation of an acceptable Taylor cone, and a uniform layer was achieved. Then electrospray process, as outlined in Figure 1, was implemented on carbon fiber samples measuring 60 x 60 cm2 for scaling up and mass production. The samples were treated using a 14 kV voltage, with two nozzles positioned 7.5 cm away from the sample, and a flow rate of 400 µL/min was set. The nozzle's movement speed was controlled at 6 mm/s in both the x and y directions. The process involved initially electrospraying one side of the carbon fibers, followed by a drying period of 24 h at room temperature, before electrospraying the other side. The set-up of the electrospraying process is provided in Figure. S1 in Supporting Information.

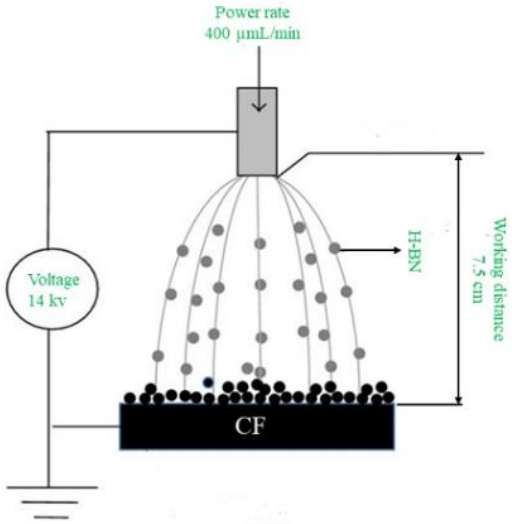

Figure 5.1 The scheme of the electrospraying process on carbon fabrics (CF).

5.2.4.2 Epoxy resin modification with h-BN particles

Initially, 250 g of ethanol were combined with 70 g of filler (either neat h-BN or APTES/heat-treated h-BN) and sonicated for 2 h. Subsequently, 350 g of epoxy were heated to 60 °C. After sonication, this mixture was added to the warmed epoxy and stirred continuously for 2 days at 50 °C to allow ethanol evaporation. This was followed by a 60-min degassing process. Next, 98 g of hardener were incorporated into the mixture, which was then mixed and degassed for an additional 30 min. This final mixture was then ready for application to CF and hot pressing. The resins were labeled as (20 wt% neat micron h-BN-e) and (20 wt% APTES/heat-treated h-BN-e).

5.2.4.3 Composite manufacturing by hot pressing

Following the preparation of electrosprayed CFs with either neat h-BN or APTES/heat-treated h-BN, the fibers were cut into two sizes: 10 x 10 cm^2 with 16 layers for thermal conductivity testing, and 30 x 30 cm2 with 8 layers for mechanical testing. The resin was then applied to these fibers using the hand lay-up method. Subsequently, the prepared samples were placed under vacuum and hot-pressed for curing. This process involved applying a pressure of 2.5 tons at a temperature of 100 °C for 5 h. Figure 2 displays the composites of h-BN/carbon fiber/epoxy manufacturing stages and in Table S2 provided in supplementary document, the composite systems produced in the study and their characteristics are mentioned.

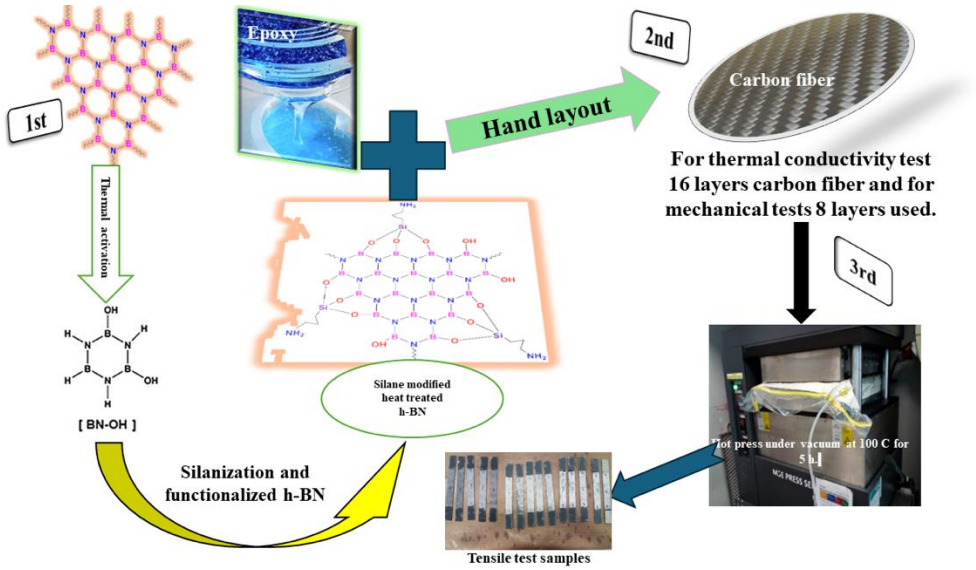

Figure 5.2 A schematic illustration of stepwise production processes of h-BN/CF/epoxy composites.

5.2.5 Characterization

Fourier transform infrared (FTIR) spectra were obtained using IS10 FT-IR spectrometer equipment to detect the active groups on the surface of the h-BN material used. Crystallinity analysis was performed on the samples through X-ray diffraction (XRD) analysis using a Bruker (Billerica, MA, USA) D2 PHASER Desktop equipment with a CuKα radiation source spanning

from 2θ = 5° to 80°. X-ray photoelectron spectroscopy (XPS) utilizing the X-Ray008 400um - FG ON model was also employed. Thermogravimetric analysis (TGA) was carried out using a Mettler Toledo thermal analyzer (TGA/DSC 3+), heating samples at a rate of 10 K/min from 25°C to 1000°C under a 50 mL/min N2 flow. Surface morphologies were examined by using the Leo Supra 35VP Field Emission Scanning Electron Microscope (FE-SEM) machine. Microcomputed tomography (MicroCT - Baker Hughes (Waygate Technologies) - Phoenix V|tome|x M 300/180) was used to analyze the topography and porosity of fabricated membranes with a 15 μm voxel size. The operation voltage was 80 kV, the current was 200 μA, and no filters were used. The acquired CT images were reconstructed and analyzed by Datos|x (version 2.14.0) and VGSTUDIO MAX (2023.1). The thermal conductivity (TC) was assessed using the Hot Disk method with a C02-12 device. The elastic modulus and tensile strength of the composites were determined following ASTM D638 standards. During the tests, extension data was recorded using a knife-edge extensometer with a cross-head speed of 2 mm/min. Flexural properties of the specimens were obtained from three-point bending tests based on ASTM D790 standards, with a span-to-thickness ratio of 16:1. Charpy impact tests were conducted on V-notched rectangular specimens measuring 80 x 10 mm to determine the specimens' impact strength, in accordance with ISO-179 standards, using a 5 J Charpy pendulum (CEAST 9050, Instron, Canton, MA). At least five specimens were tested for each group.

5.3 Results and Discussion

5.3.1 Structural characterization of functionalized h-BN particles

The dispersion behavior and capabilities of reinforcing materials within a polymer matrix are primarily influenced by the surface morphology and chemistry of these materials. Effective dispersion and strong interfacial interactions are essential factors in determining the thermal conductivity and mechanical properties of the resulting composite material. The SEM analysis provides valuable insights into the morphological changes induced by thermal treatment and silanization processes, highlighting their importance in optimizing the dispersion and adhesion of

h-BN particles within the composite material. In the first part of the current study, the impact of thermal treatment and silanization processes on the morphology and particle size of h-BN particles was investigated using SEM analysis. There is no significant change in the platelet morphology of thermally activated h-BN and silanized h-BN compared to neat h-BN, as confirmed by SEM images showing no noticeable differences in morphologies provided in Figure S2 in the supporting document. The preservation of lamellar structure after thermal and chemical treatments carries significant importance to facility the heat transfer with the epoxy matrix and enhance the interfacial interactions with the addition of functional groups. In order to verify the effect of surface functionalization of h-BN on the performance of CF reinforced epoxy composites, crystallinity behavior and crystallite size of h-BN samples were investigated in detail to provide the understanding the nucleating agent behavior together with its reinforcement property.

Figure 3 (a) shows a comparative display of FT-IR spectra, illustrating the differences between neat micron-sized h-BN, heat-treated h-BN, and APTES modified heat-treated h-BN particles. Initially, the stretching and bending vibration peaks of the micron-sized h-BN were identified to establish the h-BN's structure before undergoing the heat treatment and silanization processes. To aid in the understanding of FTIR, it is useful to compare a vibrating bond to the physical model of a vibrating spring system. The spring system can be described by Hooke's Law, as demonstrated in the following equations, considering a bond and the connected atoms as a spring with two masses (m_1 and m_2) (H. X. Zhang et al., 2020).

$$\upsilon = \frac{1}{2\pi}\sqrt{k/\mu}$$

$$\mu = \frac{m_1 m_2}{m_1 + m_2}$$

By utilizing the force constant k (which characterizes the stiffness of the spring) along with the two masses m1 and m2, the equation demonstrates how to calculate the frequency υ of the FTIR peak, where u represents the reduced mass.

h-BN (with a space group of P63/mmc) possesses a layered structure reminiscent of graphite. Within each layer, there exist strong covalent bonds between boron and nitrogen atoms, while the layers themselves are held together by relatively weaker van der Waals forces. Consequently, the force constant (k) for covalent bonds is higher than that for van der Waals bonds. FTIR analysis has unveiled two distinctive peaks: a broad absorption peak at 1307 cm^{-1}, attributed to B-N

stretching (covalent bond), and a peak at 763 cm^{-1}, corresponding to B-N-B bending (van der Waals forces). The comprehensive B-N stretching phenomenon is evident, encompassing both in-plane stretching vibrations (at 1378 cm^{-1}) and the out-of-plane bending mode (at 809 cm^{-1}), as illustrated in (H. X. Zhang et al., 2020) and our results are consistent with their findings.

After the thermal modification of h-BN, new stretching vibration peaks were observed at 3197 cm^{-1}, corresponding to B-OH stretching, and 841 cm^{-1} for N-O, in addition to the characteristic h-BN peaks, in the FT-IR spectra. It is noteworthy that the electronegativity difference between B and O atoms is greater than that between N and O atoms, resulting in a higher force constant for the B-O bond compared to the nitrogen-oxygen bonds. As a consequence, the vibration mode for B-O, as described by equation 1, occurs at a higher frequency. The broad absorption peak at approximately 3200 cm^{-1} was attributed to the –OH bands, which were consistent with our FTIR results. In this context, this peak undoubtedly confirmed the presence of hydroxyl groups on the surface of h-BN, signifying a hydroxylation process. In the subsequent phase, during the silanization process of the hydroxylated BN particles' surface, the absorption peaks at 2961 cm^{-1} and 2804 cm^{-1} was corresponded to the asymmetric and symmetric stretching of CH_2 groups, as well as peaks at 1101 cm^{-1} and 1023 cm^{-1}, associated with the Si-O-Si bonds present in the silane molecule, respectively. The chemical transformation, which leads to the creation of B-OH and Si-O bonds within the molecular structure of h-BN, was effectively verified by comparing FT-IR spectra.

X-ray diffraction (XRD) was employed to analyze the crystalline phase identification, determine the crystallite size and purity of the synthesized particles. Figure 3 (b) displays the XRD patterns of pristine micron-sized h-BN, heat-treated h-BN, and APTES/heat-treated h-BN powders. In each XRD pattern, a distinct and prominent peak is observed at $2\theta=26.60^{o}$ (002), which corresponds to the crystallographic plane of the h-BN graphitic structure. Additionally, the XRD patterns exhibit peaks of lower intensity at $2\theta=41.55^{o}$ (100), 43.63^{o} (101), 49.87^{o} (102), and 54.89^{o} (004), respectively. These peaks are consistent with those reported in (Guerra et al., 2018). On the contrary, a novel peak at $2\theta=27.55^{o}$ (111), which can be attributed to the presence of $B(OH)_3$, was revealed in the XRD pattern of the heat-treated h-BN. This emerging peak signifies the diffraction of $B(OH)_3$, indicating the formation of B-OH groups on the surface of h-BN. It's worth noting that in some other methods for introducing OH groups, such as acid treatment, base treatment, and the Hummer's method, their XRD patterns do not exhibit the signs of B-OH formation.

It is important to take into account that on the surface of the particles, OH molecules are bonded through covalent forces and arranged in ordered patterns. This arrangement results in the appearance of an X-ray diffraction peak (111). However, upon the binding of APTES molecules to the surface of hydroxylated h-BN, Si-O bonds are formed, causing the B-OH peak to disappear. In the XRD pattern, similar peak groups to those found in pristine micron-sized h-BN were detected, likely due to the amorphous nature of the silane molecule's structure.

The structure factors denoted as F(hkl), serve as the fundamental quantities upon which the electron density function depends. These factors hold significant importance since they determine the maximum of the electron density function, ρ(xyz), which in turn reveals the positions of the atoms and thereby the internal structure of crystals. As described in Equation (3), a structure factor, F(hkl), results from the collective contribution of all waves scattered in the direction of the hkl reflection by the n atoms within the unit cell. Each of these waves exhibits an amplitude that is proportionate to the atomic scattering factor *f*j, representing the X-ray scattering capability of each atom.

$$f(hkl) = \sum_{j=1}^{n} f_j e^{2\pi j(hx+ky+lz)}$$

According to Figure 3 (b), the intensity peaks for the heat-treated h-BN are at their maximum. By taking into account the structure factor theory, it can be affirmed that the rate of crystallization is higher in this case, allowing a greater number of crystal planes to participate in diffraction. The Scherrer equation (Vinila & Isac, 2022), used to determine the average crystallite size D, is:

$$D=\frac{k\lambda}{\beta\cos\theta}$$

In this equation, K represents the Scherrer constant, λ denotes the wavelength of the X-ray beam employed (typically 1.54184 Å), β signifies the full width at half maximum (FWHM) of the peak, and θ represents the Bragg angle. Table 1 presents the average crystallite size for neat micron h-BN, heat-treated h-BN, and APTES/heat-treated h-BN powders obtained by calculating β from XRD results and the Scherrer equation. Taking into account the distance between h-BN layers of 0.5 nm, the number of layers within a crystallite can be determined by using the average crystallite size (Table 2). Additionally, Table 1 displays the calculated values for the crystalline degree of neat h-BN, heat-treated h-BN, and APTES/heat-treated h-BN powders.

Table 5.1 Crystallinity degree values of functionalized h-BN particles derived from XRD.

Samples	The average crystallite size	The number of layers	The crystalline degree
Neat micron h-BN	17.04 nm	34	70.1 %
Activated h-BN	10.6 nm	21	72.2 %
Functionalized h-BN	10.3 nm	21	70.9 %

Figure 3 (c) shows XPS survey scan spectra for various samples of micron-sized h-BN, including the pristine material, heat-treated h-BN, and silane-modified h-BN. The XPS wide-scan analysis of the pristine micron-sized h-BN reveals a chemical composition consisting of 45.9% nitrogen (N), 47.85% boron (B), 2.56% oxygen (O), and 3.7% carbon (C). Upon subjecting the micron-sized h-BN to heat treatment, the oxygen content experiences a notable increase, rising from 2.56% to 13.67%. This augmentation is attributed to the formation of hydroxyl groups at the edges of the boron atoms within the micron-sized h-BN structure during the heat treatment process. The XPS analysis further verifies this by detecting the presence of B-OH bonds in the O1s scans of the hydroxylated h-BN at 531.9 eV. Subsequently, when the APTES molecule is introduced to the heat-treated h-BN via silanization, the oxygen content rises further, reaching 14.75%. Importantly, the successful binding of APTES as a silane coupling agent to the heat-treated h-BN surface is confirmed by the XPS spectrum. This is evident from the appearance of Si2s peak at 150.1 eV and Si2p peak at 100.3 eV, as illustrated in Figure 3 (c).

Thermogravimetric analysis (TGA) was utilized to investigate the effects of surface modifications on micron-sized h-BN and to evaluate its thermal stability. Figure 3 (d) presents the TGA curves for pristine micron h-BN, thermally treated h-BN, and silane-modified thermally treated h-BN. Each sample exhibited weight loss over distinct temperature ranges: pristine micron h-BN between 308.9°C and 506.8°C, thermally treated h-BN between 101.7°C and 163.0°C, and silane-modified thermally treated h-BN between 289.3°C and 461.1°C. The thermally treated h-BN showed a weight loss of only 6.7% during the nitrogen flow, which can be attributed to the presence of hydroxyl groups on its surface, leading to an oxygen content of 13.67 wt.% (based on XPS results). For the silane-modified sample, the weight loss is primarily due to the detachment of silane

molecules. This thermal behavior demonstrates that micron-sized h-BN maintains significant thermal stability, with high thermal resistance up to 1000°C. These findings highlight the material's potential for high-temperature applications, where maintaining structural integrity under extreme conditions is crucial.

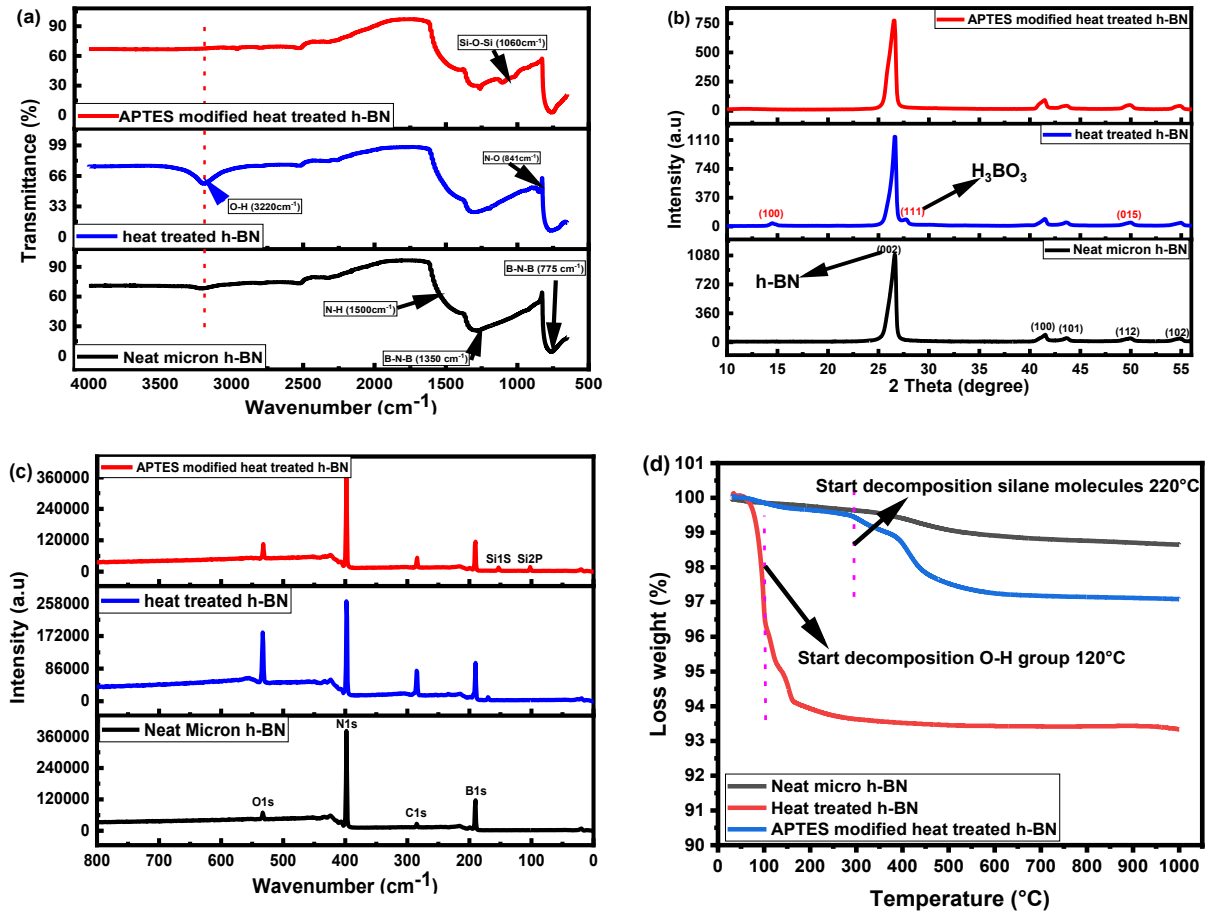

Figure 5.3 (a) FT-IR spectra, (b) XRD patterns, (c) XPS survey scan spectra and (d) TGA curves under N_2 atmosphere of neat micron h-BN, heat-treated h-BN, and APTES modified heat-treated h-BN samples

5.3.2 Morphological analysis of h-BN coated carbon fabrics

The uniformity of hexagonal boron nitride (h-BN) particles when applied via electrospraying is a crucial factor that significantly influences both the mechanical and thermal properties of the

resultant composites. In the electrospraying process, achieving a consistent and even distribution of h-BN particles is essential for ensuring homogeneous reinforcement throughout the matrix. Uniformly dispersed h-BN particles can effectively enhance the mechanical properties, such as tensile strength and modulus, by providing uniform stress distribution and reducing stress concentrations. Additionally, the thermal properties, particularly thermal conductivity and stability, are also markedly improved with uniform dispersion. This is because h-BN, known for its excellent thermal management capabilities, when evenly distributed, forms an efficient thermal pathway across the composite material. This uniformity is especially critical in applications where high thermal conductivity and mechanical strength are required simultaneously. Thus, the effectiveness of electrospraying in achieving uniform dispersion of h-BN particles plays a pivotal role in optimizing the performance characteristics of advanced composite materials. Figure 4 (a) optical microscopy image and Figure 4 (b) FE-SEM image present CF coated with APTES-treated h-BN particles using a 10 wt. % ethanol-based solution. Herein, the APTES-treated h-BN particles are visibly prominent on the fibers, and the distribution of APTES-treated h-BN particles is remarkably uniform (compared with Figure 4 (c)). This uniformity is crucial for ensuring consistent properties across the composite material. Ethanol, due to its properties, appears to facilitate a more even distribution of h-BN particles. As a result, ethanol was selected as the preferred solvent for further composite preparation processes, optimizing the material for better performance and reliability. Further insights into particles are provided by SEM analysis in Figure 4 (b) and how they are oriented on the CFs are presented by SEM analysis in Figure. S2. This image reveals that the application of APTES-treated h-BN results in a more homogeneous coating across most of the carbon fibers. Such uniform coverage is likely to enhance the mechanical integrity and thermal properties of the final composite, as it ensures consistent interaction between the h-BN particles and the carbon fiber substrate. This uniformity is especially critical in applications where balanced mechanical strength and thermal conductivity are essential, as it ensures the composite material performs reliably under varying conditions.

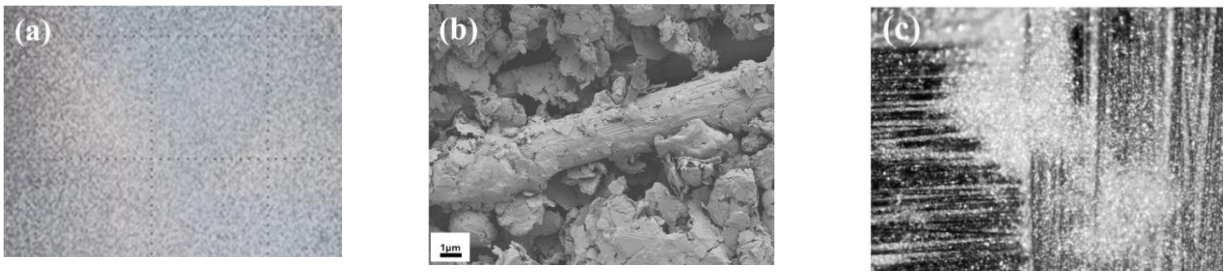

Figure 5.4 (a) Optical picture, (b) SEM image of APTES modifed heat treated h-BN coated CF sample and (c) optical image of h-BN deposited CF.

5.3.3 The effect of h-BN configuration within the composite structure on the thermal conductivity of epoxy composites

Thermal conductivity is vital for optimizing performance, efficiency, and safety in various technological applications, making it a fundamental consideration in material selection and engineering design. In this way, Figure 5 (a) presents the results of out-of-plane thermal conductivity measurements conducted through isotropic tests. The out-of-plane thermal conductivity was measured to be 1.07 W/mK for the CF+/EP composite. This value experienced a notable increase to 1.2 W/mK, a rise of approximately 12.15%, following the incorporation of neat micron-sized h-BN. This increase can be attributed to the inherently high thermal conductivity of h-BN particles, owing to their planar structure which facilitates efficient heat transfer. To further explore the thermal conduction mechanisms, it is crucial to consider the anisotropic thermal conductivity properties of h-BN. As a ceramic filler, h-BN contributes significantly to thermal conduction due to its unique layered structure, which allows heat transfer primarily in-plane. The deposition of exfoliated h-BN on carbon fibers (CF) enhances this effect by creating efficient heat transfer pathways at the fiber-matrix interface. Especially the presence of B-N interactions in composite specimen is critical since the thermal conduction occurred between h-BN layers exfoliated in matrix and also deposited on CF. In addition, SEM analysis confirmed the uniform dispersion and deposition of exfoliated h-BN layers on CF and in the epoxy matrix. FTIR results are shown in Figure S3, where the observed peaks primarily correspond to the epoxy matrix. These peaks, located at 770, 1050, 1640, 2840, and 3360 cm^{-1}, are attributed to the vibrations of the C–C, benzene ring, C–O, C–H, and O–H functional groups, respectively. The structural composition

of the epoxy unit is illustrated in Figure. S3, clearly indicating that the FTIR peaks are related to various molecular vibrations of the atoms in the epoxy resin. When h-BN is incorporated into the resin, particularly in the CF+/EP-20%hBN composite, a new peak appears around 1397 cm^{-1}, corresponding to the in-plane vibration of the boron-nitrogen (B–N) bond. Additionally, another peak associated with the out-of-plane B–N–B vibration is observed around 770 cm^{-1}, though it overlaps with the C–C vibration of the epoxy structure, making it less distinct. FTIR results demonstrate the successful incorporation of h-BN into the resin on the carbon fibers (CFs). However, a more significant enhancement in thermal conductivity was observed in carbon fibers coated with both neat micron h-BN and APTES-treated h-BN through the electrospray process. For instance, CF electrosprayed with neat micron h-BN embedded in epoxy exhibited a thermal conductivity of 2.02 W/mK. The peak value was achieved with the (eMhBN)CF+/EP-20%hBN sample, reaching 2.31 W/mK – an impressive increment of about 115.89% relative to the neat CF/EP composites. This substantial increase in thermal conductivity can be partially explained by the electrospraying process. During electrospraying, particles impact the carbon fibers at high velocities, enabling deeper penetration and more effective filling of voids within the fibers. This deeper integration of particles enhances phonon transport in the composites, thereby boosting thermal conductivity. Furthermore, APTES treatment likely strengthens the bond between the h-BN particles and the carbon fibers, contributing to an even higher thermal conductivity. The combination of these factors demonstrates the profound effect of particle treatment and application methods on the thermal performance of these composite materials. Our findings stand out in the context of previous research, as evidenced by comparisons with several studies. For instance, in one of the studies (Song et al., 2023), a composite consisting of room temperature vulcanized silicone rubber (RTV-SiR) combined with h-BN, when hot pressed, achieved a thermal conductivity (TC) of only 0.6 W/mK. This is significantly lower compared to our results. Similarly, in study (R. Chen et al., 2023), a composite fabricated using hydroxylated h-BN with a natural ester yielded a TC of approximately 0.21 W/mK, which is markedly less than our findings. Another relevant comparison can be made with study (N. Zhang et al., 2022), where a composite comprising graphene oxide and h-BN within an epoxy matrix reached a maximum TC of about 1.5 W/mK. This value, while higher than the previous examples, still falls short of the TC levels we have achieved. Furthermore, study (X. Zhang et al., 2021) explored enhancing the compatibility of inorganic fillers with silicone rubber by biologically modifying h-BN with a

polydopamine (PDA) coating. In that instance, the composite, containing 30 wt.% filler, exhibited a thermal conductivity of 0.95 W/mK. This represents a reasonable enhancement, yet it does not quite reach the level of improvement demonstrated by our findings. In one of the studies, h-BN was chemically modified with polypyrrole 4-styrenesulfonate (PSS), achieving a TC of 2.3 W/mK under a magnetic field, which dropped to 1.5 W/mK without it, comparable to the highest values obtained (Luo et al., 2022). Fang et al. fabricated modified h-BN with epoxy for incorporation into glass fibers, achieving a maximum out-of-plane thermal conductivity of 1.53 W/mK at high loading ratio of h-BN 35%. Kirubakaran et al. manufactured hybrid filler polymer (HFP) composites by incorporating nano h-BN into epoxy, achieving a maximum thermal conductivity of 1.01 W/mK (Kirubakaran et al., 2024). These comparisons underscore the significance of our results, particularly in achieving high TC values without the need for external stimuli like magnetic fields and highlight the effectiveness of our methods in enhancing thermal conductivity in the prepared composites.

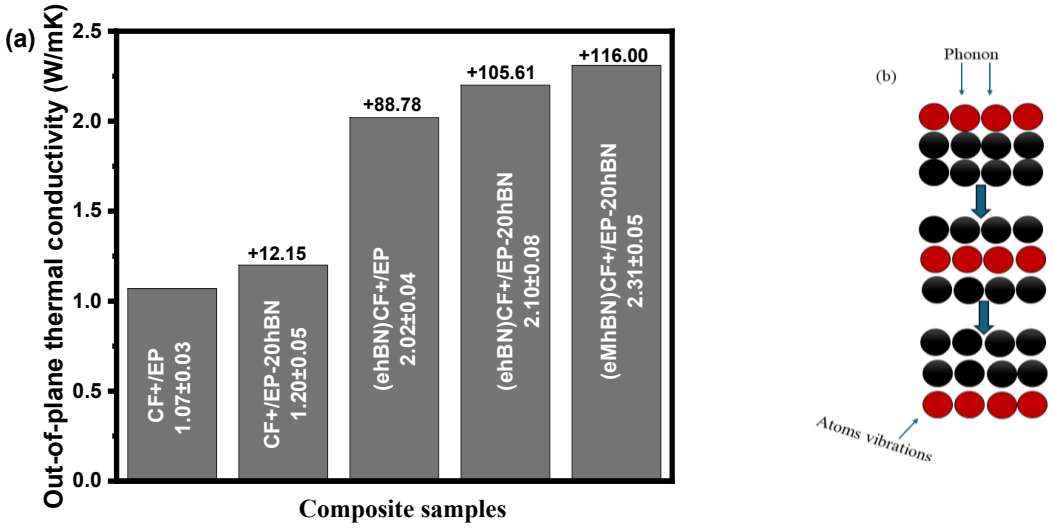

Figure 5.5 (a) Out-of-plane TC (isotropic mode) values of h-BN treated CF/epoxy samples and (b) the schematic representation of out of plane heat transmission by the collision of particles.

Figure 6 (a) displays the results from anisotropic tests measuring in-plane thermal conductivity. Initially, when only neat epoxy was applied to carbon fibers, the thermal conductivity was recorded at 2.5 W/mK. Intriguingly, this value did not exhibit any change upon the introduction of neat

micron-sized h-BN, suggesting that in the context of in-plane thermal conductivity, the addition of neat h-BN did not significantly affect the heat transfer capabilities of the composite. However, the scenario alters when considering carbon fibers (CFs) that have been coated with both neat micron h-BN and APTES-treated h-BN via the electrospray process. These samples showed a notable increase in thermal conductivity (TC) compared to the basic CF+/EP (carbon fiber/epoxy) composite. This enhancement can be attributed to the improved alignment and distribution of h-BN particles along the fiber axis, which is more effective in conducting heat in the in-plane direction. The highest thermal conductivity was observed in carbon fibers that were electrosprayed with APTES-treated h-BN and incorporated into an epoxy matrix containing 20 wt% neat micron h-BN. This combination achieved a maximum TC of 3 W/mK. This significant increase underscores the impact of both the type of h-BN treatment and its concentration on the composite's thermal properties. The APTES treatment, in particular, seems to enhance the interface between the h-BN particles and the carbon fibers, thereby facilitating more efficient thermal transfer. These results demonstrate the critical role of both the h-BN modification process and the application technique in optimizing the thermal performance of composite materials, especially when specific directional properties, like in-plane thermal conductivity, are targeted.

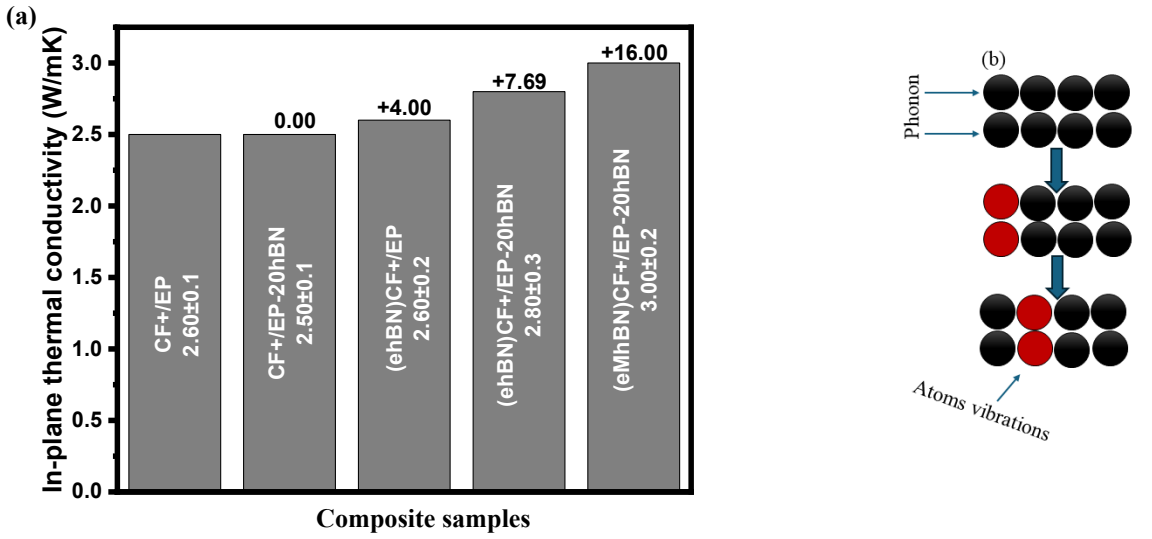

Figure 5.6 (a) In-plane TC (anisotropic mode) values of h-BN treated CF/epoxy samples and (b) the schematic representation of in- plane heat transmission behavior by collision of particles.

5.3.4 Mechanical performance of the configuration h-BN in carbon fiber reinforced epoxy composites

Figure 7 illustrates the tensile and flexural test results for the prepared composites analyzed in detail. The data clearly demonstrates that the incorporation of neat micron h-BN significantly enhances the mechanical performance of the composites. Specifically, the addition of h-BN led to an increase in the elastic modulus from 36.82 GPa for the CF+/epoxy composite to 53.9 GPa for the CF+/EP-20%hBN composite, with the maximum tensile strength reaching 600 MPa. This substantial improvement can be attributed to the reinforcing effect of the h-BN particles within the epoxy matrix, which aids in better stress distribution and load transfer. It is also evident in the CF+/EP-20%hBN composite that the carbon fibers (CFs) exhibit a more extensive coating, which likely facilitates a stronger bond between the epoxy matrix and the CFs. This enhanced interfacial adhesion is a key factor contributing to the higher mechanical properties observed in this composite. The more comprehensive the coating on the fibers, the more effective the load transfer from the matrix to the fibers, leading to improved overall mechanical strength and stiffness. When the electrospray process is employed to coat CFs with neat micron h-BN and APTES-treated h-BN, there is also an increase in tensile properties, though not to the same extent as observed in the CF+/EP-20%hBN composite. This difference might come from the coating uniformity, the interaction between the h-BN particles and the carbon fibers, or the distribution of h-BN within the epoxy matrix. Moreover, it is noteworthy that samples coated through electrospraying exhibit a more brittle behavior compared to composites containing uncoated CFs or those with only micron h-BN in the resin that could be attributed to the nature of the electrosprayed coating. While the coating can enhance bond strength and load transfer, it might also constrain the flexibility of the fibers to some extent, leading to a more brittle fracture behavior. The thickness, uniformity, and mechanical compatibility of the electrosprayed layer with the CF and the epoxy matrix are critical in determining the balance between strength enhancement and brittleness. Therefore, while electrospraying can improve certain mechanical properties, it also necessitates careful optimization to avoid undesirable increases in brittleness.

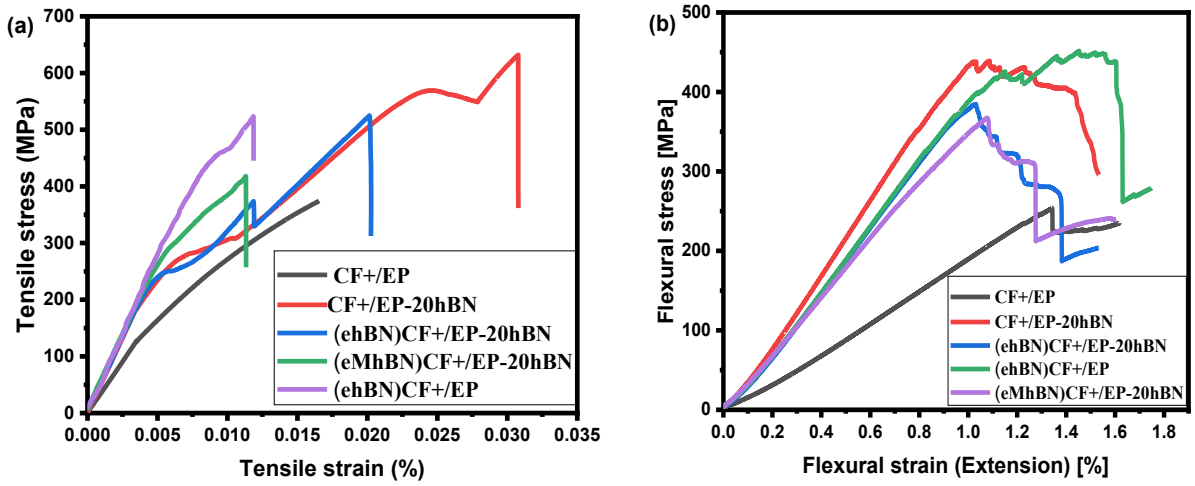

Figure 5.7 Stress-strain curves of CF/EP/h-BN composite samples: (a) tensile loading and (b) flexural loading.

In the samples treated with APTES, the strong bonding at the interfaces inhibits debonding during crack propagation, resulting in a high degree of brittle behavior. This is a critical observation that APTES treatment enhances bonding and thus increasing the brittleness of the composite. Nonetheless, the tensile performance of our composites is highly notable, especially when benchmarked against data from other studies. These comparisons underscore the superior mechanical properties of our composites, particularly in terms of tensile strength and elastic modulus. The incorporation of h-BN, combined with specific treatment processes like APTES, plays a significant role in these enhancements. However, the increased brittleness observed in APTES-treated samples underscores the need for a balanced approach in composite design, where the improvement in mechanical properties is carefully weighed against the potential for increased brittleness. Table S3 summarizes the details of tensile modulus and strength of multilayered carbon fiber incoperated into h-BN/epoxy composites provided in the Supporting Information.

The stress-strain curves of the composites under flexural loading are shown in Figure 7 (b). When neat micron h-BN is added to create the CF+/EP-20%hBN composite, both the initial slope and the peak of the curve are noticeably higher than that of neat CF+/EP, indicating that h-BN enhances the stiffness and strength of the material. The (ehBNCF)+/EP -20%hBN composite, which is the result of electrospraying neat micron h-BN onto carbon fibers, also surpasses the baseline in terms of UTS, yet it does not achieve the same performance as CF+/EP-20%hBN, suggesting that while electrospraying confers benefits, it may not be as efficacious as blending h-BN directly into the

epoxy. In contrast, the (eMhBNCF)+/EP-20%hBN composite-representing fibers electrosprayed with APTES-treated h-BN-shows an even higher peak than (ehBNCF)+/EP-20%hBN, which points to the APTES treatment's effectiveness in improving mechanical properties. However, its curve also exhibits a precipitous drop post-peak, which could be indicative of an increased brittleness. But it is better to inform that (ehBNCF)+/EP has very close results with CF+/EP-20%hBN and its flexural modulus reached 39.79 GPa. This phenomenon implies that while certain treatments and application methods can significantly bolster the interface bonding and, consequently, the composite's strength, they may also inadvertently reduce the material's ductility, leading to a trade-off between enhanced mechanical properties and material toughness. A substantial increase in flexural strength to 415 MPa, or 62.1%, is observed in the CF+/EP-20%hBN composite, wherein neat micron h-BN has been incorporated. This augmentation in strength underscores the reinforcing effect that the addition of h-BN has on the matrix, bolstering its resistance to bending stresses. For the (ehBNCF)+/EP composite, where electrospraying has been employed to apply neat micron h-BN onto the fibers, an enhanced flexural strength of 440 MPa is recorded, which represents a 71.3% improvement over the baseline. This enhancement is better than CF+/EP-20%hBN composite, indicating that electrospraying confers advantages. The composite with electrosprayed carbon fibers treated with APTES, designated as (eMhBNCF)+/EP-20%hBN, exhibits a 37.5% increase in flexural strength to 352 MPa. This is noted to be the least improvement among the modified composites, suggesting that the APTES treatment, while potentially bettering the h-BN to epoxy interface, might not significantly contribute to the flexural strength as much as untreated h-BN does. Table S4 summarizes flexural modulus and strength values of multi-scale h-BN/CF epoxy composites in different conFigureurations with the improvement percentages provided in Supporting Information.

Figure S4 shows the comparison of charpy impact strength values of the composite systems. The neat CF+/EP composite has the Charpy impact strength at 47.89 MPa, indicating its baseline toughness level. As a standard carbon fiber reinforced epoxy, it lacks any modification or additional reinforcement that could potentially absorb or dissipate impact energy more effectively. With the addition of neat micron h-BN, the CF+/EP-20%hBN composite exhibits a Charpy impact strength of 49.67 (KJ/m2), a modest increase over the CF+/EP. This suggests that the inclusion of h-BN particles at a 20% weight concentration slightly enhances the material's ability to withstand impact without catastrophic failure. The improvement indicates that h-BN could be contributing

to energy absorption within the composite matrix. The (ehBNCF)+/EP-20%hBN composite shows a Charpy impact strength of 49.76 (KJ/m2). This is a marginal improvement from the CF+/EP-20%hBN composite. The electrospray method may facilitate a more uniform distribution of h-BN particles, potentially leading to a slight increase in toughness. However, the small difference between the (ehBNCF)+/EP-20%hBN and CF+/EP-20%hBN suggests that the electrospray application method does not significantly enhance impact energy absorption compared to direct mixing. Interestingly, the (eMhBNCF)+/EP-20%hBN composite demonstrates a lower Charpy impact strength of 39.72 (KJ/m2), which is a reduction from the baseline CF+/EP composite. This indicates that the modifications made to this composite, possibly involving APTES treatment on the electrosprayed h-BN, do not enhance and may even detract from the material's impact toughness. The reduction could be due to several factors, including a potential compromise of the fiber-matrix interface, alterations in the h-BN structure that affect its interaction with the matrix, or the introduction of defects during the treatment process.

The slightly increased impact strength in the CF+/EP-20%hBN composites suggests that the incorporation of h-BN, to a certain extent, contributes positively to the energy dissipation during impact, possibly by preventing crack propagation or by absorbing energy through particle fracture and pull-out mechanisms. The decrease in impact strength for the (eMhBNCF)+/EP-20%hBN composite raises some concerns. It could suggest that the APTES treatment, while it may improve the chemical bonding between h-BN and the epoxy, may also lead to a stiffer and more brittle composite. This can result in a lower impact strength, as more brittle material tends to absorb less energy before failing. It is also possible that the APTES treatment could cause a change in the h-BN particle morphology or agglomeration, which might negatively affect the energy absorption capabilities. The overall toughness of a composite is governed by the synergistic effects of its constituents. In optimizing the toughness, one must balance the properties of the matrix, the reinforcement, and any coupling agents or treatments used. The results indicate that while h-BN has the potential to enhance the impact strength of carbon fiber/epoxy composites, the method of h-BN application and any subsequent treatments must be carefully controlled to avoid compromising the toughness. While h-BN is generally considered to improve the thermal and mechanical properties of composites, its impact on toughness, as measured by Charpy impact tests, is less straightforward and seems highly dependent on the preparation process and treatment of the material. For practical applications, it is essential to understand the balance between stiffness,

strength, and toughness. In industries where impact resistance is critical, such as automotive or aerospace, the drop in toughness for (eMhBNCF)+/EP-20%hBN would be a significant concern and could outweigh any other mechanical advantages. It may also inform material scientists and engineers about the need to adjust the composite formulation or processing techniques to achieve the desired balance of properties.

5.3.5 Cross sectional analysis of h-BN/carbon fiber reinforced composites

Figure. 8 presents FE-SEM images of the fractured regions of composite specimens, revealing distinct differences in the composite structures based on the composition and processing methods. As shown in Figure 8 (a), the CF+/EP composite displays noticeable delamination and cracks. The epoxy resin does not completely cover all of the carbon fibers, and the gaps between the carbon fibers and the epoxy matrix are clearly visible, indicating poor adhesion and interfacial bonding. In contrast, when neat h-BN is introduced into the epoxy resin to create the CF+/EP-20%hBN composite, as depicted in Figure 8(b), the size of the cracks is significantly reduced. A larger number of carbon fibers are coated with the resin, and the wettability between the h-BN reinforced epoxy resin and the carbon fibers is improved, enhancing the overall interfacial bonding. Furthermore, when the electrospray process is employed, both with unmodified and APTES-treated h-BN (shown in Figures 8(c) to 8(e)), there is a noticeable increase in the amount of carbon fibers coated with the epoxy resin. This improved coating is especially evident in the (eMhBNCF)+/EP-20%hBN composite, as seen in Figure. 8(e), where the carbon fibers are entirely covered by the coating, indicating thorough and uniform coverage. This indicates that the electrospray process, combined with the addition of h-BN, significantly enhances the interfacial bonding and distribution of the resin around the carbon fibers, leading to better mechanical and thermal properties in the composite material. The use of silane-modified h-BN powders in the electrospray process enhances this effect by fostering a stronger interfacial bond with epoxy. This improved bonding helps disperse the h-BN more effectively within the epoxy matrix, filling any gaps or vacancies and leading to a more uniform coating of the carbon fibers. Such uniformity in coating is essential for enhancing the thermal conductivity of the composites. A consistent layer helps minimize phonon scattering centers, which are points where energy carrying particles

(phonons) can be deflected. Reducing these scattering centers allows phonons to move more freely and efficiently through the composite material, directly contributing to improved thermal conductivity. This demonstrates the importance of both the modification of h-BN and the electrospray application technique in achieving optimal thermal properties in these composites.

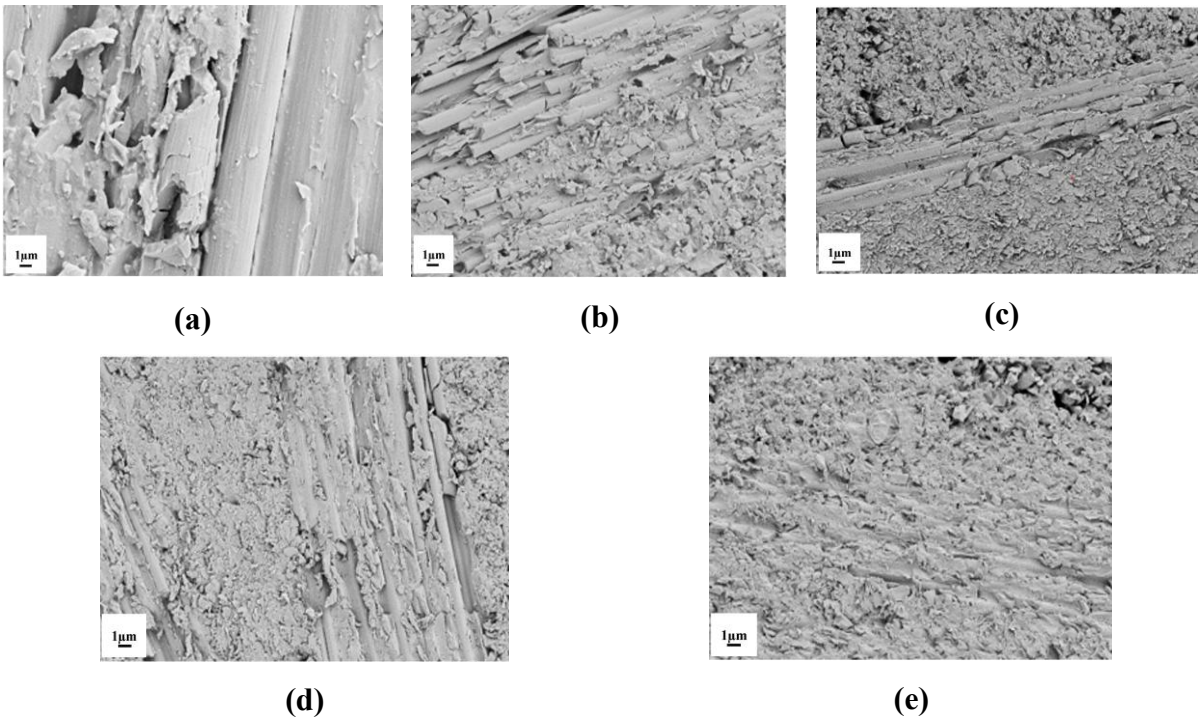

Figure 5.8 SEM images of (a) neat CF+/EP, (b) CF+/EP-20%hBN, (c) (ehBNCF)+/EP, (d) (ehBNCF)+/EP-20%hBN, and (e) (eMhBNCF)+/EP-20%hBN.

CT scans and X-ray imaging provide significant benefits for studying composite materials, enabling detailed internal inspection, non-destructive testing (NDT), 3D visualization, quantitative analysis, material characterization, and failure analysis. The CT scan images of h-BN/CF/epoxy composites are presented in Figure 9. It is observed that the incorporation of h-BN and silanized h-BN via the electrospraying process significantly reduces voids and defects within the composites. In addition, the porosity calculations for these composites were performed shown in Figure. 10. The porosity percentage of the CF+/EP composite was calculated as 10.47%. When h-BN was incorporated into the resin, this value decreased down to 8.23%. Samples treated with the electrospraying process showed an even greater reduction in porosity, with the minimum value observed in the (eMhBNCF)+/EP-20%hBN sample. The CT scan images confirmed that reducing

porosity is essential for improving heat transfer. This is due to the high packing density, which facilitates the easier movement of phonons. Additional details of the porosity images from different angles and views are provided in Figure S5. This data indicates that the reduction of porosity through the electrospraying process and silanization not only enhances the structural integrity of the composites but also significantly improves their thermal conductivity. Comprehensive analysis from various imaging techniques highlights the importance of optimizing porosity to attain better thermal performance in the composite materials, aligning with the thermal conductivity results.

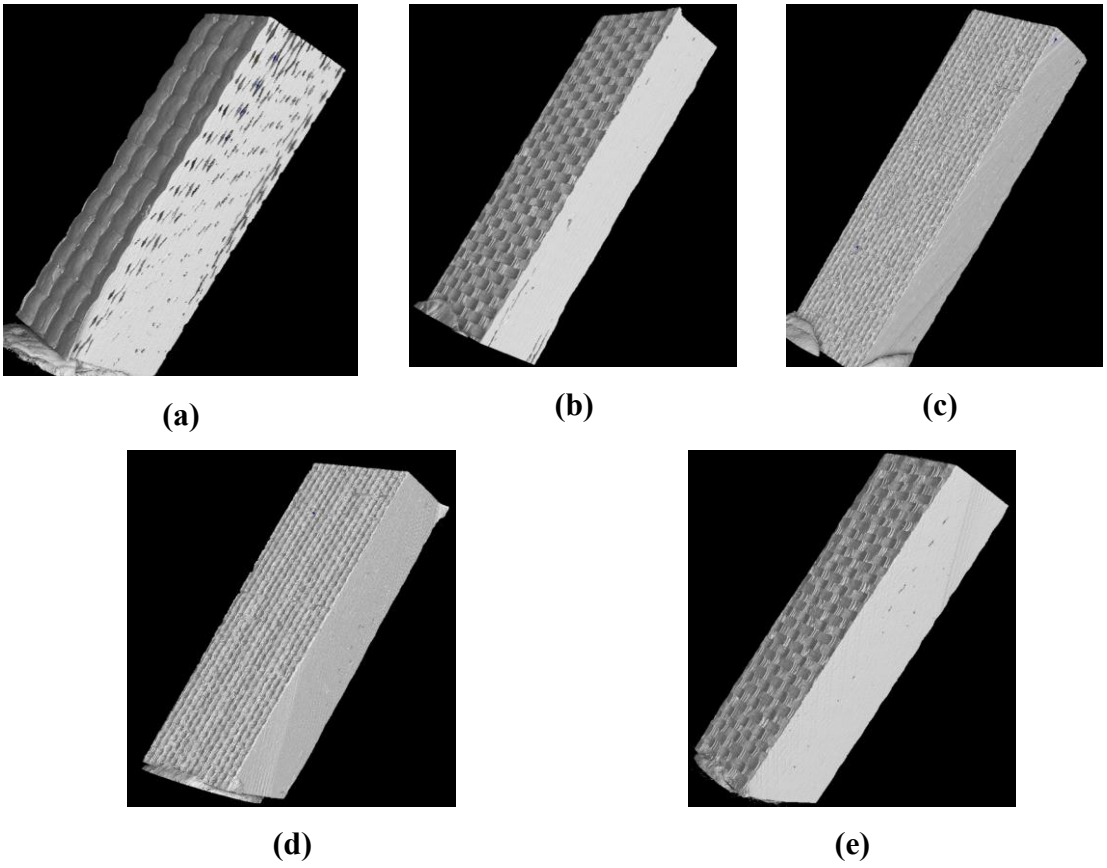

Figure 5.9 CT scans X-ray images of (a) CF%/EP, (b) CF+/EP-20%hBN, (c) (ehBNCF)+/EP, (d) (ehBNCF)+/EP-20%hBN, and (e) (eMhBNCF)+/EP-20%hBN specimens.

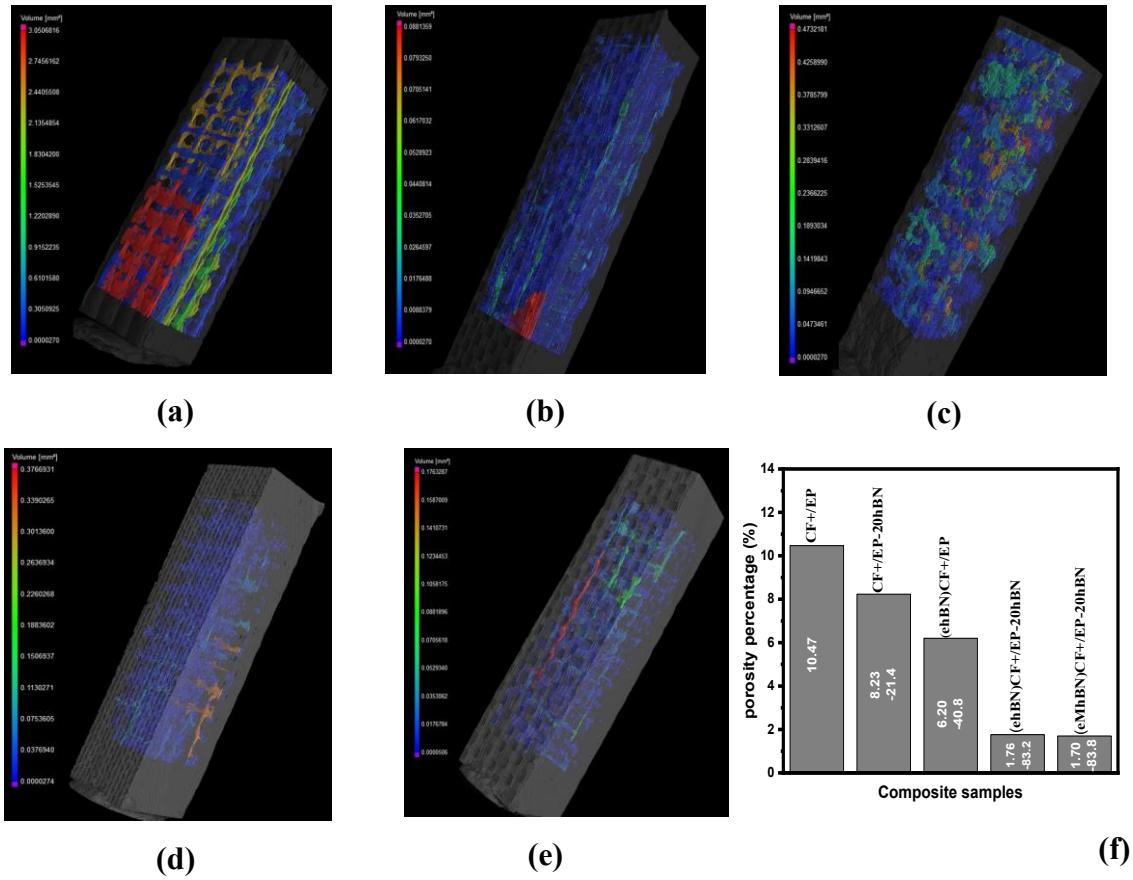

Figure 5.10 Porosity by CT scans-X-ray images of (a) CF+/EP, (b) CF+/EP-20%hBN, (c) (ehBNCF)+/EP, (d) (ehBNCF)+/EP-20%hBN (e) (eMhBNCF)+/EP-20%hBN and (f) porosity calculations for h-BN/CF/epoxy composite specimens.

5.4 Conclusions

This study effectively managed the directional thermal conductivity and mechanical performance of a CF reinforced epoxy matrix by incorporating both neat h-BN and silanized h-BN, carefully controlling their physical and chemical interactions. Three main conFigureurations of h-BN were employed to optimize heat transfer by forming efficient thermal bridges: embedded within the matrix, electrosprayed onto the carbon fabric, and a combination of both within a single composite structure. During thermal treatment, hydroxyl groups were introduced to the h-BN surface,

increasing the oxygen content up 13.76 %. Subsequently, five different composite samples were fabricated for thermal conductivity and mechanical testing, utilizing various combinations of materials, including carbon fiber, pristine h-BN, APTES-treated h-BN, and epoxy. Thermal conductivity analysis demonstrated that all manufacturing processes, including APTES treatment and electrospraying, improved thermal conductivity compared to the reference sample CF+/EP, which had a thermal conductivity of 1.07 W/mK. The highest thermal conductivity, 2.31 W/mK, was achieved in the (eMhBNCF)+/EP-20%hBN sample. This particular composite was prepared by electrospraying carbon fibers with APTES/heat-treated h-BN and using a resin mixture of epoxy with 20 wt% neat micron h-BN. CT scan images of the h-BN/CF/epoxy composites revealed that the application of h-BN and silanized h-BN via electrospraying significantly reduced voids and defects within the composites. Additionally, mechanical testing showed that all treatment methods used in this study improved the mechanical properties compared to the reference sample (CF+/EP). This study highlights the potential for customized thermal conductivity solutions in sectors such as aerospace and high-performance automotive manufacturing. The composites developed here offer significant advantages over traditional materials like steel or aluminum, including superior thermal management and mechanical strength by providing a seamless transition to advanced material technologies in various manufacturing environments.

Supplementary

Table 5.S1 DOE of the Electrospraying of h-BN on CFs.

Run	Applied Voltage (kV)	Distance (cm)	Flow Rate (ul/min)
1	12	8,5	320
2	7	5	320
3	7	5	160
4	7	8	320
5	10	10	240
6	12	5	320

7	7	5	320
8	10	7	240
9	12	5	160
10	10	7	240
11	10	7	240
12	10	7	240
13	12	8	160
14	10	7	240
15	7	8	320
16	10	7	400
17	5	7	240
18	10	7	80
19	10	7	240
20	12	5	160
21	12	8	160
22	7	8	160
23	12	5	320
24	10	7	240
25	10	7	240
26	7	5	160
27	10	4	240
28	14	7	400
29	12	8	320
30	7	8	160

Table 5.S2 Summary of the manufacturing conditions of h-BN/carbon fiber/epoxy composites.

Sample Name	Silane agent	hBN/epoxy (wt.%)	Hot press Temperature (°C)	Hot press Time (h)	Composite system definition
CF+/EP	-		100	5	Neat carbon fiber and through CFs resin neat epoxy
CF+/EP-20%hBN	-	20	100	5	Neat carbon fiber and through CFs resin 20 wt% neat micron h-BN
(ehBN)CF+/EP	-		100	5	CFs electrosprayed by neat h-BN and through CFs resin neat epoxy
(ehBN)CF+/EP-20%hBN	-	20	100	5	CFs electrosprayed by neat h-BN and through CFs resin 20 wt% neat micron h-BN
(eMhBN)CF+/EP-20%hBN	APTES	20	100	5	CFs electrosprayed by APTES modified heat treated h-BN and through CFs resin

	20 wt% neat micron h-BN

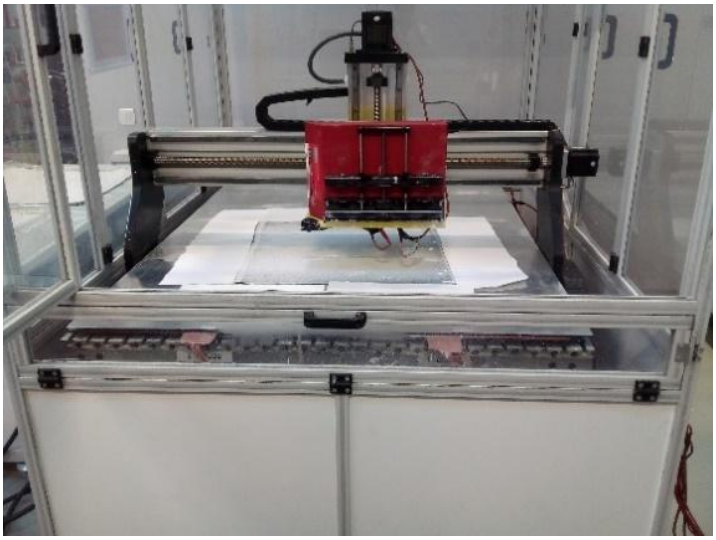

Figure 5.S1 Electrospraying set-up for the deposion of h-BN particles onto carbon fabrics.

Table 5.S3 The summary of Tensile modulus and strength values of multi-scale h-BN/CF epoxy composites in different conFigureurations with improvement percentages

Specimens	Tensile modulus (GPa)	Improvement (%)	Tensile strength (MPa)	Improvement (%)
CF+/EP	36.82 ±1.95	-	358.00 ±21.89	-
CF+/EP-20%hBN	53.90 ±1.80	46.38	600.00 ±46.80	67.50
(ehBNCF)+/EP	51.71 ±1.87	40.43	496.40 ±25.60	38.60

(ehBNCF)+/EP - 20%hBN	53.07 ±1.92	44.07	512.50 ±27.34	43.15
(eMhBNCF)+/EP - 20%hBN	50.48 ±6.02	40.20	426.20 ±29.35	19.00

Table 5.S4 The summary of flexural modulus and strength values of multi-scale h-BN/CF epoxy composites in different conFigureurations with improvement percentages.

Specimens	**Flexural modulus (GPa)**	**Improvement (%)**	**Flexural strength (MPa)**	**Improvement (%)**
CF+/EP	19.41 ±2.45	-	256.00 ±15.67	-
CF+/EP-20%hBN	39.12 ±3.70	101.50	415.00 ±23.78	62.10
(ehBNCF)+/EP	39.79 ±1.16	105.00	440.00 ±45.65	71.30
(ehBNCF)+/EP-20%hBN	30.95 ±6.42	59.40	363.00 ±21.83	41.70
(eMhBNCF)+/EP-20%hBN	31.85 ±2.08	64.09	352.00 ±11.95	37.50

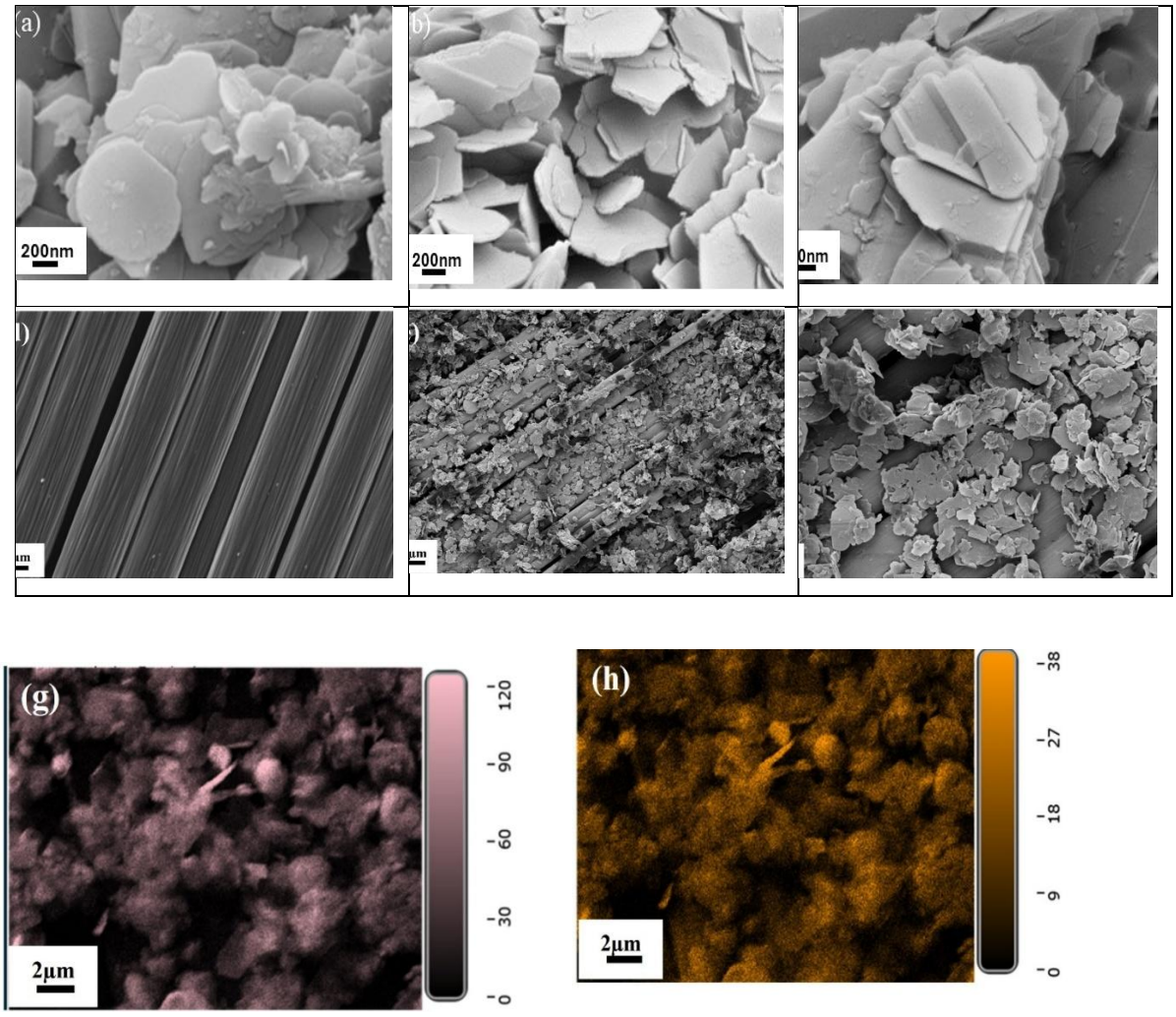

Figure 5.S2 SEM images of (a) neat h-BN, (b) heat-treated h-BN, (c) APTES modified h-BN particles, (d) neat CFs, (e,f) h-BN deposited CFs at different magnifications, (g) Nitrogen EDX analysis of h-BN deposited CFs and (h) Boron EDX analysis of h-BN deposited CFs.

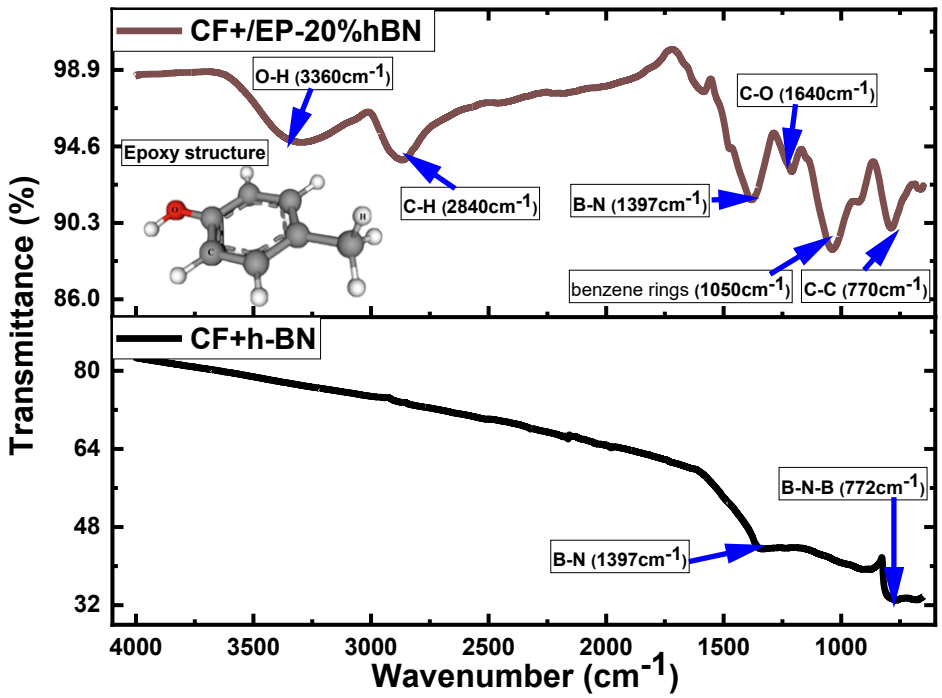

Figure 5.S3 FTIR spectra of h-BN deposited on CFs (CF+h-BN) and CF+/EP-20%hBN composite specimen.

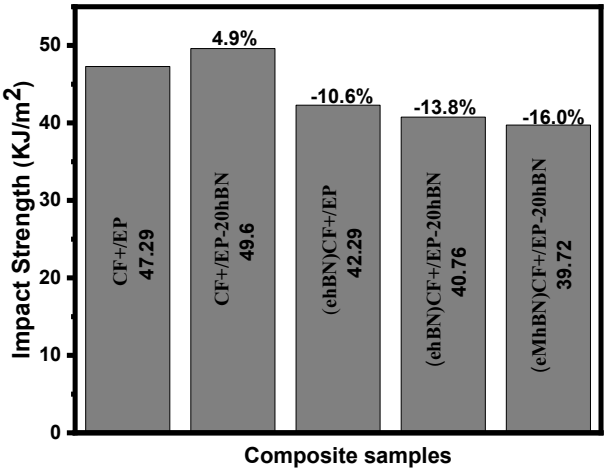

Figure 5.S4 Impact strength values of the composite systems from Charpy tests.

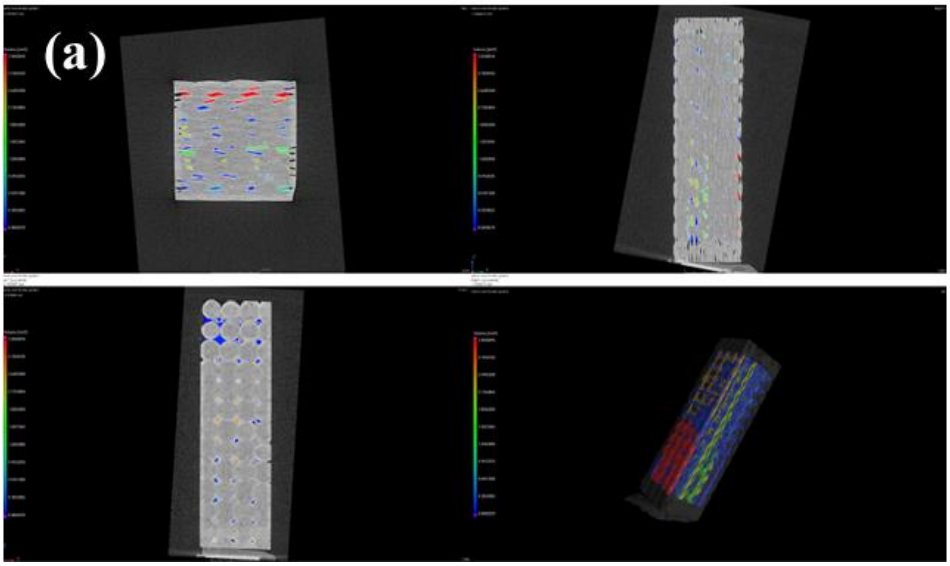
(a)

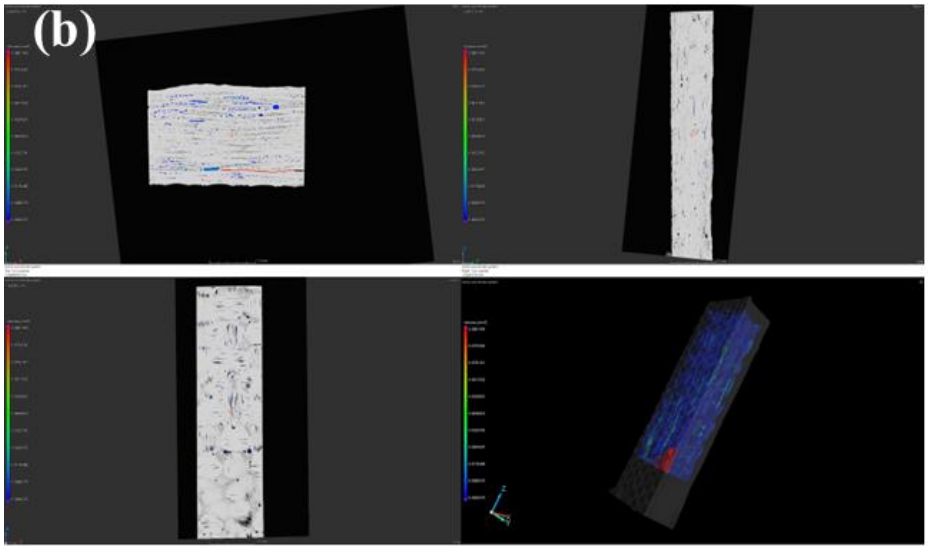
(b)

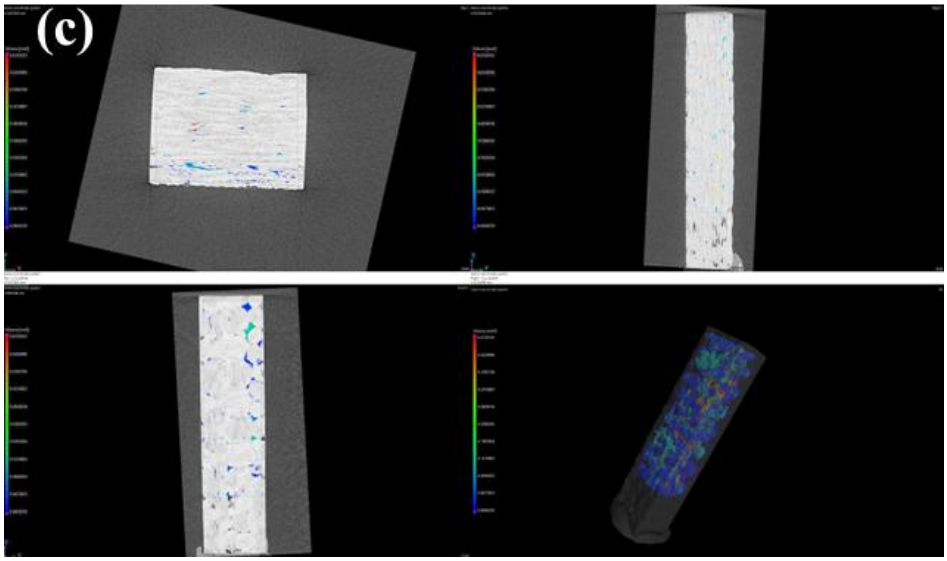
(c)

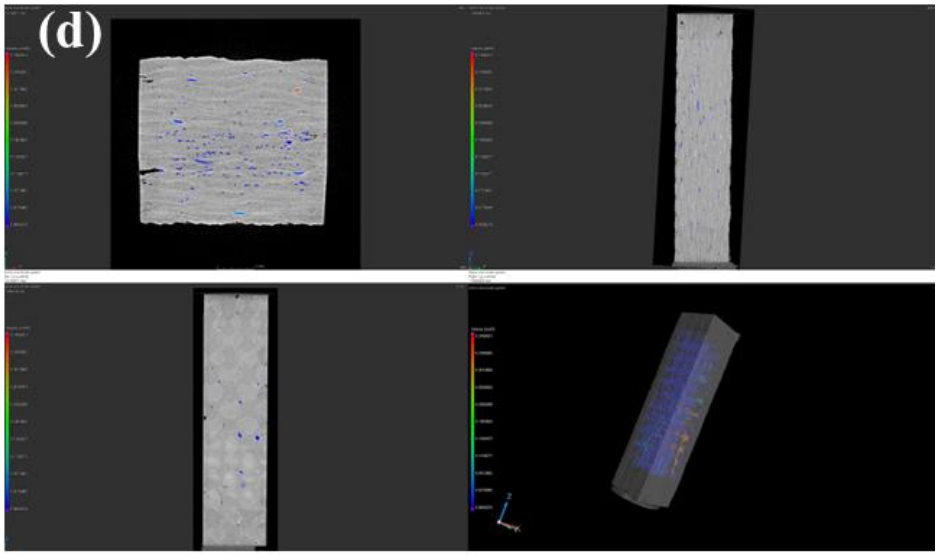
(d)

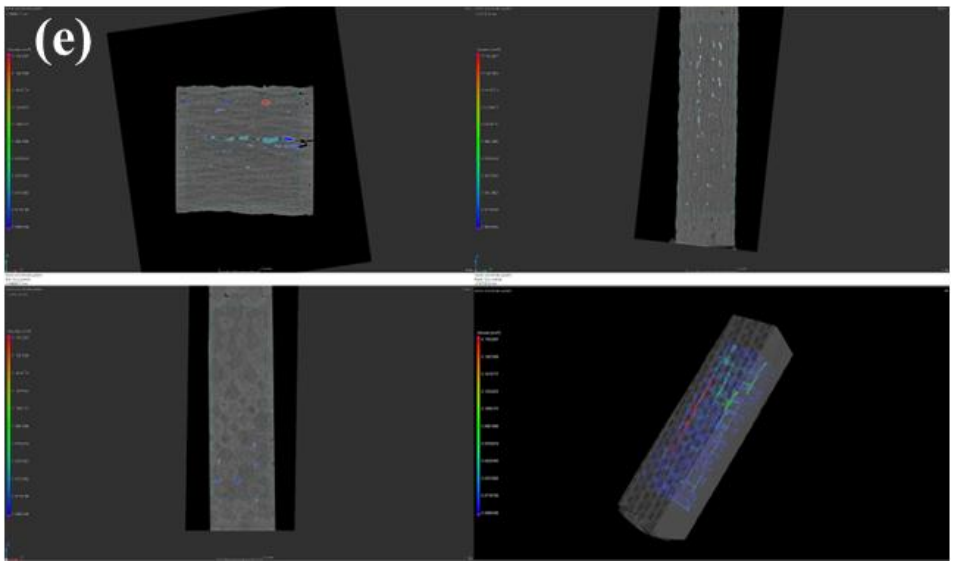

Figure 5.S5 Porosity by CT scans-X-ray images of (a) CF+/EP, (b) CF+/EP-20%hBN, (c) (ehBN)CF+/EP, (d) (ehBN)CF+/EP-20%hBN, and (e) (eMhBN)CF+/EP-20%hBN composite specimens.

6. MULTI-SCALE INTERFACE ENGINEERING OF EPOXY COMPOSITES REINFORCED WITH HEXAGONAL BORON NITRIDE AND CARBON FIBERS BY CONTROLLING DIRECTIONAL PERFORMANCE THROUGH PHYSICAL AND CHEMICAL INTERACTIONS

The low thermal conductivity of carbon fiber (CF) reinforced epoxy composites primarily arises from porosity and fabrication-induced defects, which disrupt thermal pathways and hinder heat transfer efficiency. This study demonstrates pathway heat control in both out-of-plane and in-plane directions by incorporating hexagonal boron nitride (h-BN) as a thermally conductive agent by conFigureuring interface interactions on the CF fabric and within the epoxy resin while evaluating physical and chemical interactions. Two integration techniques of dip coating and electrospraying were employed to apply h-BN, effectively creating robust h-BN layers on CF fabrics and dispersing neat or silane-modified h-BN within the epoxy matrix by combining vacuum bag and hot compression processes to reduce void content. The highest out-of-plane thermal conductivity achieved was 1.3 W/mK, a 166 % improvement over the epoxy's thermal conductivity of 0.2 W/mK, using electrosprayed silane-modified h-BN on carbon fibers combined with a 20 wt. % silane-modified h-BN loading in the epoxy matrix with overall 11 % h-BN loading in the composite structure. Regarding mechanical properties, the composite incorporating neat h-BN in both the epoxy matrix and dip-coated layers on carbon fibers demonstrated exceptional performance, achieving a 127 % increase in flexural modulus and a 49 % enhancement in Charpy impact strength compared to reference carbon fiber reinforced epoxy composites. Delamination and porosity were controlled by CT scan X-ray and microscopic techniques indicating that resizing CF fabrics enhances directional thermal conductivity in CF/epoxy composites by controlling porosity, achieving an approximately 81% reduction in porosity for the silanized h-BN sample. These findings underscore that functionalized h-BN particles triggered phonon transfer much better than neat h-BN in resin whereas h-BN particles sprayed by electrospraying process providing much more alignment of particles compared the bulk dispersion of dip-coating

6.1 Review

Two-dimensional (2D) solid materials can significantly enhance phonon transport, thereby boosting thermal conductivity. This improvement arises from several key factors, including high atomic packing density, robust in-plane covalent bonding, reduced dimensional scattering, high phonon group velocity, and minimized anharmonic effects. Consequently, 2D van der Waals layered materials such as graphene, semiconductors like GaS, boron nitride, and transition metal dichalcogenides like TiS_2 have garnered substantial interest for their superior heat transfer and mechanical properties, making them promising candidates for advanced thermal management applications [140]. Hexagonal boron nitride (h-BN) distinguishes itself among two-dimensional (2D) materials as an exceptional candidate for thermal management applications due to its unique combination of properties that surpasses alternatives like graphene and transition metal dichalcogenides. While graphene offers extremely high thermal conductivity, its conductive nature can restrict its use in systems requiring electrical insulation. In contrast, h-BN provides both high thermal conductivity and excellent electrical insulation, making it particularly suitable for applications in electronics and thermal interface materials where dielectric properties are critical. Additionally, h-BN exhibits high chemical and thermal stability, retaining its structural integrity at elevated temperatures and in harsh chemical environments, which significantly expands its range of potential applications (W. Chen et al., 2024). While h-BN offers numerous advantages for thermal management applications, there are several disadvantages like processing challenges, agglomeration and compatibility issues.

Surface modification of h-BN is crucial for improving its integration into composite structures, especially in thermal management applications that utilize woven carbon fibers and epoxy matrices. The modification of h-BN with silane or other agents enhances compatibility between the inorganic h-BN and the organic epoxy matrix, resulting in stronger interfacial bonds that promote effective thermal transport throughout the composite (Oh & Kim, 2019). During this process, silane molecules are chemically grafted onto the surface of h-BN plates. This attachment forms a functional layer on the h-BN particles, enhancing compatibility with organic matrices by introducing reactive sites that facilitate stronger interfacial bonding in composite structures. Several studies have explored the impact of silanization on materials properties, particularly

focusing on how silanization affects performance and compatibility within composite structure. For instance, Lu et al. selected several typical modifiers (silane coupling agents KH550 and KH570) to modify boron nitride to improve its interfacial compatibility with epoxy resin. The thermal conductivity of BN-KH570/Epoxy composite at 26 wt.% loading reached 1.2 W/mK, which is 7.6 times that of pure epoxy resin. In addition, Atefe et al. investigated surface modification of h-BN nanoparticles using varying concentrations of vinyltrimethoxysilane (VTMS) to enhance their compatibility within composite matrices (Farahani et al., 2023). Prior to silane treatment, the h-BN nanoparticles were hydroxylated with a 5 M sodium hydroxide solution to introduce hydroxyl groups, facilitating subsequent silanization. The surface modification led to notable improvements in the mechanical properties, with the maximum tensile stress observed in the silanized samples reaching 9.3 MPa. Moreover, Yongbo et al. examined the effects of silanization on h-BN using APTES molecules, focusing on the enhancement of thermal conductivity and increased the thermal conductivity of the composite, reaching a peak of 0.85 W/mK at a filler loading of 30 wt.% (Yan et al., 2024). A review of the literature indicates that surface modification of h-BN is essential prior to its use in composite manufacturing. All these functionalization processes on h-BN indicate that silanization is a crucial surface modification technique that enhances its compatibility with polymer matrices, improving the thermal performance of composites.

Beyond surface treatment, controlling adhesion and curing during manufacturing is crucial for optimizing the thermal and mechanical properties of h-BN-based composites. Stronger interfacial bonding ensures uniform h-BN dispersion, enhancing conductivity and strength. Surface modifications and optimized manufacturing processing maximize h-BN's benefits, making these composites ideal for thermal management and structural applications. For instance, Zhang et al. used electrospinning to create a polymer-based modified-BN composite with uniform orientation, achieving a thermal conductivity of 7.29 W at 30 wt.% modified-BN and a tensile strength of 24.06 MPa. Additionally, Gu et al. developed a boron nitride/polyamide acid (mBN/PAA) composite via electrospinning, which was then converted into a thermally conductive mBN/polyimide (mBN/PI) composite through hot pressing at 320°C and 5 MPa for 20–30 min. The resulting mBN/PI composite, containing 30 wt.% mBN, achieved a thermal conductivity of 0.696 W/mK. Building on these advantages, incorporating h-BN with various surface modifications and composite

fabrication methods offers diverse approaches for enhancing thermal conductivity and mechanical properties in composite materials.

Up to now, there have been several attempts to control surface chemistry and process techniques separately and not providing the ideal method to integrate h-BN in both matrix and interface. In our previous work, graphene and h-BN were configured in carbon fiber reinforced epoxy composites to tailor mechanical performance and electrical conductivity. In the current study, six distinct configured were developed to optimize thermal conductivity in both in-plane and out-of-plane directions while enhancing mechanical properties by applying different sizing methods to enhance the interfacial interactions between the fiber and matrix. These configurations included applying h-BN on woven carbon fabric via electrospraying and dip coating, incorporating h-BN directly into the epoxy resin, and combining both techniques. The h-BN was functionalized with APTES to improve interfacial bonding and reduce stress concentrations, facilitating efficient conduction pathways. This comprehensive approach achieved significantly high thermal conductivity, a result not previously reported, while at 20 wt.% filler loading, mechanical performance was notably enhanced by integrating h-BN through electrospraying and dip coating. The study presents a detailed examination of key fabrication parameters, including electrospraying and dip coating techniques, hot pressing methods, h-BN incorporation, the silanization process, and the development of multilayered structures specifically, 32-layer assemblies of CF and h-BN resin layers for thermal conductivity tests and 16-layer assemblies for mechanical tests. The enhancements in thermal conductivity and mechanical strength were comprehensively examined through spectroscopic, gravimetric, and morphological characterizations, offering detailed insights into the physical and chemical interactions within the composite structure.

6.2 Experimental Part

6.2.1 Materials

Hexagonal boron nitride (h-BN) with a particle size of 1 to 10 μm and a purity of 99.5% was obtained from Civelek Porselen Company, Turkiye. The silane coupling agent, 3-

aminopropyltriethoxysilane (>98%), was sourced from Sigma-Aldrich. Acetic acid (100%), ethanol and n-hexane, used as a solvent in the silanization and manufacturing processes, were obtained from Tekkim. All chemicals were used directly without further purification. Plain carbon fabrics with a weight of 200 gsm, supplied by Dost Chemistry Company, were utilized in the fabrication of h-BN-reinforced epoxy-based composites. Sika Biresin® CR131, composed of 50%–100% bisphenol A diglycidyl ether (DGEBA), 10%–20% bisphenol F diglycidyl ether (DGEBF), and 5%–10% 1,4-bis (2,3 epoxypropoxy) butane, along with the CH132-5 hardener (based on triethylenetetramine [TETA]), was provided by Tekno Chemicals Inc, Turkiye.

6.2.2 Surface modification of h-BN particles by silanization

The surface of h-BN was activated through thermal treatment at 1000°C for 5 min in air, increasing its oxygen content and enhancing its interaction with silane molecules during silanization. After treatment, the furnace was cooled to room temperature. Then, the silanization of h-BN in composite production is crucial for several reasons done. Chemical functionalization enhances dispersion, and adhesion, and prevents agglomeration of h-BN particles within the polymer matrix. In order to modify the surface of thermally treated micron h-BN, 5.0 g of h-BN was dispersed in 50 mL of n-hexane containing 2.5 mL APTES. This mixture was sonicated for 15 min using an ultrasonic probe sonicator. After sonication, 15 drops of acetic acid were added to adjust the pH of the mixture to 4-5. The reaction mixture was then stirred at room temperature for an additional 15 min using a magnetic stirrer. Once the reaction was complete and the mixture cooled, it was filtered and washed twice with distilled water. Finally, the silane-modified h-BN was dried in an oven at 80°C for 1 h to remove any remaining solvent.

6.2.3 Resizing carbon fabrics by electrospraying and dip coating techniques

6.2.3.1 Carbon Fabric resizing by electrospraying of h-BN particles

Silanized h-BN particles were first gone to a solution-making process, where 10 wt.% silanized h-BN was dispersed in ethanol and mixed for 15 min using a magnetic stirrer to ensure uniform dispersion. Subsequently, the electrospray process, illustrated in Figure 1, was employed to coat the silanized h-BN onto woven carbon fibers measuring 60 cm × 60 cm, demonstrating scalability and potential for mass production. During the process, a voltage of 14 kV was applied, with the nozzle positioned 7.5 cm from the carbon fiber surface. The h-BN suspension was delivered at a controlled flow rate of 400 µL/min, while the nozzles moved at a speed of 6 mm/s in both the x and y directions to achieve an even coating. The procedure involved electrospraying one side of the CF fabric, followed by a drying period of 24 h at room temperature to ensure the ethanol evaporated completely and the coating adhered properly. After drying, the process was repeated on the opposite side of the fabric to achieve uniform coverage on both sides. This precise and controlled electrospray method not only ensured an even distribution of silanized h-BN on the carbon fibers but also demonstrated its feasibility for producing high quality coatings suitable for scaled up applications.

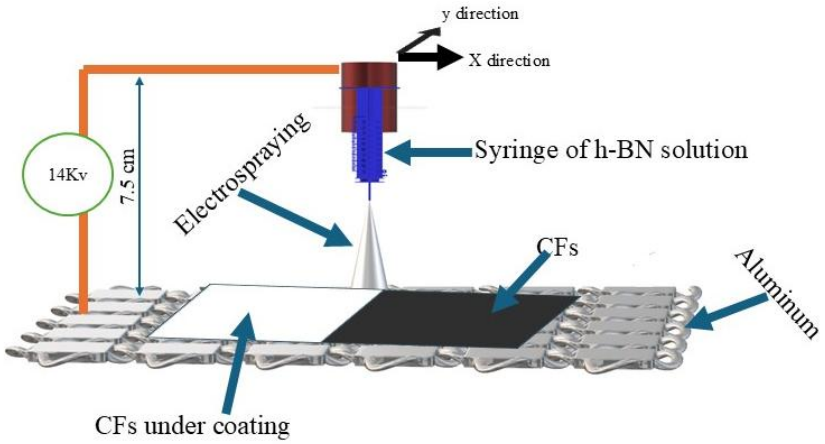

Figure 6.1 The schematic representation of electrospraying process on carbon fabrics (CFs).

6.2.3.2 Carbon Fabric resizing by dip coating of h-BN particles

To assess the integrity and performance of the h-BN layer applied to carbon fibers through electrospraying in terms of thermal and electrical conductivity, an alternative dip-coating method was also employed for comparison. In the dip-coating process, carbon fiber sheets aligned vertically, each measuring 20 x 20 cm, were immersed in a 10 wt. % h-BN suspension for 15 min to ensure uniform coating by stretching the fabrics. Following the immersion, the coated carbon fibers were dried at 60°C for 24 h to promote adhesion and achieve stable layer formation. The process images, shown in Figure S.1 (Supplementary document), illustrate the immersion and drying stages, highlighting the preparation conditions.

6.2.4 Epoxy resin manufacturing with h-BN particles

Initially, 250 g of ethanol were combined with 70 g of filler (either neat h-BN or silanized h-BN) and sonicated for 2 h to reach high degree of stability. Subsequently, 350 g of epoxy were heated to 60 °C in order to attain high degrees of h-BN dispersion. After the completion of sonication process, the prepared mixture was added to the heated epoxy and stirred continuously for 48 h at 50 °C to allow ethanol evaporation. Subsequently, a 30-min degassing process was applied and then 98 g of hardener was incorporated into the mixture, which was then mixed and degassed for an additional 15 min. The pre-treated composition becomes ready for the curing process to attain final structure.

6.2.5 h-BN integrated CF reinforced epoxy composites by vacuum bagging and hot compression processes

After preparing the electrosprayed and dip-coated carbon fibers (CFs) with either neat h-BN or silanized h-BN, the fibers were cut into two sizes: 10 x 10 cm^2 with 16 layers for thermal conductivity testing and 30 x 30 cm^2 with 8 layers for mechanical testing. The resin, prepared as described in section 2.3.3, was then applied to the fibers using the hand lay-up method. Following

this, the samples were placed under vacuum and subjected to hot pressing for curing. This process involved applying a pressure of 2.5 tons at 100°C for 5 h. The manufacturing stages of the h-BN/carbon fiber/epoxy composites are shown in Figure 2, and the composite systems along with their characteristics are provided in Table 1.

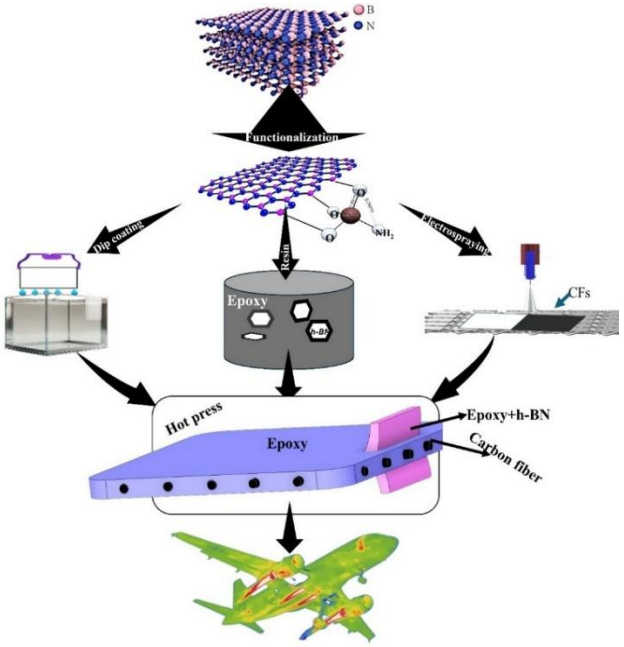

Figure 6.2 A schematic illustration of a stepwise production process of h-BN/CF/epoxy composites.

Table 6.1 Summary of the configuration designs of h-BN/carbon fiber/epoxy composite specimens.

configuration	**Methods**	**Sample Name**	**h-BN content in composite (wt. %)**	**Hot press Temperature (°C)/Time (h)**	**Composite system definition**

Type 1	-	-	Resin preparation	CF+/EP	-	100/5	Neat carbon fiber and through CFs, resin neat epoxy used.
Type 2	-	-	Resin preparation	CF+/EP-20%hBN	6.0	100/5	Neat carbon fiber and through CFs, resin 20 wt.% neat h-BN used.
Type 3	Dip coating	-	Resin preparation	(dhBN)CF+/EP	8.0	100/5	CFs dip coated by neat h-BN and through CFs, resin neat epoxy used.
Type 4	Dip coating	-	Resin preparation	(dhBN)CF+/EP-20%hBN	12.0	100/5	CFs dip coated by neat h-BN and through CFs, resin 20 wt.% neat h-BN used.
Type 5	Dip coating	silanization	Resin preparation	(dhBN)CF+/EP-20%MhBN	11.5	100/5	CFs dip coated by neat h-BN

							and through CFs, resin 20 wt.% APTES modified h-BN used.
Type 6	Elec tro-spra ying	silani zatio n	Resin prepar ation	(eMhBN)CF +/EP-20%MhBN	11.0	100/5	CFs electrospray ed by APTES modified h-BN and through CFs, resin 20 wt.% neat h-BN used.

6.2.6 Characterization

Fourier transform infrared (FTIR) spectra were obtained using an IS10 FT-IR spectrometer to identify the active functional groups on the surface of the h-BN material. Crystallinity was analyzed through X-ray diffraction (XRD) using a Bruker D2 PHASER Desktop equipped with a CuKα radiation source, covering a 2θ range from 5° to 80°. A Renishaw inVia Reflex Raman Microscope with a 532 nm edge laser was employed at room temperature, scanning the range from 100 to 3500 cm^{-1}. Thermogravimetric analysis (TGA) was conducted with a Mettler Toledo TGA/DSC 3+ thermal analyzer, heating the samples at 10 K/min from 25°C to 1000°C under a 50 mL/min N2 flow. Surface morphology was examined using a Leo Supra 35VP Field Emission Scanning Electron Microscope (FE-SEM). Microcomputed tomography (MicroCT) analysis was performed using a Phoenix V|tome|x M 300/180 system (Baker Hughes/Waygate Technologies),

with a voxel size of 15 µm, operating at 80 kV, 200 µA, and no filters. The CT images were reconstructed and analyzed with Datos|x (version 2.14.0) and VGSTUDIO MAX (2023.1) software. Thermal conductivity (TC) was measured using the Hot Disk method with a C02-12 device. The flexural properties of the specimens were determined via three-point bending tests according to ASTM D790 standards, with a span-to-thickness ratio of 16:1. Charpy impact tests were performed on V-notched rectangular specimens (80 x 10 mm) to assess impact strength, following ISO-179 standards, using a 5 J Charpy pendulum (CEAST 9050, Instron, Canton, MA). At least five specimens per group were tested. Additionally, Dynamic Mechanical Analysis (DMA) was conducted on samples measuring 65 x 10 x 4 mm using a Mettler Toledo DMA device, with tests performed in single cantilever mode at a heating rate of 3 °C/min, a frequency of 1 Hz, and a temperature range of 25 to 250°C, with a minimum of five specimens per group to ensure reliable results.

6.3 Results and Discussion

6.3.1 Structural characterization of functionalized h-BN particles

The functionalization of h-BN by silanization is carried out to enhance its compatibility with polymer matrices, improving interfacial adhesion, dispersion, and thermal conductivity in composites. In this way, the FTIR results of multilayered structures of h-BN/CF/epoxy and modified h-BN/CF/epoxy, prepared via dip coating and electrospraying methods, are presented in Figure.3. In the case of carbon fibers (CFs), the molecular vibrations of atoms are generally inactive in FTIR due to their symmetrical atomic arrangements, resulting in the absence of detectable functional groups in the FTIR spectra (Ismail et al., 1997). Therefore, as shown in Figure 3 (a), the peaks observed correspond primarily to the epoxy matrix. These peaks, located at 770, 1050, 1640, 2840, and 3360 cm^{-1}, are attributed to vibrations of the C–C, benzene ring, C–O, C–H, and O–H functional groups, respectively. It is evident that the FTIR peaks correspond to various molecular vibrations associated with the atoms that make up the epoxy resin. Upon the introduction of h-BN into the resin, specifically in the CF+/EP-20%hBN composite, a new peak

appears around 1397 cm^{-1}, which can be attributed to the in-plane vibration of boron and nitrogen (B-N). Additionally, another peak related to the out-of-plane B-N-B vibration appears around 770 cm^{-1}. However, this peak overlaps with the C–C vibration of the epoxy structure, making it less distinguishable. In the case of applying h-BN to carbon fibers via dip coating, the FTIR spectra for (dhBN)CF+/EP and (dhBN)CF+/EP-20%hBN primarily show peaks corresponding to both epoxy and h-BN. Notably, the intensity ratio of the h-BN-related peaks relative to those of the epoxy matrix increases, indicating a higher presence of h-BN in the composite when compared to CF+/EP-20%hBN sample. An interesting observation arises when silanized h-BN is introduced to the multilayered structure via dip coating and electrospraying. In these samples, a new peak around 1070 cm^{-1} appears, which is attributed to the Si–O–Si stretching vibration, confirming the successful incorporation of silanized h-BN into the h-BN/CF/epoxy composite structure. In summary, the FTIR analysis reveals the successful incorporation of h-BN and silanized h-BN into the CF/epoxy composite, as well as the evolution of new peaks that reflect the presence of these additives and their interaction with the epoxy matrix.

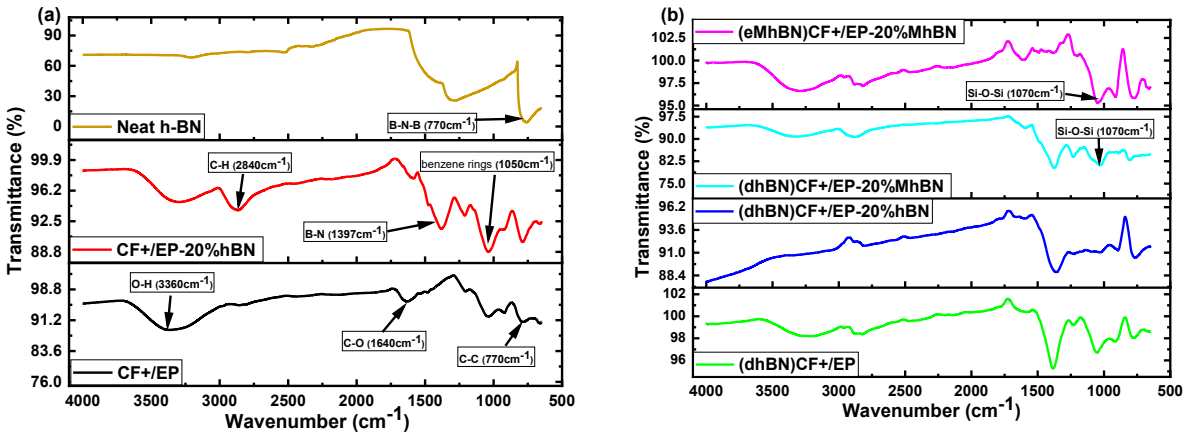

Figure 6.3 FTIR spectra (a) comparison of CF+/EP, CF+/EP-20%hBN, b) comparison of (dhBN)CF+/EP, (dhBN)CF+/EP-20%hBN, (dhBN)CF+/EP-20%MhBN, (eMhBN)CF+/EP-20%MhBN.

Raman spectroscopy analysis of the composites fabricated in this study is shown in Figure S.2. in order to evaluate molecular vibrations and the changes in polarization of atoms since Raman characterization is particularly effective in the identification of vibrational modes associated with symmetrical atomic movements (Thapliyal et al., 2022). In the Raman spectra of the composite

specimens, two prominent peaks are observed at 1357 cm^{-1} (D band) and 1600 cm^{-1} (G band), which are characteristic of carbon-based materials such as carbon fibers (CFs). The D band corresponds to the disorder or the defect content in the carbon structure, while the G band is associated with the E_{2g} phonon mode, a key feature of graphitic carbon materials. In addition to these carbon-related peaks, two other peaks are attributed to C-H symmetrical vibrational modes. These peaks arise from vibrations of carbon and hydrogen atoms, often due to the moisture or adsorbed water on the surface of the carbon fibers. These modes reflect the presence of adsorbed water or organic species on the CFs. For the CF+/EP-20%hBN multilayered structure, the most dominant peak in the Raman spectrum is associated with the E2g mode of hexagonal boron nitride (h-BN), which is a signature of this material's in-plane optical vibration. The E2g mode involves the opposite motion of boron and nitrogen atoms within the hexagonal lattice of h-BN, with boron atoms vibrating in one direction and nitrogen atoms vibrating in the opposite direction. This symmetrical vibration mode is highly characteristic of h-BN and confirms its incorporation into the composite. A very small peak corresponding to the G band of CFs is also observed, suggesting the presence of carbon fibers but indicating that their contribution is secondary in this structure compared to h-BN (Yuzuriha & Hess, 1986). In contrast, for the (dhBN)CF+EP composite, which was fabricated using a dip-coating technique, the Raman spectrum reveals a different behavior. The E_{2g} peak of h-BN is pronounced match with the peaks from the CFs. However, in the (dhBN)CF+EP-20%hBN composite, where h-BN is added through the resin and carbon fibers, the intensity of the h-BN E2g peak increases. Furthermore, the use of silanized h-BN in the composite results in a noticeable reduction in the intensity of the h-BN E_{2g} peak. This reduction could be due to the interaction between the silane molecules and the h-BN, potentially altering its vibrational characteristics or diminishing its Raman scattering efficiency. The silane treatment may also create a surface coating that interferes with the intrinsic Raman signals of h-BN, thereby modifying the overall spectral profile. An intriguing observation from the Raman analysis of the epoxy-based multilayered composite structures is the apparent attenuation of the CF-related peaks (D and G bands). This suggests that the epoxy resin included h-BN acts as a filter, dampening the contributions from the CFs. This effect may be attributed to the resin's interaction with the carbon fibers, which could modify the local environment of the fibers, potentially reducing their exposure to the Raman laser or altering their vibrational modes in a way that diminishes the intensity of the D and G bands. Overall, the Raman results provide valuable insights into the molecular structure

and interactions within the composites, shedding light on how different fabrication techniques, such as dip-coating and silane treatment, influence the distribution and vibrational characteristics of the materials within the composite matrix.

To further substantiate the findings, X-ray diffraction (XRD) analysis was performed to identify the crystalline phases present of the synthesized samples. The XRD results for the composite materials fabricated in this study are presented in Figure 4. In the case of the CF+/EP composite, three sharp diffraction peaks are observed at 2θ values of 31.6°, 43.5°, and 45.4°. These peaks correspond to the (200), (100), and (101) Miller index planes, respectively. Additionally, a broad peak at 25.9° is observed, which is attributed to the (002) plane, indicative of the graphite phase. These findings confirm the presence of carbon fibers (CFs) embedded in the epoxy resin, with the graphite structure playing a significant role. The epoxy resin, on the other hand, is amorphous, and the deviation from the baseline in the XRD curve compared to a straight line can be attributed to the amorphous nature of the resin, which contributes to this baseline shift. When h-BN is introduced into the composite as in CF+/EP-20%hBN, the XRD pattern reveals the emergence of peaks that are characteristic of the hexagonal structure of h-BN. These peaks become more prominent, indicating that the h-BN phase is now more dominant compared to the CF-related peaks. This result mirrors the observations from the Raman spectroscopy analysis, where the presence of h-BN is clearly detectable. Furthermore, in the composite containing both CFs and dip coated h-BN (designated as (dhBN)CF+/EP), the XRD peaks corresponding to both the h-BN and CF phases are identifiable. Additionally, the method of incorporating h-BN into the composites either through electrospraying or dip coating has a noticeable effect on the XRD peaks. In the case of composites containing electrosprayed and dip-coated h-BN, the intensity of the h-BN peaks increases, reflecting a higher concentration of the material within the composite. In contrast, when the h-BN is silanized before being added to the composites, the XRD peaks corresponding to h-BN are reduced, indicating a decrease in the crystallinity of h-BN in the composite structure. Similarly to the Raman results, the inclusion of epoxy resin in the system, especially with h-BN, leads to the attenuation of the CF-related peaks, suggesting that the epoxy resin included h-BN acts as a filter. These XRD results corroborate the Raman spectroscopy findings and offer a more comprehensive understanding of the structural characteristics and interfacial interactions within the composites, particularly in relation to the incorporation of h-BN. Table 2 provides a

comprehensive analysis of the crystallinity and amorphousness levels for all configurations. It offers detailed insights into the structural composition of each configuration.

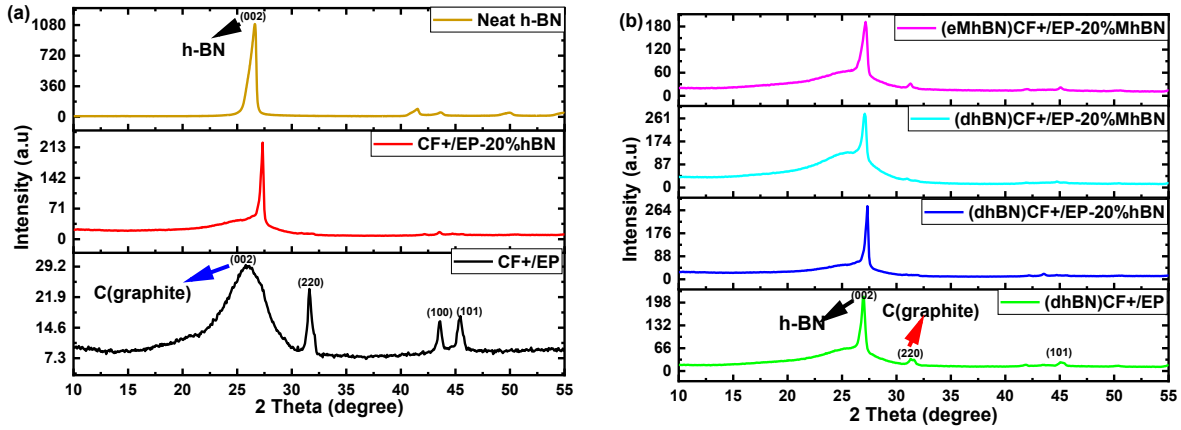

Figure 6.4 XRD patterns (a) comparison of CF+/EP, CF+/EP-20%hBN, b) comparison of (dhBN)CF+/EP, (dB)CF+/EP-20%hBN, (dhBN)CF+/EP-20%MhBN, (eMhBN)CF+/EP-20%MhBN.

Table 6.2 Crystallinity and amorphous degrees of h-BN and multilayer composite CF/h-BN/epoxy samples.

Sample Name	Crystallinity (%)	Amorphous (%)
h-BN	70	30
CF+/EP	4	96
CF+/EP-20%hBN	19	81
(dhBN)CF+/EP	23	77
(dhBN)CF+/EP-20%hBN	24	76
(dhBN)CF+/EP-20%MhBN	17	83
(eMhBN)CF+/EP-20%MhBN	23	77

The TGA results were further analyzed to quantify the decomposition characteristics of the multilayered composite structure consisting of h-BN, CFs, and epoxy resin. These findings are

illustrated in Figure 5. The composites fabricated in this study exhibited thermal stability up to 320 °C, beyond which decomposition began. The decomposition process continued until approximately 470 °C. Both the carbon fibers (CF) and h-BN demonstrated stability up to 1000 °C, indicating that the observed weight loss is primarily attributed to the epoxy resin used in the composites. A key observation from the TGA results is that the weight loss increases as the amount of h-BN introduced into the composites increases. The highest weight loss (27.5%) was recorded for the composite labeled (eMhBN)CF+/EP-20%MhBN. This trend of enhanced weight loss with higher h-BN content can be attributed to the unique properties of h-BN, specifically its high thermal conductivity. As the h-BN material known for its excellent heat management properties, h-BN facilitates more efficient heat transfer within the composite. When the composite is exposed to elevated temperatures, the presence of h-BN improves the distribution of heat across the material, potentially accelerating the thermal degradation of the epoxy matrix. This improved heat distribution likely leads to a higher rate of decomposition, thus resulting in more pronounced weight loss as the temperature increases. Furthermore, silanization not only improves the bonding between the filler and the matrix but also enhances the thermal conductivity of the composite material. In the following section, the effects of silanization will be discussed in detail, specifically, in the case of silanized h-BN, the composites exhibit significantly higher thermal conductivity, which facilitates more efficient heat transfer throughout the system. This enhanced thermal conductivity can lead to increased heat dissipation, thereby promoting a higher rate of thermal degradation during the TGA decomposition process in epoxy resins. Table 3 presents key characteristics derived from the TGA results of the CF/h-BN/epoxy samples.

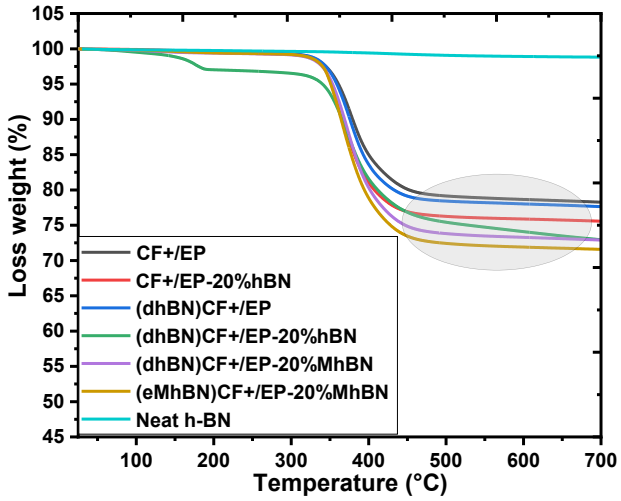

Figure 6.5 TGA curves of neat CF/epoxy composite and h-BN reinforced CF/epoxy composite specimens in different configurations.

Table 6.3 TGA results of multi-scale and multilayered CF/h-BN/epoxy composite samples.

Sample Name	TGA (˚C)		Remaining substance amounts until 700 ˚C (%)
	T_{on}	T_{dm}	
h-BN	-	-	98.8
CF+/EP	325	493	78.3
CF+/EP-20%hBN	325	450	75.6
(dhBN)CF+/EP	325	455	77.7
(dhBN)CF+/EP-20%hBN	325	450	72.9
(dhBN)CF+/EP-20%MhBN	325	457	72.9
(eMhBN)CF+/EP-20%MhBN	325	449	71.6

T_{on}: Onset temperature, starting point of the decomposition processes.

T_{dm}: Maximum point of decomposition.

6.3.2 Mechanical performance of the configured h-BN in carbon fiber reinforced epoxy composites

Figure 6 illustrates the flexural test results of the prepared composites, demonstrating the significant impact of CFs and h-BN particles on their mechanical properties. The data clearly

shows that the incorporation of CFs markedly enhances the mechanical performance of the composites. The integration of h-BN through the resin, as evidenced in the CF+/EP-20%hBN composite, exhibited enhanced flexural properties. This composite achieved a flexural modulus of 39.1 GPa and a flexural strength of 415 MPa, a significant improvement over CF+/EP. The increase in mechanical performance can be attributed to the ability of h-BN particles to impede crack propagation through mechanisms such as crack pinning, deflection, and branching. These mechanisms enhance the toughness and load-bearing capacity of the composite. Moreover, advanced fabrication techniques such as dip-coating and electrospraying, combined with the incorporation of silanized h-BN particles, further improved the mechanical performance. The (dhBN)CF+/EP-20%MhBN composite exhibited the highest flexural modulus of approximately 42.9 GPa, representing an impressive 84% increase compared to neat CF+/EP. The functionalization of h-BN ensures better dispersion within the matrix and stronger interfacial bonding with the carbon fibers, which enhances stress transfer efficiency. The detailed results of the flexural strength and modulus for all composites are presented in Table 4.

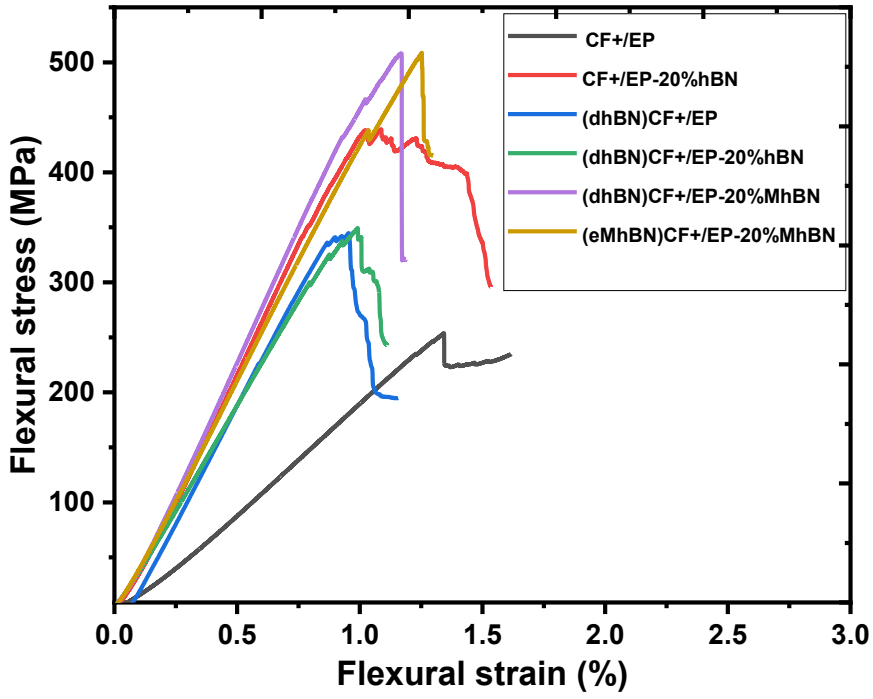

Figure 6.6 Comparison of flexural stress-strain curves for neat CF/EP composites and h-BN-integrated CF/epoxy composites in various configurations.

Table 6.4 The improvement percentages of flexural modulus and strength values of multi-scale and multi-layered h-BN/CF/epoxy composites.

Specimen type	Flexural strength (MPa)	Improvement (%)	Flexural Modulus (GPa)	Improvement (%)
CF+/EP	256±2.87	-	19.4±1.15	-
CF+/EP-20%hBN	415±3.49	63	39.1±6.83	110
(dhBN)CF+/EP	327±6.48	28	20.5±4.79	11
(dhBN)CF+/EP-20%hBN	331±2.70	30	26.1±5.04	43
(dhBN)CF+/EP-20%MhBN	458±2.83	79	42.9±5.57	127
(eMhBN)CF+/EP-20%MhBN	471±5.38	84	40.9±8.47	116

Figure 7 presents the Charpy impact strength values for the composite systems, showcasing the influence of CF reinforcement and h-BN particle inclusion, and advanced processing techniques. The neat CF+/EP composite demonstrates a Charpy impact strength of 47.89 kJ/m². The incorporation of neat h-BN particles into the matrix led to an improvement in impact strength. The CF+/EP-20%hBN composite achieved a Charpy impact strength of 49.67 kJ/m², a modest increase compared to the CF+/EP composite. This enhancement suggests that the addition of h-BN particles at a 20% weight concentration contributes to the composite's ability to absorb impact energy. H-BN particles likely act as micro-scale toughening agents within the epoxy matrix, dissipating energy through mechanisms such as crack pinning and deflection. However, the improvement is modest because neat h-BN particles may not fully integrate into the matrix or interface with the fibers. Significant advances in impact strength were observed with the use of dip coating and electrospraying techniques, which incorporated silanized h-BN. These methods facilitated better dispersion and bonding of the h-BN particles within the composite matrix and at the fiber-matrix interface. The (dhBN)CF+/EP-20%hBN composite exhibited the highest Charpy impact strength, reaching 70 kJ/m², corresponding to a 44% increase compared to the neat CF+/EP. This substantial

improvement can be attributed to several factors. Functionalized h-BN particles improve the matrix's ability to absorb and dissipate impact energy through mechanisms like crack branching and particle debonding. Moreover, silanized h-BN particles enhance the bonding at the fiber-matrix interface, ensuring efficient load transfer during impact and reducing the likelihood of delamination or catastrophic failure. Also, advanced coating techniques ensure a more homogenous distribution of h-BN particles, minimizing stress concentrations and enhancing overall composite toughness.

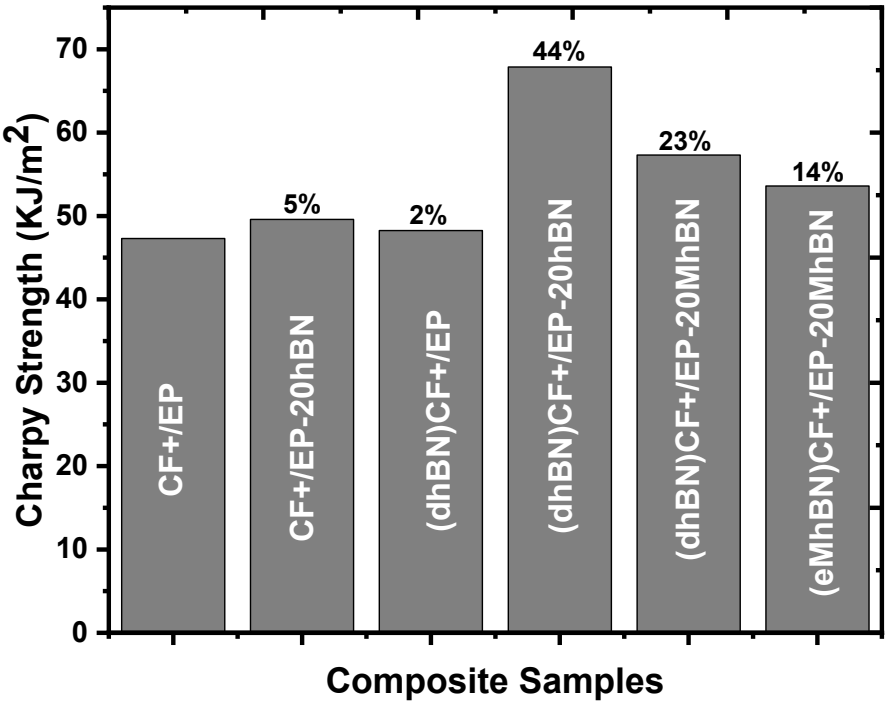

Figure 6.7 Comparison Charpy impact results of neat CF/EP composites and h-BN-integrated CF/epoxy composites.

Dynamic mechanical analysis (DMA) was performed to assess the storage modulus, loss modulus, and tan δ of the prepared composite samples. The results are presented in Figure 8, highlight the significant effects of CFs reinforcement and h-BN incorporation on the composites' mechanical and thermal behavior. The storage modulus, a key parameter indicating the stiffness of a material under oscillatory loading, measures the elastic energy stored during deformation. It provides a direct insight into the material's resistance to deformation under dynamic loads (Gracia-Fernández

et al., 2010). The data showed that incorporating CFs into the epoxy matrix resulted in a significant increase in storage modulus compared to neat epoxy. This increase can be attributed to the woven architecture of the CFs, which effectively distributes applied loads evenly across the composite structure. This distribution enhances stiffness in multiple directions and ensures balanced mechanical reinforcement. Importantly, despite the substantial improvement in stiffness, the glass transition temperature T_g which represents the transition from a hard, brittle state to a rubbery, flexible state due to increased polymer chain mobility, remained unchanged in the CF+/EP composite. This observation suggests that the addition of CFs did not alter the thermal mobility or molecular dynamics of the epoxy matrix. When h-BN particles were introduced into the composite, further improvements in storage modulus were observed. The CF+/EP-20%hBN composite demonstrated a storage modulus of 6000 MPa, indicating a significant enhancement over the CF+/EP system. However, the T_g of this composite decreased slightly to 90°C, which could be attributed to the disruption of the epoxy network by the non-functionalized h-BN particles. This disruption may increase the mobility of polymer chains, slightly reducing the thermal stability of the composite. To overcome this limitation, a dip-coating process was applied to uniformly coat the CFs with h-BN particles before incorporating them into the epoxy matrix. This process significantly improved both the mechanical and thermal properties of the composite. The resulting (dhBN)CF+/EP composite exhibited a remarkable storage modulus of 10,000 MPa, representing a 456% increase compared to neat epoxy. Additionally, the T_g increased to 125°C, indicating enhanced thermal stability. The observed improvements in the dip-coated h-BN composite can be attributed to several factors. First, the dip-coating process ensured a uniform and consistent distribution of h-BN particles on the CF surface, minimizing stress concentrations and enabling smoother stress transfer across the composite. Second, the presence of h-BN particles near the fiber-matrix interface restricted the mobility of the polymer chains, thereby stiffening the composite and increasing its thermal stability. Third, the strong interfacial bonding between the CFs and the epoxy matrix, facilitated by the coated h-BN particles, improved load transfer efficiency and overall material stiffness. The detailed results of the DMA tests are summarized in Table 5, showing the significant enhancements achieved through these materials and processing innovations.

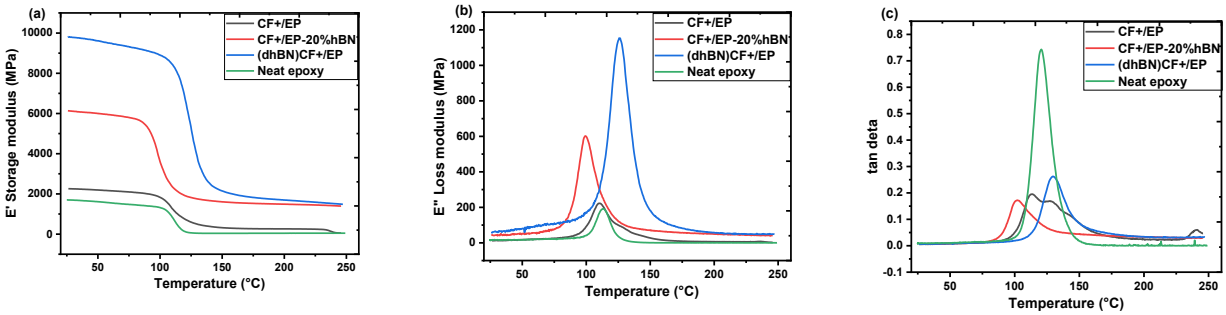

Figure 6.8 Comparison of DMA curves (a) changes of E' storage modulus (b) E'' loss modulus and (c) tan delta of epoxy for epoxy, neat CF+/EP composite and h-BN integrated CF+/EP composite specimen.

Table 6.5 The summary of DMA results of multilayered structure of CF/epoxy.

Specimen type	Glass transition temperature (T_g)	Storage modulus (MPa)	Maximum loss modulus (MPa)
Epoxy	113	1800	198
CF+/EP	100	2000	200
CF+/EP-20%hBN	90	6000	600
(dhBN)CF+/EP	125	10000	1200

6.3.3 The effect of h-BN Configuration within the composite structure on the thermal conductivity of epoxy composites

Its importance extends from electronics cooling to the design of advanced composite materials, where the ability to manage heat efficiently can significantly affect the durability and functionality of the material. In this context, Figure 9 (a) presents the results of out-of-plane thermal conductivity measurements performed on anisotropic mode composites. These measurements are critical for understanding how heat flows through materials, particularly when their structure influences phonon transport, which is the primary mode of heat transfer in solid materials. The

reference out-of-plane thermal conductivity of the epoxy resin composite was measured to be 0.2 W/mK. However, this value showed a remarkable value of 0.49 W/mK for carbon fibers (CF) were introduced into the epoxy resin composite, resulting in the neat CF+/EP conFigureuration. When 20% h-BN was introduced into the CF+/EP composite, the thermal conductivity increased, reaching 0.58 W/mK, representing a 19% enhancement over the neat epoxy resin. The h-BN particles, known for their 2D structure, contribute to the increase in thermal conductivity by facilitating phonon transport in the composite. In solid materials, phonons primarily carry heat in the in-plane direction, and h-BN, being a 2D material with excellent phonon transport properties, helps extend the phonon conduction pathways, thereby enhancing heat transfer across the material. The alignment of these h-BN particles with the epoxy resin during processing further aids in this phonon transport, boosting the composite's thermal conductivity. The process of dip coating, which involves applying a thin, uniform layer of h-BN to the composite material, also significantly improved the thermal conductivity. When the dip-coated h-BN was used in combination with CFs, the thermal conductivity reached 0.6 W/mK for the (dhBN)CF+/EP-20%hBN conFigureuration. This enhancement can be attributed to the efficient coating of h-BN particles onto the carbon fibers, which allows for better integration and alignment of the 2D h-BN crystals with the carbon fibers, promoting enhanced phonon coupling between the two materials. This increased phonon transport network is responsible for the noticeable rise in thermal conductivity. However, the most remarkable increase in thermal conductivity was observed when carbon fibers were coated with APTES-treated h-BN using the electrospray process. In the (eMhBN)CF+/EP-20%MhBN composite, the thermal conductivity peaked at 1.3 W/mK an outstanding 166% increase compared to the neat CF+/EP. This substantial improvement can be explained through a combination of factors. The electrospraying process allows for a finer, more uniform distribution of h-BN particles onto the carbon fibers, facilitating deeper penetration and a more comprehensive filling of voids within the fiber matrix. The high-velocity impact of electrosprayed particles improves the interaction between the h-BN particles and the carbon fibers, leading to a more effective integration of the two materials. This process not only enhances phonon transport within the material but also significantly strengthens the bond between the h-BN and the carbon fibers. Moreover, the APTES treatment of h-BN likely contributes to the formation of stronger interfacial bonds between the particles and the fibers. This treatment increases the chemical compatibility of the h-BN with the carbon fibers, ensuring that phonons can more effectively transfer from the

carbon fiber network to the h-BN, and vice versa. As a result, the overall thermal conductivity of the composite is significantly improved. These findings highlight the importance of particle treatment and the selection of deposition methods in determining the thermal properties of composite materials. The enhancement in thermal conductivity observed through these various methods in this work is also notable when compared to previous studies in the field.

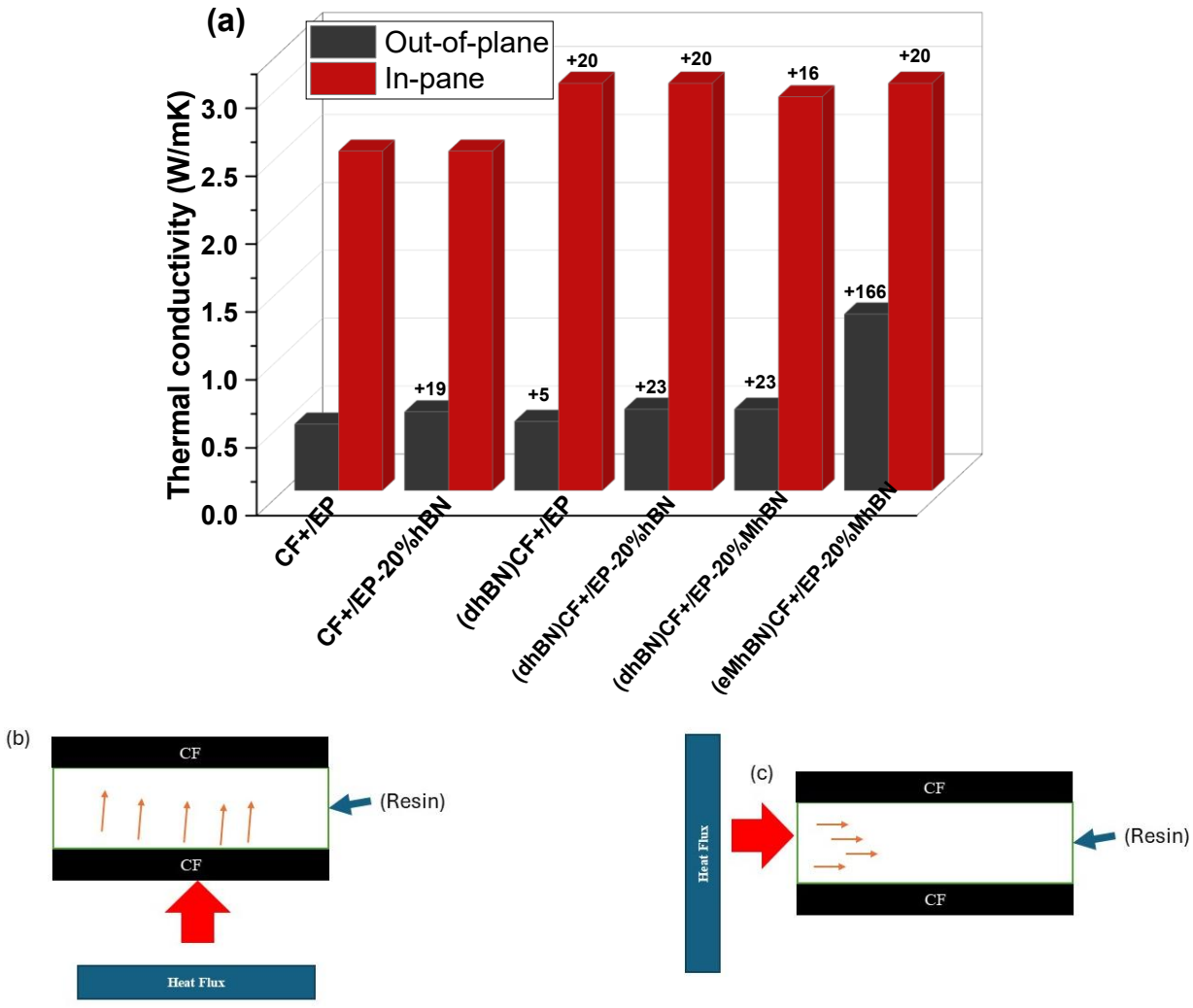

Figure 6.9 (a) Out-of-plane and in-plane thermal conductivity (anisotropic mode) values of epoxy, CF+/EP, CF+/EP-20%hBN, (dhBN)CF+/EP, (dhBN)CF+/EP-20%hBN, (dhBN)CF+/EP-20%MhBN, (eMhBN)CF+/EP-20%MhBN, (b) the schematic representation of out of plane heat transmission by the collision of particles and (c) the schematic representation of in-plane heat transmission.

Figure 9 (a) also presents the results from anisotropic tests measuring the in-plane thermal conductivity of the composites. Initially, when only neat epoxy through CFs was used (CF+/EP), the thermal conductivity was measured at 2.5 W/mK. However, when h-BN is combined with silanized h-BN, using techniques such as electrospraying and dip coating, the thermal conductivity improves. Among the different Configurations tested, the highest thermal conductivity was observed in the (eMhBN)CF+/EP-20%MhBN composite, which reached a remarkable 3 W/mK. This represents a 20% increase compared to the neat CF+/EP, highlighting the considerable enhancement in thermal performance. When comparing these results with those from out-of-plane thermal conductivity tests, it is clear that the introduction of h-BN into the resin has a more pronounced effect on heat transfer in the out-of-plane direction compared to in-plane direction. This suggests that the presence of h-BN plays a pivotal role in improving thermal conductivity in the direction perpendicular to the plane of the composite, further enhancing the overall heat dissipation capabilities of the material.

6.3.4 Cross sectional analysis of h-BN/carbon fiber reinforced composites

CT scans and X-ray imaging provide essential benefits for the study of composite materials by allowing for detailed internal examination, non-destructive testing (NDT), 3D visualization, and quantitative analysis. The CT scan images of h-BN/CF/epoxy composite specimens are presented in Figure 10 (a-c), highlighting the effects of incorporating h-BN and silanized h-BN through electrospraying and dip-coating techniques. These processes effectively minimize voids and defects within the composites, enhancing their overall quality. Furthermore, the cross-sectional CT X-ray images of the (dhBN)CF+/EP-20%hBN and (eMhBN)CF+/EP-20%MhBN samples are shown in Figure 10 (d-e). Notably, in the case of (eMhBN)CF+/EP-20%MhBN, the electrospraying and APTES treatment of h-BN create a much denser packing structure, as observed in the CT scan images. This process contributes to improved composite integrity by reducing voids and enhancing material distribution. Porosity calculations for these composites are provided in Figure 10 (f), where the porosity of the CF+/EP composite is calculated to be 10.47%. Remarkably, the samples treated with the electrospraying process exhibited a significant reduction in porosity, with the lowest value observed in the (eMhBNCF)+/EP-20%hBN sample. The CT scan images

emphasize the critical importance of minimizing porosity to improve heat transfer efficiency. A higher packing density facilitates more effective phonon movement, thereby enhancing the thermal conductivity of the composites. Overall, these results demonstrate that reducing porosity through electrospraying and silanization not only strengthens the structural integrity of the composites but also significantly boosts their thermal performance, making them more effective for applications requiring efficient heat management.

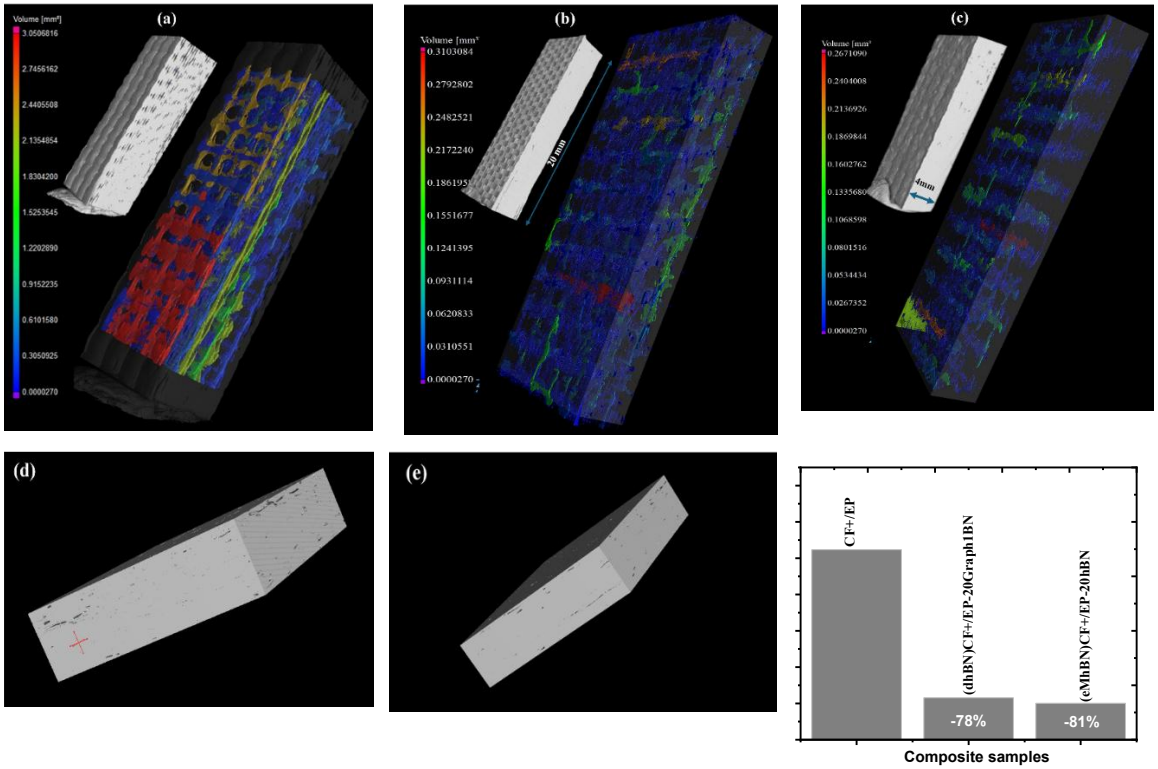

Figure 6.10 CT scans X-ray images of (a) CF+/EP (b) (dhBN)CF+/EP-20%hBN, (c) (eMhBN)CF+/EP-20%MhBN, cross-sectional view CT X-ray images of (d) (dhBN)CF+/EP-20%hBN, (e) (eMhBN)CF+/EP-20%MhBN and (f) porosity analysis of h-BN/CF/epoxy composite specimens.

Figure 11 shows FE-SEM images of the cross-sectional views of composite specimens, illustrating distinct variations in composite structures influenced by composition and processing techniques. Figure 11 (a) presents the neat carbon fibers as a reference to assess delamination and interfacial adhesion in the newly composite structures. In Figure 11 (b), the CF+/EP composite exhibits prominent delamination and cracks. The epoxy resin fails to fully encapsulate all carbon fibers,

leaving visible gaps between the carbon fibers and the epoxy matrix, indicative of poor adhesion and weak interfacial bonding. In contrast, introducing neat h-BN into CFs through the dip coating process to form the (dhBN)CF+/EP-20%hBN composite, as shown in Figure 11 (c), significantly reduces the size of cracks. More carbon fibers are coated with resin, and the wettability between the h-BN-reinforced epoxy resin and the carbon fibers is noticeably improved, resulting in enhanced interfacial bonding. Further improvements are observed when the electrospray process is applied using APTES-treated h-BN, as depicted in Figure 11 (d). This method leads to a substantial increase in the number of carbon fibers coated with epoxy resin. In the (eMhBN)CF+/EP-20%hBN composite, the carbon fibers are entirely enveloped by a uniform and thorough resin coating. This demonstrates that the electrospray process, combined with the incorporation of h-BN, significantly improves interfacial bonding and the distribution of resin around the carbon fibers, enhancing the mechanical and thermal performance of the composite compared to CF+/EP. The use of silane-modified h-BN powders in the electrospray process amplifies this improvement by creating a stronger interfacial bond with the epoxy. This stronger bonding facilitates more effective dispersion of h-BN within the epoxy matrix, filling voids and achieving a highly uniform coating of the carbon fibers. Such uniformity is critical for boosting the thermal conductivity of the composites. A consistent resin layer minimizes phonon scattering centers, which are points where energy-carrying particles (phonons) can be deflected, thereby optimizing the thermal performance of the material.

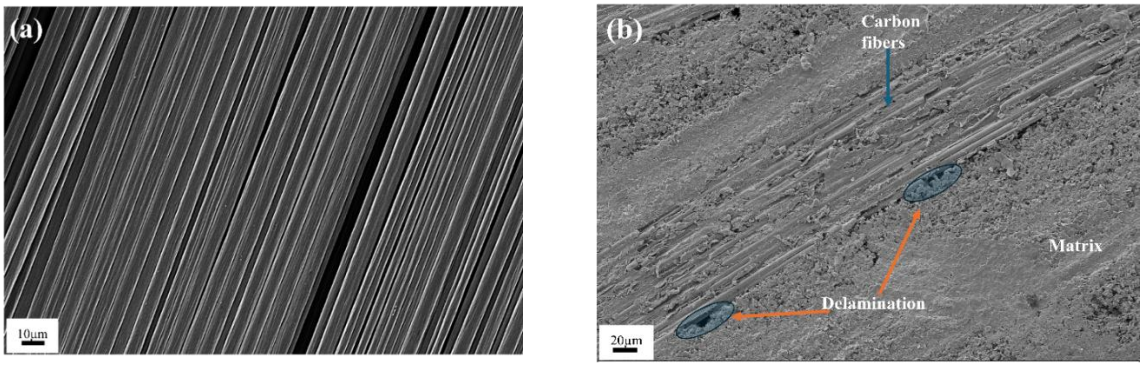

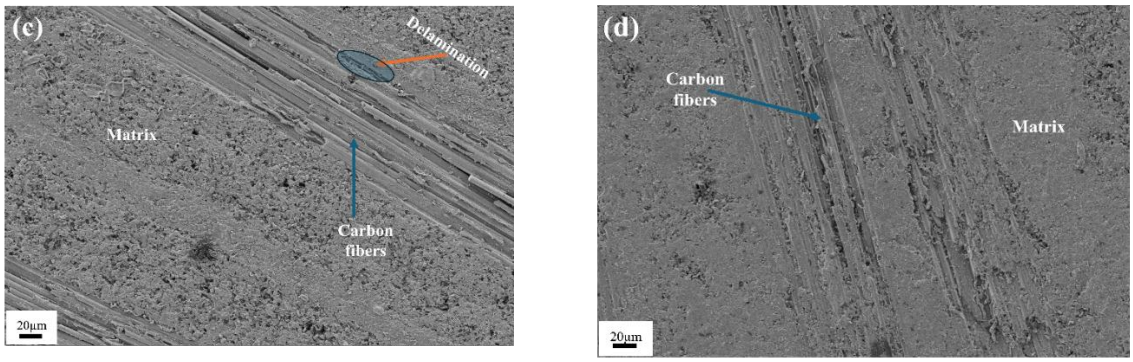

Figure 6.11 SEM images of (a) neat CFs, (b) CF+/EP, (c) (dhBN) CF+/EP-20%hBN and (d) (eMhBN) CF+/EP-20%MhBN specimens.

6.4 Conclusions

In this study, a multi-scale interface engineering strategy was successfully developed to enhance the directional thermal and mechanical performance of carbon fiber (CF) reinforced epoxy composites through the integration of h-BN and silanized h-BN. By employing six distinct composite Configurations, embedding h-BN into the matrix and applying it onto CF fabrics via electrospraying and dip-coating techniques—both physical dispersion and chemical interfacial interactions were carefully optimized. Among the Configurations, the highest thermal conductivity value of 1.3 W/mK was achieved with the (eMhBN)CF+/EP-20%MhBN sample, underscoring the efficacy of combining APTES-modified and heat-treated h-BN on CF surfaces with a 20 wt.% h-BN-loaded epoxy matrix. In addition, the electrospraying technique proved particularly effective in enhancing h-BN distribution and removing residual solvent, thus minimizing void content and improving interfacial bonding. CT analyses further highlighted the role of h-BN in reducing porosity and defects within the composite structure, which was critical in achieving consistent mechanical reinforcement. Mechanical tests confirmed that all surface treatments led to improved stiffness and strength relative to the neat epoxy system.

To provide a comprehensive overview of improvement of all the mechanical properties and thermal conductivity (TC) results compared to neat CF+/EP, a radar chart has been created. This

chart, presented in Figure 12, effectively visualizes and compares the performance metrics of the various Configurations. The maximum improvement in TC was achieved with the electrosprayed sample (eMhBN)CF+/EP-20%MhBN), showing a 166% increase. Additionally, the bending strength for the electrosprayed case improved by 84%.

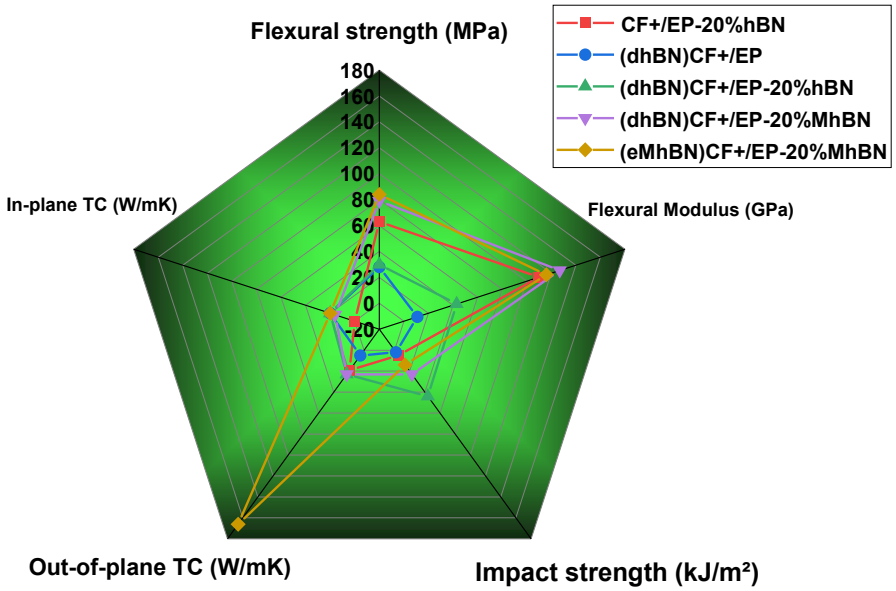

Figure 6.12 Radar chart of comparative analysis of mechanical and thermal properties of h-BN placement in configured CF/epoxy composites.

These findings emphasize the critical role of interfacial design and filler alignment in the development of high-performance structural composites. The demonstrated approach holds significant promise for aerospace applications where directional control over thermal dissipation and mechanical integrity is vital.

Supplementary

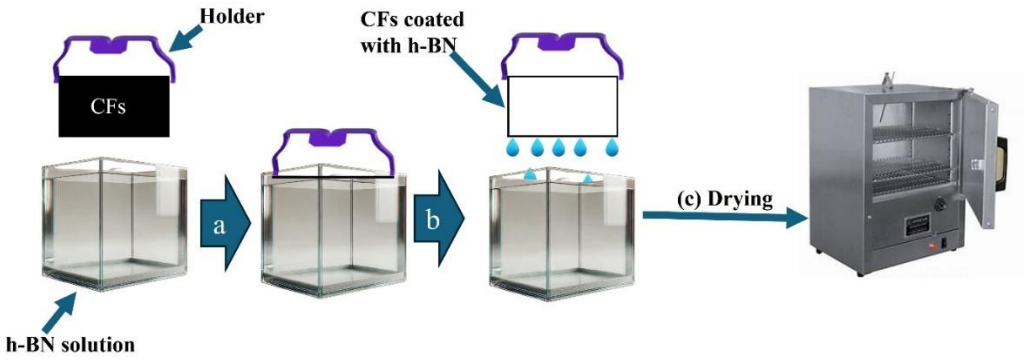

Figure 6. S.1 The dip coating process for applying neat micron h-BN on CF (a) inserting CF at h-BN solution, (b) leaving it after 15 min and (c) drying.

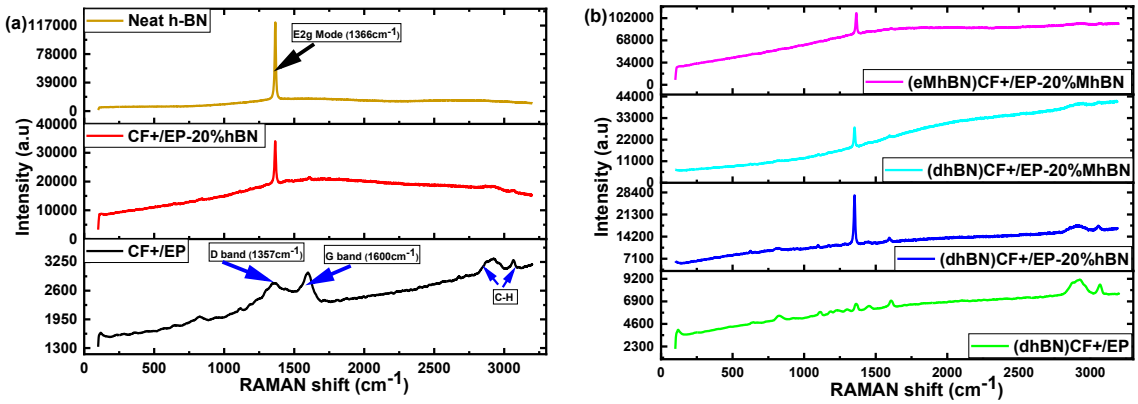

Figure 6.S.2 Raman spectra (a) comparison of CF+/EP, CF+/EP-20%hBN, b) comparison of (dhBN)CF+/EP, (dhBN)CF+/EP-20%hBN, (dhBN)CF+/EP-20%MhBN, (eMhBN)CF+/EP-20%MhBN.

Table 6.S.1 Error bars represent the standard deviation of the measured thermal conductivity values of h-BN/CF/epoxy composites.

Sample Name	Out-of-plane thermal conductivity (W/mK)	In-plane thermal conductivity (W/mK)
CF+/EP	0.49±0.009	2.5±0.070
CF+/EP-20%hBN	0.58±0.022	2.5±0.030
(dhBN)CF+/EP	0.51±0.025	3.0±0.005
(dhBN)CF+/EP-20%hBN	0.60±0.0146	3.0±0.051
(dhBN)CF+/EP-20%MhBN	0.60±0.0282	2.9±0.005
(eMhBN)CF+/EP-20%MhBN	1.30±0.0073	3.0±0.004

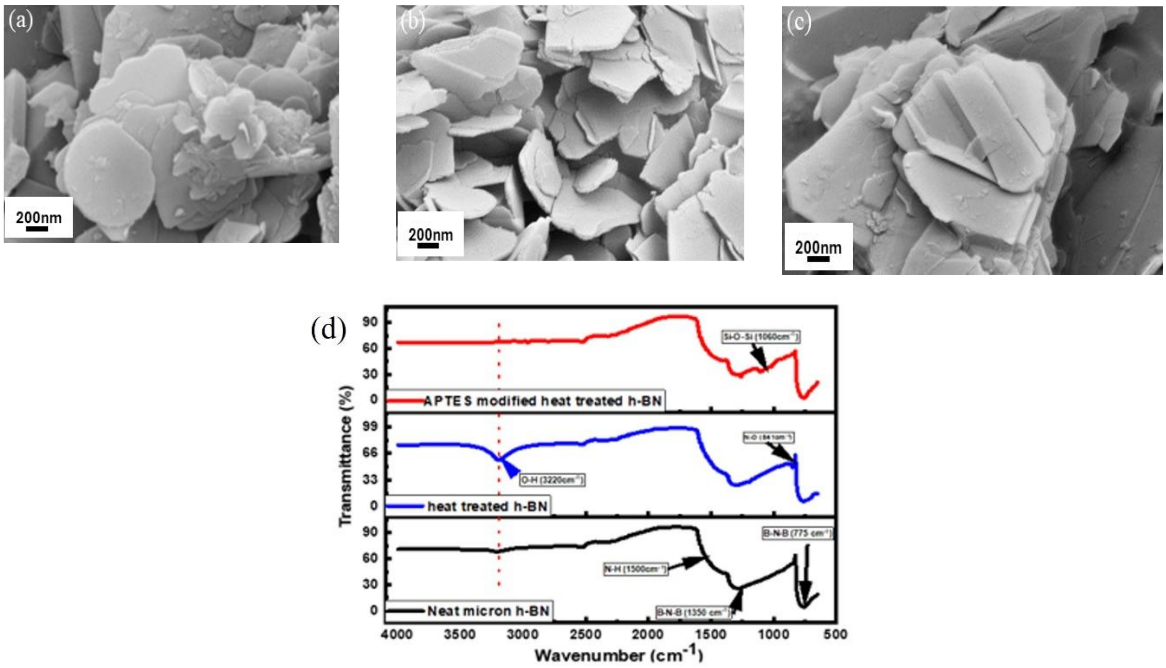

Figure 6.S.3 SEM images of (a) neat h-BN, (b) heat-treated h-BN, (c) APTES modified h-BN particles and (d) FT-IR spectra of neat micron h-BN, heat-treated h-BN, and APTES modified heat-treated h-BN samples.

General Conclusion

This comprehensive study demonstrates the successful enhancement of thermal and mechanical properties in epoxy-based composites through strategic integration and surface modification of hexagonal boron nitride (h-BN) particles. By varying particle size, filler concentration, and surface treatment methods including thermal activation and silanization with APTES, significant improvements in both in-plane and through-thickness thermal conductivity, as well as mechanical strength were achieved. Notably, micron-sized h-BN particles at 20 wt.% led to the highest thermal conductivity gains (up to 112%) and mechanical reinforcement (up to 47% increase in tensile modulus), outperforming nano-sized counterparts. Surface modification techniques, especially silanization, enhanced interfacial bonding, although excessive silane content negatively impacted

thermal conductivity and tensile strength. Electrospraying h-BN onto carbon fiber fabrics and embedding it in the matrix further optimized h-BN dispersion, minimized void formation, and improved the overall structural integrity of the composites. CT imaging confirmed reduced porosity, while mechanical and thermal tests validated the efficacy of the multi-scale engineering approach. Overall, this work provides a scalable and cost-effective pathway to engineer high-performance, thermally conductive, and mechanically robust epoxy composites. These advancements are particularly valuable for thermal management in demanding applications such as aerospace, electronics, and automotive systems, where efficient heat dissipation and structural durability are critical.

This thesis systematically demonstrates that directional thermal conductivity and mechanical performance in epoxy- and carbon fiber-reinforced epoxy composites can be effectively tailored through a multi-scale interface engineering strategy that integrates hexagonal boron nitride (h-BN) and its surface-functionalized derivatives. Across the chapters, the correlation between h-BN particle size and loading ratio was established, showing that micron-sized h-BN at optimal concentrations can achieve over 100% improvement in both in-plane and through-thickness thermal conductivity while maintaining or enhancing tensile and flexural properties. Surface modification through thermal activation, acid treatment, and silanization with APTES proved highly effective in strengthening interfacial bonding, significantly boosting directional thermal conductivity—up to 1.7 W/mK with high filler loadings—while preserving thermal stability at elevated temperatures. Numerical simulations validated the experimental trends, underscoring the importance of controlling silane content to balance thermal and mechanical performance. The integration of h-BN into carbon fiber composites via electrospraying and dip-coating enabled the formation of aligned thermal pathways, reduced porosity, and improved stiffness and strength. The highest recorded performance—a 166% increase in thermal conductivity and an 84% improvement in bending strength—was achieved by combining electrosprayed APTES/heat-treated h-BN on carbon fibers with a 20 wt.% h-BN-filled epoxy matrix. Collectively, these findings establish a clear pathway for designing multi-functional, scalable composite systems that meet the demanding requirements of aerospace, electronics, and advanced thermal management applications, where precise control of heat dissipation and mechanical integrity is critical.

Key Highlights of the Thesis are summarized below

- **Optimized filler parameters:** 20 wt.% micron-sized h-BN enhanced in-plane and through-thickness thermal conductivity by 107% and 112%, respectively.
- **Mechanical reinforcement:** 20 wt.% micron-sized h-BN improved tensile modulus by 47%, while 10 wt.% improved flexural modulus by 41%.
- **Surface functionalization impact:** Thermal activation + APTES silanization boosted through-thickness TC from 0.21 W/mK to 0.47 W/mK at 10 wt.% loading.
- **High-loading performance:** 60 wt.% thermally treated h-BN + APTES silanization increased epoxy TC from 0.31 W/mK to 1.4 W/mK.
- **Numerical validation:** ANSYS simulations confirmed optimal silane ratio before decline in TC with excess silane.
- **Interfacial engineering in CF systems:** Electrosprayed APTES/heat-treated h-BN onto carbon fibers+ 20 wt.% micron h-BN in epoxy achieved 2.31 W/mK TC and 127% increase in flexural modulus.
- **Defect reduction:** Electrospraying reduced porosity and voids, as confirmed by CT scans, leading to improved structural integrity.
- **Top performance:** Maximum gains of 166% in thermal conductivity and 84% in bending strength compared to neat CF+/EP reference.
- **Scalability:** Pre-dispersion, surface functionalization, and electrospraying techniques are adaptable for industrial-scale production.
- Application potential: Developed composites are well-suited for aerospace, electronics, and high-performance automotive sectors where heat dissipation and mechanical strength are critical.

BIBLIOGRAPHY

Ahmad, S., Habib, S., Nawaz, M., Shakoor, R. A., Kahraman, R., & Tahtamouni, T. M. Al. (2023). The role of polymeric matrices on the performance of smart self-healing coatings: A review. *Journal of Industrial and Engineering Chemistry*, *124*, 40–67. https://doi.org/10.1016/J.JIEC.2023.04.024

Ambreen, T., & Kim, M. H. (2020). Influence of particle size on the effective thermal conductivity of nanofluids: A critical review. *Applied Energy*, *264*, 114684. https://doi.org/10.1016/J.APENERGY.2020.114684

Bashir, A., Maqbool, M., Usman, A., Lv, R., Niu, H., Kang, L., Ashraf, Z., & Bai, S. (2023). Enhancing Thermal Conductivity and Mechanical Strength of TPU Composites Through Modulating o-PDA-BN/rGO Heterointerface Networks. *Composites Part A: Applied Science and Manufacturing*, *173*, 107676. https://doi.org/10.1016/J.COMPOSITESA.2023.107676

Berktas, I., Chaudhari, O., Ghafar, A. N., Menceloglu, Y., & Okan, B. S. (2021). Silanization of SiO2 decorated carbon nanosheets from rice husk ash and its effect on workability and hydration of cement grouts. *Nanomaterials*, *11*(3), 1–18. https://doi.org/10.3390/NANO11030655,

Berktas, I., Ghafar, A. N., Fontana, P., Caputcu, A., Menceloglu, Y., & Okan, B. S. (2020). Facile Synthesis of Graphene from Waste Tire/Silica Hybrid Additives and Optimization Study for the Fabrication of Thermally Enhanced Cement Grouts. *Molecules 2020, Vol. 25, Page 886*, *25*(4), 886. https://doi.org/10.3390/MOLECULES25040886

Bianco, V., De Rosa, M., & Vafai, K. (2022). Phase-change materials for thermal management of electronic devices. *Applied Thermal Engineering*, *214*, 118839. https://doi.org/10.1016/J.APPLTHERMALENG.2022.118839

Chen, F., Xiao, H., Peng, Z. Q., Zhang, Z. P., Rong, M. Z., & Zhang, M. Q. (2021). Thermally conductive glass fiber reinforced epoxy composites with intrinsic self-healing capability. *Advanced Composites and Hybrid Materials*, *4*(4), 1048–1058. https://doi.org/10.1007/S42114-021-00303-3/FIGURES/5

Chen, R., Qiu, Q., Peng, X., & Tang, C. (2023). Surface modified h-BN towards enhanced electrical properties and thermal conductivity of natural ester insulating oil. *Renewable Energy*, *204*, 185–196. https://doi.org/10.1016/J.RENENE.2022.12.108

Chen, W., Huang, M., Chen, Q., Luo, S., Huang, Z., & Qi, X. (2024). Vibration modes of phonons

in few-layer NbOCl2 modulated by uniaxial strain. *Applied Materials Today*, *40*, 102384. https://doi.org/10.1016/J.APMT.2024.102384

Dericiler, K., Sadeghi, H. M., Yagci, Y. E., Sas, H. S., & Okan, B. S. (2021). Experimental and Numerical Investigation of Flow and Alignment Behavior of Waste Tire-Derived Graphene Nanoplatelets in PA66 Matrix during Melt-Mixing and Injection. *Polymers 2021, Vol. 13, Page 949*, *13*(6), 949. https://doi.org/10.3390/POLYM13060949

Dong, Y., Yu, H., Feng, Y., & Feng, W. (2024). Structure, properties and applications of multi-functional thermally conductive polymer composites. *Journal of Materials Science \& Technology*, *200*, 141–161. https://doi.org/10.1016/J.JMST.2024.02.070

Farahani, A., Jamshidi, M., & Foroutan, M. (2023). Effects of functionalization and silane modification of hexagonal boron nitride on thermal/mechanical/morphological properties of silicon rubber nanocomposite. *Scientific Reports*, *13*(1). https://doi.org/10.1038/S41598-023-39203-5,

Gaonkar, N., & Vaidya, R. G. (2020). Phonon mode-dependent lattice thermal conductivity of nanoscale black phosphorus. *Physics Letters A*, *384*(36), 126912. https://doi.org/10.1016/J.PHYSLETA.2020.126912

Gautam, C., & Chelliah, S. (2021). Methods of hexagonal boron nitride exfoliation and its functionalization: covalent and non-covalent approaches. *RSC Advances*, *11*(50), 31284–31327. https://doi.org/10.1039/D1RA05727H

Gong, Y., Xu, Z. Q., Li, D., Zhang, J., Aharonovich, I., & Zhang, Y. (2021). Two-Dimensional Hexagonal Boron Nitride for Building Next-Generation Energy-Efficient Devices. *ACS Energy Letters*, *6*(3), 985–996. https://doi.org/10.1021/ACSENERGYLETT.0C02427/ASSET/IMAGES/LARGE/NZ0C02427_0005.JPEG

Gracia-Fernández, C. A., Gómez-Barreiro, S., López-Beceiro, J., Saavedra, J. T., Naya, S., & Artiaga, R. (2010). Comparative study of the dynamic glass transition temperature by DMA and TMDSC. *Polymer Testing*, *29*(8), 1002–1006. https://doi.org/10.1016/J.POLYMERTESTING.2010.09.005

Gu, J., Lv, Z., Wu, Y., Guo, Y., Tian, L., Qiu, H., Li, W., & Zhang, Q. (2017). Dielectric thermally conductive boron nitride/polyimide composites with outstanding thermal stabilities via in-situ polymerization-electrospinning-hot press method. *Composites Part A: Applied Science and Manufacturing*, *94*, 209–216. https://doi.org/10.1016/J.COMPOSITESA.2016.12.014

Gu, J., Zhang, Q., Dang, J., & Xie, C. (2012). Thermal conductivity epoxy resin composites filled

with boron nitride. *Polymers for Advanced Technologies*, *23*(6), 1025–1028. https://doi.org/10.1002/PAT.2063;PAGE:STRING:ARTICLE/CHAPTER

Guerra, V., Wan, C., Degirmenci, V., Sloan, J., Presvytis, D., & McNally, T. (2018). 2D boron nitride nanosheets (BNNS) prepared by high-pressure homogenisation: structure and morphology. *Nanoscale*, *10*(41), 19469–19477. https://doi.org/10.1039/C8NR06429F

Gul, S., Arican, S., Cansever, M., Beylergil, B., Yildiz, M., & Okan, B. S. (2023). Design of Highly Thermally Conductive Hexagonal Boron Nitride-Reinforced PEEK Composites with Tailored Heat Conduction Through-Plane and Rheological Behaviors by a Scalable Extrusion. *ACS Applied Polymer Materials*, *5*(1), 329–341. https://doi.org/10.1021/ACSAPM.2C01534/ASSET/IMAGES/LARGE/AP2C01534_0007.JPEG

H., Z. C., & Peter, B. (2018). Comprehensive Composite Materials II. *Comprehensive Composite Materials II*, *II*, 100534. http://www.sciencedirect.com:5070/referencework/9780081005347/comprehensive-composite-materials-ii

Hassan, E. A. M., Yang, L., Elagib, T. H. H., Ge, D., Lv, X., Zhou, J., Yu, M., & Zhu, S. (2019). Synergistic effect of hydrogen bonding and π-π stacking in interface of CF/PEEK composites. *Composites Part B: Engineering*, *171*, 70–77. https://doi.org/10.1016/J.COMPOSITESB.2019.04.015

He, L., Wang, H., Chen, L., Wang, X., Xie, H., Jiang, C., Li, C., Elibol, K., Meyer, J., Watanabe, K., Taniguchi, T., Wu, Z., Wang, W., Ni, Z., Miao, X., Zhang, C., Zhang, D., Wang, H., & Xie, X. (2019). Isolating hydrogen in hexagonal boron nitride bubbles by a plasma treatment. *Nature Communications 2019 10:1*, *10*(1), 1–9. https://doi.org/10.1038/s41467-019-10660-9

Hou, J., Li, G., Yang, N., Qin, L., Grami, M. E., Zhang, Q., Wang, N., & Qu, X. (2014). Preparation and characterization of surface modified boron nitride epoxy composites with enhanced thermal conductivity. *RSC Advances*, *4*(83), 44282–44290. https://doi.org/10.1039/C4RA07394K

Huang, L., Yang, Y., Wu, R., Fan, W., Dai, Q., He, J., & Bai, C. (2020). Boron nitride and hyperbranched polyamide assembled recyclable polyisoprene vitrimer with robust mechanical properties, high thermal conductivity and remoldability. *Polymer*, *208*, 122964. https://doi.org/10.1016/J.POLYMER.2020.122964

Ismail, A. A., van de Voort, F. R., & Sedman, J. (1997). Chapter 4 Fourier transform infrared spectroscopy: Principles and applications. *Techniques and Instrumentation in Analytical Chemistry*, *18*(C), 93–139. https://doi.org/10.1016/S0167-9244(97)80013-3

Kasirer, S., & Meir, Y. (2022). Hysteresis and jumps in the I-V curves of disordered two-dimensional materials. *Physical Review B*, *105*(13), 134508. https://doi.org/10.1103/PHYSREVB.105.134508/FIGURES/7/THUMBNAIL

Kim, K., Kim, M., Hwang, Y., & Kim, J. (2014). Chemically modified boron nitride-epoxy terminated dimethylsiloxane composite for improving the thermal conductivity. *Ceramics International*, *40*(1), 2047–2056. https://doi.org/10.1016/J.CERAMINT.2013.07.117

Kirubakaran, R., Salunke, D. R., Pitchumani, S. V., Gopalan, V., & Sampath, A. (2024). Investigation of nano-hBN/ natural fibers reinforced epoxy composites for thermal and electrical applications using GRA and ANFIS optimization methods. *Polymer Testing*, *139*, 108561. https://doi.org/10.1016/J.POLYMERTESTING.2024.108561

Kong, N., Tian, Y., Huang, M., Ye, C., Yan, Y., Peng, C., Liu, J., & Han, F. (2023). Conformal BN coating to enhance the electrical insulation and thermal conductivity of spherical graphite fillers for electronic encapsulation field. *Journal of Alloys and Compounds*, *968*, 172039. https://doi.org/10.1016/J.JALLCOM.2023.172039

Kuila, C., Maji, A., Murmu, N. C., & Kuila, T. (2025). Hexagonal boron nitride (h-BN) "a miracle in white": An emerging two-dimensional material for the advanced powered electronics and energy harvesting application. *Composites Part B: Engineering*, *301*, 112531. https://doi.org/10.1016/J.COMPOSITESB.2025.112531

Lee, J. H., Shin, H., & Rhee, K. Y. (2019). Surface functionalization of boron nitride platelets via a catalytic oxidation/silanization process and thermomechanical properties of boron nitride-epoxy composites. *Composites Part B: Engineering*, *157*, 276–282. https://doi.org/10.1016/J.COMPOSITESB.2018.08.050

Li, S., Wang, H., Mao, H., Li, L., & Shi, H. (2021). Enhanced thermal management performance of comb-like polymer/boron nitride composite phase change materials for the thermoregulated fabric application. *Journal of Energy Storage*, *40*, 102826. https://doi.org/10.1016/J.EST.2021.102826

Li, X., Qiu, H., Liu, X., Yin, J., Guo, W., Li, X., Qiu, H., Liu, X., Yin, J., & Guo, W. (2017). Wettability of Supported Monolayer Hexagonal Boron Nitride in Air. *Advanced Functional Materials*, *27*(19), 1603181. https://doi.org/10.1002/ADFM.201603181

Liu, F., Yi, M., Ran, L., Ge, Y., & Peng, K. (2021). Effect of silane grafted h-BN fillers on microstructure and mechanical properties of CVI-based C/C-BN composites. *Materials Characterization*, *171*, 110765. https://doi.org/10.1016/J.MATCHAR.2020.110765

Liu, M., Chiang, S. W., Chu, X., Li, J., Gan, L., He, Y., Li, B., Kang, F., & Du, H. (2020). Polymer composites with enhanced thermal conductivity via oriented boron nitride and alumina hybrid fillers assisted by 3-D printing. *Ceramics International*, *46*(13), 20810–20818. https://doi.org/10.1016/J.CERAMINT.2020.05.096

Liu, M., Lin, K., Yao, X., Vallés, C., Bissett, M. A., Young, R. J., & Kinloch, I. A. (2023). Mechanics of reinforcement in a hybrid graphene and continuous glass fibre reinforced thermoplastic. *Composites Science and Technology*, *237*, 110001. https://doi.org/10.1016/J.COMPSCITECH.2023.110001

Liu, Y., Cheng, Y., Ma, D., Hu, N., Han, W., Liu, D., Wu, S., An, Y., & Wang, A. (2022). Continuous carbon fiber reinforced ZrB2-SiC composites fabricated by direct ink writing combined with low-temperature hot-pressing. *Journal of the European Ceramic Society*, *42*(9), 3699–3707. https://doi.org/10.1016/J.JEURCERAMSOC.2022.03.045

Lunelli, L., Caradonna, F., Potrich, C., Piotto, C., Bettotti, P., Vanzetti, L., Pederzolli, C., & Guella, G. (2019). A new silanizing agent tailored to surface bio-functionalization. *Colloids and Surfaces B: Biointerfaces*, *181*, 166–173. https://doi.org/10.1016/J.COLSURFB.2019.05.034

Luo, W., Wu, C., Li, L., Jia, T., Yu, S., & Yao, Y. (2022). Control of alignment of h-BN in polyetherimide composite by magnetic field and enhancement of its thermal conductivity. *Journal of Alloys and Compounds*, *912*, 165248. https://doi.org/10.1016/J.JALLCOM.2022.165248

Ma, X. K., Lee, N. H., Oh, H. J., Jung, S. C., Lee, W. J., & Kim, S. J. (2011). Morphology control of hexagonal boron nitride by a silane coupling agent. *Journal of Crystal Growth*, *316*(1), 185–190. https://doi.org/10.1016/J.JCRYSGRO.2010.12.066

Mehdipour, M., Doğan, S., Hezarkhani, M., Dericiler, K., Arık, M. N., Yıldırım, C., Beylergil, B., Yildiz, M., & Saner Okan, B. (2025). Enhancing directional thermal conductivity in hexagonal boron nitride reinforced epoxy composites through robust interfacial bonding. *Polymer Composites*, *46*(3), 2740–2755. https://doi.org/10.1002/PC.29136

Moore, A. L., & Shi, L. (2014). Emerging challenges and materials for thermal management of electronics. *Materials Today*, *17*(4), 163–174. https://doi.org/10.1016/J.MATTOD.2014.04.003

Mostovoy, A. S., Vikulova, M. A., & Lopukhova, M. I. (2020). Reinforcing effects of aminosilane-functionalized h-BN on the physicochemical and mechanical behaviors of epoxy nanocomposites. *Scientific Reports 2020 10:1*, *10*(1), 1–11. https://doi.org/10.1038/s41598-020-67759-z

Muratov, D. S., Kuznetsov, D. V., Il'inykh, I. A., Burmistrov, I. N., & Mazov, I. N. (2015a). Thermal conductivity of polypropylene composites filled with silane-modified hexagonal BN. *Composites Science and Technology*, *111*, 40–43. https://doi.org/10.1016/J.COMPSCITECH.2015.03.003

Muratov, D. S., Kuznetsov, D. V, Il'inykh, I. A., Burmistrov, I. N., & Mazov, I. N. (2015b). Thermal conductivity of polypropylene composites filled with silane-modified hexagonal BN. *Composites Science and Technology*, *111*, 40–43. https://doi.org/10.1016/J.COMPSCITECH.2015.03.003

Namba, S., Takagaki, A., Jimura, K., Hayashi, S., Kikuchi, R., & Oyama, S. T. (2019). Effects of ball-milling treatment on physicochemical properties and solid base activity of hexagonal boron nitrides. *Catalysis Science \& Technology*, *9*(2), 302–309. https://doi.org/10.1039/C8CY00940F

Oh, H., & Kim, J. (2019). Fabrication of polymethyl methacrylate composites with silanized boron nitride by in-situ polymerization for high thermal conductivity. *Composites Science and Technology*, *172*, 153–162. https://doi.org/10.1016/J.COMPSCITECH.2019.01.021

Omini, M., & Sparavigna, A. (1997). Effect of phonon scattering by isotope impurities on the thermal conductivity of dielectric solids. *Physica B: Condensed Matter*, *233*(2–3), 230–240. https://doi.org/10.1016/S0921-4526(97)00296-2

Ozyigit, S., Mehdipour, M., Al-Nadhari, A., Tabrizi, A. T., Dogan, S., Dericiler, K., Beylergil, B., Yildiz, M., & Okan, B. S. (2024). A comprehensive experimental study on the effects of hexagonal boron nitride particle size and loading ratio on thermal and mechanical performance in epoxy composites. *Journal of Composite Materials*, *58*(13), 1605–1616. https://doi.org/10.1177/00219983241247910/SUPPL_FILE/SJ-PDF-1-JCM-10.1177_00219983241247910.PDF

Park, H., Shin, G. H., Lee, K. J., & Choi, S. Y. (2018). Atomic-scale etching of hexagonal boron nitride for device integration based on two-dimensional materials. *Nanoscale*, *10*(32), 15205–15212. https://doi.org/10.1039/C8NR02451K

Peng, T., Huang, J., Gong, Z., Chen, X., & Chen, Y. (2022). Self-healing of reversibly cross-linked thermoplastic vulcanizates. *Materials Chemistry and Physics*, *292*, 126804. https://doi.org/10.1016/J.MATCHEMPHYS.2022.126804

Pradhan, P., Purohit, A., Jena, H., Singh, J., & Sahoo, B. B. (2025). Effects of spherical fillers reinforcement on the efficacy of thermal conductivity in epoxy and polyester matrices: Experimental validation and prediction using finite element method. *Journal of Vinyl and*

Additive Technology, *31*(1), 109–120. https://doi.org/10.1002/VNL.22159

Purohit, A., & Satapathy, A. (2016). Epoxy matrix composites filled with micro-sized LD sludge: Wear characterization and analysis. *IOP Conference Series: Materials Science and Engineering*, *115*(1). https://doi.org/10.1088/1757-899X/115/1/012006

Ryu, S., Oh, H. W., & Kim, J. (2019). A study on the mechanical properties and thermal conductivity enhancement through TPU/BN composites by hybrid surface treatment (mechanically and chemically) of boron nitride. *Materials Chemistry and Physics*, *223*, 607–612. https://doi.org/10.1016/J.MATCHEMPHYS.2018.11.052

Sabri, F. N. A. M., Zakaria, M. R., Akil, H. M., Abidin, M. S. Z., Rahman, A. A. A., & Omar, M. F. (2021). Interlaminar fracture toughness properties of hybrid glass fiber-reinforced composite interlayered with carbon nanotube using electrospray deposition. *Nanotechnology Reviews*, *10*(1), 1766–1775. https://doi.org/10.1515/NTREV-2021-0103/ASSET/GRAPHIC/J_NTREV-2021-0103_FIG_012.JPG

Salunke, D. R., & Gopalan, V. (2021). Thermal and Electrical behaviors of Boron Nitride/Epoxy reinforced polymer matrix composite—A review. *Polymer Composites*, *42*(4), 1659–1669. https://doi.org/10.1002/PC.25952;JOURNAL:JOURNAL:15480569;PAGE:STRING:ARTICLE/CHAPTER

Seyhan, A. T., Göncü, Y., Durukan, O., Akay, A., & Ay, N. (2017). Silanization of boron nitride nanosheets (BNNSs) through microfluidization and their use for producing thermally conductive and electrically insulating polymer nanocomposites. *Journal of Solid State Chemistry*, *249*, 98–107. https://doi.org/10.1016/J.JSSC.2017.02.020

Shen, T., Liu, S., Yan, W., & Wang, J. (2019). Highly efficient preparation of hexagonal boron nitride by direct microwave heating for dye removal. *Journal of Materials Science*, *54*(12), 8852–8859. https://doi.org/10.1007/S10853-019-03514-8/FIGURES/7

Shi, Y., Lin, G., Ma, X. F., Huang, X., Zhao, J., Luo, H., & Sun, D. (2020). Boron nitride nanoplatelets as two-dimensional thermal fillers in epoxy composites: new scenarios at very low filler loadings. *Journal of Polymer Engineering*, *40*(10), 859–867. https://doi.org/10.1515/POLYENG-2020-0046/ASSET/GRAPHIC/J_POLYENG-2020-0046_FIG_007.JPG

Song, J., Zhang, K., Guo, Z., Liang, T., Chen, C., Liu, J., & Shi, D. (2023). h-BN orientation degree on the thermal conductivity anisotropy of their silicone rubber composites: A quantitative study. *Composites Part A: Applied Science and Manufacturing*, *166*, 107389. https://doi.org/10.1016/J.COMPOSITESA.2022.107389

Sroka, J., Rybak, A., Sekula, R., & Sitarz, M. (2016). An Investigation into the Influence of Filler Silanization Conditions on Mechanical and Thermal Parameters of Epoxy Resin-Fly Ash Composites. *Journal of Polymers and the Environment*, *24*(4), 298–308. https://doi.org/10.1007/S10924-016-0773-8/FIGURES/9

Sun, Y., Yanagisawa, M., Kunimoto, M., Nakamura, M., & Homma, T. (2016). Estimated phase transition and melting temperature of APTES self-assembled monolayer using surface-enhanced anti-stokes and stokes Raman scattering. *Applied Surface Science*, *363*, 572–577. https://doi.org/10.1016/J.APSUSC.2015.12.035

Sun, Y., Zhou, L., Han, Y., Cui, L., & Chen, L. (2020). A new anisotropic thermal conductivity equation for h-BN/polymer composites using finite element analysis. *International Journal of Heat and Mass Transfer*, *160*, 120157. https://doi.org/10.1016/J.IJHEATMASSTRANSFER.2020.120157

Thapliyal, V., Alabdulkarim, M. E., Whelan, D. R., Mainali, B., & Maxwell, J. L. (2022). A concise review of the Raman spectra of carbon allotropes. *Diamond and Related Materials*, *127*, 109180. https://doi.org/10.1016/J.DIAMOND.2022.109180

Vinila, V. S., & Isac, J. (2022). Synthesis and structural studies of superconducting perovskite GdBa2Ca3Cu4O10.5+δ nanosystems. *Design, Fabrication, and Characterization of Multifunctional Nanomaterials*, 319–341. https://doi.org/10.1016/B978-0-12-820558-7.00022-4

Wang, S., Cao, K., Wang, G., Chen, M., & Wang, H. (2022). Preparation and Properties of Epoxy Composites with Multi-Scale BN Sheets. *Applied Sciences*, *12*(12), 6171. https://doi.org/10.3390/APP12126171

Wang, W., Zhao, M., Jiang, D., Zhou, X., & He, J. (2022). Amino functionalized boron nitride and enhanced thermal conductivity of epoxy composites via combining mixed sizes of fillers. *Ceramics International*, *48*(2), 2763–2770. https://doi.org/10.1016/J.CERAMINT.2021.10.063

Wang, Y., Wu, J., Han, T., & Yin, A. Y. (2019). Enhanced Thermal Conductive Boron Nitride/ Silicon Carbide/ Silicone Elastomer with Nonlinear Conductive Characteristic and Partial Discharge Resistance. *Annual Report - Conference on Electrical Insulation and Dielectric Phenomena, CEIDP*, *2019-October*, 70–73. https://doi.org/10.1109/CEIDP47102.2019.9009730

Wie, J., Kim, M., & Kim, J. (2020). Enhanced thermal conductivity of a polysilazane-coated A-BN/epoxy composite following surface treatment with silane coupling agents. *Applied Surface Science*, *529*, 147091. https://doi.org/10.1016/J.APSUSC.2020.147091

Xiao, C., Guo, Y., Tang, Y., Ding, J., Zhang, X., Zheng, K., & Tian, X. (2020a). Epoxy composite with significantly improved thermal conductivity by constructing a vertically aligned three-dimensional network of silicon carbide nanowires/ boron nitride nanosheets. *Composites Part B: Engineering*, *187*, 107855. https://doi.org/10.1016/J.COMPOSITESB.2020.107855

Xiao, C., Guo, Y., Tang, Y., Ding, J., Zhang, X., Zheng, K., & Tian, X. (2020b). Epoxy composite with significantly improved thermal conductivity by constructing a vertically aligned three-dimensional network of silicon carbide nanowires/ boron nitride nanosheets. *Composites Part B: Engineering*, *187*, 107855. https://doi.org/10.1016/J.COMPOSITESB.2020.107855

Yan, Y., Liao, K., Hu, J., Qin, M., He, T., Ou, T., Fan, Y., Leng, J., & He, G. (2024). Effects of h-BN content and silane functionalization on thermal conductivity and corrosion resistance of h-BN/EPN coating. *Surface and Coatings Technology*, *476*, 130185. https://doi.org/10.1016/J.SURFCOAT.2023.130185

Yang, H., Chen, Q., Wang, X., Chi, M., Liu, H., & Ning, X. (2019). Dielectric and Thermal Conductivity of Epoxy Resin Impregnated Nano-h-BN Modified Insulating Paper. *Polymers 2019, Vol. 11, Page 1359*, *11*(8), 1359. https://doi.org/10.3390/POLYM11081359

Yang, L., Zhang, L., & Li, C. (2020). Bridging boron nitride nanosheets with oriented carbon nanotubes by electrospinning for the fabrication of thermal conductivity enhanced flexible nanocomposites. *Composites Science and Technology*, *200*, 108429. https://doi.org/10.1016/J.COMPSCITECH.2020.108429

Yang, N., Xu, C., Hou, J., Yao, Y., Zhang, Q., Grami, M. E., He, L., Wang, N., & Qu, X. (2016). Preparation and properties of thermally conductive polyimide/boron nitride composites. *RSC Advances*, *6*(22), 18279–18287. https://doi.org/10.1039/C6RA01084A

Yang, W., Lin, Y., Zhu, Y., Zhen, C., Tao, W., Luo, Y., & Wang, X. (2025). Synergistic effect of dual-modification strategy on thermal conductivity and thermal stability of h-BN/silicone rubber composites: Experiments and simulations. *International Communications in Heat and Mass Transfer*, *163*, 108716. https://doi.org/10.1016/J.ICHEATMASSTRANSFER.2025.108716

Yi, H., Solís-Fernández, P., Hibino, H., & Ago, H. (2022). Surface etching and edge control of hexagonal boron nitride assisted by triangular Sn nanoplates. *Nanoscale Advances*, *4*(18), 3786–3792. https://doi.org/10.1039/D2NA00479H

Yi, L., Hu, H., li, C., Zhang, Y., Yang, S., & Pan, M. (2022). Experimental investigation on enhanced flow and heat transfer performance of micro-jet impingement vapor chamber for high power electronics. *International Journal of Thermal Sciences*, *173*, 107380.

https://doi.org/10.1016/J.IJTHERMALSCI.2021.107380

Yu, B., Xing, W., Guo, W., Qiu, S., Wang, X., Lo, S., & Hu, Y. (2016). Thermal exfoliation of hexagonal boron nitride for effective enhancements on thermal stability, flame retardancy and smoke suppression of epoxy resin nanocomposites via sol–gel process. *Journal of Materials Chemistry A*, *4*(19), 7330–7340. https://doi.org/10.1039/C6TA01565D

Yuan, C., Li, J., Lindsay, L., Cherns, D., Pomeroy, J. W., Liu, S., Edgar, J. H., & Kuball, M. (2019). Modulating the thermal conductivity in hexagonal boron nitride via controlled boron isotope concentration. *Communications Physics*, *2*(1), 1–8. https://doi.org/10.1038/S42005-019-0145-5;SUBJMETA=1005,119,301,639,766;KWRD=CONDENSED-MATTER+PHYSICS,MATERIALS+FOR+DEVICES

Yuzuriha, T. H., & Hess, D. W. (1986). Structural and optical properties of plasma-deposited boron nitride films. *Thin Solid Films*, *140*(2), 199–207. https://doi.org/10.1016/0040-6090(86)90263-4

Zanjani, J. S. M., Okan, B. S., Menceloglu, Y. Z., & Yildiz, M. (2016). Nano-engineered design and manufacturing of high-performance epoxy matrix composites with carbon fiber/selectively integrated graphene as multi-scale reinforcements. *RSC Advances*, *6*(12), 9495–9506. https://doi.org/10.1039/C5RA23665G

Zhang, D. L., Zha, J. W., Li, W. K., Li, C. Q., Wang, S. J., Wen, Y., & Dang, Z. M. (2018). Enhanced thermal conductivity and mechanical property through boron nitride hot string in polyvinylidene fluoride fibers by electrospinning. *Composites Science and Technology*, *156*, 1–7. https://doi.org/10.1016/J.COMPSCITECH.2017.12.008

Zhang, H. X., Shin, B. G., Lee, D. E., & Yoon, K. B. (2020). Preparation of PP/2D-Nanosheet Composites Using MoS2/MgCl2- and BN/MgCl2-Bisupported Ziegler–Natta Catalysts. *Catalysts 2020, Vol. 10, Page 596*, *10*(6), 596. https://doi.org/10.3390/CATAL10060596

Zhang, N., Zhang, Y., Li, S., Guo, L., Yang, Z., Zhang, X., Wang, T., & Wang, Q. (2022). 3D structurally advanced graphene oxide/h-BN hybrid for solid self-lubrication with enhanced thermal conductivity. *Tribology International*, *176*, 107918. https://doi.org/10.1016/J.TRIBOINT.2022.107918

Zhang, S., Li, X., Guan, X., Shi, Y., Wu, K., Liang, L., Shi, J., & Lu, M. (2017). Synthesis of pyridine-containing diamine and properties of its polyimides and polyimide/hexagonal boron nitride composite films. *Composites Science and Technology*, *152*, 165–172. https://doi.org/10.1016/J.COMPSCITECH.2017.09.026

Zhang, X., Yi, J., Yin, Y., Song, Y., & Xiong, C. (2021). Thermal conductivity and electrical insulation properties of h-BN@PDA/silicone rubber composites. *Diamond and Related*

Materials, *117*, 108485. https://doi.org/10.1016/J.DIAMOND.2021.108485